# Regulation of Floral Ontogeny in Pigeonpea (Cajanus cajan L.) Under Elevated CO<sub>2</sub> and Drought Stress

# Thesis Submitted for the Award of the Degree of DOCTOR OF PHILOSOPHY

DIVYA K UNNIKRISHNAN

(Registration No. 16LPPH04)



School Of Life Sciences

Department Of Plant Sciences

University Of Hyderabad

Hyderabad 500046

December 2022



University of Hyderabad

(A Central University established in 1974 by an act of parliament)

#### HYDERABAD - 500 046, INDIA

#### CERTIFICATE

This is to certify that Ms DIVYA K UNNIKRISHNAN has carried out the research work embodied in the present thesis under the supervision and guidance of Professor Attipalli R. Reddy for a full period prescribed under the Ph.D. ordinances of this University. We recommend her thesis entitled "Regulation of Floral Ontogeny in Pigeonpea (Cajanus cajan L.) Under Elevated CO2 and Drought Stress" for submission for the degree of Doctor of Philosophy of the University.

Prof. Attipalli R. Reddy

Prof. Subramanyam Rajagopal

(Supervisor)

(Supervisor)

Prof. Attipalli R. Reddy, FNASc Dept. of Plant Sciences University of Hyderabad Hyderabad-500 046, India. Prof. S. RAJAGOPAL
Dept. of Plant Sciences
School of Life Sciences
University of Hyderabad
Hyderabad-500 046.



University of Hyderabad
(A Central University established in 1974 by an act of parliament)

HYDERABAD - 500 046, INDIA

#### DECLARATION

Ontogeny in Pigeonpea (Cajanus cajan L.) Under Elevated CO2 and Drought Stress" has been carried out by me under the supervision of Prof. Attipalli R. Reddy, Department of Plant Sciences, School of Life Sciences. The work presented in this thesis is a bonafide research work and has not been submitted for any degree or diploma in any other University or Institute. A report on plagiarism statistics from the University Librarian is enclosed.

Divya K. Unnikrishnan

Prof. Attipalli R. Reddy

(Supervisor)

Prof. Attipalli R. Reddy, FNASc Dept. of Plant Sciences University of Hyderabad Hyderabad-500 046, India. Prof. Subramanyam Rajagopal

(Supervisor)

Prof. S. RAJAGOPAL Dept. of Plant Sciences School of Life Sciences University of Hyderabad Hyderabad-500 046.



# **Department of Plant Sciences**

## **School of Life Sciences**

## University of Hyderabad

# Hyderabad – 500046, Telangana, India

#### CERTIFICATE

This is to certify that this thesis entitled "Regulation of Floral Ontogeny in Pigeonpea (Cajanus cajan L.) Under Elevated CO2 and Drought Stress" is a record of Bonafide work done by Ms. Divya K Unnikrishnan, a research scholar for Ph. D. programme under the Department of Plant Sciences, School of Life Sciences, University of Hyderabad under my guidance and supervision. This thesis is free from plagiarism and has not been submitted in part or in full to this or any other University or institution for the award of any degree or diploma.

Parts of the thesis have been:

- A. Published in the following publications:
- 1. Acta Physiologiae Plantarum (2021) 43:1-15.
- B. Presented in the following conferences:
- 1. Poster presentation in 8th International Conference on "Photosynthesis and Hydrogen Energy Research for Sustainability 2017". Effect of elevated CO<sub>2</sub> on growth, yield, and seed quality of Pigeonpea.
- 2. Oral presentation in National Conference on Frontiers in Plant Biology (January 31-February 1, 2020) Impact of Elevated Atmospheric CO<sub>2</sub> on Growth, Yield and Seed quality of Pigeonpea.

Further, the student has passed the following courses towards the fulfilment of the coursework requirement for Ph.D.

S.No.	Course code	Name	Credits	Pass/Fail
1	PL801	Analytical Techniques	4	Pass
2	PL802	Research ethics, Data analysis and biostatistics and management	3	Pass
3	PL803	Lab work and Seminar	5	Pass

Supervisor

Dept. of Plant Sciences School of Life Sciences University of Hyderabad Hyderabad-500 046. Head HEAD

Dept. of Plant Sciences School of Life Sciences University of Hyderabad Hyderabad-500 046 INDIA Dean DEAN

School of Life Sciences University of Hyderabad Hyderabad-500 046.

#### **ACKNOWLEDGEMENTS**

I express my immense gratitude to my supervisor **Prof.** Attipalli R Reddy, for giving me an opportunity to work in his lab. Words can't express my gratefulness for his constant support and guidance during my tenure of doctoral research. I would like to thank him for building my courage, his inputs to improve my work. I am inspired by his dedication to the scientific field. I am fortunate and privileged to have him as my Supervisor.

I am grateful to my co- supervisor and former doctoral committee member **Prof. S**Rajagopal for his kind support and guidance throughout my doctoral research. I am thankful for his suggestions and providing lab resources during my research.

I thank my doctoral committee members **Prof. G Padmaja and Dr. Rahul Kumar** for their valuable suggestions and guidance throughout my research.

I extend my sincere gratitude to Head of the Department of Plant Sciences, **Prof. S**Rajagopal, and former Heads, **Prof. G Padmaja** and **Prof Ch. Venkata Ramana**providing the necessary department facilities for my research work.

I am thankful to Dean **Prof.** N Siva Kumar and former Deans, **Prof.** S. Dayananda, **Prof.** M. Ramanadham, **Prof.** P. Reddanna for extending the facilities in School of Life Sciences.

I am extremely thankful to Faculty members, Department of Plant Sciences and School of Life Sciences for their support and suggestions.

I am grateful to all my seniors **Dr. Debashree**, **Dr. Madhana Sekhar**, **Dr. Sree Harsha**, **Dr. Shalini**, **Dr. Sumit**, **Dr. Sitaram**, **Dr. Suresh** for their help and support during my research tenure.

I am especially grateful to **Dr. Sree Harsha** for his support and guidance throughout my research work.

I am thankful to all seniors and colleagues Dr. Elsin, Dr. Sai, Dr. Manjunath, Dr. Nageshrao, Dr. Venkateswara, Dr. Ranay, Dr. Nisha, Tamna di, Yusuf, Jayendra, Jerome, Jyothi Ranjan, Pavitra, Praveena, Sailaja, Vijay and Ganesh for their support and maintaining a cheerful environment in the lab. I am thankful to CSIR, BBL and all

funding bodies supporting departmental facilities helping in completion of my research work.

"It's not what we have in life, but who we have in our life that matters." I have been fortunate to meet wonderful people in my life whom I can call my people. They have helped me to believe in myself, gave me courage and support. They have given me my best and happy time of my life. I am grateful to all my friends- Anusha, Mouboni, Anusree Indu, Smita and Rutuparna who have supported me and were pillars of support. Mouboni di and Anusree di thank you for cheering me, supporting me and for the happy memorable times. I am grateful to have met my friend Anusha, thank you for being my moral support. I am grateful to Smita, for being a support at all times.

I am grateful to all my friends – Pragyansini, Mounica, Ammu, Aiswarya for always supporting and cheering me. I am also grateful to my other friends Ipsita, Pavitra, Shreya, Vandana, Risha, Prodosh and Deepak.

Words can't express my gratitude to my sister and best friend Vinaya. Thank you for being my pillar of support and believing in me when I couldn't believe in myself. I am fortunate to know Bangtan. Thank you for helping me to have faith in myself and impart the courage to pursue my dreams.

I am indebted to my parents for believing in me and helping me achieve my dreams. I am so grateful to my mother for always listening to my worries and being my biggest supporter. I am who I am because of you Amma. I am grateful to my brother Dhinu, Laila, and Pluto for cheering me up during my bad times. I am thankful to my family-grandparents, aunts, uncles and cousins for their support. I finally thank God almighty for all the blessings.

# **Table of contents**

Content	Pages
Chapter 1: Introduction and Objectives	1- 26
Chapter 2: Materials and Methods	27-52
Chapter 3: Results	53-171
Chapter 4: Discussion	172-206
Chapter 5: Summary and conclusions	207-211
Chapter 6: Literature cited	212-230

#### **List of Figures and Tables**

#### **Figures**

- Fig. 1. Schematic illustration representing major flowering pathways and flower formation in plants.
- Fig. 2. Variations in atmospheric CO<sub>2</sub> levels over the years. (NOAA, 3 April 2022). 280 ppm is the chart baseline, as it is the preindustrial average.
- Fig. 3. Survey showing global drought risk index areas by IPCC climate report 2022.
- Fig. 4. Various responses induced by drought stress in plants.
- Fig. 5. Pigeonpea flowering (left) and pigeonpea seeds (right).
- Fig. 6. a) Open top chambers (OTC) (4x4x4 m) for elevated CO<sub>2</sub> studies at the University of Hyderabad. b) Setup for CO<sub>2</sub> gas cylinders and pumping c) NDIR (non-dispersive infra-red) based CO<sub>2</sub> analyser and d) SCADA software controlling CO<sub>2</sub> pumping.
- Fig. 7. Experimental layout for the elevated CO<sub>2</sub> studies.
- Fig. 8. Experimental layout for drought studies under different developmental stages in pigeonpea.
- Fig. 9. Growth characteristics of pigeonpea under elevated  $CO_2$  a) height of the plant, b) the number of nodes, and c) days to anthesis. Values are given as mean  $\pm$  SD (n=3), and ns denotes no significance.
- Fig. 10. Photosynthetic parameters under elevated  $CO_2$  a) Fv/Fm, b) Fv/Fo, c) Fo, and d) Fm. Values are given as mean  $\pm$  SD and significant difference between ambient and elevated  $CO_2$  grown plants at \*\*p < 0.01.

- Fig. 11. Foliar carbohydrates under ambient and elevated  $CO_2$  conditions a) fructose, b) glucose, c) sucrose, and d) H/S ratio. Values are given as mean  $\pm$  SD, with significant difference wherein p value denotes \* < 0.05, \*\* < 0.01.
- Fig. 12. Analysis of flowering gene transcripts under ambient and elevated CO<sub>2</sub> conditions a) Photoperiod and floral regulator gene transcripts, b) miRNA transcripts, and c) genes involved in sugar signalling.
- Fig. 13. Correlation network of floral regulatory genes under elevated CO<sub>2</sub> conditions.
- Fig. 14. ABCE gene transcript expression patterns in inflorescence under elevated CO<sub>2</sub> conditions.
- Fig. 15. Yield characteristics of pigeonpea under elevated  $CO_2$  conditions a) pod weight, b) seed weight, c) weight/ 100 seeds, and d) total dry weight. Values are given as mean  $\pm$  SD (n=3) and significant difference between ambient and elevated  $CO_2$  grown plants at \*p < 0.05, \*\*p<0.001, ns: no statistical significance.
- Fig. 16. Biochemical characteristics of pigeonpea seeds under elevated CO<sub>2</sub>.
- Fig. 17. Metabolite analysis of pigeonpea seeds under elevated CO<sub>2</sub> a) characterization of metabolites into different categories and b) fold change of metabolites in pigeonpea seeds under elevated CO<sub>2</sub>.
- Fig. 18. PCA analysis of metabolites in ambient and elevated CO<sub>2</sub> grown pigeonpea seeds.
- Fig. 19. Correlation heatmap between metabolites in pigeonpea seeds under elevated CO<sub>2</sub>.

Fig. 20. a) Characterization of the proteome of pigeonpea seed based on significance, b) downregulated proteins in pigeonpea seeds under elevated CO<sub>2</sub>, and c) upregulated proteins in pigeonpea seeds under elevated CO<sub>2</sub> based on their functionality.

Fig. 21. a) Gene ontology of upregulated proteins in pigeonpea seed under elevated CO<sub>2</sub> and b) gene ontology of downregulated proteins in pigeonpea seed under elevated CO<sub>2</sub>.

Fig. 22. a) Gene ontology of proteins exclusively expressed in elevated CO<sub>2</sub> grown pigeonpea seeds and b) Gene ontology of proteins exclusively expressed in ambient CO<sub>2</sub> grown pigeonpea seeds.

Fig. 23. Functional characterization of elevated seed specific proteins within each category of gene ontology a) Metabolism, b) Genetic information and processing and c) Environmental sensing and processing.

Fig. 24. Total transposon elements (TEs) exclusively expressed in ambient and elevated CO<sub>2</sub> grown seeds.

Fig. 25. Functional characterization of ambient seed specific proteins within each category of gene ontology a) Metabolism, b) Genetic information and processing and c) Environmental sensing and processing.

Fig. 26. a) Leaf relative water content (RWC) at preflowering stage drought (PFSS) and b) RWC at flowering stage drought (FSS) in pigeonpea.

Fig. 27. a) Leaf moisture content (LMC) in pigeonpea at preflowering stage drought (PFSS) and b) LMC at flowering stage drought (FSS).

- Fig. 28. Photosynthetic physiology of pigeonpea under drought at two developmental stages- preflowering stage (PFSS) and flowering stage (FSS). a) Photosynthetic rate, b) transpiration rate, c) Water use efficiency, and d) stomatal conductance.
- Fig. 29. Foliar free sugar contents in pigeonpea under drought stress at two developmental phases- preflowering stage (PFSS) and flowering stage (FSS). Values are given as mean  $\pm$  SD.
- Fig. 30. Fold change of amino acid contents in pigeonpea leaves under drought stress at the preflowering stage (PFSS).
- Fig. 31. Fold change of amino acid contents in pigeonpea leaves under drought stress at flowering stage (FSS).
- Fig. 32. Analysis of major phytohormones (GA3, IAA, ABA, IBA) in pigeonpea leaves under drought stress at the preflowering stage (PFSS) and flowering stage (FSS). Values are given as mean  $\pm$  SD, and significant differences between control and drought stressed plants were calculated wherein \*\*p < 0.001 and \*p < 0.5.
- Fig. 33. Correlation heatmap among the phytohormones under PFSS.
- Fig. 34. Correlation heatmap among the phytohormones under FSS.
- Fig. 35. Correlation heatmap between phytohormones and metabolites under PFSS.
- Fig. 36. Correlation heatmap between phytohormones and metabolites under FSS.
- Fig. 37. Transcript levels of flowering regulatory genes, phytohormone, and sugar signaling genes in pigeonpea leaves at PFSS and FSS stress.

- Fig. 38. Transcript levels of flowering regulatory genes, phytohormone, and sugar signaling genes in meristem at a) PFSS and b) FSS stress.
- Fig. 39. Correlation network analysis to illustrate relationships among the flowering regulatory genes under a) PFSS and b) FSS stress conditions.
- Fig. 40. Correlation network analysis to illustrate relationships among the flowering regulatory genes in meristem under a) PFSS and b) FSS stress conditions.
- Fig. 41. Transcript analysis of ABCE genes in inflorescence from control plant inflorescence (CF), drought recovered PFSS plants (RF) and inflorescence from drought stressed FSS plants (DF).
- Fig. 42. a) Number of inflorescences observed in drought stressed plants, and b) Number of pods observed from drought recovered plants. Statistical analysis shows P value \*\* < 0.01.
- Fig. 43. Analysis of reproductive characteristics from drought recovered pigeonpea plants.
- Fig. 44. Correlation heatmap of reproductive characteristics in pigeonpea under drought.
- Fig. 45. Analysis of free amino acids in pigeonpea seeds from drought recovered plants.
- Fig. 46. Proposed model on the molecular regulation of delayed flowering under elevated CO<sub>2</sub>. The brown color shows the presence of metabolites and gene transcripts in leaves and green in roots, and the ascending intensity of the color shows an increase in concentration at the time point in elevated CO<sub>2</sub> grown plants.

The arrow represents upregulation or downregulation compared to ambient CO<sub>2</sub> grown plants. The remobilization of sucrose (C) is considered a signal for the suppression of TPS, causing enhanced expression of miR156, which results in the suppression of various other genes required for floral initiation.

Fig. 47. Correlation analysis among LMC, Pn, LRWC, and Proline under drought stress a) PFSS and b) FSS conditions.

Fig. 48. Proposed model on delayed flowering and sequential effects on the reproductive physiology of pigeonpea under drought at the preflowering stage. The arrows show upregulation and downregulation in drought stressed plants compared to the control.

Fig. 49. Proposed model on delayed flowering and sequential effects on the reproductive physiology of pigeonpea under drought at flowering stage. The arrows show upregulation and downregulation in drought stressed plants compared to the control. The width of the arrows shows an increase in the intensity of either upregulation or downregulation compared to the control plants and PFSS drought stressed plants.

#### **Tables**

Table. 1 Literature review to understand eCO<sub>2</sub> responses on a few crop and tree species.

Table. 2 Selected JIP parameters and their descriptions.

Table. 3 List of primers used for the expression of flowering regulatory gene transcripts.

Table.4 Pearson correlation coefficient and their correlation significance levels.

Table. 5 List of primers used for the expression of flowering, sugar signaling, and phytohormone gene transcripts.

Table. 6 Photosynthetic parameters under ambient and elevated CO<sub>2</sub> conditions.

Table. 7 Correlation between metabolites in elevated  $CO_2$  seeds. Pearson correlation coefficient (r) > 0.5 is considered a strong positive correlation (red), and < -0.5 is a strong negative correlation (yellow), and follows into categories of moderate or no correlation.

Table. 8 Description of differentially regulated proteins in seeds collected from ambient and elevated CO<sub>2</sub> grown pigeonpea plants.

Table. 9 Gene ontology for proteins exclusively observed in ambient and elevated CO<sub>2</sub> grown seeds.

Table. 10 Correlation between metabolites and phytohormones under PFSS. Pearson correlation coefficient (r) > 0.5 is considered a strong positive correlation (red), and < -0.5 is a strong negative correlation (yellow), and follows into categories of moderate or no correlation.

Table. 11 Correlation between metabolites and phytohormones under FSS. Pearson correlation coefficient (r) > 0.5, a strong positive correlation (red), and < -0.5, a strong negative correlation (yellow), and following into categories of moderate or no correlation.

## **List of Abbreviations**

Fo	Minimum fluorescence value after the onset of actinic		
	illumination at 50μs		
Fp=Fm	Maximum fluorescence intensity under saturating illumination at		
	P-step		
Fv	Variable chlorophyll fluorescence		
DIo/RC	Dissipated energy flux per RC		
RC/CSm	Density of active reaction centers per cross-section (CS)		
ABS/CSm	Absorption flux per excited CS		
ETo/CSm	Electron transport flux per excited CS		
DIo/CSm	Dissipated energy flux per excited CS		
PI(ABS)	Performance index on absorption basis		
GI	Gigantea		
CO	Constans		
FT	Flowering Locus T		
TOC1	Timing of CAB 1		
CCA1	Circadian clock associated 1		
SOC1	Suppressor of Overexpression of CO1		
SPL	Squamosa promoter binding like		
CWIN	Cell wall invertase		
PRR5	Pseudo response regulator 5		
ZTL	Zeitlupe		
TPS6	Trehalose 6 phosphate synthase 6		
AP1	Apetala 1		
AP2	Apetala 2		
AP3	Apetala 3		
PST	Pistillata		
AGA	Agamous		
SEP	Sepallata		
SPS	Sucrose phosphate synthase		
SUT	Sucrose transporter		
ARF	Auxin response factor		
IAA	Auxin/ IAA responsive gene		
GID	GA insensitive dwarf		
TPS9	Trehalose 6 phosphate synthase 9		
GA20OX	GA 20 Oxidase		
SPA	Suppressor of PHYA		
SnRK	Sucrose non fermenting related protein kinase		
LFY	Leafy		
CO <sub>2</sub>	Carbon dioxide		
N <sub>2</sub> O	Nitric oxide		
LRWC	Leaf relative water content		
LMC	Leaf moisture content		
WUE	Water use efficiency		
GA3	Gibberellin		
ABA	Abscisic acid		
IAA	Indole acetic acid		

IBA	Indole butyric acid			
Suc	Sucrose			
Gluc	Glucose			
Fru	Fructose			
Lys	Lysine			
Trp	Tryptophan			
Met	Methionine			
Val	Valine			
Leu	Leucine			
His	Histidine			
Asp	Aspartic acid			
Glu	Glutamate			
Ala	Alanine			
Ser	Serine			
Arg	Arginine			
Pro	Proline			
Gly	Glycine			
C	Carbon			
N	Nitrogen			
P	Phosphorus			
S	Sulfur			
OTC	Open Top Chambers			
PFSS	Preflowering stage stress			
FSS	Flowering stage stress			
CDF				
TSF	Cycling DOF Factors Twin sister of FT			
FLC				
LD	Flowering Locus C Luminidependens			
FUL	Fruitful			
CAL	Cauliflower			
RCA	Rubisco activase			
PEPc	Phosphoenolpyruvate carboxylase			
IPCC	Intergovernmental Panel on Climate Change			
ROS	Reactive oxygen species			
SCADA	Supervisory control and data acquisition			
HPLC	High performance liquid chromatography			
LFQ	Label free quantification			
DAE	Days after emergence			
FW	Fresh weight			
DW	Dry weight			
TW	Turgid weight			
OPA	Ortho phthalaldehyde			
FMOC	Fluroenylmethyloxycarbonyl			
TE	Transposon elements			
MEP	Methylerythritol 4 phosphate			
DAS	Days after stress			
DAS	Days after stress			

# CHAPTER 1 INTRODUCTION AND OBJECTIVES

#### INTRODUCTION

Climate change is a global concern today, impacting the environment and agronomy. It poses a significant threat to agriculture and affects millions of lives. The primary culprits of this climate change include greenhouse gases like methane, CO<sub>2</sub>, and N<sub>2</sub>O. As years pass by, more climate-related problems emerge, leading to issues in agriculture and the food industry. It is projected that cereal and maize production will be reduced by 3.8 % and 5.5 % by the year 2050 (Mahli et al., 2021). Hence, understanding plant behaviour and its developmental processes, in crop plants under these climate-related stresses is crucial to improve crop productivity. Flowering is a critical development process in the plant life cycle, as timely floral initiation directly dictates the plant's reproductive success. Hence, it is necessary to understand the mechanism of floral patterns under different environmental conditions, especially under climate change stress. Flowering is a multifaceted process involving various endogenous and exogenous factors. The culmination of multiple pathways leads to a successful floral transition. Photoperiod, vernalization, and aging are significant pathways in flowering. New aspects contributing to flowering are forthcoming, such as hormonal regulation of flowering, role of miRNAs, and epigenetic regulation.

#### Major flowering pathways and mechanisms

The photoperiod pathway is the most well-studied pathway that depends on the day length required for flowering. The photoperiod pathway depends on the circadian clock and photoreceptors helping activate gigantea (GI) and constans (CO) for the flowering initiation. The induction of CO depends on the day length and accordingly leads to the initiation of florigen or Flowering locus T gene (FT). CO is a B box-type zinc finger transcription factor (TF) with the CCT domain accumulating only during daytime as it requires light for activation (Putterill et al., 1995). The levels of CO are maintained by

repressors, including CYCLING DOF FACTORs (CDFs), based on the time of the day as GI and photoreceptors repress these factors. During the night, the CDFs accumulate to degrade CO (Quiroz et al., 2021). Later CO activates FT expression, which is transported to meristem and, in conjunction with its homologs, the Twin sister of FT (TSF).

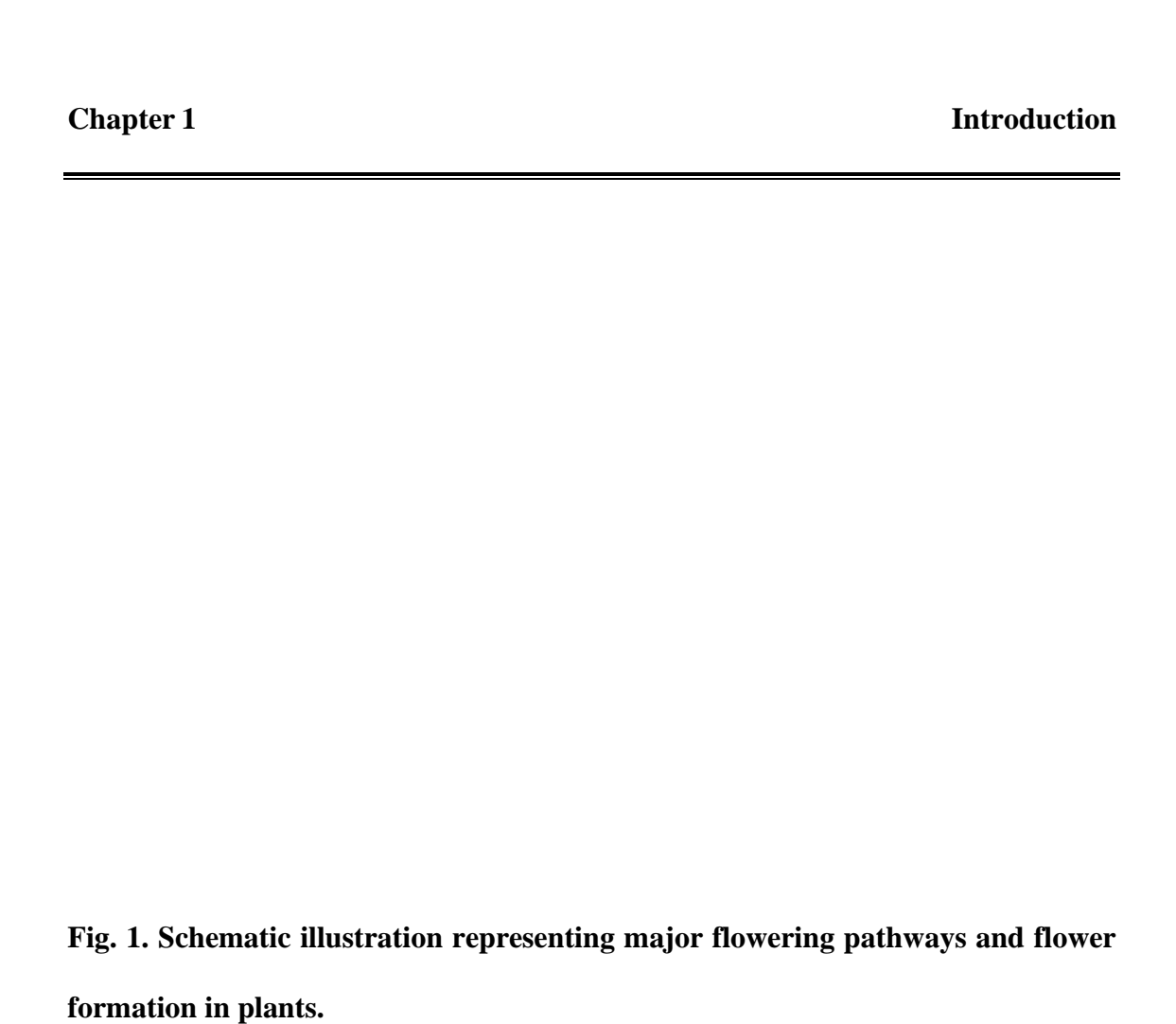
Once FT/TSF reach meristem, they form a complex with FD to activate other floral integrators for floral initiation. These floral integrators are activated by various pathways and internal cues alongside the photoperiod pathway (Quiroz et al., 2021). The autonomous and vernalization pathway represses the activity of Flowering Locus C (FLC), a well-known flowering repressor. The vernalization pathway comes into play in plants on exposure to low temperatures for a prolonged period. Autonomous pathways regulate flowering based on internal signals with the help of genes, including FCA, FLD, FY, FVE, and LD, which also repress the floral repressor FLC (Putterill et al., 2004).

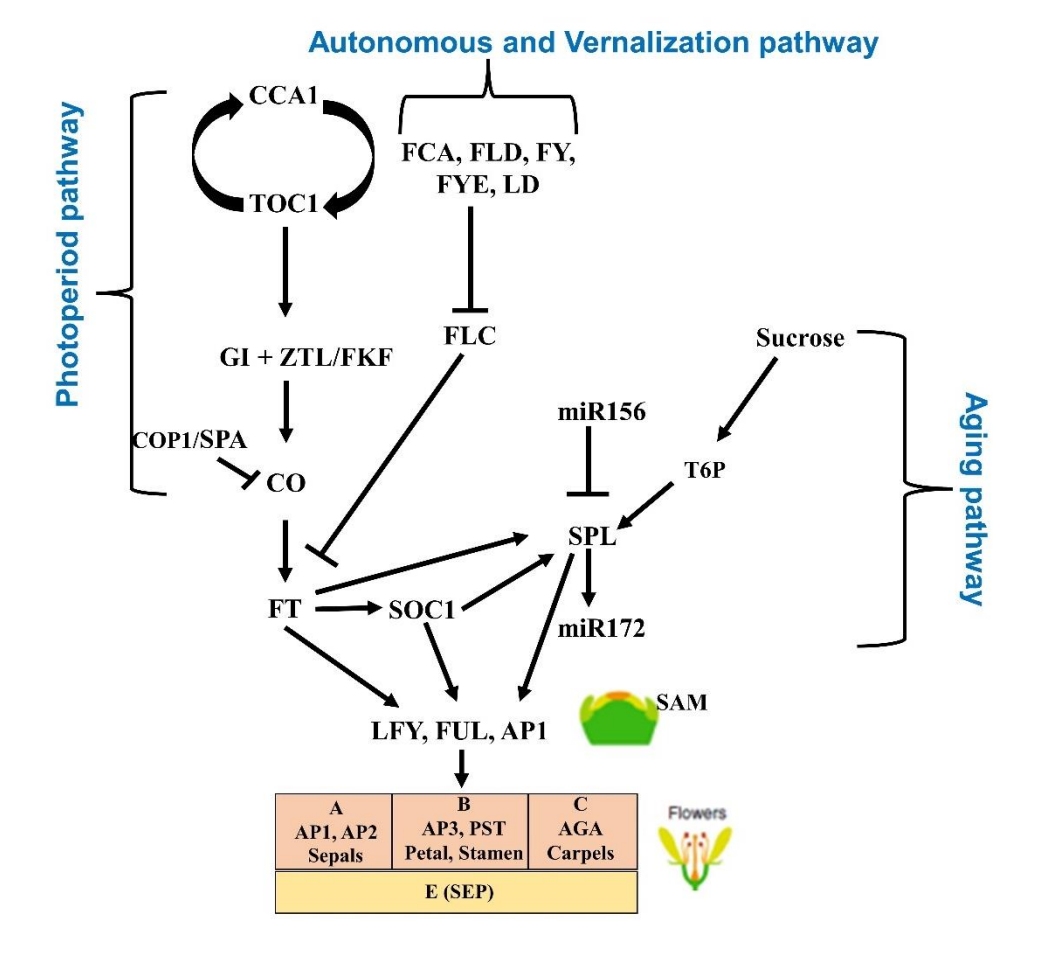
Nevertheless, as long as the plant is not developmentally equipped or aged, the other cues will not be able to promote flowering. Here, the aging pathway comes into play as it initiates plant maturation and helps transition to the reproductive stage for floral initiation. Plants align their developmental transitions in accordance with a favorable environment for successful reproduction. Sugars and miR156-SPL-miR172 are essential players in the aging pathway that sense signals and help in plant vegetative to reproductive transition. miRNAs like miR156 and miR172 are mainly conserved throughout plant species. These miRNAs with the RNA silencing mechanism play a

significant role in this developmental stage transition (Baurle and Dean 2006). miRNAs are 21-22 nucleotides that down-regulate the expression of specific target genes by directing the cleavage of mRNAs or interfering with translation. miRNA genes are transcribed by RNA polymerase II into primary transcripts (pri-miRNAs), wherein they are later transformed into mature miRNA by the action of the Dicer (DCL1) enzyme (Sun et al., 2019). The mature miRNA forms a complex with RNA-induced silencing complex (RISC), leading to the degradation of target genes or translational inhibition (Chen 2005). Lately, studies have also reported that phytohormones, mainly gibberellins, play a role in the aging pathway. Sugar levels in the plant also act as sensors for the floral transition. For example, sucrose and trehalose 6 phosphate act as signaling molecules that activate the vegetative to reproductive transition.

Plants have two major developmental stages; vegetative and reproductive with multiple in-between developmental transitions. After germination, the first developmental transition is the juvenile to the adult vegetative phase. Once the plant enters the adult vegetative phase, it can respond to the cues required for the floral transition (Baurle and Dean 2006). Usually, plants during the vegetative phase have higher levels of miR156, and as the plant matures these miR156 levels are replaced by miR172, which further initiates floral induction or the reproductive phase (Huijser and Schmid 2011). These miRNA levels are activated or repressed by the levels of sugars and carbon availability in plants. Trehalose 6 phosphate is an important signaling molecule that senses carbon availability, mainly sucrose in plants. These miRNAs target transcription factors including SQUAMOSA PROMOTER BINDING PROTEIN LIKE (SPL). Studies have

shown that constitutively expressing miR156 delays flowering (Schwab et al., 2005). miR156 represses SPL during the vegetative phase; as plants mature, the change in sugar levels is sensed with the help of T6P, causing miR156 suppression, subsequently releasing SPL and activating the miR172 to further initiate floral transition. Each pathway's role in flowering varies from species to species and on the local environment. Deletion studies of SPL in Arabidopsis have shown that SPLs are required for transcriptional initiation of FM, LFY, and AP1 genes in SAM along with SOC1 (Hyun et al., 2016, Yamaguchi et al., 2009). The culmination of all these prodigious signals at SAM converge floral pathway integrators and activate the inflorescence meristem identity (IM),including APETALA1 (AP1), **FRUITFUL** (FUL), CAULIFLOWER (CAL), and LEAFY (LFY) to initiate transition of apical meristem to inflorescence meristem (Jack 2004, Irish 2017). Later, IM genes help in the downstream action of ABCE genes for floral organ formation and prompt the final flower formation (Jack 2004, Irish 2017) (Fig. 1). Still, studies are limited to understand the factors involved in floral regulation in various plant species to get comprehensive knowledge of flowering in order to maximize the reproductive success of plants, especially crops. Along with these endogenous cues influencing flowering, exogenous factors, mainly the environment plays a significant role in successful flowering (Cho et al., 2017). Environmental stress and climate change can influence the flowering patterns and impact yield. Studying the effect of each environmental stress on the floral pattern is crucial to understand the mechanisms instigated by each stress to improve plant productivity.

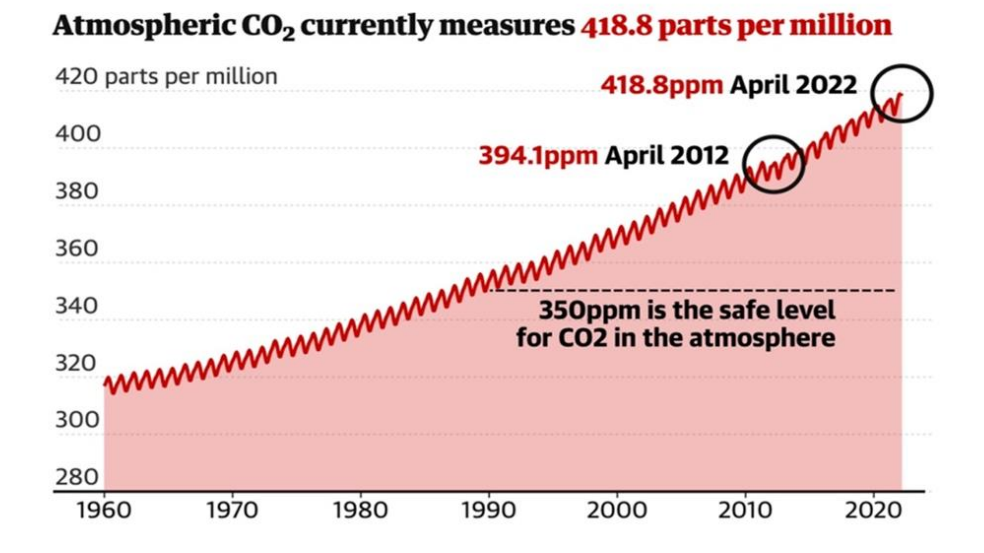




#### Rising CO<sub>2</sub> and its influence on the plant life cycle

In today's climate change scenarios, greenhouse gases mainly rising CO<sub>2</sub> levels affect plant growth and yield. Over the last 60 years, atmospheric CO<sub>2</sub> has been increasing steeply. The CO<sub>2</sub> levels in the atmosphere have increased from 280 ppm during the preindustrial era to the current 418 ppm and are expected to rise to 550 ppm by the year 2050 (Fig. 2). Rising CO<sub>2</sub> levels are mainly due to various anthropogenic activities including burning fossil fuels, industrial processes, and automobiles. It is known that till now 1.5 trillion metric tons of CO<sub>2</sub> have been emitted since 1751 (Malhi et al., 2021). These elevated levels of CO<sub>2</sub> will trap the heat in the earth's atmosphere leading to elevated temperature and drought, further snowballing the climate change issue.

Fig. 2. Variations in atmospheric CO<sub>2</sub> levels over years. (NOAA, 3 April 2022). 280 ppm is the chart baseline as it is the preindustrial average.



Crop productivity depends upon plant type and its adaptation ability. Crop responses to elevated CO<sub>2</sub> vary depending on whether it is C3 or C4 type, leguminous or nonleguminous, tree species, etc. Hence understanding the impact of elevated CO<sub>2</sub> on each plant species is necessary. Usually, under elevated CO2, plants show various physiological changes like photosynthetic carbon gain, net primary production, improved nitrogen use efficiency, and enhanced stomatal closure (Table 1). Higher CO<sub>2</sub> levels increase the photosynthetic rate leading to increased levels of carbohydrate (C), increasing the total biomass (Bhargava and Mitra 2021, Hogy et al., 2009, Sasaki et al., 2005). However, after the initially enhanced photosynthesis under elevated CO<sub>2</sub>, plants exhibit photosynthetic acclimation upon prolonged growth due to N limitation (Ainsworth and Long 2020, Ainsworth and Long 2005). Increased photosynthesis in C3 plants (eg- soybean, pigeonpea, pongamia) under elevated CO<sub>2</sub> is observed as part of Rubisco's increased carboxylation rate (Vcmax). Rubisco favors CO<sub>2</sub> over O<sub>2</sub> and Rubisco carboxylation is ampler as the excess CO<sub>2</sub> is used to increase photosynthate or carbohydrate levels. However, this surplus carbohydrate exceeds the C export causing an imbalance in C: N ratio, which leads to sucrose cycling, reducing Rubisco quantity to suppress the photosynthesis (photosynthetic acclimation) (Ainsworth and Long 2020, Ainsworth and Long 2005). Homeostasis between Rubisco activase (RCA) activity, RuBP carbamylation, and RuBP regeneration governs the acclimation process (Cen and Sage 2005, Hussain et al., 2021). RCA are enzymes dissociating inhibitory sugar phosphates from RuBPCase, promoting carbamylation. RCA's content and activity are lower under elevated CO<sub>2</sub> (Tomimatsu and Tang 2016).

Legumes can avoid this photosynthetic acclimation due to their ability to fix nitrogen and overcome the problem of N limitation. With their ability to fix atmospheric nitrogen, legumes can overcome the C: N imbalance by redirecting the excess carbon to rhizobium growth and development, leading to better nodule development and causing more N fixation which is utilized for the synthesis of various proteins, including Rubisco. Elevated CO<sub>2</sub> also increases the bacterial diversity in roots as the excess C attracts various symbiotic organisms leading to increased nutrient acquisition, mainly N and P (Bhargava and Mitra 2021). Hence, improved growth and vegetative biomass increases have been observed in C3 plants including legumes. Due to apparent anatomical differences between the C3 and C4 plants, the behavior of the C4 plant under elevated CO<sub>2</sub> varies. Studies have shown that elevated CO<sub>2</sub> does not stimulate C4 photosynthesis as CO<sub>2</sub> saturates the C uptake at lower Ci. The primary carboxylase in C4 plants is phosphoenolpyruvate carboxylase (PEPc) with lower Km for CO<sub>2</sub>, can concentrate CO<sub>2</sub> six times more than ambient around bundle sheath cells (Pignon and Long 2020). Hence greater CO<sub>2</sub> saturates carboxylation in C4, causing no direct impact on C uptake. FACE studies on sorghum, and maize have confirmed that elevated CO<sub>2</sub> has no direct impact on carbon uptake. However, on exposure to drought, elevated CO<sub>2</sub> helped improve leaf water potential, increasing photosynthesis and yield (Pignon and Long 2020). An increase in the guard cell membrane depolarization cause stomatal closure under elevated CO<sub>2</sub>. Turgor pressure in guard cells regulates the stomatal aperture by maintaining ion and organic solute concentrations. Depolarization of the guard cell membrane is essential for stomatal closure. Elevated CO<sub>2</sub> increases depolarization of the guard cell membrane by increasing the Ca<sup>2+</sup> concentration inside the guard cell while enhancing the Cl<sup>-</sup> release from guard cells resulting increased

stomatal closure (Ainsworth and Rogers 2007). In general, elevated CO<sub>2</sub> studies under both FACE and other controlled conditions have shown an increase in photosynthesis, decreased stomatal conductance, and crop yields but with a significant decrease in quality of yield (Ainsworth and Long 2007, Jena et al., 2018, Pan et al., 2018, Pilbeam 2015). Elevated CO<sub>2</sub> also helps plants to overcome drought through their increased photosynthetic rates, better water use efficiency by stomatal closure, and increased antioxidant levels, which help in scavenging more ROS compared to plants singularly exposed to drought (Sreeharsa et al., 2019, Wang et al., 2017).

An imbalance in C-N stoichiometry and disharmony between source-sink tissues results in altered temporal flowering patterns, wherein 60% of the crop plants show either delayed or accelerated flowering when grown under elevated CO<sub>2</sub> (Sreeharsha et al., 2015; Springer and Ward 2007). Different plant species have shown early, delayed, or no change in flowering time (Springer and Ward 2007). Studies have shown that the effect of elevated CO<sub>2</sub> varies within the species; e.g., Arabidopsis and soybean have exhibited delayed and accelerated flowering under elevated CO<sub>2</sub> (Becklin et al., 2017). Early flowering happens in plants that have reached the required size due to enhanced growth and increased photosynthesis. However, it also costs the plant's growth to its full potential due to photosynthetic acclimation. Increased sugars, mainly sucrose, accelerate flowering—higher levels of sucrose act as a developmental sensor promoting vegetative to reproductive transition. Cases of delayed flowering under elevated CO<sub>2</sub> have also been observed in various plants including soybean, wheat, and Arabidopsis. This varying flowering pattern in plants is due to stoichiometry changes in carbohydrate levels. In most cases, elevated CO<sub>2</sub> is shown to increase the number of lateral branches, flower buds, and flowers in many plant species including pigeonpea, pepper, and

Phalaenopsis (Sreeharsha et al., 2015, Pereyda-Gonzalez et al., 2022, Cho et al., 2020). On the other hand, exceptions have also been observed wherein elevated CO<sub>2</sub> showed effects only on pepper and zucchini and none on tomato (Lopez-Cubillos and Hughes 2016). Zucchini had more male flowers than female flowers under elevated CO<sub>2</sub>, while pepper showed reduced flowers under elevated CO<sub>2</sub> (Lopez-Cubillos and Hughes 2016). These contrasting observations under elevated CO<sub>2</sub> result from factors like the duration of elevated CO<sub>2</sub> exposure, plant species, and there is limited knowledge on the behavior of different plant species under elevated CO<sub>2</sub>. However, much is to be done to comprehend the molecular mechanisms behind this varying flowering patterns.

The effects of elevated CO<sub>2</sub> also differ from vegetative to reproductive tissues, wherein a meta-analysis of crop plants showed an increase of 31% in vegetative biomass while fruit and seed production showed only 12 and 25% increases respectively under elevated CO<sub>2</sub> (Hikosaka et al., 2011). Elevated CO<sub>2</sub> studies on soybean have shown a 24% increased seed yield (Ainsworth et al., 2002, Ainsworth and Long 2020). Though there was a quantitative enhancement in seed biomass, major non-legume food crops with few exceptions, showed an average of 14% decrease in seed N content under elevated CO<sub>2</sub>, thus making the seed deficient in crucial proteins and amino acids leading to diminished seed nutritional quality (Hikosaka et al., 2011, Hampton et al., 2012). Studies have shown that plants invest more in leaves and vegetative tissues than reproductive tissues causing N deprivation to overcome photosynthetic acclimation (Bhargava and Mitra 2020). This decrease in seed N is due to the dilution effect of carbohydrates on N. A decrease in P and S by 9%, along with other minor nutrients in seeds by 8% was also reported (Loladze 2014). Respiratory ATP is necessary for seed filling as it helps to translocate the photosynthate from vegetative tissue during grain

filling. Under elevated CO<sub>2</sub>, photosynthetic rates are increased but not respiratory rates, which might be one reason for high C and low N content. Some legumes showed decreased minerals like Fe and Zn under elevated CO<sub>2</sub> (Myers et al., 2014). They led to the primary concern that seed quality was reduced in most crops when grown under elevated CO<sub>2</sub>. However, detailed studies on seed quality are required as each plant species vary in its response to elevated CO<sub>2</sub>.

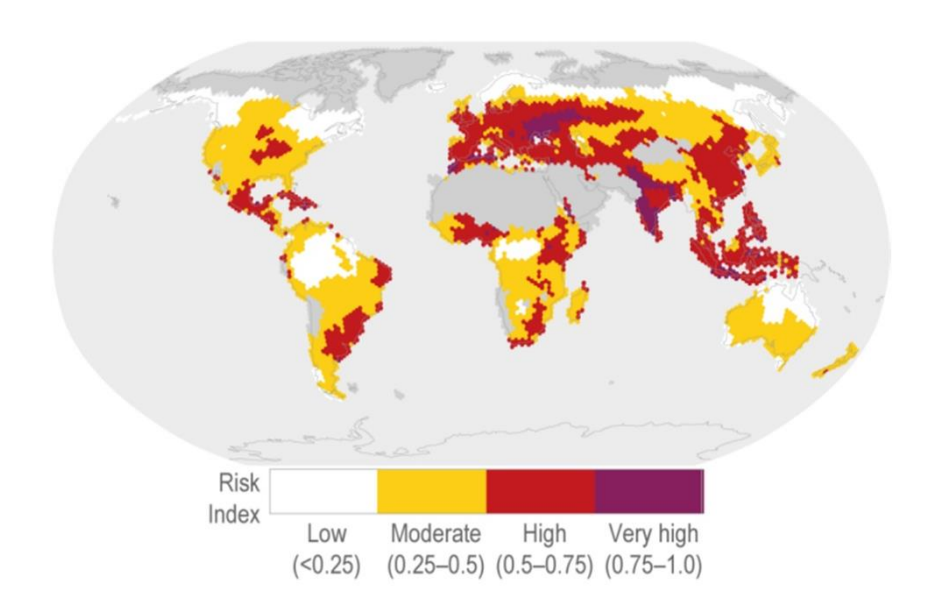
Table. 1 Literature review to understand eCO<sub>2</sub> responses on a few crop and tree species.

S.NO	Plant Species	Response	Reference
1.	Oryza sativa	Decreased lodging resistance was observed, leading to improved yield under eCO <sub>2</sub> .	Zhao et al., 2019
2.	Glycine max	<ul> <li>Seed fats and oils were increased under eCO<sub>2</sub>.</li> <li>eCO<sub>2</sub> improved drought resistance by enhancing photosynthesis and WUE.</li> </ul>	Li et al., 2018 Wang et al., 2018
3.	Cajanus cajan	<ul> <li>Higher root length area</li> <li>Enhanced photosynthesis, nodule number, nodule biomass, and yield.</li> <li>eCO<sub>2</sub> helps in mitigating drought with the help of</li> </ul>	Saha et al., 2012 Sreeharsha et al., 2015 Sreeharsha et al.,
		<ul> <li>increased antioxidant levels.</li> <li>❖ eCO₂ increased seed yields and enhanced seeds'</li> </ul>	2019 Unnikrishnan et al.,
		carbohydrate content and essential amino acids.	2021
4.	Jatropha curcas	<ul> <li>Sustained enhanced rate of photosynthesis under eCO<sub>2</sub>.</li> </ul>	Kumar et al., 2014
5.	Morus alba	<ul> <li>The yield was increased.</li> <li>Elevated CO<sub>2</sub> increased photosynthesis and biomass in coppice-grown mulberry.</li> </ul>	Sekhar et al., 2014  Liu et al., 2019
		<ul> <li>eCO2 improved drought resistance by improving PSII function.</li> </ul>	,
6.	Triticum durum	<ul> <li>Enhanced biomass and grain yield were observed under eCO<sub>2</sub>.</li> </ul>	Soba et al., 2019
		<ul> <li>Decreased N content, protein, and amino acid (glutamine) was observed in grains.</li> </ul>	
7.	Vicia faba	Under early growth stages, eCO <sub>2</sub> improved yield and N2 fixation by reducing soil water use.	Parvin et al., 2019

#### Drought - aftermath of climate change and its influence on the plant life cycle

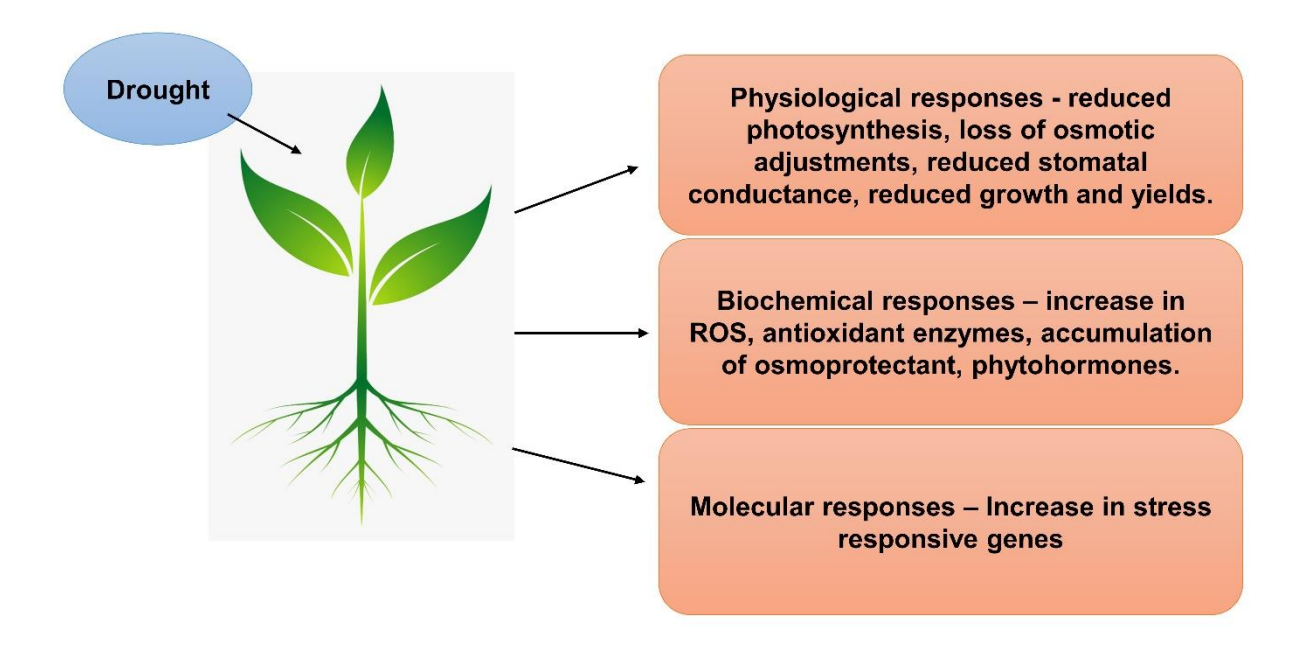
Increasing levels of CO<sub>2</sub> also bring about various other problems such as high temperatures and most importantly drought. Hence understanding the plant life cycle, mainly flowering processes under drought, is crucial for plant growth and yield. Drought can pose a big problem for crop survival and constrain agricultural productivity. It was shown that drought destroyed 9.42 and 3.72 million ha of cropland and 20.64 million tons of rainfed crops in Southeast Asia were lost due to drought between 2015 to 2019 (Venkatappa et al., 2021). According to a real-time droughtmonitoring platform named Drought Early Warning System (DEWS), 2021: Over a fifth of India's land area (21.06 percent) is facing drought-like conditions. Also, the new IPCC climate report 2022 shows that most countries fall into the varying category of drought risk index, with most parts of India under high and very high drought risk index (Fig. 3).

Fig. 3. Survey showing global drought risk index areas by IPCC climate report 2022.



The impact of drought depends on the ability of the plant species, developmental stage, and severity and duration of drought. Plants are either exposed to slow water shortage, which takes days to weeks or months, or rapid water shortage, which lasts hours to days (Nadeem et al., 2019). Plants respond to drought in either of the following ways drought escape, drought tolerance, and drought avoidance strategies (Nadeem et al., 2019). Plants usually use a drought escape strategy when subjected to a slow water shortage, which takes longer to recover. The fast and slow drought prompt varying responses in plants that are either long-term or short-term. Approaches to mitigate drought stress include water efficient practices, innovative breeding, and the development of traits for drought tolerance. Drought elicits various physiological, biochemical, and molecular responses in plants (Fig. 4). These responses include a reduction in photosynthesis, stomatal closure, reduction in flowering, and subsequent decrease in yield (Reddy et al., 2004, Nadeem et al., 2019). In response to these changes, plants invoke strategies for protection and survival. Hence, understanding the mechanisms of crop plants on how they perceive the drought and respond is extremely important to developing drought-tolerant crops.

Fig. 4. Various responses induced by drought stress in plants.



#### Physiological responses under drought

Some of the physiological responses elicited in plants under drought are reduced stomatal conductance, decreased photosynthesis, low shoot growth, and reduced yields. The signals corresponding to drought are foremost sensed by roots and sent to other plant parts through inter-organ signaling in the form of Ca<sup>2+</sup> waves, ROS signals, and electric currents (Kuromori et al., 2022). These signals cause stomatal closure to avoid water loss by transpiration to overcome the drought. To maintain leaf water potential, plant's first response under drought is stomatal closure (Laxa et al., 2019). An ionic imbalance of K<sup>+</sup>, Cl<sup>-</sup>, and H<sup>+</sup> is triggered by drought piloting turgor pressure in guard cells, causing stomatal closure (Mukarram et al., 2021). Another physiological response under drought is lower relative leaf water content (RWC). As the transpiration rate reduces, leaf water potential also decreases leading to reduced RWC. Reduced stomatal conductance and transpiration leads to high water use efficiency (WUE), a part of the drought avoidance/ tolerance strategy. Stomatal closure limits the CO<sub>2</sub> uptake, which causes limitations in Rubisco carboxylation, ultimately decreasing the photosynthetic rate. Drought was also shown to affect chlorophyll pigments in Nicotiana tabacum, subsequently affecting photosynthesis (Hu et al., 2018). Drought reduces chlorophyll concentration due to oxidative stress, degeneration, or photooxidation (Wahab et al., 2022). Reduced stomatal conductance and CO<sub>2</sub> uptake lead to the production of ROS as a part of the over-reduction of the electron transport system and carbon starvation in organelles (Laxa et al., 2019). ROS production also reduces photosynthesis, damaging the organelle membranes. Drought also downregulates noncyclic electron transport to match required NADPH production, thus reducing ATP synthesis and prompting a decline in photosynthesis (Farooq et al., 2009). It also affects complex systems like

photosystem I and II. Reduced photosynthesis then decreases carbohydrate synthesis, mainly starch, as the Calvin cycle and Ribulose phosphate are also affected under drought (Wahab et al., 2022). The lower carbohydrate synthesis leads to alteration in the partitioning of photoassimilates between the sink organs. Under drought, more photoassimilates are directed towards the root for enhanced root growth and distribution to overcome water limitations. However, this enhanced root growth causes limited shoot growth as the energy and resources are redirected towards roots instead of shoot, as recorded with reduced shoot growth, vegetative yield, and subsequently low reproductive yields.

#### Biochemical responses under drought

Drought-induced oxidative damage to proteins, lipids, and nucleic acids results in reactive oxygen species production in plants. Various antioxidant enzymes, osmoprotectants, and solutes are produced in plants to overcome ROS toxicity. Reactive oxygen species including superoxides, hydroxyl radicals, peroxides, singlet oxygen, and alpha oxygen, are produced in response to drought. In response to ROS, plants also produce osmoprotectants like sugar alcohols, amino acids including proline, glycine betaine, as well as several secondary metabolites. These act together in concomitance and initiates cross talk to maintain the ROS concentrations. Antioxidants are produced to combat ROS toxicity. They can be enzymatic or non-enzymatic. Some principal enzymatic antioxidants include catalase, superoxide dismutase, glutathione peroxidase, glutathione reductase, and peroxidase. On the other hand, non-enzymatic antioxidants include glutathione, ascorbic acid, carotenoids, and phenols (Mukarram et al., 2021). Drought increased phenolic content in tomato plants (Wahab et al., 2022).

Amino acids accumulate in response to abiotic stress, including drought, due to mechanisms like decreased protein synthesis, increased protein degradation, or enhanced biosynthesis (Yadav et al., 2019, Huang and Jander 2017). Proline regulates cellular redox status and acts as a ROS scavenger (Wahab et al., 2022). Sugars including soluble sugars, trehalose, and fructans, act as both osmotic agents and osmoprotectants (Mukarram et al., 2021). Trehalose is considered a carbon and energy source and can stabilize proteins and membranes under stress (Mukarram et al., 2021). Phytohormones are also known to play an essential role in sensing drought stress and mitigating the stress. ABA is known to act as the primary chemical messenger under drought (Mukarram et al., 2021). Drought activates specific responses by the ABA independent or ABA dependent signaling pathways. ABA signal transduction consists of ABA receptors (PYR/PYL/RCAR type), group A 2C type protein phosphatase (PP2C), and SnRK2 proteins. ABA accumulates as ABRE element of ABA-induced genes binds with bZip TFs (e.g., EMP1) (Mukarram et al., 2021, Zhang et al., 2006). Accumulated ABA binds to ABA receptors (PYR/PYL/RCAR), inactivating PP2C and releasing SnRK2. Then the activated SnRK2 initiates several responses including stomatal closure. Methyl jasmonate is also known to induce stomatal closure by increasing pH levels and ROS, similar to ABA (Kuromori et al., 2022). Independent of ABA, brassinosteroids induce osmoprotectant molecules by modulating hydrotropic responses in roots. These phytohormones then regulate the expression of stressresponsive genes to mitigate drought stress.

#### Molecular responses under drought

Drought induces various molecular responses, including the expression of drought responsive genes. Most of these drought responsive genes lead to the production of proteins involved in signaling and transcriptional regulation, including protein kinases, phosphatase, and transcription factors, proteins protecting cellular membranes like late embryogenesis abundant proteins (LEA), osmotin, and proteins involved in water and ion transport like aquaporins and sugar transporters (Fang and Xiong 2015, Kaur and Asthir 2017). Most drought responsive genes fall into two categories- ABA dependent or ABA independent based on their dependency on ABA for initiation (Kaur and Asthir 2017). Genes like ABI 1 and 3 are associated with ABA mediated response. Under drought, ABI 1 is upregulated while ABI 3 is downregulated (Pinheiro and Chaves 2011). Recent studies have shown AB1 3 is a part of drought recovery (Pinheiro and Chaves 2011). The expression of drought responsive genes is interconnected with biochemical and physiological responses, helping to overcome drought stress.

Drought affects various developmental processes including flowering. Usually, flowering gets accelerated during drought as part of a drought escape strategy wherein the plant tries to complete its lifecycle before the stress gets severe (Kooyers 2015). In some other cases, flowering is delayed as a part of the dehydration avoidance strategy of plants (Kooyers 2015). During the dehydration avoidance strategy, plants become dormant to avoid the effects of stress by pausing all critical developmental processes. Late flowering is correlated with high water use efficiency, usually observed in plants undergoing drought avoidance (Kooyers 2015). This accelerated or delayed flowering is due to the aftereffect of the drought stress responses in plants. Drought stress

accelerates flowering under long days but delays under short days in Arabidopsis (Riboni et al., 2013). Under short days, it is hypothesized that drought and ABA activate floral repressors inhibiting FT/TSF expression leading to delayed flowering (Riboni et al., 2013). However, different types of Arabidopsis ecotypes differ in their response to drought stress. Mild drought stress caused fitness costs in early flowering lines of Arabidopsis compared to the late ones (Kazan and Lyons 2015). However, on exposure to terminal drought, early flowering was correlated with higher biomass showing that these Arabidopsis ecotypes were adapted toward drought escape response (Kazan and Lyons 2015). The ecotypes that survive longer under drought are shown to have high WUE and are correlated with late flowering, a part of the drought avoidance strategy (Kenny et al., 2014). Phytohormones also play an essential role in floral transition under stress. Most of the hormones either accelerate or delay flowering depending on the plant species' severity of stress. Despite the varied flower patterns, yield is reduced under drought stress. Drought reduced yield by 60 % and seed weight by 25 % in common bean (Smith et al., 2019). The primary issue due to drought is the reduction in yield which affects agronomy detrimentally. Hence, it is crucial to study crop physiological responses under these climate-changing scenarios with particular reference to elevated CO<sub>2</sub> and drought.

#### Pigeonpea- Our model plant for the studies

We have chosen *Cajanus cajan* L. (Pigeonpea), a widely grown semi-arid legume crop, as our experimental plant because of its importance as a significant protein source and widely used fodder. Legume crops are valuable sources of dietary proteins for human consumption, synthesis of natural products, and cattle fodder (Maphosa and Jideani

2017). In addition to proteins, the legume seed is a primary source of starch, oil, and phytic acid with a significant inter-species variation (Dam et al., 2009). Elevated CO<sub>2</sub> has shown heightened vegetative growth in legumes (Irigoyen et al., 2014). Legumes can overcome photosynthetic acclimation, giving them advantages over other crops (Soares et al., 2019, Parvin et al., 2019, Sreeharsha et al., 2015). Most legumes showed increased seed yields: 32.7% in bean, 23.8-39.6% in soybean, 29% in pigeonpea and 18 % in pigeonpea (Soares et al., 2019, Sreeharsha et al., 2015, Unnikrishnan et al., 2021). Drought studies on legumes have shown reduced photosynthesis and lower yields. The impact of drought on low yields varied depending on the stage stress was subjected. Drought reduced yield by 46-71% in soybean when exposed at the reproductive phase and 73-82% at the pod set stage (Nadeem et al., 2019). Reduced yields were observed in legumes when drought was subjected at flowering, reproductive, and pod set/filling stages. Pigeonpea is majorly cultivated in Asia, Africa, South America, and the Caribbean islands. In Asia, pigeonpea is majorly grown in India, Myanmar, and Nepal. It is an important protein source (with 22% of the seed). It is majorly cultivated in rain-fed conditions, mainly in hot-humid climates. It is considered as one of the orphan crops that has not benefited from advanced research as it is grown in marginal parts of the world with low inputs. Of late, several studies reported enhanced C assimilation and yield as well as radiation use efficiency and canopy structure in pigeonpea under elevated CO<sub>2</sub> (Saha et al., 2012, Sreeharsha et al., 2015). Further, when grown under elevated CO<sub>2</sub>, pigeonpea was shown to withstand moderate oxidative stress by modulating the antioxidative metabolism (Sreeharsha et al., 2019). However, the molecular mechanisms behind the regulation of flowering,

including the changes in floral regulatory pathway genes, are not yet established in pigeonpea under elevated CO<sub>2</sub> and drought conditions.

Fig. 5. Pigeonpea flowering (left) and pigeonpea seeds (right).





Here we attempt to find answers to two significant questions which form the crux of this research-

- 1. How does flowering in pigeonpea get affected by two environmental variables: elevated CO<sub>2</sub> and drought?
- 2. How do these changes in floral timing translate into the reproductive status of pigeonpea?

Based on these questions, we have framed the following objectives for the present study.

## **Objectives**

• To decipher the physiological and molecular regulation of flowering under elevated CO<sub>2</sub> in pigeonpea.

- Sequential changes in the reproductive characteristics in pigeonpea grown under elevated CO<sub>2</sub>.
- To assess the regulation of flowering under drought stress in pigeonpea.
- To investigate the drought-induced changes in reproductive status and seed yields of pigeonpea.

## **CHAPTER 2**

# MATERIALS AND METHODS

#### MATERIALS AND METHODS

#### I. Experimental layout for elevated CO<sub>2</sub> studies

#### 1. Experimental facility

The elevated CO<sub>2</sub> studies were carried out in Open Top Chambers (OTC) (Neo genesis engineering, Mumbai, India) with 4×4×4m dimensions and octagonal shape. The OTCs were constructed in the Botanical gardens of the University of Hyderabad, India (17.3°10′ N and 78°23′E at an altitude of 542.6 m above sea level) (Fig. 6). Sensors are used to detect the temperature, humidity, and flow rate of the CO<sub>2</sub> injection in the OTCs. The software supervisory control and data acquisition (SCADA) was used to control the pumping of CO<sub>2</sub>. Commercial grade 100% CO<sub>2</sub> gas cylinders were used for the studies wherein gas was sent into chambers through manifold fitted with solenoid valve to regulate the gas supply. A NDIR (non-dispersive infra-red) based CO<sub>2</sub> analyser is used to monitor and analyze the CO<sub>2</sub> concentration in the OTCs. For elevated CO<sub>2</sub> conditions one chamber was supplied with elevated CO<sub>2</sub> (600 μmol mol<sup>-1</sup>), and the other OTC received ambient atmospheric CO<sub>2</sub> (400 μmol mol<sup>-1</sup>).

#### 2. Experimental layout and plant growth

Seeds of Pigeonpea variety ICP 15011 were procured from ICRISAT, Patancheru, Hyderabad. The experiment was carried out in the OTC chambers at the University of Hyderabad, India (17.3°10' N and 78°23'E at an altitude of 542.6 m above sea level) for two growing seasons of 4 months each. Seeds were surface sterilized with mercuric chloride (0.2%) for 5 min, washed, and soaked overnight. The seeds were kept for germination in germination trays for two days. The germinated seedlings were transferred to pots (of volume 11.0 L) for further growth in Open Top Chambers (OTC), wherein one chamber was supplied with elevated CO<sub>2</sub> (600

 $\mu$ mol/mol), and the other OTC received ambient atmospheric CO<sub>2</sub> (400  $\mu$ mol/mol) (Fig. 7). The experiments were designed with multiple sets of pots in ambient and elevated chambers, which acted as biological replicates. The plants are grown for the complete life cycle, and the materials required for various analyses were collected accordingly.

Fig. 6. a) Open top chambers (OTC) (4x4x4 m) for elevated CO<sub>2</sub> studies at the University of Hyderabad. b) Setup for CO<sub>2</sub> gas cylinders and pumping c) NDIR (non-dispersive infra-red) based CO<sub>2</sub> analyser and d) SCADA software controlling CO<sub>2</sub> pumping.

a)



b)



c)



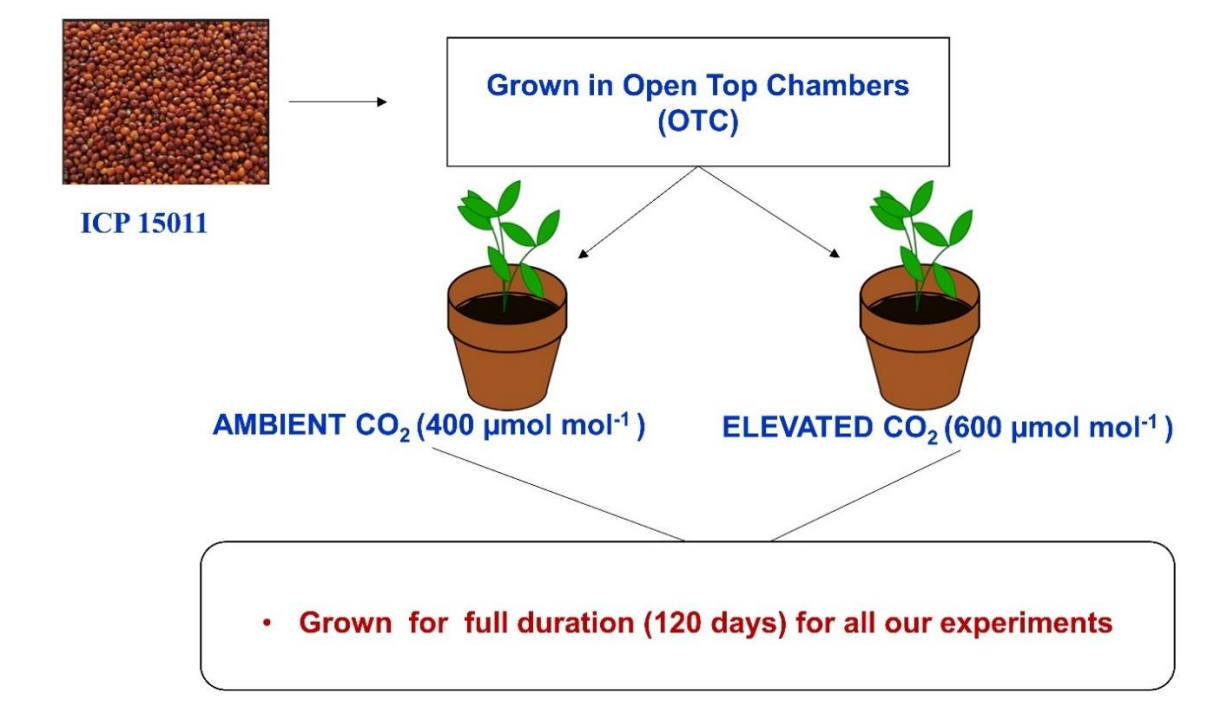
d)





**Materials and Methods** 

Fig. 7. Experimental layout for the elevated  $CO_2$  studies.



## 3. Photosynthetic characteristics of pigeonpea under elevated CO<sub>2</sub>

Photosynthetic efficiency was analyzed using portable Handy-PEA (Hansatech Instruments, King's Lynn, UK) in pigeonpea plants. Pigeonpea's life cycle is divided into preflowering, flowering, and postflowering phases. Chlorophyll a fluorescence was measured in pigeonpea at all 3 phases grown under ambient and elevated CO<sub>2</sub> conditions. The upper canopy leaves at the 3<sup>rd</sup> or 4<sup>th</sup> position of the apex were used for the measurements. The leaves were then dark adapted for 30 min by using leaf clips, and the fluorescence intensities were recorded after illuminating with a saturating light intensity of 3000 µmol m<sup>-2</sup> s<sup>-1</sup> (an excitation intensity sufficient to ensure closure of all PSII reaction centers) provided by an array of three light emitting diodes, for 1s. The fluorescence intensities at 50 µs (Fo), 150 μs(L), 300 μs (K), 2 ms (J), 30 ms (I), and 500 ms to 1 s (P or FM) were recorded and used for all analyses. Fv/Fm estimates the efficiency of PSII, which is calculated by Fv/Fm = (Fm-Fo)/Fm. Raw (without normalization) OJIP chla fluorescence transient (Ft) curves were transferred with WINPEA 32 and analyzed with Biolyzer. JIP test parameters (Table 2) were calculated accordingly from OJIP chlorophyll a fluorescence transient to provide structural and functional information of PSII in ambient and elevated CO<sub>2</sub> conditions.

Table. 2 Selected JIP parameters and their descriptions.

JIP Parameters	Description
Fo	Minimum fluorescence value after the onset of actinic illumination at $50\mu s$
Fp=Fm	Maximum fluorescence intensity under saturating illumination at P-step
Fv	Variable chlorophyll fluorescence
DIo/RC	Dissipated energy flux per RC
RC/CSm	Density of active reaction centers per cross-section (CS)
ABS/CSm	Absorption flux per excited CS
ETo/CSm	Electron transport flux per excited CS
DIo/CSm	Dissipated energy flux per excited CS
PI(ABS)	Performance index on absorption basis

#### 4. Plant material for ambient and elevated CO<sub>2</sub> studies

To study the effect of elevated CO<sub>2</sub> on the growth of pigeonpea, especially floral ontogeny, leaf samples were collected from 3 different time points in the pigeonpea life cycle grown in ambient and elevated CO<sub>2</sub> conditions. The stages were carefully chosen based on the age of the pigeonpea plant, i.e., days after emergence (DAE) - 35 DAE (juvenile phase), 55 DAE (transition phase), and 65 DAE (reproductive phase). The phases were decided based on the anthesis observed in the ambient CO<sub>2</sub>-grown plant. Further, the pigeonpea inflorescence was collected to check the expression patterns of ABCE genes in both ambient and elevated CO<sub>2</sub>-grown plants. The reproductive characteristics of pigeonpea under elevated CO<sub>2</sub> were studied and characterized with the help of mature, dry seeds collected after 120 days.

#### 5. Foliar sugar analysis by HPLC

The leaf samples were dried and used for analyzing free sugars by HPLC. 100 mg of the sample was homogenized in 1 mL of Milli-Q water and vortexed for 15 min (Giannoccaro et al.,2006). The sample was centrifuged at 13,000 rpm at room

temperature for 10 min, and 500 μl supernatant was taken to which 1.5 ml 95% acetonitrile was added and mixed for 30 min at room temperature rotor spin. The sample was centrifuged at 13,000 rpm for 10 minutes at room temperature, and the supernatant was collected. The supernatant was evaporated in a dry bath at 95 °C, and the residue obtained was dissolved in 1 mL milliQ water. This extract was filtered through 0.22 μm filter paper with syringe filters. The filtrate was used to quantify free sugars through reverse phase HPLC using the NH<sub>2</sub> column (Shodex-Asahipak NH<sub>2</sub> P-50-4E). Acetonitrile and water in 70:30 ratios were used as the mobile phase; the flow rate was 1 mL/min, and peaks were detected at an absorbance of 190 nm using a PDA detector. Standards of sugars (20 mg/ml) (Sucrose, glucose, and fructose) were prepared using Himedia and used for subsequent quantification.

### 6. qRT- PCR of floral regulatory and ABCE genes

Total RNA was extracted from the samples (leaf, inflorescence) using Spectrum Plant Total RNA isolation kit (Sigma, USA). 1 μg of RNA was used for cDNA synthesis by Revert aid first-strand cDNA synthesis kit (Takara cDNA synthesis kit, Japan). cDNA for miRNA was synthesized by miRNA cDNA synthesis kit (Takara, Japan) using 1 μg of RNA from the total RNA initially isolated. Expression of mRNA for genes involved in flowering (Table 3) was measured by qRT – PCR in Eppendorf thermal cycler using SYBR FAST qPCR universal master mix (2X) (KAPA Biosystems, USA). Each reaction contained 1 μl of the first-strand cDNA as the template in a 10 μl reaction mixture. The amplification program was performed at 95° C for 2 min, followed by 95° C for 20 s and Tm for 20 s (40 cycles).

The relative expression was calculated using the formula  $2^{-\Delta\Delta Ct}$  (Livak and Schmittgen. 2001), with actin as a housekeeping gene for data normalization.

Table. 3 List of primers used for the expression of flowering regulatory gene transcripts.

Genes	Forward Primer	Reverse Primer
GI	TCAGCCTCACCAACAAAAGC	TCCATCAACCAGCATCCCAT
CO	GTCGTCGATGGAGGTAGGAG	TGATCCTTGGCCTCGTTTCA
FT	GTGTTGGCGGAGATGACTTC	CATCCAGGAGCATACACCCT
TOC1	GGATAGGGGAGTCATCAGCC	AGTGCTGCTGGGTAAGTCAT
CCA1	GCTGCTACATTTTGGCCGTA	GGAGCACACAAAGGAAGCAA
SOC1	AGAAGGTTTGGGGTCTTGCT	TTGTTGTTGGCTGTGGATCG
SPL	GCCCTGTGAAGATGCTGATG	AGCAAACATCCTCCTCCACA
CWIN	TAGGAAGTGGCATGTGGGAG	GCATCCTTGGCAGCATTGTA
PRR5	TGATTCAGTTGGCATGGTGT	TCGCTTGCAGAATTGTCATC
CS	TTGTTCTCAGCGAGGTCCTT	GGGTCAACCCAAGTCAAAGA
ZTL	GGGTTCTACAGCACCTCCAA	AGAATGGTTTGCCAGAATGC
TPS6	CACCACAGATTCACCACCTG	AGCACCCAGCAATAACAACC
AP1	GGTTTCTCAAGGGGGAGTTC	GCAGGTTTCATCTCGCTCTC
AP2	GCAAGTGGTTAGAGAGAGAGAG	TGAAGAGAGAGAGGTAGGTG
AP3	TCACAGGGAAATTGGACCAT	CTGCGGGTACGAATTTGTTT
PST	CAAGGTTGTTCGTGAGCGTA	CATTAGGATGGCTTGGCTGT
AGA	GGAGATAGACTTGCACAACA	AAGGCAAACTACAAGTAGCA
SEP	GAACGCCATCTTGGAGACAT	TTCTGCCGGGTAATCCATAG

### 7. Quantification of miRNA transcripts

To check the expression levels of miR156 and miR172, a qRT analysis was done. The 5'primers for the miRNAs were generated, and 3'primers provided in the Mir-X for kit (Takara, Japan) were used the analysis (miR156-TGACAGAAGAGAGTGAGCACA, miR172-AGAATCTTGATGATGCTGCAT). SYBR FAST qPCR universal master mix (2X) (KAPA Biosystems, USA) was used with minor modifications to the protocol. The relative expression was calculated using the formula  $2^{-\Delta\Delta Ct}$  (Livak and Schmittgen. 2001), with U6 as the housekeeping gene for data normalization.

#### 8. Growth and yield measurements

The growth of plants was measured by recording total dry weight, the number of nodes, and height of the plants. Mature seeds were collected from elevated and ambient CO<sub>2</sub> grown plants after 120 days, and parameters including pod weight, seed weight, and weight per 100 seeds were measured for the seeds collected from ambient and elevated CO<sub>2</sub> grown pigeonpea plants.

#### 9. Seed biochemical analysis

The seed samples were dried to analyze reducing sugars, free sugars, starch, and total carbohydrate. The sample was homogenized in 80% hot ethanol, centrifuged, and the supernatant was used to estimate soluble sugars by the DNS method (Miller 1972). The residue was dissolved in 5 mL of water and extracted using 6.5 mL (52%) perchloric acid, followed by centrifugation. The supernatant was used to estimate starch by anthrone method (Hedge and Hofreiter 1962). Free sugars were extracted by homogenizing 100 mg of seed sample in 1 mL of milliQ water and vortexed for 15 min (Giannoccaro et al., 2006). The sample was centrifuged at 13,000 rpm for 10 min at room temperature, and 500 µl of supernatant was taken to which 700 µl of 95% acetonitrile was added and mixed for 30 min at room temperature in a rotor spin. The sample was centrifuged at 13,000 rpm for 10 minutes at room temperature and collected the supernatant. The supernatant was evaporated in the dry bath at 95 °C, and the residue was dissolved in 1 mL milliQ water. This extract was filtered through 0.22 µm filter paper with the help of syringe filters. The filtrate was used to quantify free sugars, mainly sucrose, through reverse phase HPLC using the NH<sub>2</sub> column (Shodex-Asahipak NH<sub>2</sub> P-50-4E). Acetonitrile and water in 70:30 ratios were used as the mobile phase; the flow rate was 1 ml/min,

and peaks were detected at an absorbance of 190 nm using a PDA detector. Standards of sugars (20 mg/ml) (sucrose, glucose, and fructose) were prepared from Himedia to prepare a standard graph and used for all subsequent quantifications. The total nitrogen content, protein content, and ash content of seeds were estimated by the Dumas method (McGill and Figueiredo 1993).

#### 10. GC-MS analysis of metabolites

The metabolite extraction for GC MS was done according to standard protocol (Singha et al., 2019). The seed sample (100 mg) was ground to powder using liquid nitrogen and was used for metabolite extraction. The sample extraction was done in 1.4 mL of precooled methanol. The mixture was then homogenized for 10 sec by vortexing, and then 60 µL of ribitol (0.2mg mL<sup>-1</sup>) internal standard was added to the mixture, followed by vortexing again for 10 sec. The mixture was ultrasonicated for 10 min and centrifuged at 11,000 g for 10 min. The supernatant was mixed with 750 µL of precooled chloroform and 1.5 mL of precooled water, followed by centrifugation at 2200 g for 15 min. The supernatant from the upper phase (150  $\mu$ L) was dried under a vacuum. The dried extract was derivatized by dissolving in 20 µl of methoxyamine hydrochloride pyridine solution (40 mg/mL) and incubated at 30°C with shaking for 90 min. 80 μL of N-methyl-N-(trimethylsilyl) trifluoroacetamide solution is mixed with the sample, followed by 30 min incubation at 37°C with shaking. This derivatized sample was centrifuged for 8 min at 20,000 g, and the supernatant obtained was used for GC MS analysis, wherein GC coupled with LECO Pegasus R 4D GC-TOF-MS (Agilent 6890, USA) was used for the analysis. The metabolites were annotated by comparing their retention time and mass spectra against the GMD database (Kopka et al., 2005). Metabolites crossing the match

factor of 700 were used for quantification. The normalization of the data was done using ribitol, and the concentration of the metabolite was calculated with respect to the known concentration of standard ribitol (Singha et al., 2019). Statistical analysis including PCA and correlation analyses were done with aid of online software Metaboanalyst 5.0.

#### 11. Label-free quantification (LFQ) of seed protein

The seed samples were collected randomly from three different pots and seed protein was then extracted from 500 mg of seed sample using 2 ml of extraction buffer (25 mM Tris HCl, 15 mM MgCl<sub>2</sub>, 15 mM EGTA, 75 mM NaCl, 2 mM 1,4-DTT, 0.1% nonidet P-40, 1 mM NaF, 1 mM PMSF). The extract was centrifuged at 10,000 rpm for 15 min at 4°C, and the supernatant was collected. 0.2 mL of supernatant was aliquoted into tubes, and 4 volumes of ice-cold 0.1 M ammonium bicarbonate in methanol were added and kept for protein precipitation at -20°C overnight. The incubated protein was precipitated by centrifuging at 10,000 rpm at 0°C. The pellet was retained and washed 3 times with methanol and 2 times with acetone, followed by drying, and was used for LFQ. An equimolar concentration of 100 µg from the pooled protein sample is taken for LC quantification, wherein technical repetitions were performed to arrive at valid conclusions about fold change. The sample was treated with 100 mM DTT for 1 hr at 95°C followed by 250 mM IDA at room temperature for 45 min at dark, digested with trypsin, and incubated overnight at 37°C. The digested peptides were extracted in 0.1% formic acid and incubated at 37°C for 45 min, followed by centrifugation at 10,000 g. The supernatant was collected, vacuum dried, and dissolved in 20 µL of 0.1% formic acid in water. 10 µL of volume was used for the separation of peptides. The liquid

chromatography (LC) was performed on the ACQUITY UPLC system (Waters, UK) with a 75 um x150 mm x1.7 um BEH C18 column (Waters, UK). The sample (10  $\mu$ l) was injected into the column, and the separated peptides were directed to Waters Synapt G2 Q-TOF instrument for MS and MS/MS analysis with 60 min program for separation using the following buffer A: 0.1% formic acid in water and buffer B: 0.1% formic acid in acetonitrile with a program of gradient elution. The raw data acquired from the instrument was processed using Protein Lynx Global Server (PLGS) software 3.0.2, which performed a Data Processing and Database search. 1% FDR was used for analysis. The ratio  $\leq$  0.5 was considered as significantly downregulated and  $\geq$  2 as significantly upregulated. The gene ontology for the proteins was assigned with Uniprot.

#### 12. Statistical analysis

All experiments were performed by randomly collecting samples from ambient and elevated  $CO_2$  grown plants. Each experiment was done in triplicates, and the data were represented as mean  $\pm$  SD (n=3). Data was checked for statistical differences using t-test (\* p  $\leq$  0.05, \*\* p  $\leq$  0.01, \*\*\* p  $\leq$  0.001) using software Sigmaplot 11.0. Pearson correlation analysis and subsequent network were constructed for the flowering genes using OriginPro, where the -1 to 1 range of correlation was considered (Table 4).

Table.4 Pearson correlation coefficient and their correlation significance levels.

S.NO	Pearson correlation coefficient	The significance level of correlation
1.	> 0.5	Strong positive correlation
2.	0-0.5	Moderate positive correlation
3.	0	No correlation
4.	0- (-0.5)	Moderate negative correlation
5.	< -0.5	Strong negative correlation

### II. Experimental layout for drought studies

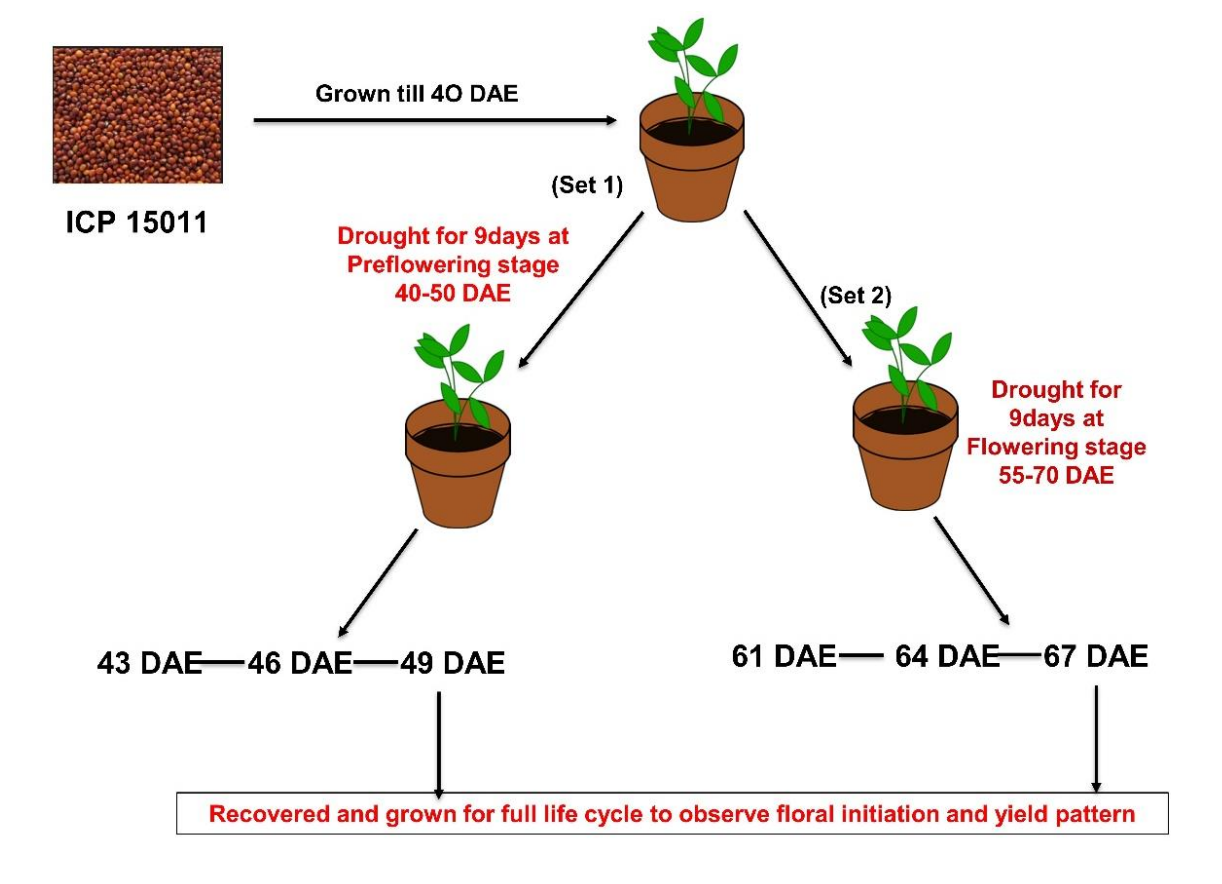
#### 1. Plant growth for drought studies

Pigeonpea seeds (ICP 15011; ICRISAT Patancheru) with 120 days of the life cycle were used for the study. All experiments were carried out at the University of Hyderabad, India (17.3°10' N and 78°23'E at an altitude of 542.6 m above sea level) for a growing season of 4 months. The seeds were surface sterilized with mercuric chloride (0.2% for 5 min), soaked overnight and germinated in germination trays for 2 days. Later, they are transferred to pots, grown up to 40 days after emergence (DAE), and divided into two sets for further experiments. Drought was subjected to pigeonpea at the pre-flowering stage (PFSS), i.e., 40 -50 DAE for 9 days, and recovered on the 10th day after stress to observe the flowering pattern and yield forming the first set of experiments. For the second set of experiments, drought was given during the flowering stage (FSS), i.e., 55-70 DAE starting from 59 DAE for 9 days, recovered on the 10th day and allowed further to grow for an entire life cycle to observe floral initiation and yield pattern.



**Materials and Methods** 

Fig. 8. Experimental layout for drought studies under different developmental stages in pigeonpea.



### 2. Measurement of photosynthetic parameters

Portable Infra-red gas analyzer (IRGA) (LI 6400) was used for the measurement of leaf gas exchange parameters, including photosynthetic assimilation rate (A), transpiration (E), stomatal conductance (gs), internal CO<sub>2</sub> concentration (Ci) and water use efficiency (WUE). Water use efficiency was calculated by the formula of photosynthetic assimilation rate (A)/ transpiration (E). The parameters were measured at a saturating photosynthetically active radiation (PAR) of 1600 μmol m<sup>-2</sup> s<sup>-1</sup> with an LED light source (6400-02 LED) connected to a leaf chamber along with air temperature at 25°-26° C, CO<sub>2</sub> concentrations at 400 μmol mol<sup>-1</sup> and relative humidity at 55-60 %. The upper canopy leaves at the 3<sup>rd</sup> or 4<sup>th</sup> positions from the apex were relatively used for the measurements. Leaves were enclosed in a leaf chamber, allowing for acclimation for 2 min after stabilization of readings were recorded. All measurements were done during the morning hours of 9:00 to 11:00 hours after a 3-day interval of drought stress for 10 days.

#### 3. Physiological parameters under drought

Leaf relative water content (LRWC) and leaf moisture content were used to calculate the plant water status. The formula to calculate LRWC: LRWC (%) = (FW–DW)/(TW-DW)\*100, where FW is the fresh weight of leaves collected from three different plants, TW is the turgid weight of the leaves after they have been rehydrated in double distilled water for 24 hr at 4°C, DW is the dry weight of the leaves once they have been dehydrated in the oven drying at 80°C for 24 hr. Leaf moisture content (LMC %) was also calculated by LMC = (FW-DW)/FW\*100, by using the above mentioned parameters.

#### 4. Estimating Primary metabolites by reverse phase HPLC

Free sugars were analyzed in leaf samples and analyzed by reverse-phase HPLC using the NH2 column (Shodex-Asahipak NH2 P-50-4E) (Giannoccaro et al., 2006). Free amino acids in leaves were analyzed by reverse-phase HPLC using the C18 column, according to Sreeharsha et al. (2019). Amino acids were also analyzed by reverse phase HPLC in seed samples collected from control and drought recovered plants to check for drought-induced changes in nutritional and metabolite levels in seeds (Sreeharsha et al., 2019). The sample (0.5 g) was extracted in 2ml of cold 5% acetic acid for 1hr with gentle agitation on the shaker at room temperature. Homogenates were centrifuged at 4000 rpm for 15min, and the supernatant obtained was filtered through 0.22µm filter paper. The filtrate was then subjected to free amino acid analysis. The amino acids were analyzed by reverse phase HPLC with precolumn derivatization using OPA and FMOC. OPA derivatization was used for primary amino acids, and FMOC can derivatize only secondary amino acids. OPA reagent was prepared by dissolving 90 mg sodium tetraborate in 4.5 ml water by gentle warming; 66 mg of N-Acetyl-L-Cysteine and 27 mg of OPA dissolved in 0.5 ml methanol was added to make the reagent. FMOC was prepared by dissolving 50 mg of FMOC in 20 ml acetonitrile. C18 column (Spincho-Tech, 4.5 mM x 150 mM, 5 μM) was used to separate amino acids. The program used for the separation consists of a binary gradient with solvent A consisting of phosphate buffer (pH 6.3), methanol, and acetonitrile in a 76.5: 20:3.5 ratio and solvent B consisting of methanol, acetonitrile, and milliQ water in 45: 45:10 ratio. The flow rate was set to 1.2 ml per minute for a run time of 26 min with 0 % of B (0 - 18.1min), 57 % B

(18.1 - 18.6 min), 100 % B (18.6 - 22.3 min), and 100 % A (22.3 - 26 min). PDA detector was used for detection, and amino acids were detected at an absorbance of 262 and 334 nm. Standards of 14 amino acids (1 mg/ml) (Asp, Glu, Ser, His, Arg, Ala, Gly, Val, Met, Trp, Isoleu, Phe, Leu, and Pro) were prepared from Himedia and used for the quantification of amino acids.

#### 5. Hormone analysis by reverse phase HPLC

The contents of gibberellin (GA3), auxin (IAA, IBA), and abscisic acid were also analyzed in leaf samples. Hormones were extracted as described by Pan et al. (2010) with few modifications. 50 mg of ground tissue was extracted with 500 µl of extraction solvent of 2 propanol: miliQ water: Hcl (2: 1: 0.002) and mixed in a thermomixer at 4° C, 100 rpm for 30 min. Then 1 ml of dichloromethane was added to the mixture and repeated the previous step. After 30 min of thermomixer, the extract was centrifuged at 13,000 g for 5 min, and 900 µl of lower phase was transferred to a fresh tube followed by speed vac at zero temperature for 10 min. The concentrated sample was then redissolved in 0.1 ml of methanol and stored at -20° C till further analysis. The hormones were analyzed by reverse-phase HPLC using the C18 column (Zhu et al., 2020). The detection was done by binary gradient with solvent A comprising of water: glacial acetic acid (99.9: 0.1) and solvent B with 100 % methanol. The program was 0-40 min with 20-70 % B, 40-50 min with 70-95 % B, and 50-54 min with 95 % B at a flow rate of 0.9 ml/min and detected at an absorbance of 220 – 290 nm. Hormone standards were prepared from Himedia, with various concentrations of the standards were used to prepare a standard graph for quantifying hormones.

### 6. Transcript analysis of genes involved in flowering under drought

The transcript patterns of the floral regulatory genes involved in various pathways were analyzed in pigeonpea leaf, meristem, and inflorescence samples using qRT-PCR (Table 5). Total RNA was extracted from the samples collected using Spectrum Plant Total RNA isolation kit (Sigma, USA). 1 μg of RNA was used for cDNA synthesis by Revert aid first-strand cDNA synthesis kit (Takara cDNA synthesis kit, Japan). cDNA for miRNA was synthesized by miRNA cDNA synthesis kit (Takara, Japan) using 1 μg of RNA from the total RNA initially isolated. qRT – PCR was done in Eppendorf thermal cycler using SYBR FAST qPCR universal master mix (2X) (Thermo Fisher Scientific). Each reaction contained 1 μl of the first-strand cDNA as the template in a 10 μl reaction mixture. The amplification program was performed at 95° C for 10 min, followed by 95° C for 20 s and Tm for 20 s (40 cycles). The expression data were normalized to housekeeping gene actin. The relative fold change was estimated using the double normalization approach (Livak and Schmittgen. 2001).

Table. 5 List of primers used for the expression of flowering, sugar signaling, and phytohormone gene transcripts.

Genes	Forward Primer	Reverse Primer
GI	TCAGCCTCACCAACAAAAGC	TCCATCAACCAGCATCCCAT
CO	GTCGTCGATGGAGGTAGGAG	TGATCCTTGGCCTCGTTTCA
FT	GTGTTGGCGGAGATGACTTC	CATCCAGGAGCATACACCCT
TOC1	GGATAGGGGAGTCATCAGCC	AGTGCTGCTGGGTAAGTCAT
CCA1	GCTGCTACATTTTGGCCGTA	GGAGCACACAAAGGAAGCAA
SOC1	AGAAGGTTTGGGGTCTTGCT	TTGTTGTTGGCTGTGGATCG
SPL	GCCCTGTGAAGATGCTGATG	AGCAAACATCCTCCTCCACA
CWIN	TAGGAAGTGGCATGTGGGAG	GCATCCTTGGCAGCATTGTA
PRR5	TGATTCAGTTGGCATGGTGT	TCGCTTGCAGAATTGTCATC
CS	TTGTTCTCAGCGAGGTCCTT	GGGTCAACCCAAGTCAAAGA
ZTL	GGGTTCTACAGCACCTCCAA	AGAATGGTTTGCCAGAATGC
TPS6	CACCACAGATTCACCACCTG	AGCACCCAGCAATAACAACC
AP1	GGTTTCTCAAGGGGGAGTTC	GCAGGTTTCATCTCGCTCTC
AP2	GCAAGTGGTTAGAGAGAGAGAG	TGAAGAGAGAGAGGTAGGTG
AP3	TCACAGGGAAATTGGACCAT	CTGCGGGTACGAATTTGTTT
PST	CAAGGTTGTTCGTGAGCGTA	CATTAGGATGGCTTGGCTGT
AGA	GGAGATAGACTTGCACAACA	AAGGCAAACTACAAGTAGCA
SEP	GAACGCCATCTTGGAGACAT	TTCTGCCGGGTAATCCATAG
SPS	GGCACTAAGGTATCTGTTCG	CTGGACCTCTGAGTAACTCTTC
SUT	TCGACAATACACCCTACTCC	GTCCACTTATCACAGACACCAC
ARF	CCTATTGCATCAGGACCTTC	GCCACTTCTAGCATAACCAG
IAA	GAGAGGGTTCTCTGAGACAGT	TCCTGTATGACCTCACTGGT
GID	GAATCTATCGTCCTGCTGAG	GCCTATAGTTCACTGACACC
TPS9	AACCACAGGGTGTGAGCAAG	AACGGTGCAGGCGAATACTT
GA20OX	GACCATTCTTCACCAGGATC	GACTAACCACCTTATCACCC
BRZ	GAGTGTGACGAGTCTGATAG	GACTTCATGAATCCTCTCCC
AAO	GAATCTATCGTCCTGCTGAG	GCCTATAGTTCACTGACACC
SPA	AAAAAGGCCAGGAACAACCT	CCCGATCAAAGCTCAGAGAG
COP1	AAGGCCACTGCTGTTCTTGT	CGCAAGCAAAAAGTTGATGA
SnRK	CATAGTAGAGAAGGGTAGGCTG	CTCTGGAGCTGCATAGTTAG
TOE3	AGCGAGTTAGAGGCTGCAAG	TACAAGCTGGGCTCGAAGTT
LFY	CAACAACCTCCTCTCCACGG	TCCCTTCATCATTCTCTTCCCCT

### 7. Reproductive parameters under drought

The reproductive parameters, including the days to anthesis, number of inflorescences, number of pods, total yield, pod weight, seed weight, and weight per 100 seeds, were measured from control and drought recovered plants. Pearson correlation analysis among these reproductive parameters was done to understand the effect of drought on the reproductive phenology of pigeonpea.

#### 8. Free amino acid analysis using HPLC

Seeds collected from drought recovered plants, i.e., both from preflowering stage stress recovered plants and flowering stage stress recovered plants, were analyzed for amino acids (Sreeharsa et al., 2019). The sample (0.5 g) was extracted in 2ml of cold 5% acetic acid for 1hr with gentle agitation on the shaker at room temperature. Homogenates were centrifuged at 4000 rpm for 15min, and the supernatant obtained was filtered through 0.22µm filter paper. The filtrate was then subjected to free amino acid analysis. The amino acids were analyzed by reverse phase HPLC with precolumn derivatization using OPA and FMOC. OPA derivatization was used for primary amino acids, and FMOC can derivatize only secondary amino acids. OPA reagent is prepared by dissolving 90 mg sodium tetraborate in 4.5 ml water by gentle warming; 66 mg of N-Acetyl-L-Cysteine and 27 mg of OPA dissolved in 0.5 ml methanol was added to make the reagent. FMOC was prepared by dissolving 50 mg of FMOC in 20 ml acetonitrile. C18 column (Spincho-Tech, 4.5 mM x 150 mM, 5 μM) was used to separate amino acids. The program used for the separation consists of a binary gradient with solvent A consisting of phosphate buffer (pH 6.3), methanol, and acetonitrile in a 76.5: 20:3.5 ratio and solvent B consisting of methanol, acetonitrile, and milliQ water in 45: 45:10 ratio. The flow rate was set to

1.2 ml per minute for a run time of 26 min with 0 % of B (0 - 18.1min), 57 % B (18.1 - 18.6 min), 100 % B (18.6 - 22.3 min), and 100 % A (22.3 - 26 min). PDA detector was used for detection of amino acids at an absorbance of 262 and 334 nm. Standards of 14 amino acids (1 mg/ml) (Asp, Glu, Ser, His, Arg, Ala, Gly, Val, Met, Trp, Isoleu, Phe, Leu, and Pro) were prepared from Himedia and used for the quantification of amino acids.

### 9. Correlation and statistical analysis

Pearson correlation analysis was done to check the correlation between the metabolites and hormones which is represented as a heatmap by using OriginPro software. The statistical differences were calculated by one-way ANOVA at \*\*\*p < 0.001, \*\*p < 0.01 and \*p < 0.5 between control and treated samples using Sigmaplot 11.0 software.

# **CHAPTER 3**

# **RESULTS**

#### **RESULTS**

Objective 1 - To decipher the physiological and molecular regulation of flowering under elevated CO<sub>2</sub> in pigeonpea.

#### A. Growth and physiology of pigeonpea under elevated CO<sub>2</sub>

Pigeonpea showed a positive growth response when grown under elevated CO<sub>2</sub>. Pigeonpea was grown for 120 days (entire life cycle). Growth characteristics like the height of the plant (5.9 %) and the number of nodes (40 %) were increased in plants under elevated CO<sub>2</sub> (Fig. 9). However, delayed flowering was observed in pigeonpea under elevated CO<sub>2</sub> by 9 days compared to its ambient counterpart. Nevertheless, delayed flowering did not decrease the inflorescence number; on the contrary, elevated grown pigeonpea had a higher inflorescence.

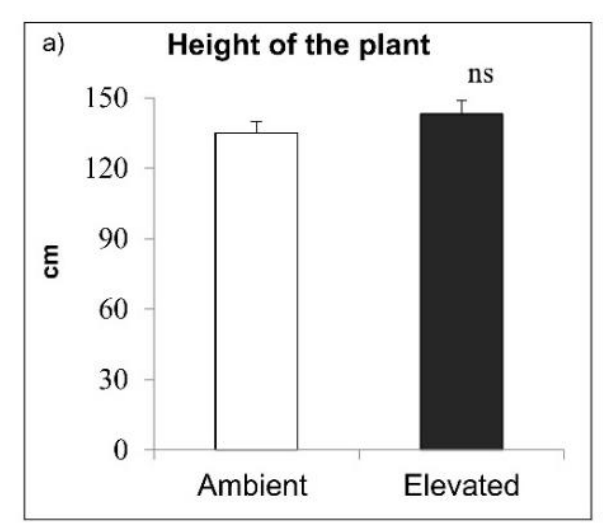
## B. Photosynthetic parameters under elevated CO<sub>2</sub>

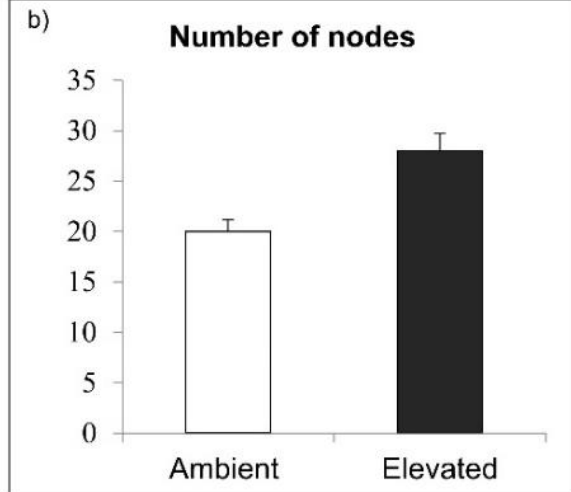
Pigeonpea grown under elevated CO<sub>2</sub> showed higher photosynthetic efficiency, which can be observed by higher Fv/Fm at all developmental stages of the plant compared to ambient-grown pigeonpea. As pigeonpea matured, Fv/Fm increased in elevated CO<sub>2</sub> grown plants, with the highest being at the flowering and postflowering phase with a ratio of 0.824, 0.826 respectively (Fig. 10 a). An increase in Fm was observed throughout the pigeonpea lifecycle under elevated CO<sub>2</sub>, causing a drop in Fo. Fm was highest during the flowering phase in elevated pigeonpea compared to other phases (Fig. 10 b). Fo decreased at all phases in pigeonpea grown under elevated CO<sub>2</sub> (Fig. 10 c). Among other photosynthetic parameters observed, the performance index that describes the overall efficiency of PSII, i.e., PI (abs), showed a significant increase in plants grown under elevated CO<sub>2</sub>, confirming that elevated CO<sub>2</sub> positively influenced photosynthesis in

Chapter 3 Results

pigeonpea. Elevated CO<sub>2</sub> grown pigeonpea showed a 74% increased performance index in the postflowering phase compared to ambient plants (Table 6). PI (abs) increased as pigeonpea matured in elevated CO<sub>2</sub> conditions. Photosynthetic parameters like RC/CSm, ABS/CSm, and ETo/CSm were increased in elevated CO<sub>2</sub> grown pigeonpea (Table 6). These parameters, mainly RC/CSm, were highest in the post-flowering phase (32.8%) in elevated CO<sub>2</sub> grown pigeonpea but were lower in the flowering phase compared to the preflowering phase. On the other hand, parameters like DIo/RC, DIo/CSm, ETo/RC, ABS/RC, and TRo/RC were downregulated in elevated CO<sub>2</sub> grown pigeonpea at all developmental phases (Table 6).

Fig. 9. Growth characteristics of pigeonpea under elevated  $CO_2$  a) height of the plant, b) the number of nodes, and c) days to anthesis. Values are given as mean  $\pm$  SD (n=3), and ns denotes no significance.





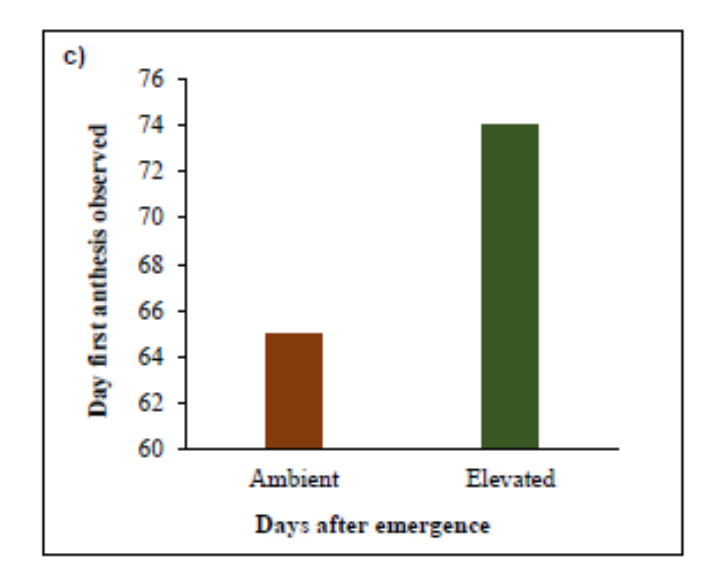
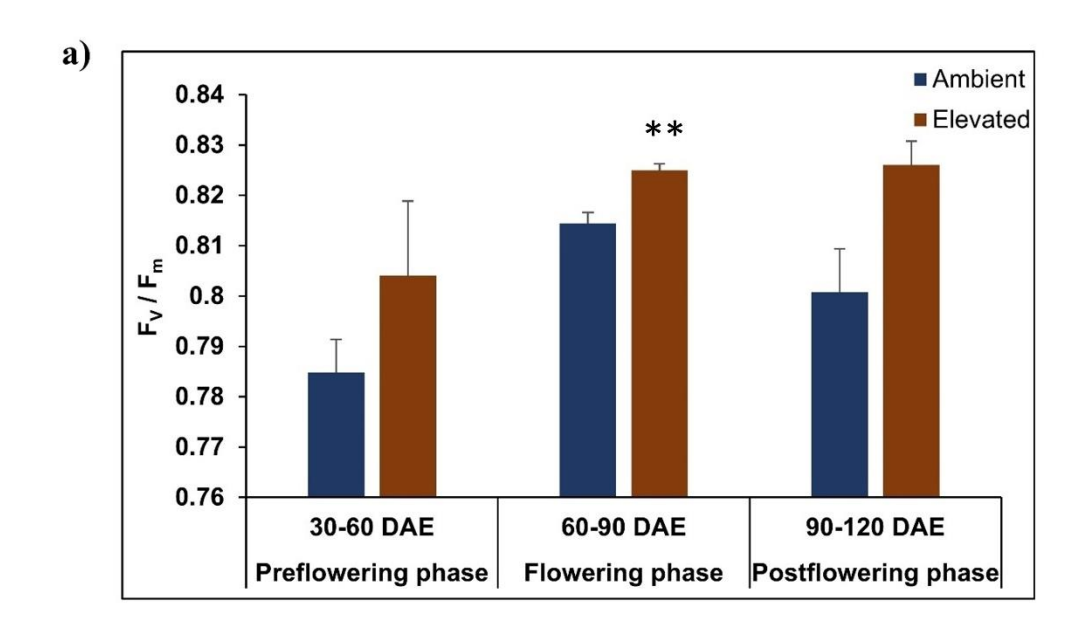
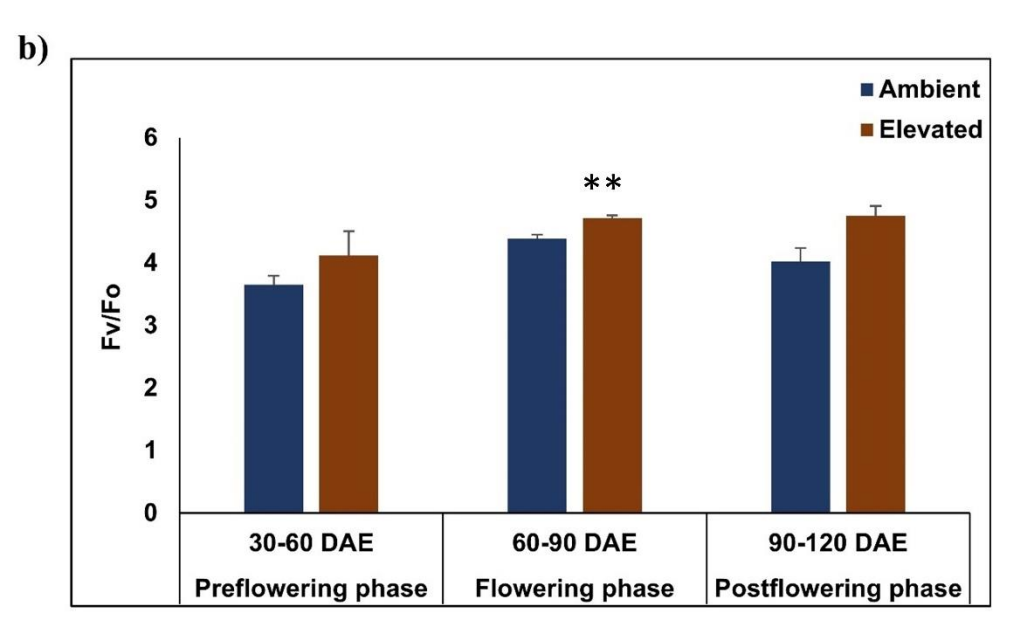
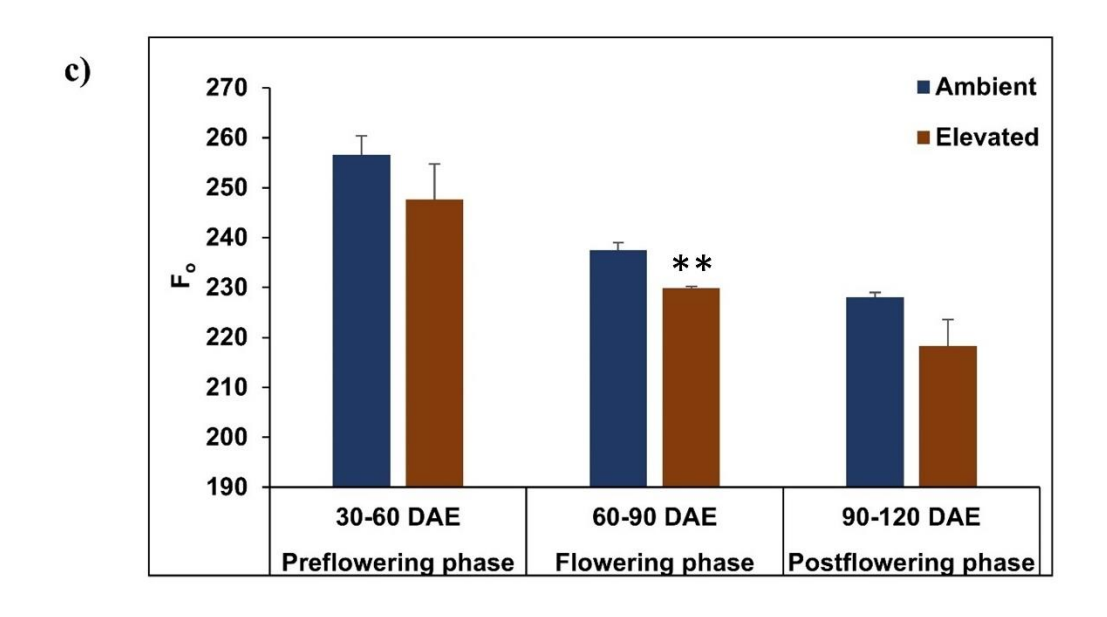


Fig. 10. Photosynthetic parameters under elevated  $CO_2$  a) Fv/Fm, b) Fv/Fo, c) Fo, and d) Fm. Values are given as mean  $\pm$  SD and significant difference between ambient and elevated  $CO_2$  grown plants at \*\*p < 0.01.







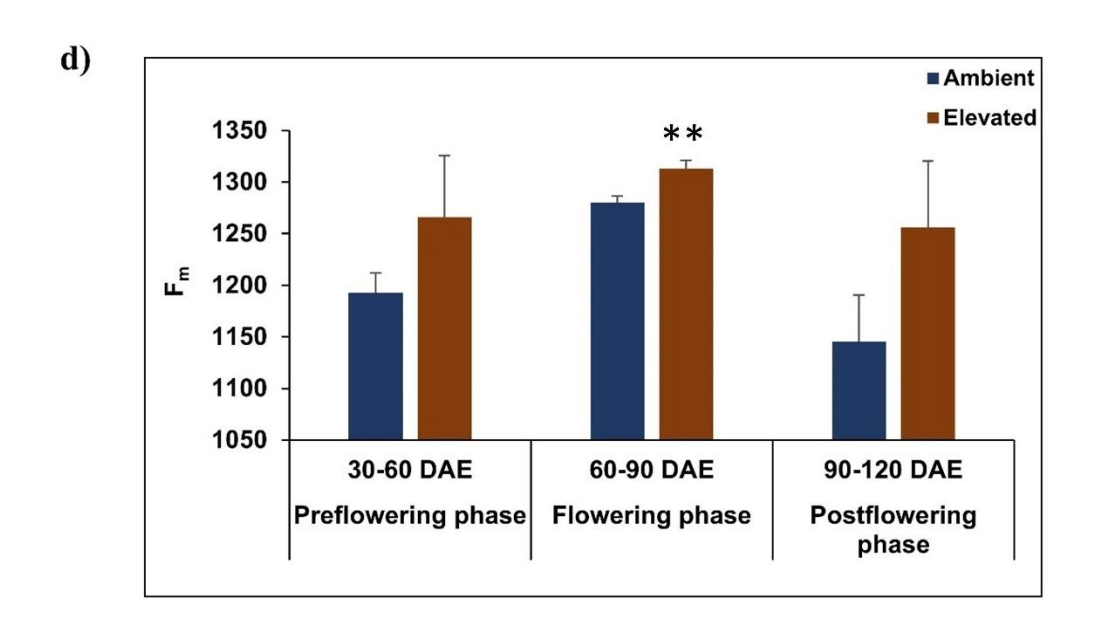


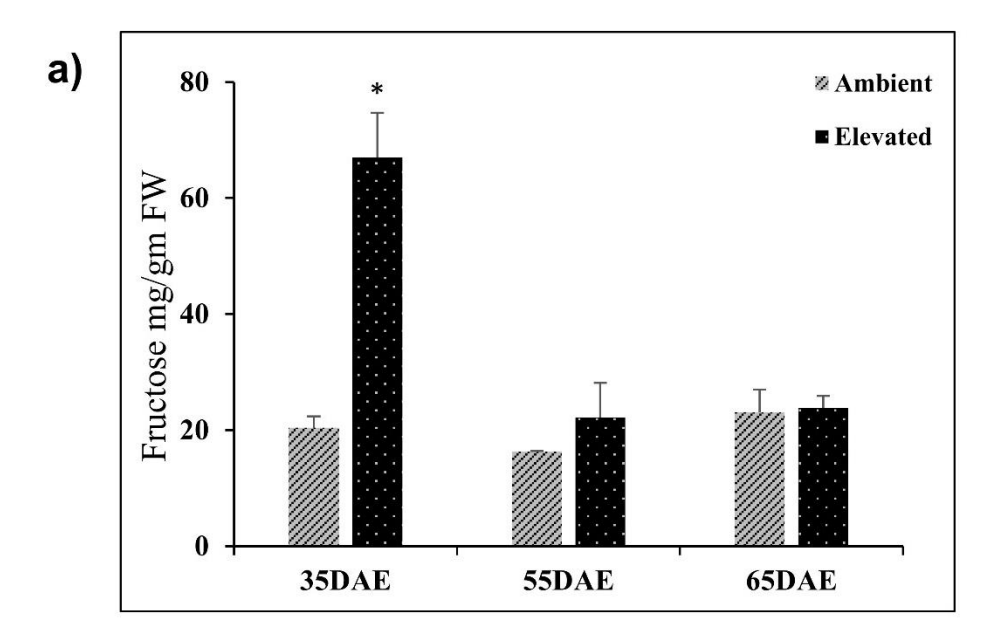
Table. 6 Photosynthetic parameters under ambient and elevated CO<sub>2</sub> conditions.

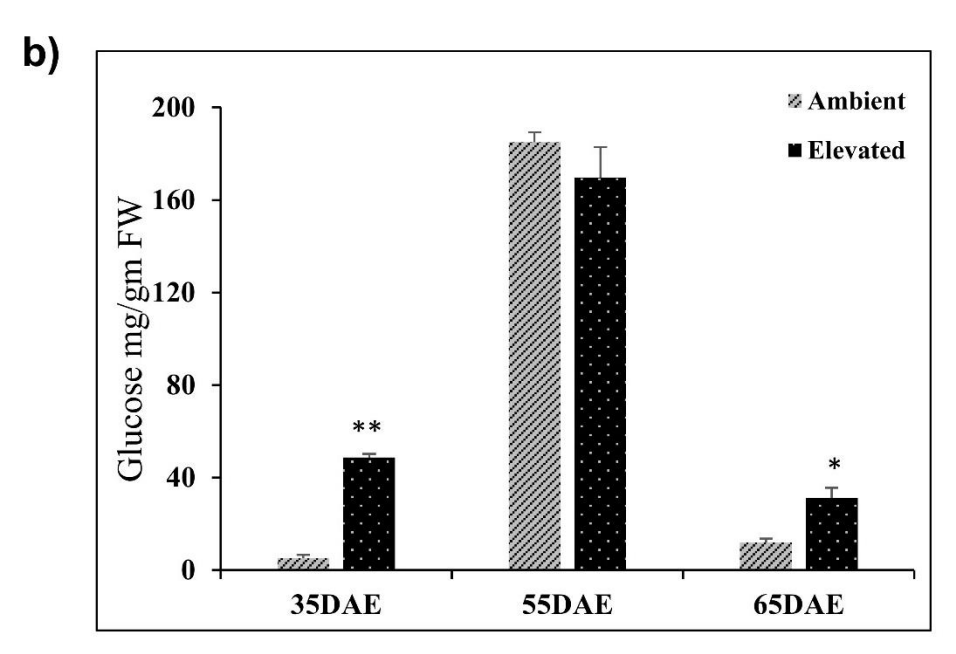
Ambient	ABS/RC	TRo/RC	ETo/RC	DIo/RC	RC/CSm	ABS/CSm	ETo/CSm	DIo/CSm	PI(abs)
Preflowering									
phase	1.45	1.12	0.74	0.33	829.82	1201.8	617.75	273.82	47.85
Flowering									
phase	1.2	0.96	0.66	0.23	1075.5	1279.9	713.16	252.52	79.51
Postflowering	5								
phase	1.33	1.04	0.72	0.28	871.52	1145.6	625.06	242.71	65.12
Elevated									
Preflowering									
phase	1.29	1.02	0.71	0.27	991.51	1266.1	703.39	263.49	72.66
Flowering									
phase	1.12	0.91	0.67	0.209	1170.9	1313.2	787.95	243.54	111.2
Postflowering	5								
phase	1.09	0.89	0.65	0.201	1157.6	1256.1	745.92	230.67	113.28
	1	l		l	l	1	l	l	

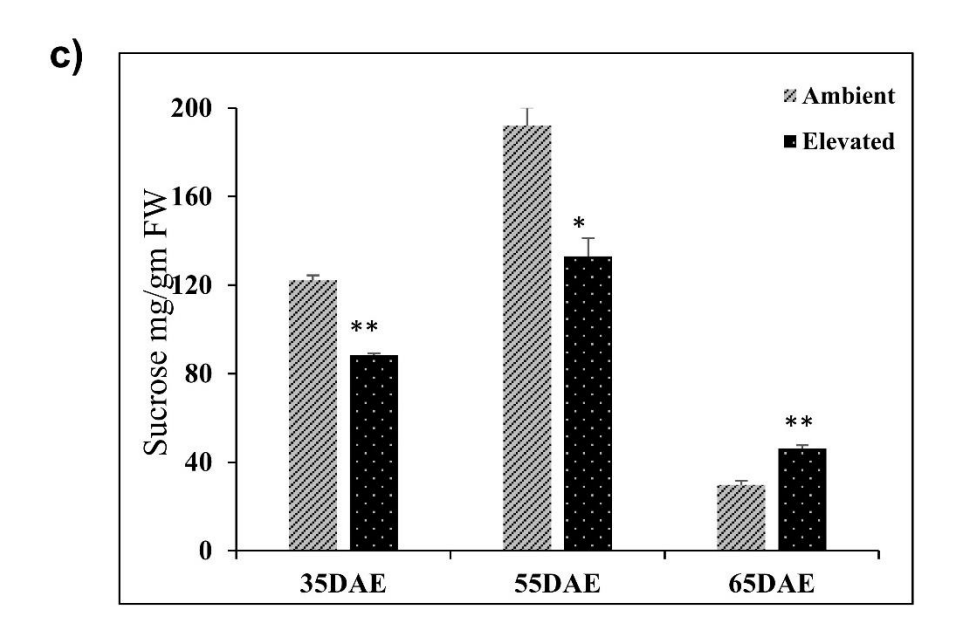
## C. Carbohydrates in Ambient and Elevated CO<sub>2</sub> grown plants

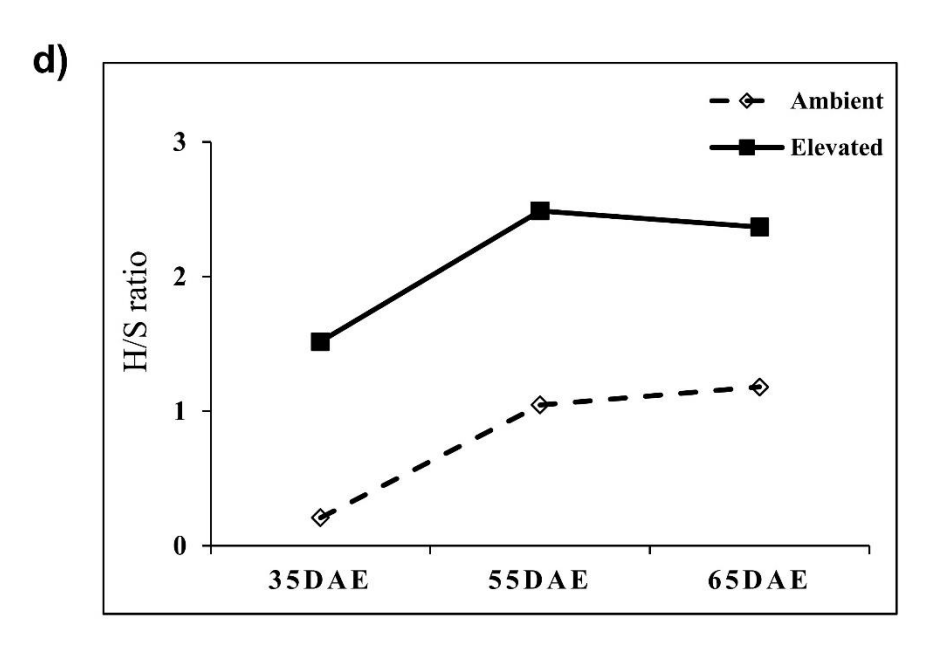
Carbohydrate levels, especially free sugars like sucrose and hexose, were analyzed in the leaf at three developmental stages, i.e., 35 DAE (vegetative), 55 DAE (transition), and 65 DAE (reproductive) from leaf samples. Glucose was higher at 35 DAE and 65 DAE in elevated CO<sub>2</sub> plants but reduced at 55 DAE. Glucose content was highest in 55 DAE (transition phase) in ambient plants compared to elevated plants (184.9 mg/gm) (Fig. 11 b). However, during 65 DAE, the glucose levels dropped in both plants but were comparatively higher in elevated CO<sub>2</sub> grown plants. Reducing monosaccharides like fructose was higher in elevated CO<sub>2</sub> grown plants at 35 DAE (vegetative phase) than in ambient CO<sub>2</sub>-grown plants (Fig. 11 a). However, as the plant progresses into other phases like the transition phase (55 DAE) and reproductive phase (65 DAE), the fructose levels dropped in elevated CO<sub>2</sub>-grown plants. At the same time, ambient CO<sub>2</sub> grown plants showed stable levels of fructose throughout the 3 phases. Sucrose levels were lower in elevated plants compared to ambient in vegetative and transition phases (Fig. 11 c). Nevertheless, at 65 DAE, sucrose levels were higher in elevated grown conditions compared to ambient, but the levels were lower compared to the previous phases. Hexose to sucrose ratios was calculated, and elevated CO<sub>2</sub> grown plants have shown a higher H/S ratio than ambient counterparts (Fig. 11 d).

Fig. 11. Foliar carbohydrates under ambient and elevated  $CO_2$  conditions a) fructose, b) glucose, c) sucrose, and d) H/S ratio. Values are given as mean  $\pm$  SD, with significant difference wherein p value denotes \* < 0.05, \*\* < 0.01.







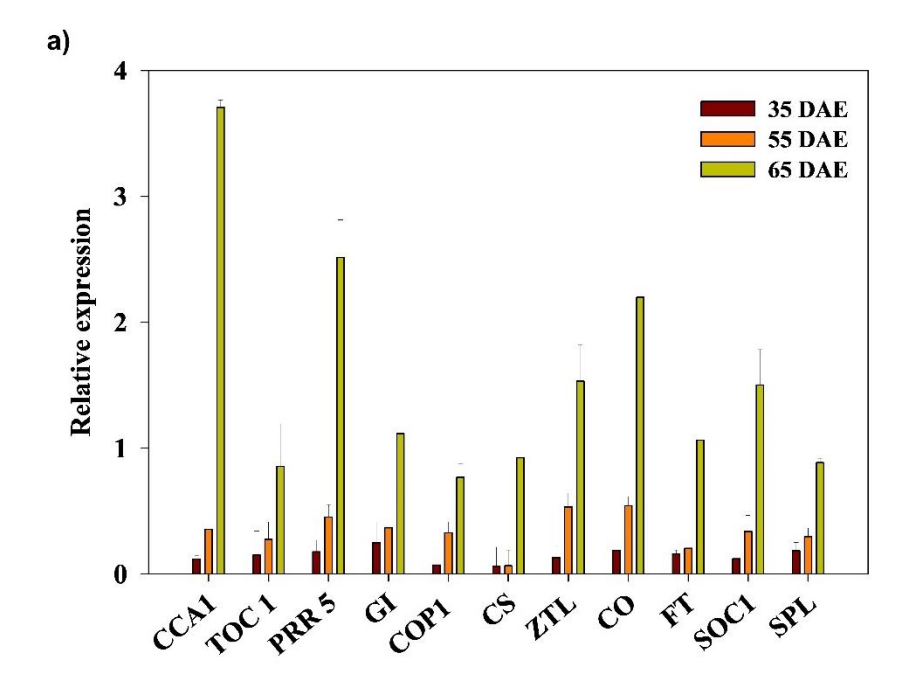


## D. Regulation of flowering under elevated CO<sub>2</sub>

To understand the effects of elevated  $CO_2$  on the molecular regulation of flowering, we analyzed the gene transcript levels of essential floral regulatory genes at all 3 stages. Genes involved in circadian rhythms like CCA 1 and TOC 1 were downregulated in elevated plants compared to ambient plants at 35 DAE and 55 DAE. CCA1 was upregulated at 65 DAE, while TOC1 was downregulated at 65 DAE compared to ambient plants. Genes involved in photoperiod pathway GI, CO, and FT were downregulated in elevated conditions at 35 and 55 DAE, but at 65 DAE, they were upregulated, especially CO, by 2-fold (Fig. 12 a). Other genes involved in the photoperiod pathway, like PRR5, COP1, and ZTL, were also analyzed. All these transcripts showed an increase in the expression levels at each time point in ascending pattern, showing the highest expression at 65 DAE in elevated plants. However, the expression was lower than its ambient counterparts at 35 DAE and 55 DAE. Except for COP1, all other genes were upregulated in elevated CO<sub>2</sub> grown plants compared to ambient plants at 65 DAE. Floral regulator SOC 1 was upregulated only at 65 DAE in elevated compared to ambient. While SPL involved in the aging pathway was found to be downregulated at three phases in elevated plants compared to ambient ones. TPS (TPS 6) was downregulated in all 3 stages in elevated plants, but 65 DAE showed an increase compared to 55 DAE in the elevated CO<sub>2</sub> grown plants, but still lower than ambient plants (Fig. 12 c). Expression levels of miR156 and miR172 involved in the aging pathway were analyzed, miR156 was upregulated in elevated plants in all 3 phases, especially at 55 DAE with 5-fold compared to ambient. miR172 was downregulated in all 3 phases in elevated plants (Fig. 12 b). Also, cell wall invertase gene (CWIN)

expression was downregulated during all the phases in elevated CO<sub>2</sub> grown plants. Correlation network analysis showed that miR156 was negatively correlated with all floral activating genes required for floral initiation (Fig. 13).

Fig. 12. Analysis of flowering gene transcripts under ambient and elevated CO<sub>2</sub> conditions a) Photoperiod and floral regulator gene transcripts, b) miRNA transcripts, and c) genes involved in sugar signalling.



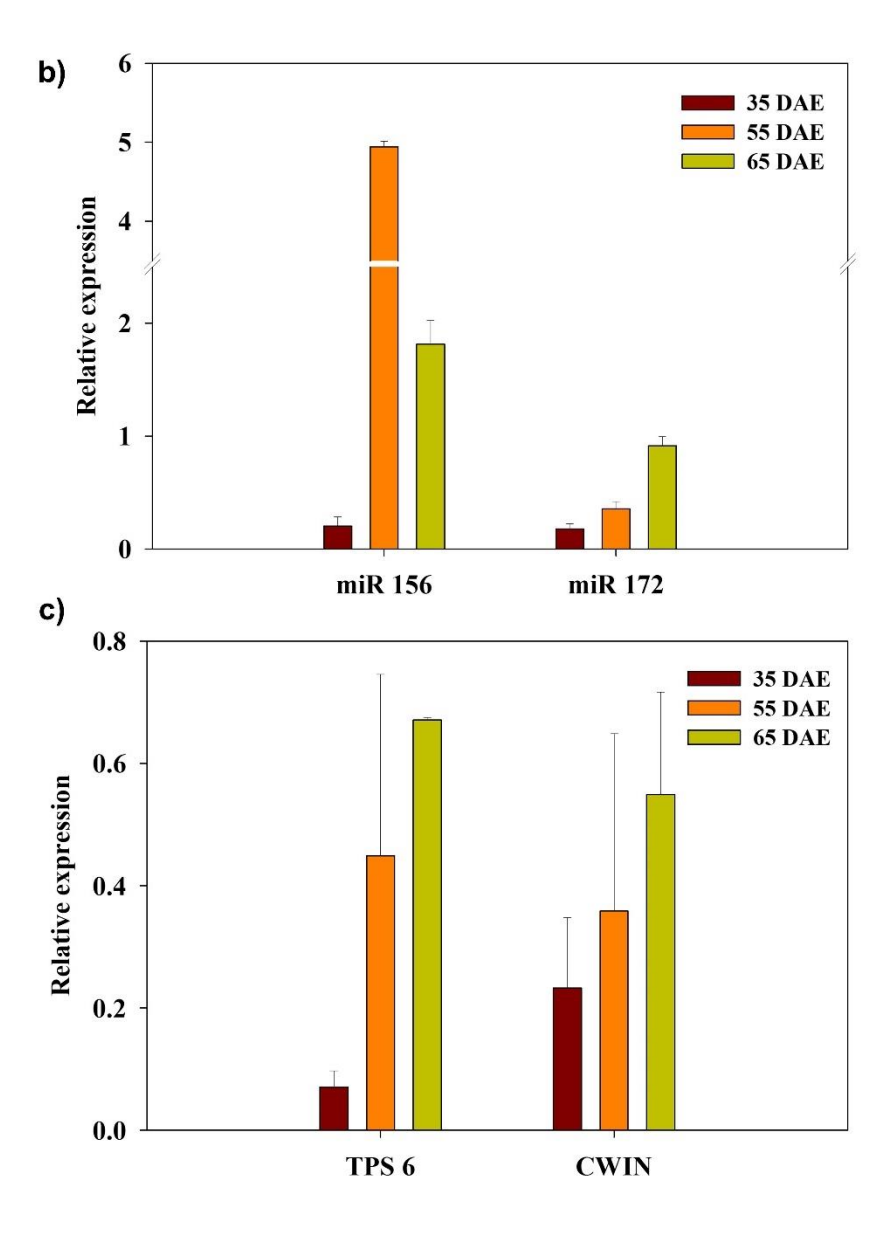
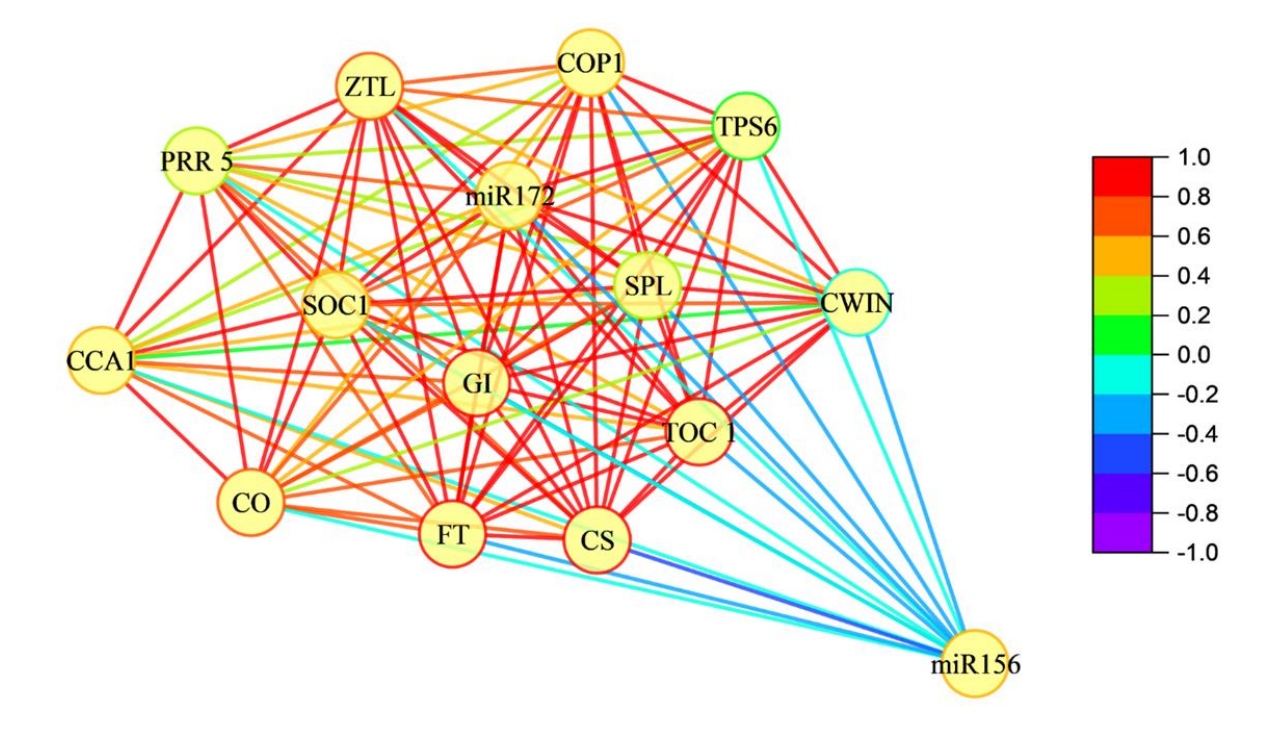




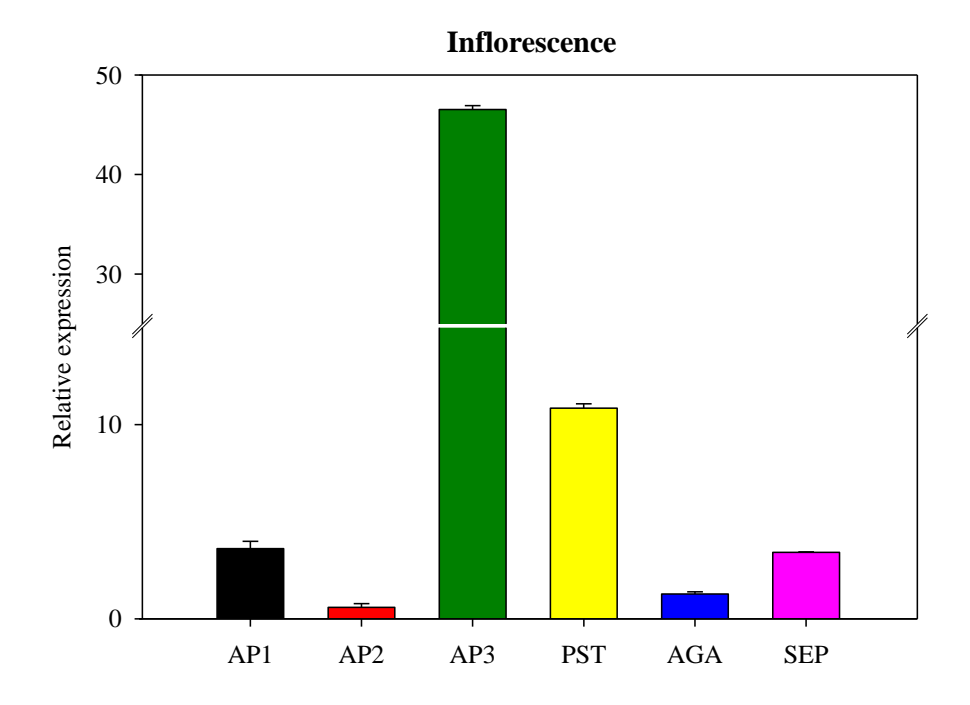
Fig. 13. Correlation network of floral regulatory genes under elevated  $CO_2$  conditions.



# E. ABCE gene expression under elevated CO<sub>2</sub>

The days required for the bud to mature into a flower in elevated plants were less compared to ambient plants. The expression of ABCE genes like Apetala 3 (AP3), Apetala 1 (AP1), Apetala 2 (AP2), Pistillata (PST), Agamous (AGA), and Sepallata (SEP) was assessed in the inflorescence collected from both ambient and elevated CO<sub>2</sub> conditions. Inflorescence collected from elevated CO<sub>2</sub> plants showed higher transcript levels of AP3, AP1, PST, AGA, and SEP compared to inflorescence in ambient plants. Among them, AP3 and PST showed higher expression levels compared to others for the faster petal and stamen differentiation which is the next stage required for flower formation (Fig. 14).

Fig. 14. ABCE gene transcript expression patterns in inflorescence under elevated CO<sub>2</sub> conditions.



Objective 2 - Sequential changes in the reproductive characteristics in pigeonpea grown under elevated CO<sub>2</sub>.

#### A. Yield characteristics of pigeonpea grown under elevated CO<sub>2</sub>

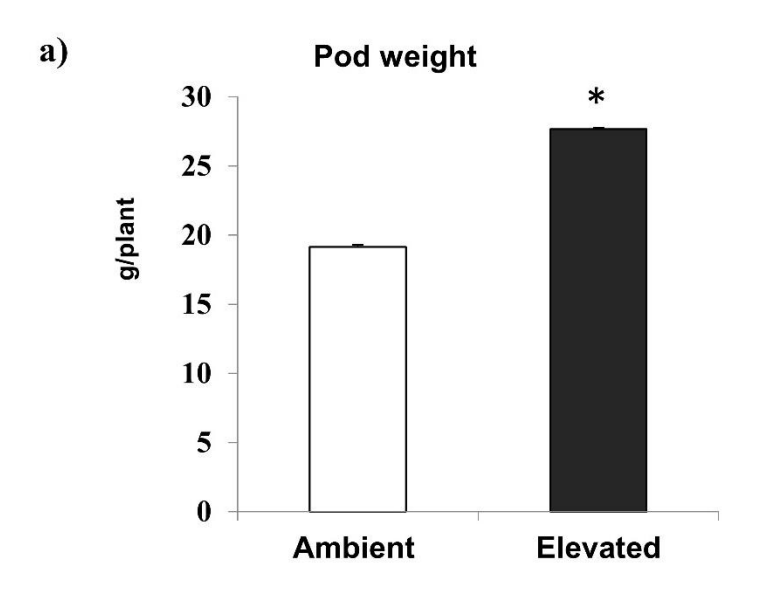
Yield characteristics like total dry weight, pod weight, seed weight, and weight per 100 seeds were measured in both ambient and elevated CO<sub>2</sub> grown pigeonpea. Elevated CO<sub>2</sub> grown plants showed higher growth rates, biomass, and seed yields. Dry weight was increased by 16% in elevated CO<sub>2</sub> grown plants compared to ambient CO<sub>2</sub> grown plants (Fig. 15 d). To assess the seed yield, mature seeds were collected at 120 days after sowing (DAS) from ambient and elevated CO<sub>2</sub> grown plants. At the end of the growth period, pigeonpea grown under elevated CO<sub>2</sub> conditions showed 18% higher seed yields than ambient CO<sub>2</sub> grown plants. The total seed weight and weight per 100 seeds in elevated CO<sub>2</sub> grown plants were recorded as 14.5 g/plant (20 %) and 10.18 g/plant (12 %) respectively, compared to ambient CO<sub>2</sub> grown plants.

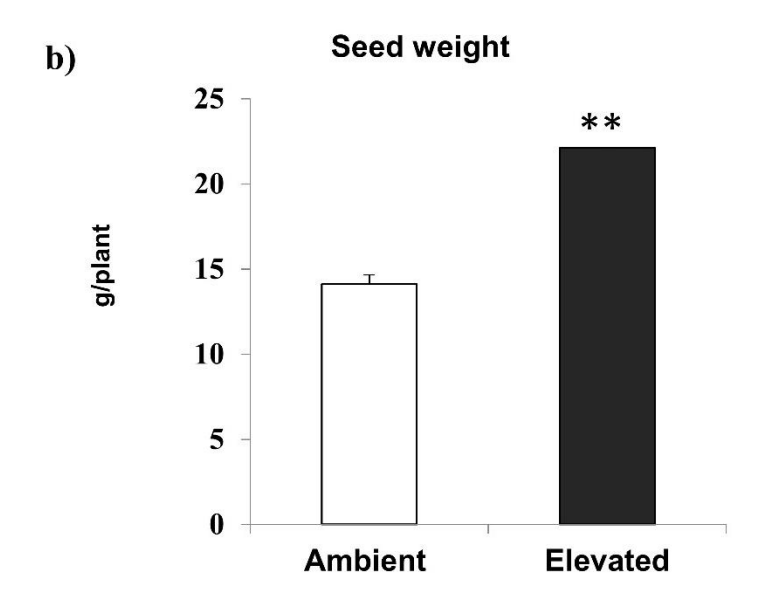
## B. Biochemical parameters analysis in pigeonpea seeds under elevated CO<sub>2</sub>

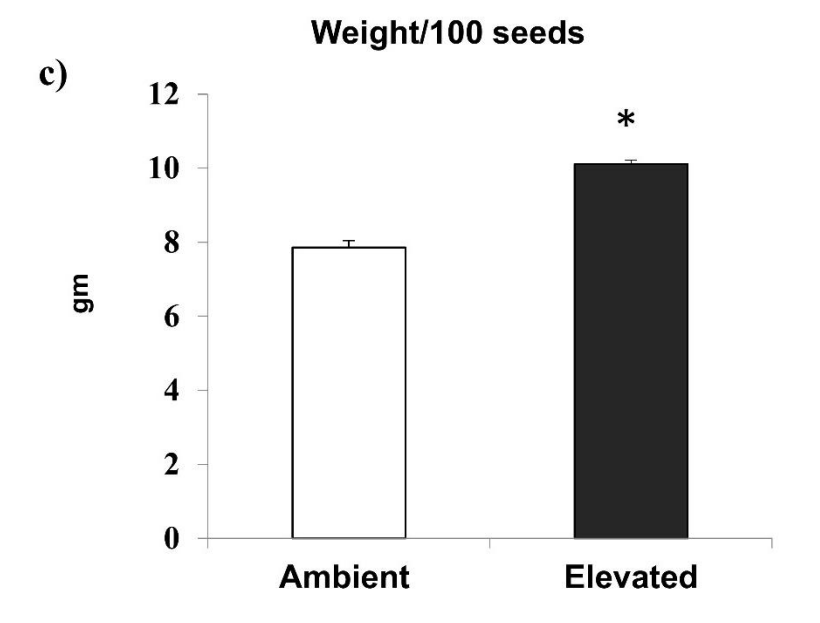
We have analyzed the total protein, ash, and nitrogen content in ambient and elevated CO<sub>2</sub> grown mature dry seeds to understand the seed's nutritional quality (Fig. 16). There was no significant difference between elevated and ambient CO<sub>2</sub> grown pigeonpea seeds concerning seed nitrogen and ash content. However, there was a slight decrease in seed protein content in elevated CO<sub>2</sub> grown plants. Biochemical analysis of seeds showed that the total carbohydrates were significantly upregulated in elevated CO<sub>2</sub> grown seeds (313 mg/gm DW) compared to ambient CO<sub>2</sub> grown seeds (187 mg/gm DW). Further, elevated CO<sub>2</sub> grown seeds

had shown 4% higher reducing sugars than ambient seeds, while starch content was almost equal in both. Sucrose was upregulated by 10% in elevated seeds (0.857 mg/gm DW) than in ambient seed (0.691 mg/gm DW) (Fig. 16).

Fig. 15. Yield characteristics of pigeonpea under elevated  $CO_2$  conditions a) pod weight, b) seed weight, c) weight/ 100 seeds, and d) total dry weight. Values are given as mean  $\pm$  SD (n=3) and significant difference between ambient and elevated  $CO_2$  grown plants at \*p < 0.05, \*\*p<0.001, ns: no statistical significance.







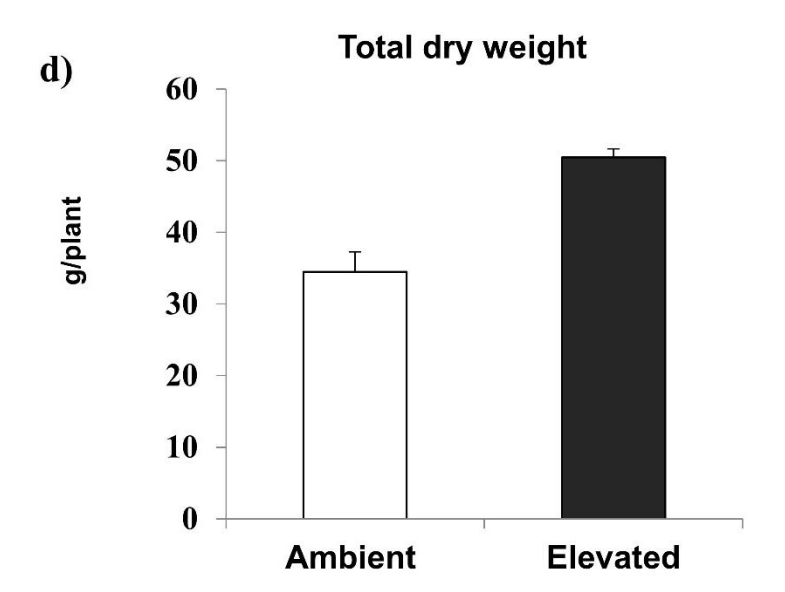
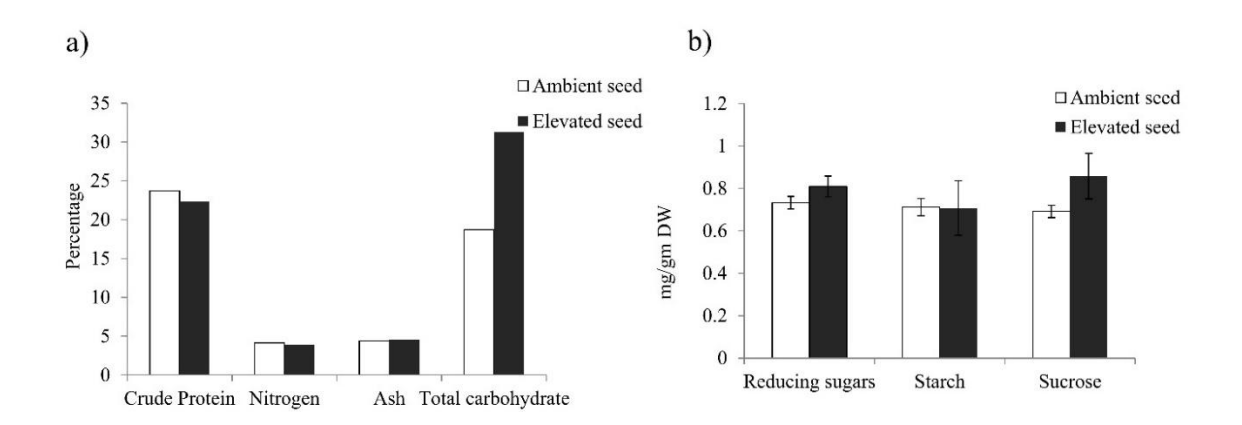
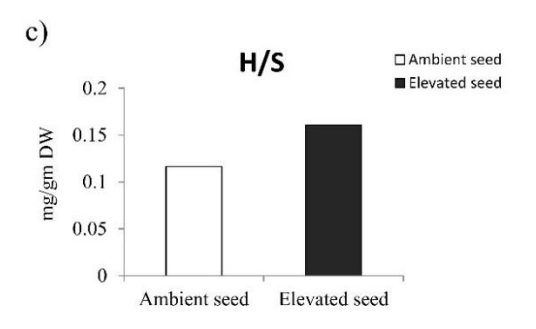




Fig. 16. Biochemical characteristics of pigeonpea seeds under elevated CO<sub>2</sub>.





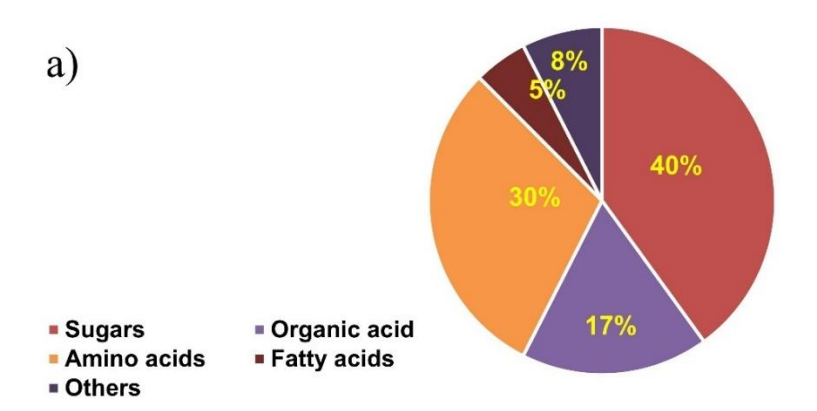
## C. Metabolite analysis of pigeonpea seeds under elevated CO<sub>2</sub>

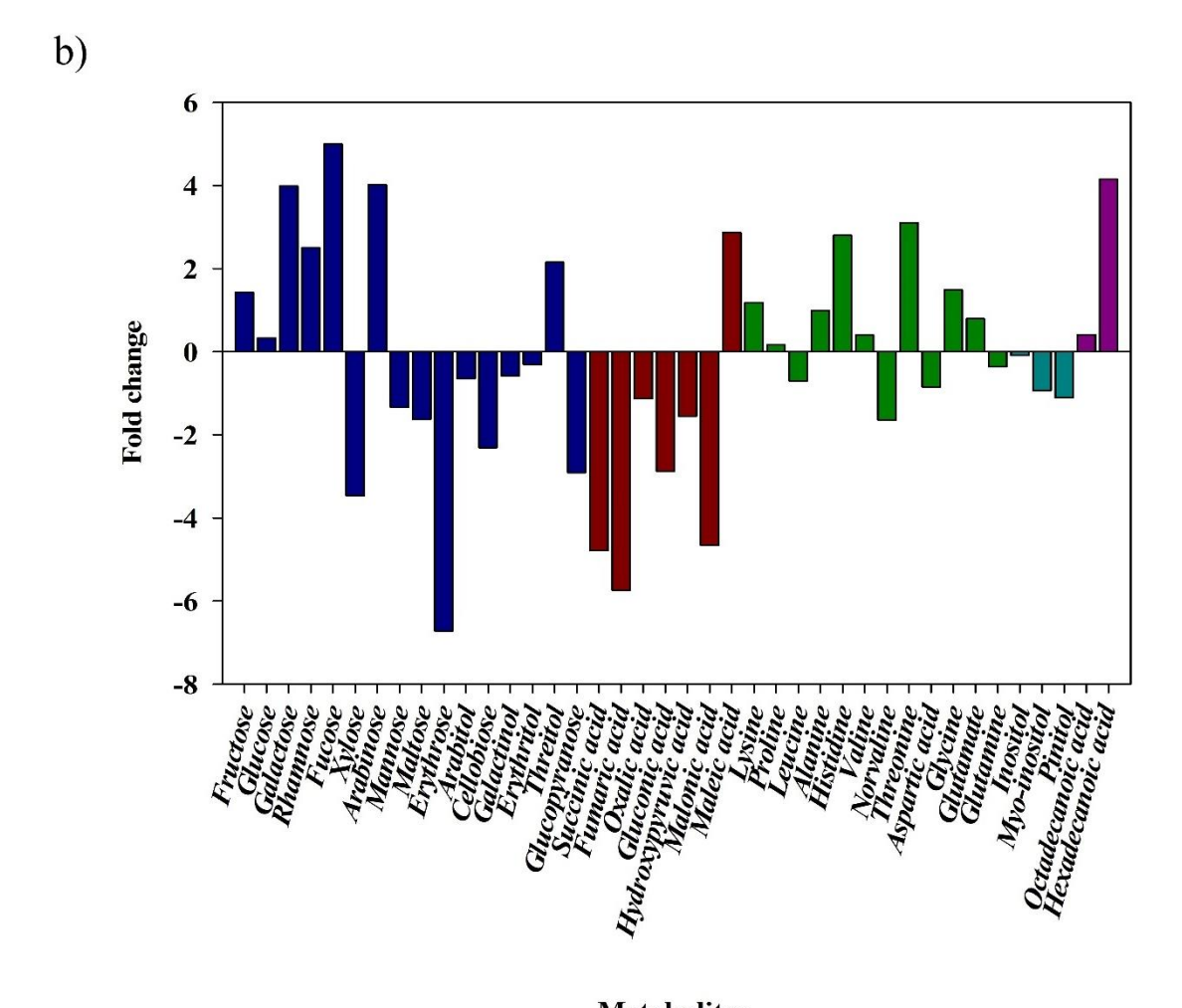
Seeds from both ambient and elevated CO<sub>2</sub> grown plants were analyzed by GC-MS for differential expression of metabolites. A total of 40 metabolites were quantified based on the retention time and spectra, which crossed the match factor of 700 among sugars (16), amino acids (12), organic acids (7), fatty acids (2), and cyclitols (3) (Fig. 17 a). Among the 16 sugars quantified, fructose, glucose, galactose, rhamnose, arabinose, threitol, and fucose were upregulated in elevated CO<sub>2</sub> grown pigeonpea seed compared to ambient CO<sub>2</sub> grown pigeonpea. Fucose showed the highest fold change whereas the remaining 9 sugars and sugar alcohol contents decreased. Among organic acids, maleic acid was upregulated 7-fold in elevated CO<sub>2</sub> grown pigeonpea seed, while the other metabolites like succinic acid, fumaric acid, oxalic acid, gluconic acid, α-hydroxypyruvic acid, and malonic acid contents were decreased (Fig. 17 b). From the 12 amino acids quantified, 8 (lysine, valine, threonine, histidine, proline, glycine, alanine and glutamate) were upregulated while 4 (leucine, norvaline, aspartic acid and glutamine) were down-regulated in elevated CO<sub>2</sub> grown pigeonpea seed. Among the upregulated amino acids, four were essential amino acids, including lysine, valine, histidine, and threonine, and the rest were non-essential amino acids. The amino acids like leucine, glutamine, aspartic acid, and norvaline were down-regulated in elevated CO<sub>2</sub> grown pigeonpea seed.

PCA analysis was done to know the variance among the samples and within the samples. PCA score plot shows that both ambient and elevated samples are varied as both fall in different quadrants (Fig. 18). Correlation analysis was done to understand the better relationship between metabolites better. Correlation analysis

showed that amino acids like leucine and lysine were negatively correlated with fumaric acid and succinic acid (Fig. 19, Table 7). Lysine was also negatively correlated with aspartic acid. Major sugar alcohols like pinitol, inositol and myoinositol showed a strong negative correlation with sugars. Pinitol was negatively correlated with fucose, arabinose, fructose while Inositol was negatively correlated with erythrose and galactinol. Myo-inositol was also negatively correlated with erythrose and galactinol. On the other hand, all sugar alcohols (pinitol, inositol, myo-inositol) were positively correlated with glucose, arabitol and erythritol (Table 7). Fatty acids (octadecanoic acid, hexadecenoic acid) were positively correlated with mannose, pinitol, rhamnose, and myo-inositol. Negative correlations were observed between fatty acids and aspartic acid, valine, erythrose and galactinol. The remaining correlations between metabolites are elucidated in Table 7.

Fig. 17. Metabolite analysis of pigeonpea seeds under elevated CO<sub>2</sub> a) characterization of metabolites into different categories and b) fold change of metabolites in pigeonpea seeds under elevated CO<sub>2</sub>.





Metabolites

Fig. 18. PCA analysis of metabolites in ambient and elevated  $CO_2$  grown pigeonpea seeds.

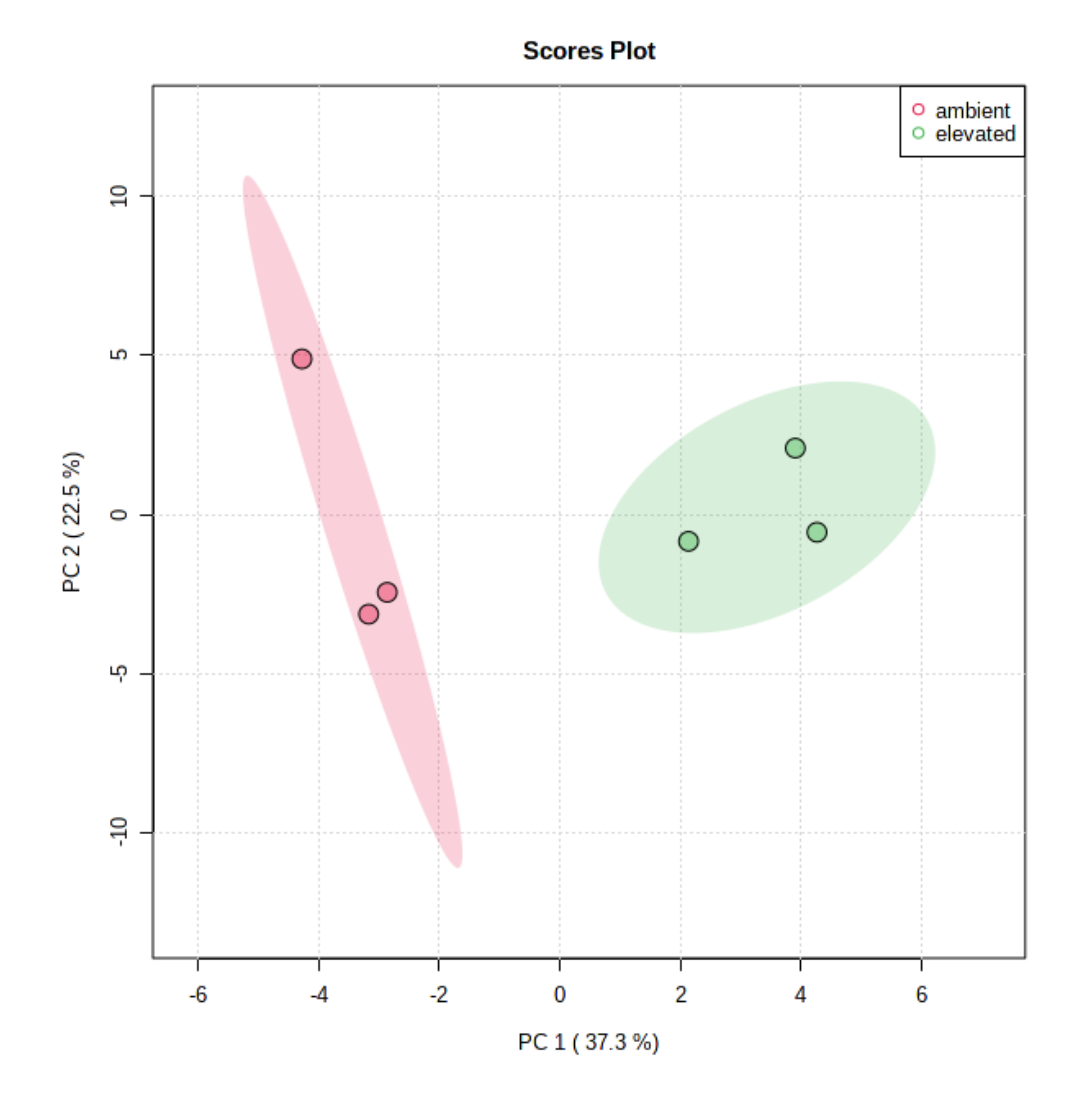




Fig. 19. Correlation heatmap between metabolites in pigeonpea seeds under elevated CO<sub>2</sub>.

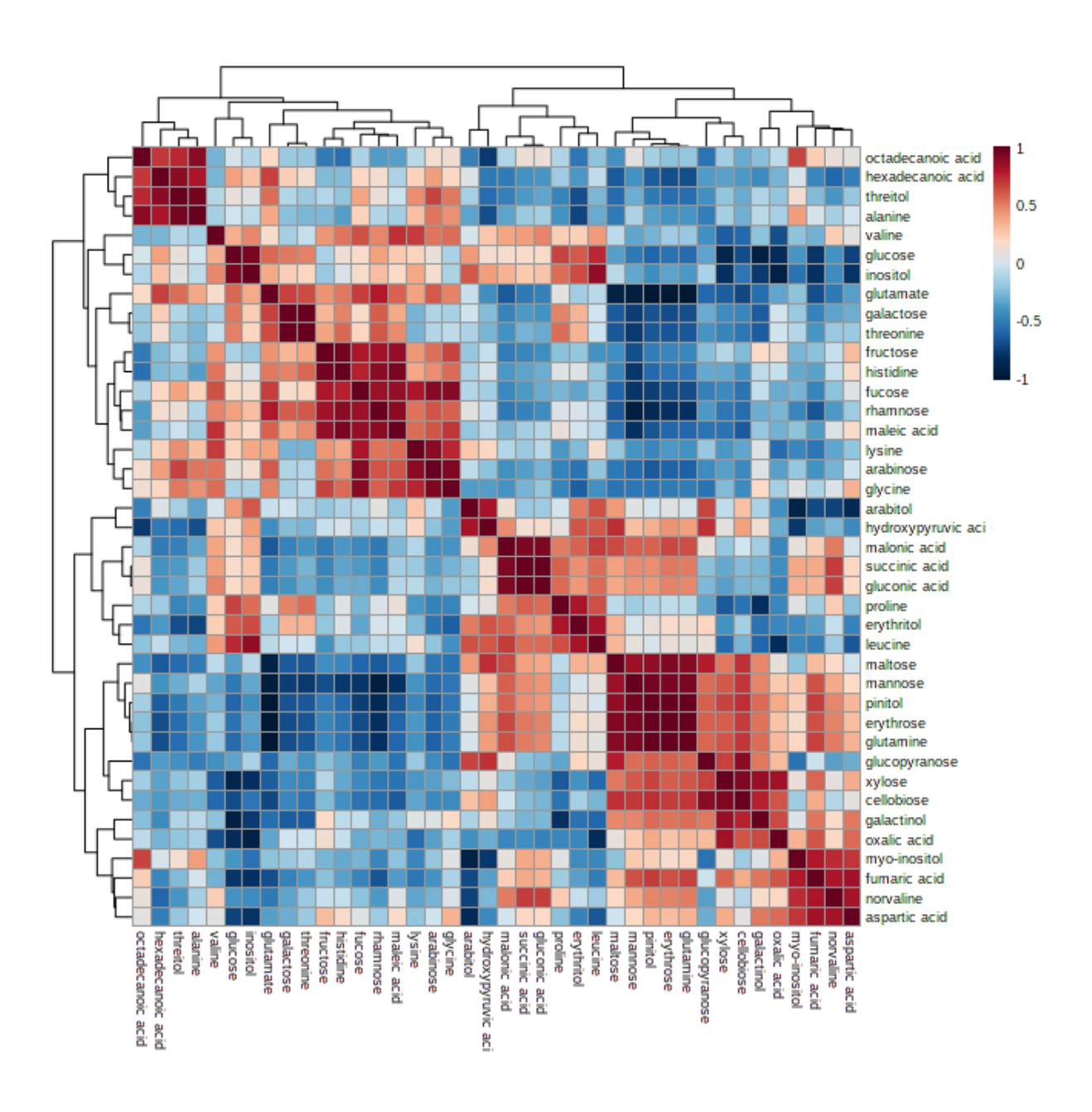


Table. 7 Correlation between metabolites in elevated  $CO_2$  seeds. Pearson correlation coefficient (r) > 0.5 is considered a strong positive correlation (red), and < -0.5 is a strong negative correlation (yellow), and follows into categories of moderate or no correlation.

Metabolites	maltose	cellobiose	glucopyranose	oxalic acid	mannose	pinitol	rhamnose	myo-inositol
maltose	1	0.79492	0.87717	0.39915	0.84606	0.73806	-0.29587	0.25683
cellobiose	0.79492	1	0.87942	0.68185	0.70731	0.60171	-0.341	0.18279
glucopyranose	0.87717	0.87942	1	0.42558	0.61918	0.5577	-0.14844	0.036812
oxalic acid	0.39915	0.68185	0.42558	1	0.62315	0.73975	0.16049	0.68829
mannose	0.84606	0.70731	0.61918	0.62315	1	0.93077	-0.16964	0.67935
pinitol	0.73806	0.60171	0.5577	0.73975	0.93077	1	0.17636	0.83487
rhamnose	-0.29587	-0.341	-0.14844	0.16049	-0.16964	0.17636	1	0.4104
myo-inositol	0.25683	0.18279	0.036812	0.68829	0.67935	0.83487	0.4104	1
octade canoic acid	0.2719	0.13235	0.10254	0.52672	0.6563	0.8082	0.52098	0.9402
glutamine	0.46972	0.30947	0.34744	0.6364	0.72343	0.9089	0.55147	0.89953
threitol	0.11315	0.053925	0.053637	0.41162	0.49146	0.64675	0.6091	0.81819
alanine	0.1658	0.092357	0.053086	0.47298	0.57128	0.71409	0.54447	0.88399
glucose	0.27408	-0.010734	0.1605	0.33578	0.48591	0.71481	0.73155	0.78037
inositol	0.30058	-0.01603	0.19046	0.26767	0.48008	0.69278	0.71278	0.72906
galactose	0.22309	0.045385	0.1614	0.50534	0.44004	0.72289	0.79505	0.81182
threonine	0.18397	0.0051845	0.11559	0.49802	0.40508	0.69829	0.8065	0.80937
hexade canoic acid	0.23802	0.086879	0.15303	0.44416	0.551	0.74246	0.66736	0.84935
glutamate	0.21187	0.06262	0.14926	0.49369	0.48851	0.73655	0.76187	0.84746
arabitol	0.53285	0.24643	0.53751	0.2383	0.52541	0.67842	0.58358	0.49586
proline	0.3202	-0.027358	0.12667	0.35986	0.51172	0.74317	0.65506	0.79943
erythritol	0.45484	0.066033	0.30987	0.29574	0.51422	0.72948	0.62309	0.65806
leucine	0.415	0.019575	0.25778	0.21296	0.53932	0.71695	0.60983	0.68428
lysine	-0.64371	-0.54292	-0.39404	-0.7265	-0.74306	-0.78421	0.11729	-0.62422
valine	-0.71924	-0.84868	-0.6672	-0.88306	-0.89175	-0.89049	0.046326	-0.67386
glycine	-0.9139	-0.53472	-0.68516	-0.30388	-0.76669	-0.737	0.13881	-0.34023
fucose	-0.90596	-0.67042	-0.61842	-0.43678	-0.88998	-0.75734	0.43779	-0.4055
arabinose	-0.81534	-0.55973	-0.56368	-0.45899	-0.71396	-0.68628	0.26429	-0.3533
fructose	-0.71911	-0.34984	-0.37677	-0.082608	-0.82322	-0.64998	0.33403	-0.43373
maleic acid	-0.8674	-0.7484	-0.65801	-0.41135	-0.92805	-0.73197	0.47118	-0.39528
histidine	-0.71266	-0.51572	-0.43226	-0.19948	-0.84641	-0.6204	0.48269	-0.38994
hydroxypyruvic ac	0.38457	0.17192	0.52279	-0.47166	-0.1526	-0.25846	-0.24799	-0.70585
malonic acid	0.31104	-0.15273	-0.01438	-0.56106	0.092886	-0.12347	-0.60206	-0.3233
succinic acid	0.11553	-0.33849	-0.30853	-0.4657	0.089154	-0.07404	-0.49606	-0.074153
gluconic acid	0.025408	-0.40727	-0.37145	-0.5615	-0.01614	-0.19295	-0.51482	-0.17168
xylose	0.51516	0.90782	0.6237	0.71156	0.50473	0.38086	-0.46659	0.098868
erythrose	0.60396	0.61851	0.47166	0.12336	0.40278	0.12115	-0.90122	-0.26122
galactinol	0.084597	0.5887	0.29154	0.30301	-0.006235	-0.19437	-0.62457	-0.37109
fumaric acid	0.14612	0.4106	-0.018472	0.46848	0.30865	0.14623	-0.67161	0.14553
norvaline	-0.19073	-0.10868		0.072709	-0.074827	-0.18533	-0.5691	-0.031623
aspartic acid	-0.3267	0.076331	-0.34857	0.3168	-0.17227	-0.23893	-0.44321	-0.055558

Metabolites	octadecanoic acid	glutamine	threitol	alanine	glucose	inositol	galactose	threonine
maltose	0.2719	0.46972	0.11315	0.1658	0.27408	0.30058	0.22309	0.18397
cellobiose	0.13235	0.30947	0.053925	0.092357	-0.010734	-0.01603	0.045385	0.0051845
glucopyranose	0.10254	0.34744	0.053637	0.053086	0.1605	0.19046	0.1614	0.11559
oxalic acid	0.52672	0.6364	0.41162	0.47298	0.33578	0.26767	0.50534	0.49802
mannose	0.6563	0.72343	0.49146	0.57128	0.48591	0.48008	0.44004	0.40508
pinitol	0.8082	0.9089	0.64675	0.71409	0.71481	0.69278	0.72289	0.69829
rhamnose	0.52098	0.55147	0.6091	0.54447	0.73155	0.71278	0.79505	0.8065
myo-inositol	0.9402	0.89953	0.81819	0.88399	0.78037	0.72906	0.81182	0.80937
octade canoic acid	1	0.9408	0.95148	0.98054	0.89742	0.87291	0.86269	0.84595
glutamine	0.9408	1	0.851	0.88111	0.92732	0.90448	0.93343	0.9158
threitol	0.95148	0.851	1	0.99028	0.85742	0.84367	0.80397	0.78047
alanine	0.98054	0.88111	0.99028	1	0.85533	0.83479	0.80843	0.78734
glucose	0.89742	0.92732	0.85742	0.85533	1	0.99519	0.9623	0.95093
inositol	0.87291	0.90448	0.84367	0.83479	0.99519	1	0.93596	0.921
galactose	0.86269	0.93343	0.80397	0.80843	0.9623	0.93596	1	0.99789
threonine	0.84595	0.9158	0.78047	0.78734	0.95093	0.921	0.99789	1
hexadecanoic acid	0.96978	0.93841	0.96949	0.96742	0.95293	0.94065	0.91278	0.89266
glutamate	0.93406	0.95137	0.9106	0.90961	0.97318	0.95171	0.97752	0.96664
arabitol	0.69756	0.81495	0.70058	0.66802	0.87629	0.90694	0.80152	0.76808
proline	0.84461	0.90805	0.72858	0.7549	0.96272	0.9484	0.94966	0.94996
erythritol	0.74	0.8676	0.6299	0.64208	0.93413	0.93747	0.90868	0.90177
le ucine	0.82565	0.88122	0.7633	0.76446	0.9699	0.98385	0.88971	0.87322
lysine	-0.40725	-0.56706	-0.12789	-0.24344	-0.31704	-0.26868	-0.41862	-0.42501
valine	-0.60384	-0.70518	-0.48517	-0.54906	-0.39703	-0.36475	-0.45514	-0.42317
glycine	-0.32111	-0.53398	-0.098185	-0.16544	-0.42026	-0.44003	-0.37755	-0.35824
fucose	-0.31486	-0.44561	-0.075821	-0.17693	-0.21481	-0.2176	-0.17532	-0.15284
arabinose	-0.20169	-0.41956	0.078933	-0.021664	-0.22627	-0.21464	-0.26444	-0.26218
fructose	-0.50556	-0.47144	-0.37628	-0.44149	-0.38328	-0.41773	-0.20086	-0.16487
maleic acid	-0.40124	-0.44174	-0.27076	-0.34247	-0.19945	-0.21629	-0.1023	-0.05795
histidine	-0.43683	-0.38121	-0.33561	-0.40269	-0.21049	-0.23679	-0.050657	-0.007895
hydroxypyruvic acid	-0.57629	-0.36814	-0.556	-0.60755	-0.27294	-0.19817	-0.34569	-0.36456
malonic acid	-0.33777	-0.32308	-0.4897	-0.43627	-0.25203	-0.20229	-0.40352	-0.39908
succinic acid	-0.154	-0.21791	-0.33813	-0.25892	-0.14695	-0.12587	-0.27307	-0.2529
gluconic acid	-0.2357	-0.32113	-0.38944	-0.32165	-0.22496	-0.19917	-0.36018	-0.33943
xylose	-0.046689	0.069104	-0.11484	-0.063982	-0.29432	-0.32604	-0.17847	-0.2033
erythrose	-0.40776	-0.30162	-0.57082	-0.49064	-0.55075	-0.54017	-0.55831	-0.57258
galactinol	-0.50473	-0.47053	-0.47328	-0.45773	-0.74264	-0.76318	-0.63723	-0.65037
fumaric acid	-0.14236	-0.17105	-0.30933	-0.19857	-0.48138	-0.53897	-0.37653	-0.36411
norvaline	-0.33538	-0.39671	-0.51918	-0.41394	-0.53855	-0.59203	-0.44724	-0.40594
aspartic acid	-0.35336	-0.41323	-0.43559	-0.36408	-0.62613	-0.6976	-0.4571	-0.42388

Metabolites	hexadecanoic acid	glutamate	arabitol	proline	e rythritol	leucine	lysine	valine
maltose	0.23802	0.21187	0.53285	0.3202	0.45484	0.415	-0.64371	-0.71924
cellobiose	0.086879	0.06262	0.24643	-0.02736	0.066033	0.019575	-0.54292	-0.84868
glucopyranose	0.15303	0.14926	0.53751	0.12667	0.30987	0.25778	-0.39404	-0.6672
oxalic acid	0.44416	0.49369	0.2383	0.35986	0.29574	0.21296	-0.7265	-0.88306
mannose	0.551	0.48851	0.52541	0.51172	0.51422	0.53932	-0.74306	-0.89175
pinitol	0.74246	0.73655	0.67842	0.74317	0.72948	0.71695	-0.78421	-0.89049
rhamnose	0.66736	0.76187	0.58358	0.65506	0.62309	0.60983	0.11729	0.046326
myo-inositol	0.84935	0.84746	0.49586	0.79943	0.65806	0.68428	-0.62422	-0.67386
octade canoic acid	0.96978	0.93406	0.69756	0.84461	0.74	0.82565	-0.40725	-0.60384
glutamine	0.93841	0.95137	0.81495	0.90805	0.8676	0.88122	-0.56706	-0.70518
threitol	0.96949	0.9106	0.70058	0.72858	0.6299	0.7633	-0.12789	-0.48517
alanine	0.96742	0.90961	0.66802	0.7549	0.64208	0.76446	-0.24344	-0.54906
glucose	0.95293	0.97318	0.87629	0.96272	0.93413	0.9699	-0.31704	-0.39703
inositol	0.94065	0.95171	0.90694	0.9484	0.93747	0.98385	-0.26868	-0.36475
galactose	0.91278	0.97752	0.80152	0.94966	0.90868	0.88971	-0.41862	-0.45514
threonine	0.89266	0.96664		0.94996	0.90177	0.87322	-0.42501	-0.42317
hexade canoic acid	1	0.97717	0.81441	0.86546	0.79874	0.8848	-0.26789	-0.51774
glutamate	0.97717	1	0.81585	0.91753	0.85904	0.8936	-0.33655	-0.49335
arabitol	0.81441	0.81585	1	0.7936	0.88218	0.91867	-0.20689	-0.43346
proline	0.86546	0.91753	0.7936	1	0.96684	0.95004	-0.49547	-0.38951
erythritol	0.79874	0.85904		0.96684	1	0.96448	-0.47059	-0.37826
leucine	0.8848	0.8936	0.91867	0.95004	0.96448	1	-0.33041	-0.3638
lysine	-0.26789	-0.33655		-0.49547	-0.47059	-0.33041	1	0.72832
valine	-0.51774	-0.49335	-0.43346	-0.38951	-0.37826	-0.3638		1
glycine	-0.28564	-0.31056		-0.5414	-0.65787	-0.57185	0.74292	0.55896
fucose	-0.18797	-0.1593		-0.33612	-0.38715	-0.33961	0.81904	0.70907
arabinose	-0.10338	-0.16373		-0.41396	-0.48287	-0.33667	0.90837	0.58747
fructose	-0.40893	-0.28382	-0.44395	-0.40056	-0.41493	-0.52227	0.42374	0.49245
maleic acid	-0.28992	-0.17949	-0.3492	-0.20454	-0.24267	-0.30295	0.56713	0.7752
histidine	-0.31549	-0.16467	-0.29894	-0.19689	-0.19747	-0.3211	0.3993	0.60228
hydroxypyruvic acid	-0.44459	-0.4195	0.15402	-0.26332	-0.01592	-0.08306	0.20773	0.27009
malonic acid	-0.40815	-0.44552		-0.10205	-0.02518			0.30159
succinic acid	-0.27862	-0.30908		0.033092	0.011365		-0.21527	0.30295
gluconic acid	-0.3497	-0.38813	-0.32546	-0.06052	-0.08139	-0.07231	-0.09463	0.40469
xylose	-0.14212	-0.15972	-0.13958	-0.29257	-0.26602	-0.32528	-0.48239	-0.74427
erythrose	-0.54139	-0.58026		-0.43135	-0.34844	-0.41625	-0.44369	-0.3233
galactinol	-0.57731	-0.60876		-0.76733	-0.74589	-0.78081	-0.02064	-0.26133
fumaric acid	-0.36167	-0.37767		-0.35127	-0.4571	-0.5202	-0.543	-0.40034
norvaline	-0.53742	-0.50623		-0.33727	-0.46145	-0.55676	-0.37441	0.091947
aspartic acid	-0.51977	-0.4855	-0.84067	-0.51625	-0.65167	-0.73885	-0.23171	-0.04446

Metabolites	glycine	fucose	arabinose	fructose	maleic acid	histidine	hydroxypyruvic acid	malonic acid
maltose	-0.9139	-0.90596	-0.81534	-0.71911	-0.8674	-0.71266	0.38457	0.31104
cellobiose	-0.53472	-0.67042	-0.55973	-0.34984	-0.7484	-0.51572	0.17192	-0.15273
glucopyranose	-0.68516	-0.61842	-0.56368	-0.37677	-0.65801	-0.43226	0.52279	-0.01438
oxalic acid	-0.30388	-0.43678	-0.45899	-0.08261	-0.41135	-0.19948	-0.47166	-0.56106
mannose	-0.76669	-0.88998	-0.71396	-0.82322	-0.92805	-0.84641	-0.1526	0.092886
pinitol	-0.737	-0.75734	-0.68628	-0.64998	-0.73197	-0.6204	-0.25846	-0.12347
rhamnose	0.13881	0.43779	0.26429	0.33403	0.47118	0.48269	-0.24799	-0.60206
myo-inositol	-0.34023	-0.4055	-0.3533	-0.43373	-0.39528	-0.38994	-0.70585	-0.3233
octade canoic acid	-0.32111	-0.31486	-0.20169	-0.50556	-0.40124	-0.43683	-0.57629	-0.33777
glutamine	-0.53398	-0.44561	-0.41956	-0.47144	-0.44174	-0.38121	-0.36814	-0.32308
threitol	-0.09819	-0.07582	0.078933	-0.37628	-0.27076	-0.33561	-0.556	-0.4897
alanine	-0.16544	-0.17693	-0.021664	-0.44149	-0.34247	-0.40269	-0.60755	-0.43627
glucose	-0.42026	-0.21481	-0.22627	-0.38328	-0.19945	-0.21049	-0.27294	-0.25203
inositol	-0.44003	-0.2176	-0.21464	-0.41773	-0.21629	-0.23679	-0.19817	-0.20229
galactose	-0.37755	-0.17532	-0.26444	-0.20086	-0.1023	-0.05066	-0.34569	-0.40352
threonine	-0.35824	-0.15284	-0.26218	-0.16487	-0.05795	-0.0079	-0.36456	-0.39908
hexadecanoic acid	-0.28564	-0.18797	-0.10338	-0.40893	-0.28992	-0.31549	-0.44459	-0.40815
glutamate	-0.31056	-0.1593	-0.16373	-0.28382	-0.17949	-0.16467	-0.4195	-0.44552
arabitol	-0.56739	-0.30405	-0.27678	-0.44395	-0.3492	-0.29894	0.15402	-0.16374
proline	-0.5414	-0.33612	-0.41396	-0.40056	-0.20454	-0.19689	-0.26332	-0.10205
e rythritol	-0.65787	-0.38715	-0.48287	-0.41493	-0.24267	-0.19747	-0.015921	-0.025182
leucine	-0.57185	-0.33961	-0.33667	-0.52227	-0.30295	-0.3211	-0.083058	-0.038043
lysine	0.74292	0.81904	0.90837	0.42374	0.56713	0.3993	0.20773	-0.12312
valine	0.55896	0.70907	0.58747	0.49245	0.7752	0.60228	0.27009	0.30159
glycine	1	0.89622	0.921	0.6957	0.70381	0.57738	-0.35688	-0.4599
fucose	0.89622	1	0.91012	0.7957	0.88977	0.78596	-0.11833	-0.45095
arabinose	0.921	0.91012	1	0.53702	0.63197	0.46535	-0.1944	-0.42596
fructose	0.6957	0.7957	0.53702	1	0.87441	0.95156	-0.021323	-0.50693
maleic acid	0.70381	0.88977	0.63197	0.87441	1	0.94775	-0.039104	-0.27641
histidine	0.57738	0.78596	0.46535	0.95156	0.94775	1	0.050232	-0.37949
hydroxypyruvic acid	-0.35688	-0.11833	-0.1944	-0.02132	-0.039104	0.050232	1	0.48321
malonic acid	-0.4599	-0.45095	-0.42596	-0.50693	-0.27641	-0.37949	0.48321	1
succinic acid	-0.34106	-0.39377	-0.38189	-0.48437	-0.18761	-0.34331	0.11835	0.91867
gluconic acid	-0.23795	-0.29309	-0.27224	-0.42067	-0.11223	-0.28839	0.14329	0.91955
xylose	-0.23207	-0.49035	-0.39575	-0.10411	-0.56866	-0.3463	-0.040512	-0.25648
erythrose	-0.47121	-0.6928	-0.60718	-0.38943	-0.62098	-0.51094	0.36178	0.55379
galactinol	0.22738	-0.06302	0.02656	0.24267	-0.19005	-0.04213	0.059011	-0.19866
fumaric acid	-0.05428	-0.43593	-0.37914	-0.11053	-0.37027	-0.29668	-0.38342	0.10277
norvaline	0.085212	-0.18544	-0.26091	0.078041	0.032018	0.01558	-0.32938	0.35452
aspartic acid	0.37558	0.054572	-0.00285	0.38314	0.14136	0.19841	-0.45548	-0.13041

Metabolites	succinic acid	gluconic acid	xylose	erythrose	galactinol	fumaric acid	norvaline	aspartic acid
maltose	0.11553	0.025408	0.51516	0.60396	0.084597	0.14612	-0.19073	-0.3267
cellobiose	-0.33849	-0.40727	0.90782	0.61851	0.5887	0.4106	-0.10868	0.076331
glucopyranose	-0.30853	-0.37145	0.6237	0.47166	0.29154	-0.018472	-0.43777	-0.34857
oxalic acid	-0.4657	-0.5615	0.71156	0.12336	0.30301	0.46848	0.072709	0.3168
mannose	0.089154	-0.01614	0.50473	0.40278	-0.006235	0.30865	-0.07483	-0.17227
pinitol	-0.07404	-0.19295	0.38086	0.12115	-0.19437	0.14623	-0.18533	-0.23893
rhamnose	-0.49606	-0.51482	-0.46659	-0.90122	-0.62457	-0.67161	-0.5691	-0.44321
myo-inositol	-0.074153	-0.17168	0.098868	-0.26122	-0.37109	0.14553	-0.03162	-0.055558
octade canoic acid	-0.154	-0.2357	-0.04669	-0.40776	-0.50473	-0.14236	-0.33538	-0.35336
glutamine	-0.21791	-0.32113	0.069104	-0.30162	-0.47053	-0.17105	-0.39671	-0.41323
threitol	-0.33813	-0.38944	-0.11484	-0.57082	-0.47328	-0.30933	-0.51918	-0.43559
alanine	-0.25892	-0.32165	-0.06398	-0.49064	-0.45773	-0.19857	-0.41394	-0.36408
glucose	-0.14695	-0.22496	-0.29432	-0.55075	-0.74264	-0.48138	-0.53855	-0.62613
inositol	-0.12587	-0.19917	-0.32604	-0.54017	-0.76318	-0.53897	-0.59203	-0.6976
galactose	-0.27307	-0.36018	-0.17847	-0.55831	-0.63723	-0.37653	-0.44724	-0.4571
threonine	-0.2529	-0.33943	-0.2033	-0.57258	-0.65037	-0.36411	-0.40594	-0.42388
hexadecanoic acid	-0.27862	-0.3497	-0.14212	-0.54139	-0.57731	-0.36167	-0.53742	-0.51977
glutamate	-0.30908	-0.38813	-0.15972	-0.58026	-0.60876	-0.37767	-0.50623	-0.4855
arabitol	-0.25792	-0.32546	-0.13958	-0.34633	-0.57255	-0.6198	-0.79241	-0.84067
proline	0.033092	-0.06052	-0.29257	-0.43135	-0.76733	-0.35127	-0.33727	-0.51625
erythritol	0.011365	-0.081389	-0.26602	-0.34844	-0.74589	-0.4571	-0.46145	-0.65167
leucine	0.0068574	-0.072312	-0.32528	-0.41625	-0.78081	-0.5202	-0.55676	-0.73885
lysine	-0.21527	-0.094632	-0.48239	-0.44369	-0.020644	-0.543	-0.37441	-0.23171
valine	0.30295	0.40469		-0.3233	-0.26133	-0.40034	0.091947	-0.044456
glycine	-0.34106	-0.23795		-0.47121	0.22738	-0.054284	0.085212	0.37558
fucose	-0.39377	-0.29309	-0.49035	-0.6928	-0.063021	-0.43593	-0.18544	0.054572
arabinose	-0.38189	-0.27224	-0.39575	-0.60718	0.02656	-0.37914		-0.0028499
fructose	-0.48437	-0.42067	-0.10411	-0.38943	0.24267	-0.11053	0.078041	0.38314
maleic acid	-0.18761	-0.11223	-0.56866	-0.62098	-0.19005	-0.37027	0.032018	
histidine	-0.34331	-0.28839	-0.3463	-0.51094	-0.042126	-0.29668	0.01558	0.19841
hydroxypyruvic acid	0.11835	0.14329	-0.04051	0.36178	0.059011	-0.38342	-0.32938	-0.45548
malonic acid	0.91867	0.91955	-0.25648	0.55379	-0.19866	0.10277	0.35452	-0.13041
succinic acid	1	0.99173	-0.35947	0.3974	-0.32141	0.22965	0.55414	0.04464
gluconic acid	0.99173	1	-0.40604	0.36997	-0.29671	0.19626	0.54738	0.053501
xylose	-0.35947	-0.40604		0.65434	0.82916	0.6816	0.19795	0.471
erythrose	0.3974	0.36997	0.65434	1	0.61662	0.68396	0.49139	0.3687
galactinol	-0.32141	-0.29671	0.82916		1	0.65757	0.33365	0.65558
fumaric acid	0.22965	0.19626		0.68396	0.65757	1	0.82936	0.86115
norvaline	0.55414	0.54738	0.19795	0.49139		0.82936		0.84968
as partic acid	0.04464	0.053501	0.471	0.3687	0.65558	0.86115	0.84968	1

### D. Proteome analysis of pigeonpea seeds under elevated CO<sub>2</sub>

The pigeonpea seed proteome was analyzed through LFQ and identified 1591 proteins in ambient and 2989 proteins in elevated  $CO_2$  grown seed. The raw data was assessed using PLGS software and the proteins with an expression ratio or fold change of  $\leq 0.5$  were considered significantly down-regulated and  $\geq 2$  as significantly upregulated. Among the 4580 proteins identified in both ambient and elevated  $CO_2$  grown pigeonpea seeds, excluding 518 uncharacterized proteins, 517 proteins were expressed in both seeds, among which 115 proteins were down-regulated, and 57 proteins were upregulated in elevated  $CO_2$  grown pigeonpea seed (Fig. 20 a). In comparison, 345 proteins were expressed in both conditions without a significant difference in fold change ratio (0.5-1.9).

## Differentially regulated proteins in pigeonpea seeds under ambient and elevated $CO_2$

Among the significantly upregulated proteins, 50% of proteins were involved in nucleic acid binding, 11% of proteins were uncharacterized, and the other significant proteins fell into categories of metabolic processes (8%), DNA repair (5%), transport (5%) and translation/ transcription (5%) (Fig. 21 a). Among the significantly down-regulated proteins, 46% of proteins were in nucleic acid binding, and the remaining fell into categories like transport (11%), metabolic process (6%), translation/ transcription (8%), and uncharacterized (13%) (Fig. 21 b). Detailed gene ontology of the significant proteins is given in Table. 8. Also, the LFQ data revealed the presence of stress-related proteins like Embryonic DC-8, EMB1, heat shock proteins, and elongation factor 2.

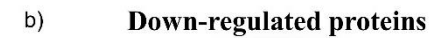
# Exclusive proteins observed in pigeonpea seeds under ambient and elevated CO<sub>2</sub>

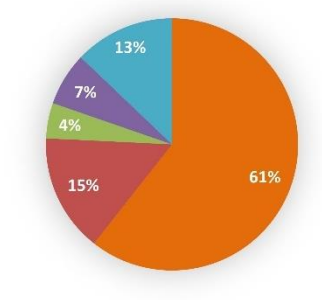
Some proteins were exclusively identified in elevated CO<sub>2</sub> grown pigeonpea seed, like Bowman-Birk type proteinase inhibitor 2 (BBI), Kunitz-type trypsin inhibitorlike 2 protein, Beta-conglycinin, GTP cyclohydrolase 1 (folate biosynthesis), PP2A protein, 4 heat shock cognate 70 kDa proteins, and 11 chaperone proteins. Proteins exclusively observed in elevated seed were characterized into the following categories based on their functions: metabolism (11%), genetic information and environmental sensing and processing (17%), processing (38%), uncharacterized (34%) (Fig. 22 a). Within the elevated seed specific proteins falling in metabolism category, majority were involved in metabolic processes, protein synthesis and modification and also in carbohydrate metabolism (Fig. 23 a). Coming to the proteins observed in genetic information and processing category, majority of them were involved in transcription/ translation (Fig. 23 b). Proteins involved in signal transduction, transport, defense response and chaperone formed major portion in environmental sensing and processing category (Fig. 23 c). Among the proteins identified (genetic information and processing), the majority were transposable element (TE) proteins. It was observed that within TE proteins, majorly occurring were Copia and Gypsy elements. In our data, elevated CO<sub>2</sub> grown seeds showed upregulated levels of these proteins (Fig. 24). Even in proteins exclusively observed in elevated conditions, 45.37% belonged to Copia proteins. On the other hand, proteins observed exclusively in ambient seed were characterized into following: metabolism (13%), genetic information and processing (35%), environmental sensing and processing (30%), uncharacterized

(30%) and unknown (6%) (Fig. 22 b). Ambient seed specific proteins under metabolism: majority fell into metabolic process, carbohydrate metabolism and protein synthesis but the number of proteins were lower comparatively to elevated seed (Fig. 25 a). Similar pattern was observed in proteins in information sensing and processing category, wherein majority were transcription and translation proteins, compared to elevated seed (Fig. 25 b). Considering the proteins in environmental sensing category, majority fell into groups of catalytic activity, metal ion binding followed by proteins in signal transduction (Fig. 25 c). Some of the important proteins exclusively observed in both ambient and elevated seed are depicted in detail in Table 9.

Fig. 20. a) Characterization of the proteome of pigeonpea seed based on significance, b) downregulated proteins in pigeonpea seeds under elevated CO<sub>2</sub>, and c) upregulated proteins in pigeonpea seeds under elevated CO<sub>2</sub> based on their functionality.

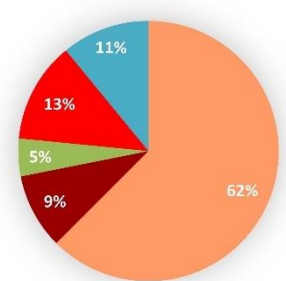
Significantly Up-regulated
 Significantly Down-regulated
 Moderately regulated





- Genetic information processing
- ■Environmental information processing
- Cellular process
- Metabolism
- Uncharacterized

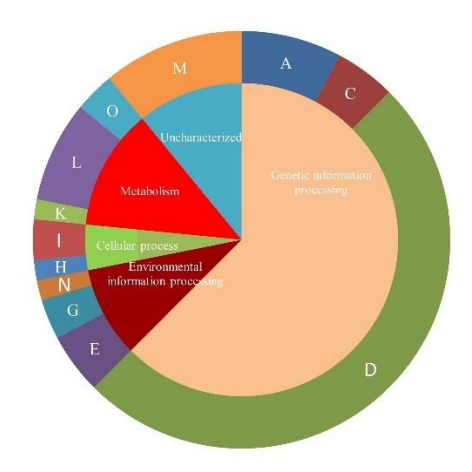
### c) Up-regulated proteins

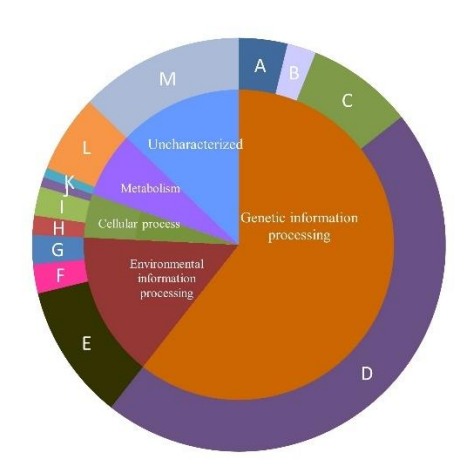


- Genetic information processing
- ■Environmental information processing
- Cellular process
- Metabolism
- Uncharacterized



Fig. 21. a) Gene ontology of upregulated proteins in pigeonpea seed under elevated CO<sub>2</sub> and b) gene ontology of downregulated proteins in pigeonpea seed under elevated CO<sub>2</sub>.





- A- DNA Replication and Repair
- B- Protein Synthesis and

Modification

- C- Transcription/Translation
- D- Nucleic acid binding
- E- Transport
- F- Signal Transduction
- G- Pollination
- H- Cell Division and Regulation
- I- Cytoskeleton
- J- Developmental and Growth
- K- Lipid Metabolism
- L- Metabolic Process
- M- Uncharacterized
- N- Defense Protein
- O- Secondary Metabolite

Table. 8 Description of differentially regulated proteins in seeds collected from ambient and elevated  $CO_2$  grown pigeonpea plants.

Accession	Description	Expressio n ratio	Gene Ontology	Molecula r weight (Da)
		Up regulated		
A0A151TM0 4	Nucleosome-remodeling factor subunit NURF301 family	12.18	Cell division and regulation	177736
A0A151U1R 1	Ankyrin repeat- containing protein At3g12360 family	3.06	Cytoskeleton	81562
A0A151U4U 0	Formin-like protein	4.90	Cytoskeleton	97608
A0A151T389	TMV resistance protein N	3.93	Defense protein	133938
A0A151TLT 2	ATPase family AAA domain-containing protein 3	2.20	DNA replication and repair	68533
A0A151U49 1	Chromodomain- helicase-DNA-binding protein 4	4.80	DNA replication and repair	98895
A0A151RA8 1	Helicase SEN1	10.07	DNA replication and repair	125510
A0A151TIB1	Replication factor C subunit 3	2.53	DNA replication and repair	78986
A0A151UA1 6	Smr domain-containing protein YPL199C	2.22	DNA replication and repair	56620
A0A151RM8 3	Cellulose synthase-like protein H1	7.53	Lipid metabolism	201253
A0A151RR8 7	Copia protein	9.87	Metabolic process	84503
A0A151UIQ 2	Copia protein	3.97	Metabolic process	40123
A0A151R7B 4	Gypsy retrotransposon integrase-like protein 1	4.66	Metabolic process	44139
A0A151R599	Gypsy retrotransposon integrase-like protein 1	11.82	Metabolic process	44365
A0A151SDS 5	Pol polyprotein	5.98	Metabolic process	90197
A0A151SPI1	Retrovirus-related Pol polyprotein from transposon 17.6 (Fragment)	8.93	Nucleic acid binding	61812

	I			1
A0A151R472	Retrovirus-related Pol	7.84	Nucleic acid binding	76329
	polyprotein from			
	transposon 17.6			
	(Fragment)			
A0A151R431	Retrovirus-related Pol	9.58	Nucleic acid binding	78742
	polyprotein from			
	transposon 17.6			
	(Fragment)			
A0A151RU2	Retrovirus-related Pol	5.00	Nucleic acid binding	93369
5	polyprotein from			
	transposon 17.6			
A0A151RNB	Retrovirus-related Pol	3.25	Nucleic acid binding	97135
8	polyprotein from			
	transposon 17.6			
A0A151RLQ	Retrovirus-related Pol	4.30	Nucleic acid binding	87972
0	polyprotein from			
	transposon 17.6			
A0A151RJ02	Retrovirus-related Pol	3.38	Nucleic acid binding	101098
	polyprotein from			
	transposon 17.6			
A0A151RGJ	Retrovirus-related Pol	8.93	Nucleic acid binding	50420
2	polyprotein from			
	transposon 17.6			
A0A151R240	Retrovirus-related Pol	6.23	Nucleic acid binding	50420
	polyprotein from			
	transposon 17.6			
A0A151UIS0	Retrovirus-related Pol	3.85	Nucleic acid binding	89335
	polyprotein from		· ·	
	transposon 17.6			
A0A151UDK	Retrovirus-related Pol	7.09	Nucleic acid binding	78993
5	polyprotein from			
	transposon 17.6			
A0A151UHL	Retrovirus-related Pol	2.43	Nucleic acid binding	80975
8	polyprotein from		· ·	
	transposon 17.6			
A0A151TFX	Retrovirus-related Pol	4.39	Nucleic acid binding	83690
8	polyprotein from			
	transposon 297 family			
	(Fragment)			
A0A151S6B	Retrovirus-related Pol	2.50	Nucleic acid binding	71537
6	polyprotein from		8	
	transposon 297 family			
A0A151R078	Retrovirus-related Pol	17.99	Nucleic acid binding	93774
	polyprotein from		6	
	transposon 297 family			
A0A151QZX	Retrovirus-related Pol	4.95	Nucleic acid binding	30999
3	polyprotein from			
	transposon 297 family			
A0A151TJD	Retrovirus-related Pol	2.22	Nucleic acid binding	36779
5	polyprotein from			
	transposon 412 family			
A0A151TW	Retrovirus-related Pol	2.29	Catalytic activity	42987
X0	polyprotein from	2.27	- 33002 5 40 41 110 5	, , ,
	transposon opus			
	anioposon opus	1		1

A O A 15103 537	D	2.00	NT 1 ' '11' '	21652
A0A151SMX	Retrovirus-related Pol	2.09	Nucleic acid binding	31652
9	polyprotein from			
	transposon TNT 1-94			
A0A151U37	Retrovirus-related Pol	25.02	Nucleic acid binding	93415
0	polyprotein from			
	transposon TNT 1-94			
A0A151UA4	Retrovirus-related Pol	7.92	Nucleic acid binding	98113
1	polyprotein from			
	transposon TNT 1-94			
A0A151RY8	Retrovirus-related Pol	2.18	Nucleic acid binding	180702
3	polyprotein from			
	transposon TNT 1-94			
A0A151RKR	Retrovirus-related Pol	9.11	Nucleic acid binding	67299
1	polyprotein from			
	transposon TNT 1-94			
A0A151R0I4	Retrovirus-related Pol	9.20	Nucleic acid binding	47577
	polyprotein from			
	transposon TNT 1-94			
A0A151QSZ	Retrovirus-related Pol	2.22	Nucleic acid binding	168646
9	polyprotein from			
	transposon TNT 1-94			
A0A151QRU	Retrovirus-related Pol	2.18	Nucleic acid binding	176217
6	polyprotein from			
	transposon TNT 1-94			
A0A151SR2	Transposon Ty3-G Gag-	11.13	Nucleic acid binding	40125
3	Pol polyprotein	11110	Tradition work officially	.0120
A0A151R2B	Transposon Ty3-G Gag-	3.63	Nucleic acid binding	146534
7	Pol polyprotein	5.05	reactive deta billating	110331
A0A151U1Y	Transposon Ty3-I Gag-	7.17	Nucleic acid binding	83762
6	Pol polyprotein	7.17	rucicie acia bilianig	03702
A0A151TWT	Transposon Ty3-I Gag-	2.24	Nucleic acid binding	40208
6	Pol polyprotein	2.24	reduction acid billiams	40200
A0A151TAN	Transposon Ty3-I Gag-	3.66	Nucleic acid binding	82944
1	Pol polyprotein	3.00	Nucleic acid billuling	02344
A0A151RTT		6 5 5	Nucleic acid binding	106951
0	Transposon Ty3-I Gag- Pol polyprotein	0.55	Nucleic acid billuling	100931
A0A151SJP5	Putative	2.06	Pollination	88746
AUAISISJES		3.06	Poliliation	00/40
	serine/threonine-protein			
A O A 151DIZE	kinase receptor	2.11	Pollination	176560
A0A151RKT	Putative	2.11	Pollination	176562
0	serine/threonine-protein			
AOA151DOX	kinase receptor	0.40	C1. 1.1.	00040
A0A151RCK	4-hydroxy-3-methylbut-	9.48	Secondary metabolite	82243
5	2-en-1-yl diphosphate			
1011515	synthase		~	44600
A0A151RHR	Anthocyanidin 3-O-	2.55	Secondary metabolite	41398
5	glucosyltransferase 5			
A0A151T3Z	DEAD-box ATP-	2.97	Transcription/translati	65952
5	dependent RNA helicase		on	
	35			
A0A151TQ5	RNA-binding protein 39	2.09	Transcription/translati	65129
9			on	
A0A151SW6	U5 small nuclear	3.70	Transcription/translati	243517
3	ribonucleoprotein		on	
	-			

A0A151U2E	Kinesin-4	2.88	Transport	119912
5	Kinesiii-4	2.00	Transport	119912
A0A151SA2	Phospholipid-	2.38	Transport	132094
8	transporting ATPase		_	
A0A151RG3	Pleiotropic drug	4.05	Transport	163584
2	resistance protein 1			
		Down-		
AOA151CAD	N1	regulated	C-11 4' 1	170006
A0A151SAR 8	Nucleosome-remodeling factor subunit BPTF	0.18	Cell division and	170906
A0A151TL9	Protein BRUSHY 1	0.18	regulation Cell division and	145430
8	Trotelli DRUSITT 1	0.16	regulation	143430
A0A151SJL2	Laminin subunit alpha-2	0.12	Cytoskeleton	102292
A0A151RNK	Myosin-J heavy chain	0.040	Cytoskeleton	180019
9	(Fragment)	0.0.0	ey toshereton	10001)
A0A151RJM	Myosin-J heavy chain	0.38	Cytoskeleton	173912
6			Ž	
A0A151S2D	Putative callose synthase	0.29	Developmental and	226966
2	8		growth	
A0A151R4U	DNA repair protein	0.33	DNA repair	142085
1	UVH3			
A0A151U0L	80 kDa MCM3-	0.19	DNA replication	145893
4	associated protein			
A0A151TAZ	(Fragment)	0.051	DNA manlication	173940
2	ATP-dependent helicase BRM	0.051	DNA replication	173940
A0A151QM	DNA polymerase	0.42	DNA replication	119416
R6	(Fragment)	0.12	Brarreprieuron	117110
A0A151TIH4	DNA polymerase	0.48	DNA replication	161913
A0A151RJ86	1-phosphatidylinositol-	0.48	Lipid metabolism	184908
	3-phosphate 5-kinase			
	FAB1			
A0A151TY	Gypsy retrotransposon	0.14	Metabolic process	42894
W6	integrase-like protein 1	0.15	36 . 1 . 12	55051
A0A151QP2 4	Gypsy retrotransposon integrase-like protein 1	0.17	Metabolic process	66861
A0A151RM	Pentatricopeptide repeat-	0.25	Metabolic process	79730
B4	containing protein		r	
	At4g18520 family			
	(Fragment)			
A0A151SI04	Putative GMC-type	0.43	Metabolic process	89203
	oxidoreductase			
	Rv0492c/MT0511/MT0			
A0A151SN6	512 family	0.22	Motobolio process	79225
9	Retrotransposable element Tf2	0.22	Metabolic process	19223
A0A151TXZ	Retrotransposable	0.364	Metabolic process	146242
2	element Tf2	0.504	1.10th offer process	110212
A0A151T2V	Retrotransposable	0.218	Metabolic process	141443
2	element Tf2		1	
A0A151S7C	Retrotransposable	0.21	Metabolic process	76929
1	element Tf2			
A0A151RQ4	Polyprotein	0.35	Nucleic acid binding	64503
4				

	T				<del>, , , , , , , , , , , , , , , , , , , </del>
A0A151SC5 9	Pro-Pol polyprotein		0.14	Nucleic acid binding	42557
A0A151SJW	Retrovirus-related	Pol	0.16	Nucleic acid binding	71298
8	polyprotein	from			
	transposon	17.6			
	(Fragment)				
A0A151TQ	Retrovirus-related	Pol	0.37	Nucleic acid binding	36264
M1	polyprotein	from			
	transposon	17.6			
	(Fragment)				
A0A151R1B	Retrovirus-related	Pol	0.37	Nucleic acid binding	94518
0	polyprotein	from			
	transposon	17.6			
	(Fragment)				
A0A151QRG	Retrovirus-related	Pol	0.41	Nucleic acid binding	114087
4	polyprotein	from			
	transposon	17.6			
	(Fragment)				
A0A151SGN	Retrovirus-related	Pol	0.35	Nucleic acid binding	42810
0	polyprotein	from			
	transposon 17.6				
A0A151SIG4	Retrovirus-related	Pol	0.14	Nucleic acid binding	34010
	polyprotein	from			
	transposon 17.6				
A0A151SMN	Retrovirus-related	Pol	0.26	Nucleic acid binding	42325
2	polyprotein	from			
	transposon 17.6				
A0A151T8F3	Retrovirus-related	Pol	0.44	Nucleic acid binding	128555
	polyprotein	from			
	transposon 17.6				
A0A151TBE	Retrovirus-related	Pol	0.24	Nucleic acid binding	86968
7	polyprotein	from			
	transposon 17.6				
A0A151S2M	Retrovirus-related	Pol	0.22	Nucleic acid binding	114773
2		from			
	transposon 17.6				
A0A151R646	Retrovirus-related	Pol	0.15	Nucleic acid binding	95368
	polyprotein	from			
	transposon 17.6				
A0A151SIP0	Retrovirus-related	Pol	0.36	Nucleic acid binding	95356
	polyprotein	from			
	transposon 297 fami	_			
A0A151SJW	Retrovirus-related	Pol	0.44	Nucleic acid binding	72160
0	1 4 1	from			
	transposon 297 fami	_			
A0A151U27	Retrovirus-related	Pol	0.18	Nucleic acid binding	86146
0	polyprotein	from			
	transposon 297 fami				
A0A151U4B	Retrovirus-related	Pol	0.15	Nucleic acid binding	43381
7		from			
	transposon 297 fami	_			
A0A151TDJ	Retrovirus-related	Pol	0.14	Nucleic acid binding	52907
2	polyprotein	from			
	transposon 297 fami	ily			

A0A151TL0	Retrovirus-related Pol	0.14	Nucleic acid binding	96482
1	polyprotein from	0.11	Tractore acra omanig	70102
	transposon 297 family			
A0A151SFD	Retrovirus-related Pol	0.21	Nucleic acid binding	77152
5	polyprotein from		_	
	transposon 297 family			
A0A151S7F6	Retrovirus-related Pol	0.15	Nucleic acid binding	43098
	polyprotein from			
101151700	transposon 297 family	0.10	X 1 1 1 1 1 1 1 1 1 1 1 1 1 1 1 1 1 1 1	00.50.5
A0A151RC9	Retrovirus-related Pol	0.18	Nucleic acid binding	88685
3	polyprotein from			
	transposon 297 family			
A0A151QT9	Retrovirus-related Pol	0.21	Nucleic acid binding	64389
8	polyprotein from			
1011510370	transposon 297 family	0.053	N. 1.1.1.1.1.1.1.1.1.1.1.1.1.1.1.1.1.1.1	120051
A0A151QNG	Retrovirus-related Pol	0.072	Nucleic acid binding	120874
0	polyprotein from			
A0A151RZN	transposon 297 family Retrovirus-related Pol	0.26	Muship said hinding	27295
6		0.36	Nucleic acid binding	37285
O	polyprotein from transposon 412 family			
A0A151TRI9	Retrovirus-related Pol	0.15	Nucleic acid binding	28944
AUAIJIIKI	polyprotein from	0.13	Trucicie acid biliding	20744
	transposon opus			
	(Fragment)			
A0A151QYZ	Retrovirus-related Pol	0.14	Nucleic acid binding	84668
9	polyprotein from			
	transposon opus			
	(Fragment)			
A0A151QZ8	Retrovirus-related Pol	0.14	Nucleic acid binding	50647
3	polyprotein from			
	transposon opus			
A0A151SM4	(Fragment) Retrovirus-related Pol	0.007	Musicia said hindina	75670
1 AUA1515M4		0.097	Nucleic acid binding	75679
1	polyprotein from transposon opus			
A0A151QSB	Retrovirus-related Pol	0.39	Nucleic acid binding	103792
3	polyprotein from	0.57	Truciere dela omanig	103772
	transposon opus			
A0A151SGE	Retrovirus-related Pol	0.35	Nucleic acid binding	52462
0	polyprotein from			
	transposon TNT 1-94			
	(Fragment)			
A0A151SGI0	Retrovirus-related Pol	0.33	Nucleic acid binding	63514
	polyprotein from			
1011517757	transposon TNT 1-94	0.25	NY 1 ' '11' ''	141002
A0A151U6I4	Retrovirus-related Pol	0.27	Nucleic acid binding	141093
	polyprotein from			
A0A151TIH6	transposon TNT 1-94 Retrovirus-related Pol	0.47	Muolojo ooid hindina	149803
AUAISIIIHO	polyprotein from	0.47	Nucleic acid binding	147003
	transposon TNT 1-94			
	1 ansposon 1111 1-34			1

A0A151SW	Retrovirus-related Pol	0.094	Nucleic acid binding	50544
U4		0.094	Nucleic acid billuling	30344
04	polyprotein from transposon TNT 1-94			
A0A151T469	Retrovirus-related Pol	0.40	Nucleic acid binding	149631
A0A1311409		0.40	Nucleic acid billding	149031
	1 71			
A O A 1 5 1 5 D A	transposon TNT 1-94	0.41	NY 1 ' '11' 1'	1.52.400
A0A151TM	Retrovirus-related Pol	0.41	Nucleic acid binding	152499
N9	polyprotein from			
	transposon TNT 1-94			
A0A151UG5	Retrovirus-related Pol	0.103	Nucleic acid binding	92507
1	polyprotein from			
	transposon TNT 1-94			
A0A151QSG	Retrovirus-related Pol	0.092	Nucleic acid binding	90699
1	polyprotein from			
	transposon TNT 1-94			
A0A151QNH	Retrovirus-related Pol	0.41	Nucleic acid binding	152572
5	polyprotein from			
	transposon TNT 1-94			
A0A151T557	Transposon Ty3-G Gag-	0.15	Nucleic acid binding	72272
	Pol polyprotein			
	(Fragment)			
A0A151STZ	Transposon Ty3-G Gag-	0.15	Nucleic acid binding	54885
9	Pol polyprotein			
A0A151U30	Transposon Ty3-G Gag-	0.14	Nucleic acid binding	40175
4	Pol polyprotein	0.1	Tradicio acia cinama	10176
A0A151TXF	Transposon Ty3-G Gag-	0.46	Nucleic acid binding	129374
8	Pol polyprotein	0.10	r tactere acta omanig	12/5/
A0A151T9U	Transposon Ty3-G Gag-	0.14	Nucleic acid binding	22064
5	Pol polyprotein	0.11	reactive dela bilianing	22001
A0A151RAU	Transposon Ty3-G Gag-	0.18	Nucleic acid binding	53241
0	Pol polyprotein	0.10	rucicie acia bilianig	33241
A0A151R7E	Transposon Ty3-G Gag-	0.15	Nucleic acid binding	31694
7	Pol polyprotein	0.13	reduction acid billiams	31074
A0A151SJG9	Transposon Ty3-I Gag-	0.44	Nuclaia said hinding	82573
AUAISISIU9		0.44	Nucleic acid binding	82373
A O A 1511150	Pol polyprotein	0.14	Nt 1 . 1 1 1 1 . 1	60.420
A0A151U58	Transposon Ty3-I Gag-	0.14	Nucleic acid binding	69439
3	Pol polyprotein	0.17	NT 1 ' '11' 1'	7.672.4
A0A151U5F	Transposon Ty3-I Gag-	0.17	Nucleic acid binding	76734
5	Pol polyprotein	0.06	NY 1 ' '11' 1'	111227
A0A151SVB	Transposon Ty3-I Gag-	0.26	Nucleic acid binding	111227
2	Pol polyprotein			10110-
A0A151SZI9	Transposon Ty3-I Gag-	0.36	Nucleic acid binding	124400
	Pol polyprotein			1
A0A151T6G	Transposon Ty3-I Gag-	0.23	Nucleic acid binding	133793
8	Pol polyprotein			
A0A151TDG	Transposon Ty3-I Gag-	0.17	Nucleic acid binding	55327
1	Pol polyprotein			
A0A151UBN	Transposon Ty3-I Gag-	0.14	Nucleic acid binding	29030
4	Pol polyprotein			
A0A151TL3	Transposon Ty3-I Gag-	0.14	Nucleic acid binding	31463
4	Pol polyprotein			
A0A151SDD	Transposon Ty3-I Gag-	0.49	Nucleic acid binding	98090
3	Pol polyprotein			
				•

A0A151RGY	Transposon Ty3-I Gag-	0.29	Nucleic acid binding	142462
6	Pol polyprotein			
A0A151RE1	Transposon Ty3-I Gag-	0.14	Nucleic acid binding	32828
9	Pol polyprotein			
A0A151R4E	Transposon Ty3-I Gag-	0.46	Nucleic acid binding	133804
2	Pol polyprotein			
A0A151R1H	Transposon Ty3-I Gag-	0.28	Nucleic acid binding	59845
7	Pol polyprotein			
A0A151S126	Putative	0.36	Pollination	93988
	serine/threonine-protein			
	kinase receptor			
A0A151RGA	Putative	0.30	Pollination	90922
5	serine/threonine-protein			
	kinase receptor			
A0A151RFX	Putative	0.25	Pollination	92612
8	serine/threonine-protein			
	kinase receptor			
A0A151SR1	Cysteine-rich receptor-	0.41	Protein synthesis and	195414
9	like protein kinase 19		modification	
A0A151T7Z	Protein VPRBP	0.38	Protein synthesis and	180268
7			modification	
A0A151U72	UDP-	0.41	Protein synthesis and	155332
4	glucose:glycoprotein	0.11	modification	100002
•	glucosyltransferase 1			
A0A151RT	E3 ubiquitin-protein	0.17	Signal transduction	178185
W9	ligase KEG (Fragment)	0.17	Signal transaction	170103
A0A151U4R	E3 ubiquitin-protein	0.37	Signal transduction	225413
9	ligase UBR2	0.57	Signal transaction	223 113
A0A151SJR2	Signal transduction	0.29	Signal transduction	105046
7107113133112	histidine-protein kinase	0.27	Signal transaction	105010
	barA (Fragment)			
A0A151SLS	Bromodomain and WD	0.19	Transcription/translati	148647
2	repeat-containing protein	0.17	on	140047
2	2		OII	
A0A151TX9	DEAD-box ATP-	0.33	Transcription/translati	83/130
2	dependent RNA helicase	0.55	on	03437
2	3		OII	
A0A151RDL	Elongation factor 2	0.27	Transcription/translati	94205
0	Liongation factor 2	0.27	on	77203
A0A151SB2	Endoribonuclease Dicer	0.38	Transcription/translati	122947
2	isogeny 2a	0.30	on	144741
A0A151QQH		0.22	Transcription/translati	132411
	Hybrid signal transduction histidine	0.22	•	132411
1	kinase J		on	
A0A151SRZ		0.41	Transcription/translati	124191
	Phytochrome	0.41	Transcription/translati	124191
8 A0A151RDD	DING finger and CHY	0.27	On Transarintian/translati	35746
	RING finger and CHY	0.37	Transcription/translati	33740
7	zinc finger domain-		on	
A0 A 151TDE	containing protein 1	0.40	Tuono oninti //1 · ·	106070
A0A151TDF	RNA-binding protein	0.48	Transcription/translati	106979
6	12B	0.40	on	120204
A0A151S591	RNA-dependent RNA	0.48	Transcription/translati	130284
	polymerase		on	

A0A151QTD	Transcription initiation	0.30	Transcription/translati	200996
8	factor TFIID subunit 1-A		on	
A0A151R8H	Zinc finger CCCH	0.19	Transcription/translati	84791
3	domain-containing		on	
	protein 55			
A0A151UIF5	ABC transporter C	0.45	Transport	42432
	family member 10		•	
A0A151RXF	Chromosome-associated	0.48	Transport	118524
4	kinesin KIF4A		•	
A0A151RYB	Clathrin heavy chain	0.30	Transport	192123
2			•	
A0A151U5W	Exocyst complex	0.25	Transport	124128
1	component SEC5		•	
A0A151TW	K(+)/H(+) antiporter 13	0.39	Transport	88251
C8			1	
A0A151SSD	Kinesin-like protein	0.30	Transport	229767
3	KIF15		•	
A0A151RAG	Kinesin-like protein	0.24	Transport	109965
4	•		•	
A0A151TUE	Kinesin-related protein	0.25	Transport	121631
5	11		•	
A0A1S5RW5	Protein TIC 214	0.34	Transport	113166
2			•	
A0A151RSS	Putative copper-	0.48	Transport	93797
9	transporting ATPase		•	
	PAA1			
A0A151R416	Putative xyloglucan	0.39	Transport	76084
	glycosyltransferase 5		•	
A0A151T6A	Sodium/hydrogen	0.31	Transport	81790
2	exchanger		1	
A0A151TXS	Vacuolar protein sorting-	0.40	Transport	80030
7	associated protein 52		1	
	isogeny			
A0A151UAB	Vesicle-fusing ATPase	0.16	Transport	80527
9				

Fig. 22. a) Gene ontology of proteins exclusively expressed in elevated  $CO_2$  grown pigeonpea seeds and b) Gene ontology of proteins exclusively expressed in ambient  $CO_2$  grown pigeonpea seeds.

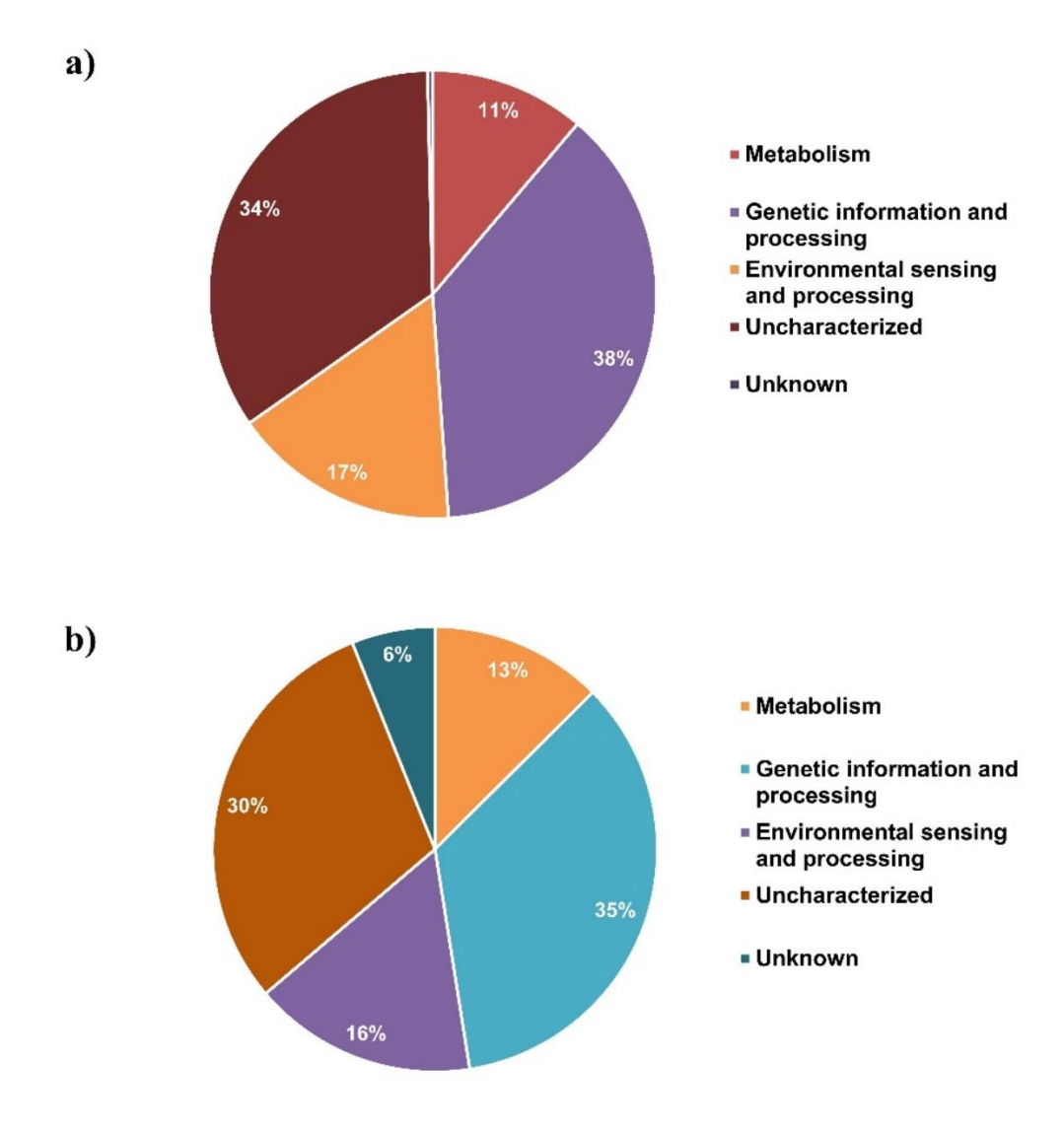
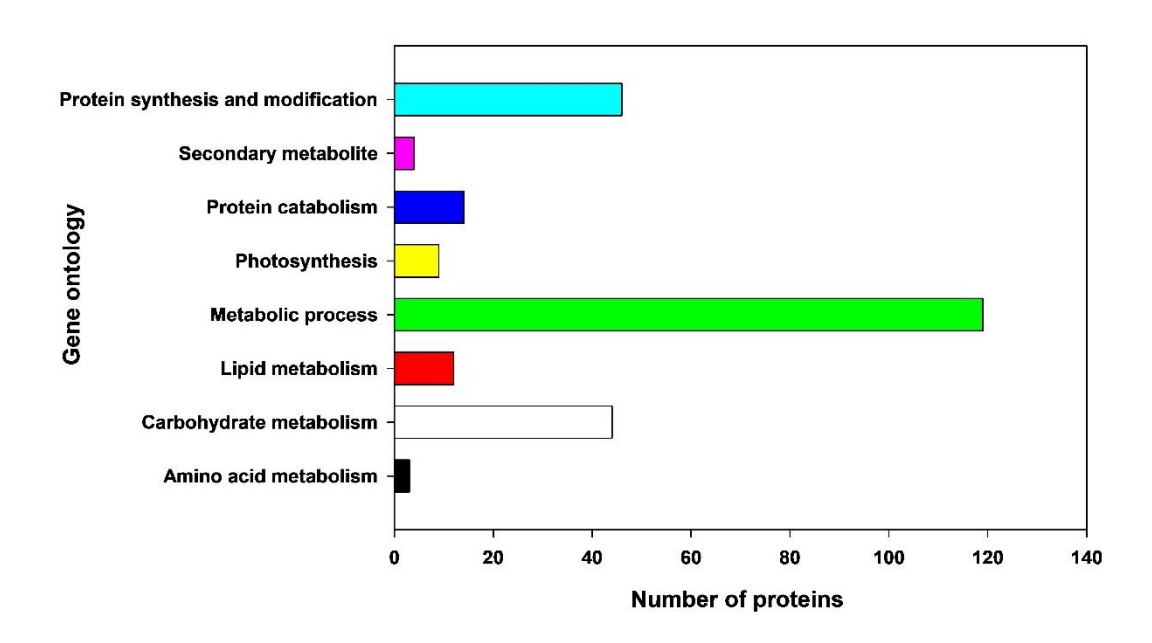
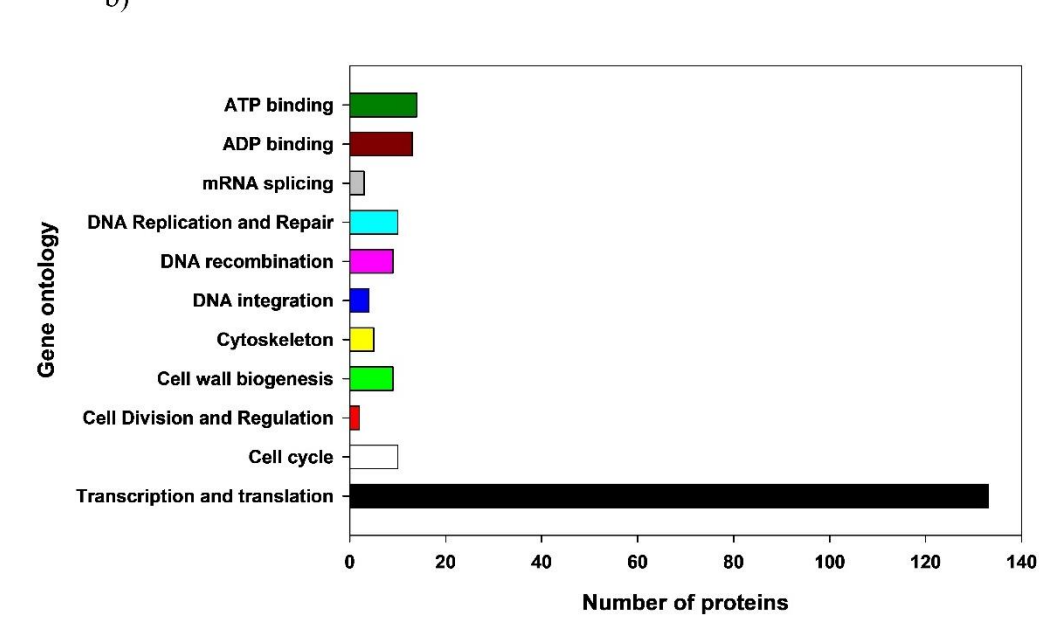


Fig. 23. Functional characterization of elevated seed specific proteins within each category of gene ontology a) Metabolism, b) Genetic information and processing and c) Environmental sensing and processing.

a)



b)



c)

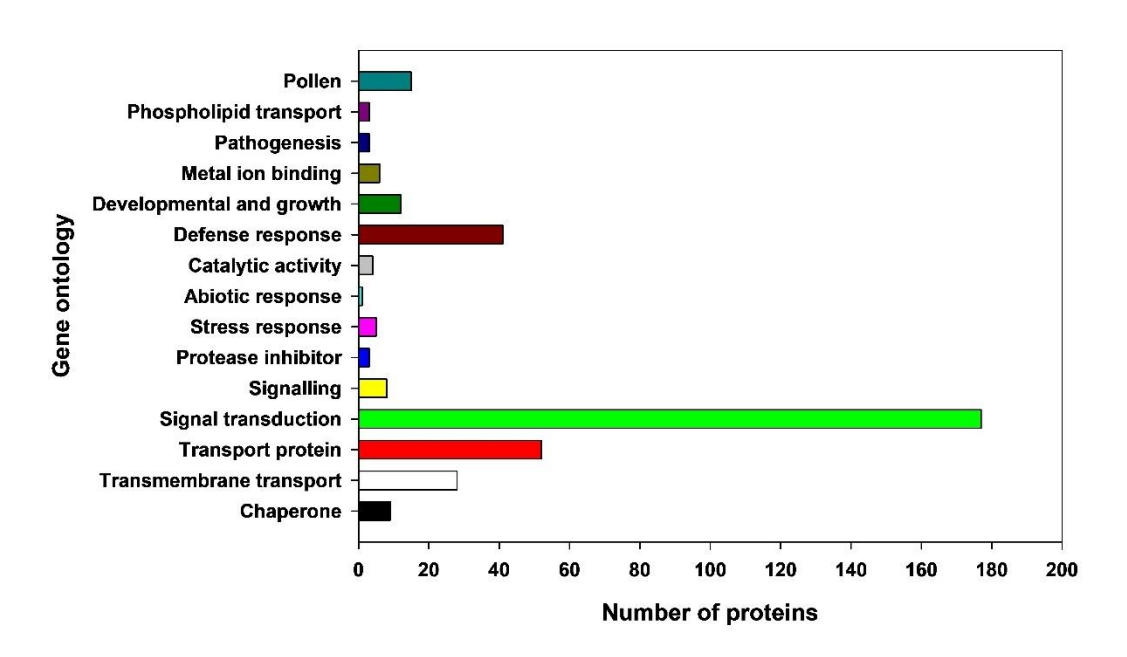


Fig. 24. Total transposon elements (TEs) exclusively expressed in ambient and elevated  $CO_2$  grown seeds.

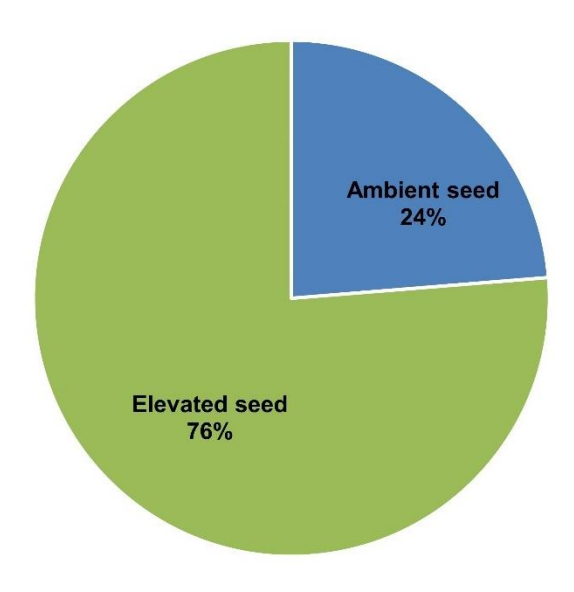
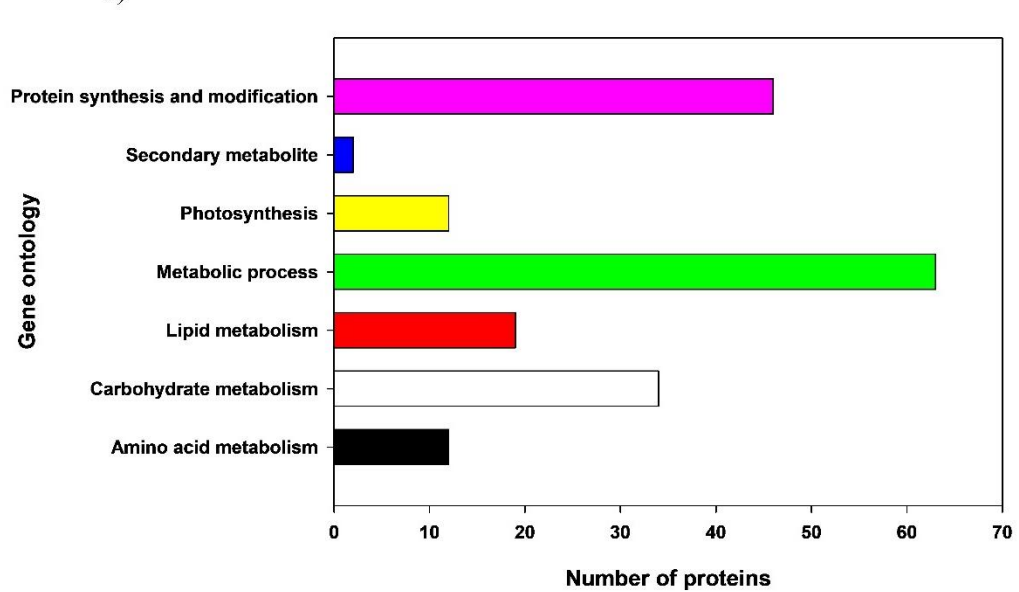
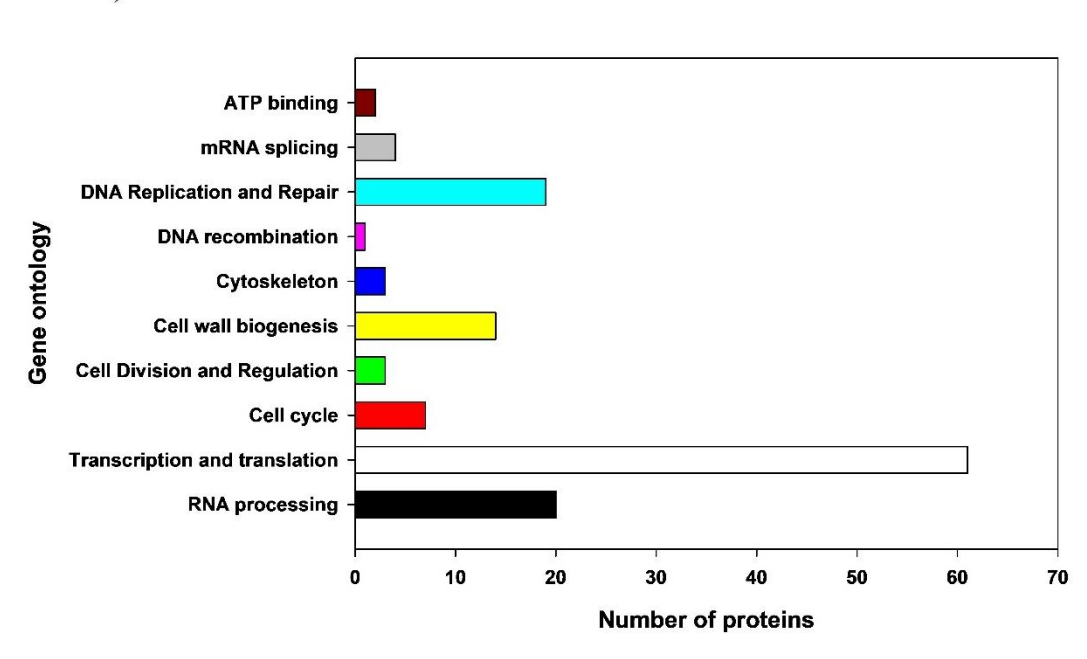


Fig. 25. Functional characterization of ambient seed specific proteins within each category of gene ontology a) Metabolism, b) Genetic information and processing and c) Environmental sensing and processing.

a)



b)



c)

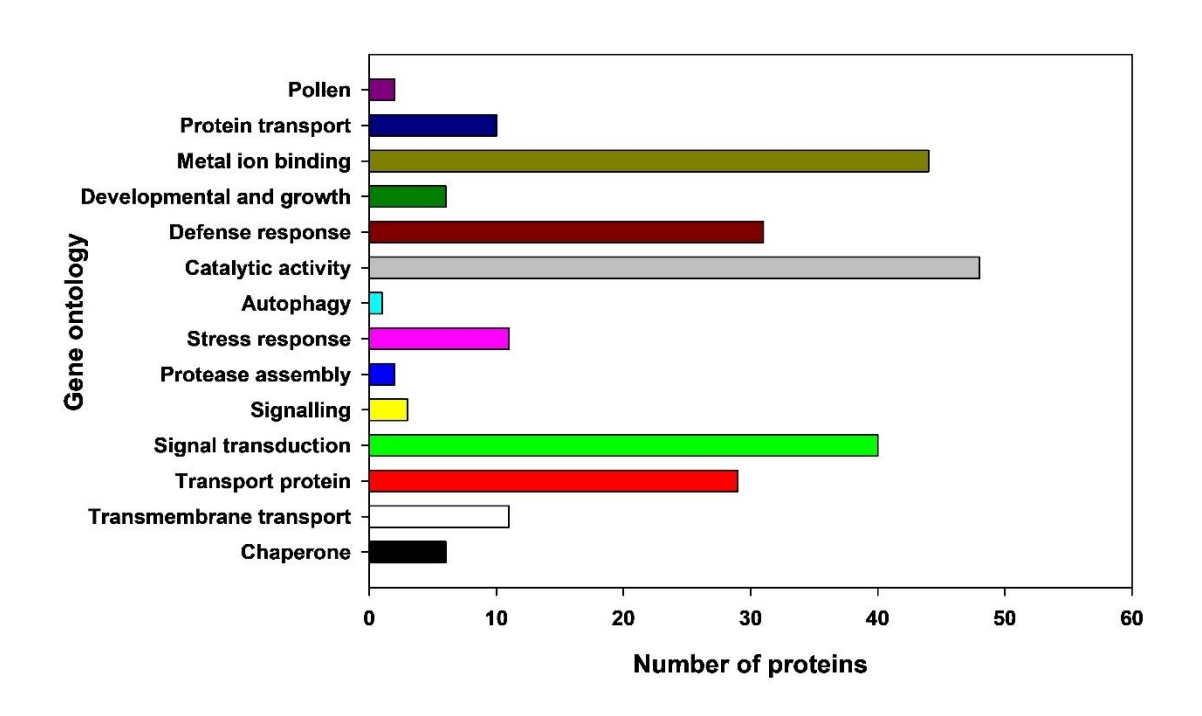


Table. 9 Gene ontology for proteins exclusively observed in ambient and elevated  $CO_2$  grown seeds.

Accession Number	Name	PLGS score	Gene ontology
	Elevated seed specific	proteins	l
A0A151RAR0	3-dehydroquinate synthase OS=Cajanus cajan OX=3821 GN=KK1_039040 PE=4 SV=1	143.04	Amino Acid Metabolism
A0A151SYE0	D-3-phosphoglycerate dehydrogenase OS=Cajanus cajan OX=3821 GN=KK1_015266 PE=3 SV=1	67.68	Amino Acid Metabolism
A0A151STU4	Aminomethyltransferase OS=Cajanus cajan OX=3821 GN=KK1_004552 PE=3 SV=1	79.94	Amino Acid Metabolism
A0A151R0U9	CTP synthase OS=Cajanus cajan OX=3821 GN=KK1_042698 PE=3 SV=1	50.63	Amino Acid Metabolism
A0A151U0J0	Dihydroxy-acid dehydratase OS=Cajanus cajan OX=3821 GN=KK1_005445 PE=4 SV=1	68.69	Amino Acid Metabolism
A0A151QM73	Phenylalanine ammonia-lyase OS=Cajanus cajan OX=3821 GN=KK1_048381 PE=3 SV=1	62.23	Amino Acid Metabolism
A0A151RU51	Selenocysteine methyltransferase OS=Cajanus cajan OX=3821 GN=KK1_032377 PE=4 SV=1	41.18	Amino Acid Metabolism
A0A151R901	Tyrosine/DOPA decarboxylase 2 OS=Cajanus cajan OX=3821 GN=KK1_039618 PE=3 SV=1	41.65	Amino Acid Metabolism
A0A151SQY8	Alpha,alpha-trehalose- phosphate synthase [UDP- forming] 1 OS=Cajanus cajan OX=3821 GN=KK1_003420 PE=4 SV=1	20.09	Carbohydrate Metabolism
A0A151TPM1	Alpha,alpha-trehalose- phosphate synthase [UDP- forming] 1 OS=Cajanus cajan OX=3821 GN=KK1_022643 PE=4 SV=1	19.2	Carbohydrate Metabolism
A0A151U764	Alpha,alpha-trehalose- phosphate synthase [UDP- forming] 5 OS=Cajanus cajan	38.22	Carbohydrate Metabolism

	OX=3821 GN=KK1_007832		
	PE=4 SV=1		
A0A151SUB4	NADP-specific glutamate	27.46	Carboxylic Acid
	dehydrogenase OS=Cajanus		Metabolism
	cajan OX=3821		
	GN=KK1_013765 PE=3 SV=1	21.50	
A0A151SJ95	Serine	24.59	Carboxylic Acid
	hydroxymethyltransferase		Metabolism
	OS=Cajanus cajan OX=3821		
10115150	GN=KK1_001072 PE=3 SV=1	17.4	0 1 1 4 1
A0A151SQI9	Serine	17.4	Carboxylic Acid
	hydroxymethyltransferase		Metabolism
	OS=Cajanus cajan OX=3821		
A O A 171D 0 CO	GN=KK1_003263 PE=3 SV=1	112.54	C + 1 + A + · · ·
A0A151R860	Histone-lysine N-	113.54	Catalytic Activity
	methyltransferase ATXR5		
	OS=Cajanus cajan OX=3821		
A0A151TCE6	GN=KK1_039920 PE=4 SV=1	64.11	Chanana
AUAISTICE6	Chaperone protein clpB 2	04.11	Chaperone
	OS=Cajanus cajan OX=3821 GN=KK1_019326 PE=3 SV=1		
A0A151T007		21.12	Chanarana
A0A1311007	Chaperone protein clpB 2 OS=Cajanus cajan OX=3821	21.12	Chaperone
	GN=KK1_022771 PE=3 SV=1		
A0A151SIV5	Chaperone protein dnaJ	83.04	Chanarana
AUAISISIVS	OS=Cajanus cajan OX=3821	63.04	Chaperone
	GN=KK1_000916 PE=4 SV=1		
A0A151TQC9	Chaperone protein dnaJ	68.83	Chaperone
AUAI311QC)	OS=Cajanus cajan OX=3821	00.03	Chaperone
	GN=KK1_008446 PE=4 SV=1		
A0A151U2B4	GrpE protein homolog	244.35	Chaperone
110111310201	OS=Cajanus cajan OX=3821	211.55	Chaperone
	GN=KK1_006072 PE=3 SV=1		
A0A151U133	Peroxidase OS=Cajanus cajan	32.31	Defence Protein
110111010100	OX=3821 GN=KK1_005563	32.31	Berence Frotein
	PE=3 SV=1		
A0A151U418	Peroxidase OS=Cajanus cajan	6.33	Defence Protein
	OX=3821 GN=KK1_006703	5.5.5	
	PE=3 SV=1		
A0A151SYE5	Phototropin-2 OS=Cajanus	13.68	Defence Protein
	cajan OX=3821		
	GN=KK1_015251 PE=4 SV=1		
A0A151QYP6	Putative disease resistance	39.82	Defence Protein
	protein At1g50180 family		
	OS=Cajanus cajan OX=3821		
	GN=KK1_043526 PE=3 SV=1		
A0A151QY87	GTP cyclohydrolase 1	167.61	Folate
	OS=Cajanus cajan OX=3821		Biosynthesis
	GN=KK1_043694 PE=4 SV=1		
A0A151U867	3-ketoacyl-CoA synthase	48.9	Lipid Metabolism
	OS=Cajanus cajan OX=3821		
	GN=KK1_008149 PE=3 SV=1		

A0A151RRP6	Acyl-coenzyme A oxidase	29.67	Lipid Metabolism
	OS=Cajanus cajan OX=3821		
	GN=KK1_033226 PE=3 SV=1		
A0A151TCK8	Phospholipase D OS=Cajanus	18.97	Lipid Metabolism
	cajan OX=3821		
	GN=KK1_019396 PE=3 SV=1		
A0A151TMF0	Putative fatty-acidCoA ligase	18.57	Lipid Metabolism
	fadD25 OS=Cajanus cajan		
	OX=3821 GN=KK1_021862		
	PE=4 SV=1		
A0A151T9B8	Lipoxygenase OS=Cajanus	166.47	Lipid Metabolism
	cajan OX=3821		
	GN=KK1_018218 PE=3 SV=1		
A0A151S7X7	Abscisic acid 8'-hydroxylase 4	60.9	Metabolic Process
	OS=Cajanus cajan OX=3821		
	GN=KK1_027249 PE=3 SV=1		
A0A151TVH6	Abscisic-aldehyde oxidase	63.51	Metabolic Process
	OS=Cajanus cajan OX=3821		
	GN=KK1_010306 PE=4 SV=1		
A0A151TVQ2	Abscisic-aldehyde oxidase	28.58	Metabolic Process
	OS=Cajanus cajan OX=3821		
	GN=KK1_010307 PE=4 SV=1		
A0A151SIC5	Copia protein OS=Cajanus	254.27	Metabolic Process
	cajan OX=3821		
	GN=KK1_000724 PE=4 SV=1		
A0A151U7W7	Cytokinin dehydrogenase 7	14.79	Metabolic Process
	OS=Cajanus cajan OX=3821		
	GN=KK1_008104 PE=4 SV=1		
A0A151U4D1	Putative E3 ubiquitin-protein	286.02	Metal Ion Binding
	ligase MGRN1 OS=Cajanus		
	cajan OX=3821		
	GN=KK1_006756 PE=4 SV=1		
A0A151T2M7	Glycine-rich RNA-binding	175.61	Nucleic Acid
	protein 10 OS=Cajanus cajan		Binding
	OX=3821 GN=KK1_023744		
	PE=4 SV=1		
A0A151TU78	Gypsy retrotransposon	164.06	Nucleic Acid
	integrase-like protein 1		Binding
	OS=Cajanus cajan OX=3821		
	GN=KK1_009781 PE=4 SV=1		
A0A151SK33	Pol polyprotein OS=Cajanus	12.15	Nucleic Acid
	cajan OX=3821		Binding
	GN=KK1_001403 PE=4 SV=1		
A0A151T8Q4	Retrotransposable element Tf2	9.74	Nucleic Acid
	OS=Cajanus cajan OX=3821		Binding
	GN=KK1_017975 PE=4 SV=1		
A0A151TSW2	Transposon Ty3-G Gag-Pol	143.41	Nucleic Acid
	polyprotein OS=Cajanus cajan		Binding
	OX=3821 GN=KK1_009322		
	PE=4 SV=1		
A0A151U6Q2	Beta-conglycinin, alpha chain	15.29	Nutrient Reservoir
	OS=Cajanus cajan OX=3821		
	GN=KK1_007701 PE=4 SV=1		

A0A151RI37	Bowman-Birk type proteinase inhibitor 2 OS=Cajanus cajan OX=3821 GN=KK1_036324 PE=3 SV=1	248.84	Protease Inhibitor
A0A151R1S0	Kunitz-type trypsin inhibitor- like 2 protein (Fragment) OS=Cajanus cajan OX=3821 GN=KK1_042342 PE=4 SV=1	27.61	Protease Inhibitor
A0A151QUM0	Kunitz-type trypsin inhibitor- like 2 protein OS=Cajanus cajan OX=3821 GN=KK1_045118 PE=4 SV=1	233.81	Protease Inhibitor
A0A151S3U1	Putative proline-rich protein 21 OS=Cajanus cajan OX=3821 GN=KK1_028839 PE=4 SV=1	42.27	Protein Synthesis and Modification
A0A151R8G7	Cucumisin OS=Cajanus cajan OX=3821 GN=KK1_039794 PE=4 SV=1	1.5	Proteolysis
A0A151TL71	Vignain OS=Cajanus cajan OX=3821 GN=KK1_024098 PE=3 SV=1	71.34	Proteolysis
A0A151RSQ1	DNA mismatch repair protein Mlh1 OS=Cajanus cajan OX=3821 GN=KK1_032871 PE=4 SV=1	126.89	Repair
A0A151RN19	DNA repair helicase UVH6 OS=Cajanus cajan OX=3821 GN=KK1_034589 PE=4 SV=1	107.1	Repair
A0A151SY02	Pre-mRNA-splicing factor ISY1 isogeny OS=Cajanus cajan OX=3821 GN=KK1_015089 PE=4 SV=1	106.96	RNA Processing
A0A151TBX0	Putative dihydroflavonol-4- reductase OS=Cajanus cajan OX=3821 GN=KK1_019123 PE=4 SV=1	45.45	Secondary Metabolite
A0A151RM92	Taxadien-5-alpha-ol O- acetyltransferase OS=Cajanus cajan OX=3821 GN=KK1_034865 PE=4 SV=1	31.87	Secondary Metabolite
A0A151T2S8	Terpene cyclase/mutase family member OS=Cajanus cajan OX=3821 GN=KK1_015843 PE=3 SV=1	21.74	Secondary Metabolite
A0A151TKI0	Terpene cyclase/mutase family member OS=Cajanus cajan OX=3821 GN=KK1_023897 PE=3 SV=1	81.1	Secondary Metabolite
A0A151T9E2	Putative LRR receptor-like serine/threonine-protein kinase At3g47570 family OS=Cajanus cajan OX=3821 GN=KK1_018203 PE=3 SV=1	181.93	Signal Transduction

etion ponse
ponse
ponse
ponse
ponse
ponse
ponse
ponse
L
ponse
ponse
ponse
ponse
ponse
ponse
otion
HOII
Acid
ism
ism
ism Acid
ism

	T		1
A0A151T1R4	Tryptophan synthase	203.31	Amino Acid
	OS=Cajanus cajan OX=3821		Metabolism
	GN=KK1_023360 PE=3 SV=1		
A0A151U9I8	Glutamate decarboxylase 1	32.75	Amino Acid
	OS=Cajanus cajan OX=3821		Metabolism
	GN=KK1_020198 PE=4 SV=1		
A0A151SHS2	Beta-galactosidase OS=Cajanus	56.97	Carbohydrate
A0A13131132	cajan OX=3821	30.77	Metabolism
			Metabolishi
4.0.4.1.5.1.EX.0.0	GN=KK1_000528 PE=3 SV=1	56.05	0.1.1.1.
A0A151TIQ9	Beta-galactosidase OS=Cajanus	56.07	Carbohydrate
	cajan OX=3821		Metabolism
	GN=KK1_013220 PE=3 SV=1		
A0A151R7L1	Glucose-6-phosphate 1-	13.15	Carbohydrate
	dehydrogenase OS=Cajanus		Metabolism
	cajan OX=3821		
	GN=KK1_040205 PE=3 SV=1		
A0A151RM55	Glucosidase 2 subunit beta	19.02	Carbohydrate
71071131111133	OS=Cajanus cajan OX=3821	17.02	Metabolism
			Metabolishi
A O A 1 5 1 FDFT O	GN=KK1_034892 PE=4 SV=1	22 ( 22	0.1.1.1.
A0A151TFL9	Pectate lyase OS=Cajanus cajan	226.23	Carbohydrate
	OX=3821 GN=KK1_012096		Metabolism
	PE=3 SV=1		
A0A151SKD8	Pectinesterase OS=Cajanus	100.09	Carbohydrate
	cajan OX=3821		Metabolism
	GN=KK1_001432 PE=3 SV=1		
A0A151QW40	Xyloglucan glycosyltransferase	67.98	Carbohydrate
710711312 11 10	4 OS=Cajanus cajan OX=3821	07.50	Metabolism
	GN=KK1_044477 PE=4 SV=1		Wictabolishi
A O A 151TC A 6		156.56	Conhohadada
A0A151TGA6	Glucan endo-1,3-beta-	130.30	Carbohydrate
	glucosidase 7 OS=Cajanus		Metabolism
	cajan OX=3821		
	GN=KK1_012352 PE=3 SV=1		
A0A151S603	Putative UDP-N-	186.51	Catalytic Activity
	acetylglucosamine		
	pyrophosphorylase		
	OS=Cajanus cajan OX=3821		
	GN=KK1_027964 PE=4 SV=1		
A0A151T803	Cell division control protein 48	25.71	Cell Cycle
710711311003	isogeny C OS=Cajanus cajan	23.71	con cycle
	OX=3821 GN=KK1_017740		
A O A 1 5 1 T 1 T 1 T O	PE=4 SV=1	7.60	0.11.01
A0A151U1J8	Cyclin-dependent kinase C-2	7.62	Cell Cycle
	OS=Cajanus cajan OX=3821		
	GN=KK1_005817 PE=3 SV=1		
A0A151TTV8	Villin-2 OS=Cajanus cajan	130.22	Cytoskeleton
	OX=3821 GN=KK1_009732		
	PE=4 SV=1		
A0A151SMB6	Copia protein (Fragment)	198.61	Metabolic Process
- 101 110 1011110	OS=Cajanus cajan OX=3821	1,0.01	1.121.11.001.01.11.000.00
	GN=KK1_002108 PE=4 SV=1		
A O A 15100 A7		204.12	Motobalia Docas
A0A151S2M7	Copia protein OS=Cajanus	294.12	Metabolic Process
	cajan OX=3821		
	GN=KK1_029249 PE=4 SV=1		

A0A151TUS3	Type Linesite 1 1 4 5	32.03	Metabolic Process
AUAISIIUSS	Type I inositol-1,4,5- trisphosphate 5-phosphatase	32.03	Metabolic Process
	CVP2 OS=Cajanus cajan		
	OX=3821 GN=KK1_010029		
	PE=4 SV=1		
A0A151T3L7	Gag-Pol polyprotein	14.95	Nucleic Acid
110111311311	OS=Cajanus cajan OX=3821	14.73	Binding
	GN=KK1_016136 PE=4 SV=1		Dinams
A0A151SR49	Gypsy retrotransposon	153.1	Nucleic Acid
11011101011	integrase-like protein 1	10011	Binding
	(Fragment) OS=Cajanus cajan		
	OX=3821 GN=KK1_003559		
	PE=4 SV=1		
A0A151U488	Putative AC transposase	96.3	Nucleic Acid
	OS=Cajanus cajan OX=3821		Binding
	GN=KK1_006773 PE=4 SV=1		
A0A151UGM7	Polyprotein OS=Cajanus cajan	77.55	Nucleic Acid
	OX=3821 GN=KK1_047574		Binding
	PE=4 SV=1		-
A0A151UHM5	Transposon Ty3-I Gag-Pol	4.28	Nucleic Acid
	polyprotein OS=Cajanus cajan		Binding
	OX=3821 GN=KK1_049164		
	PE=4 SV=1		
A0A151R7A9	Retrovirus-related Pol	294.12	Nucleic Acid
	polyprotein from transposon		Binding
	TNT 1-94 OS=Cajanus cajan		
	OX=3821 GN=KK1_040369		
101151GYY	PE=4 SV=1	204.12	NY 1 1 A 11
A0A151SXK6	Retrovirus-related Pol	294.12	Nucleic Acid
	polyprotein from transposon		Binding
	TNT 1-94 OS=Cajanus cajan		
	OX=3821 GN=KK1_014907 PE=4 SV=1		
A0A151QXA1	Structural maintenance of	143.13	Organelle
AUAISIQAAI	chromosomes protein 2-1	143.13	Organization
	OS=Cajanus cajan OX=3821		Organization
	GN=KK1_044122 PE=4 SV=1		
A0A151TT81	Elongation factor Tu	282.49	Protein
110711311101	OS=Cajanus cajan OX=3821	202.77	Biosynthesis
	GN=KK1_009425 PE=3 SV=1		Diosynthesis
A0A151SV31	1-aminocyclopropane-1-	9.79	Secondary
	carboxylate synthase		Metabolite
	OS=Cajanus cajan OX=3821		
	GN=KK1_014063 PE=4 SV=1		
A0A151SRT4	4-coumarateCoA ligase 2	85.01	Secondary
	OS=Cajanus cajan OX=3821		Metabolite
	GN=KK1_003715 PE=4 SV=1		
A0A151QMA3	LRR receptor-like	159.12	Signal
	serine/threonine-protein kinase		Transduction
	GSO2 OS=Cajanus cajan		
	OX=3821 GN=KK1_048240		
	PE=4 SV=1		

A0A151TK89	66 kDa stress protein OS=Cajanus cajan OX=3821	16.49	Stress Response
	GN=KK1_023812 PE=4 SV=1		
A0A151R666	Activator of 90 kDa heat shock	96.14	Stress Response
	protein ATPase isogeny 2		
	OS=Cajanus cajan OX=3821		
	GN=KK1_040665 PE=4 SV=1		
A0A151U7E1	Agamous-like MADS-box	101.28	Transcription
	protein AGL62 OS=Cajanus		
	cajan OX=3821		
	GN=KK1_007942 PE=4 SV=1		
A0A151U747	Putative amino-acid permease	150.38	Transport
	C15C4.04c OS=Cajanus cajan		
	OX=3821 GN=KK1_007817		
	PE=4 SV=1		

Objective 3 - To assess the regulation of flowering under drought stress in pigeonpea.

### A. Physiological parameters under drought

Leaf relative water content (RWC) was measured to analyze the impact of drought on the developmental stage of pigeonpea. Drought at the preflowering stage (PFSS) affected the RWC as it was reduced in drought stressed plants compared to control plants at all stages of stress, especially at 9 DAS with 71.15% (Fig. 26 a). RWC decreased progressively as stress progressed during the preflowering stage. Coming to drought at the flowering stage (FSS), RWC was much lower than the PFSS stage than its respective control counterpart at all stages of stress, mainly at 9 DAS (Fig. 26 b). Leaf moisture content (LMC) was also decreased in drought stressed plants. At PFSS condition, LMC decreased at 3 DAS and 6 DAS but increased slightly at 9 DAS but was still lower than the control counterpart. In comparison, LMC reduced progressively at FSS as days of stress increased, with the lowest at 9 DAS (68.26%) in pigeonpea plants (Fig. 27).

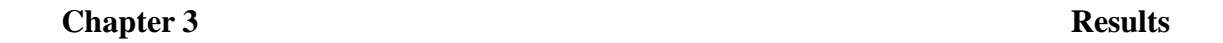
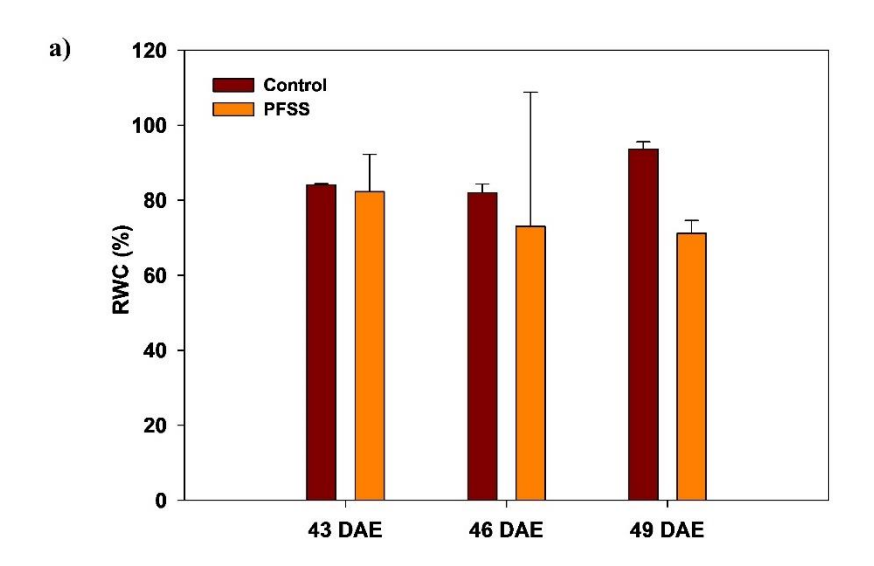


Fig. 26. a) Leaf relative water content (RWC) at preflowering stage drought (PFSS) and b) RWC at flowering stage drought (FSS) in pigeonpea.



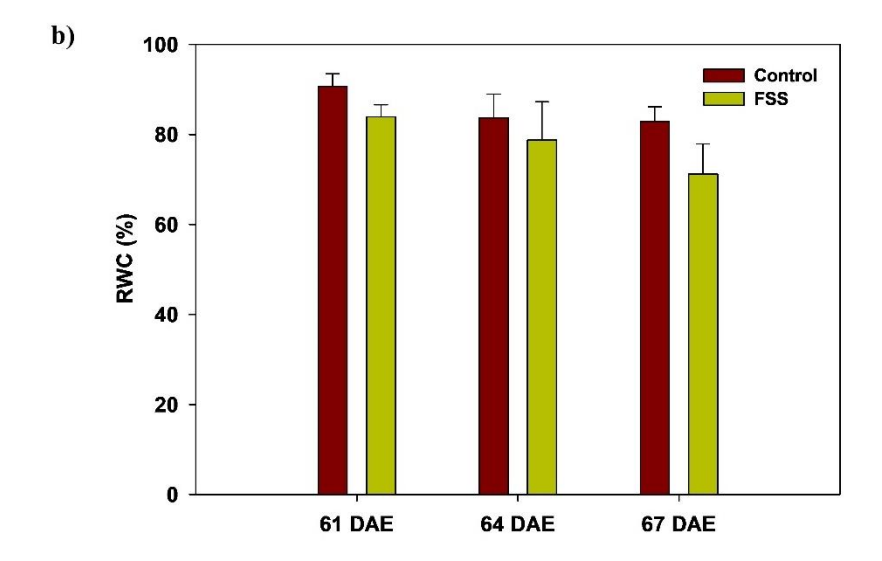
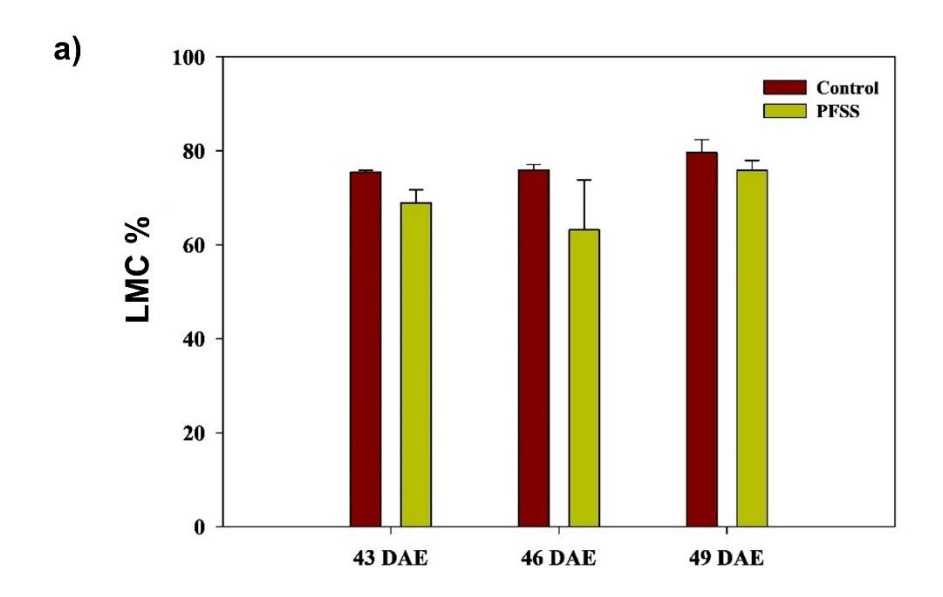
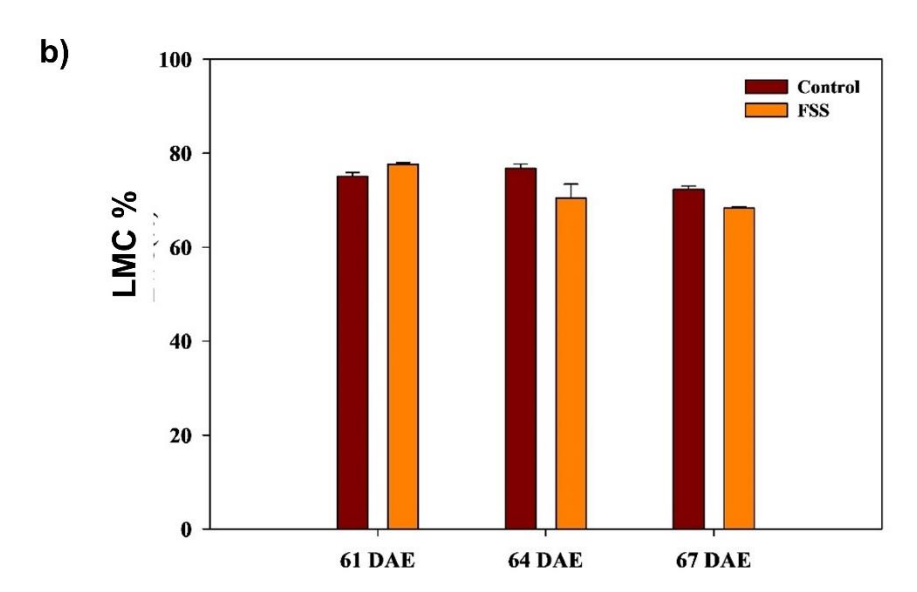


Fig. 27. a) Leaf moisture content (LMC) in pigeonpea at preflowering stage drought (PFSS) and b) LMC at flowering stage drought (FSS).

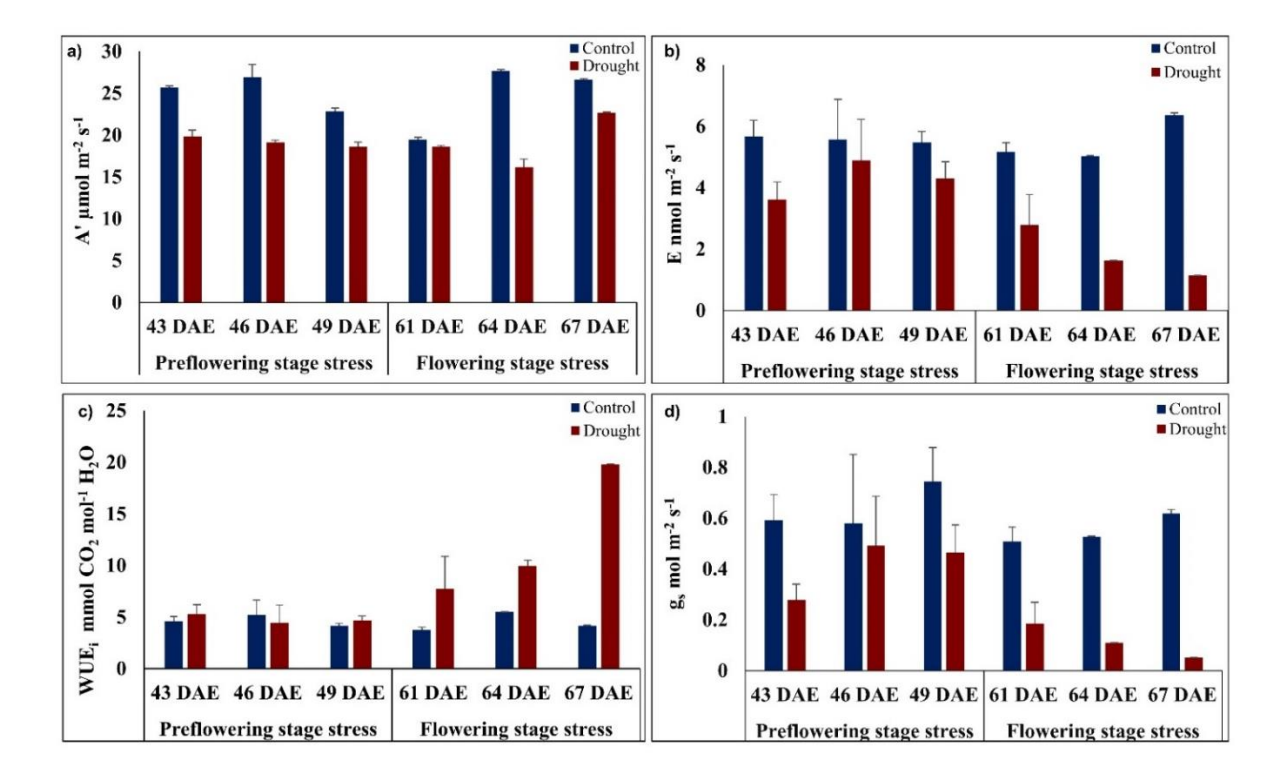




# B. Photosynthetic parameters in pigeonpea under drought

Foliar photosynthetic rates (A) decreased at all drought stages in both preflowering and flowering stress conditions. At preflowering stress, the photosynthetic rate decreased as the days of stress progressed, with a significant decrease of 19 % and 29 % at 6 and 9 DAS respectively (Fig. 28 a). A similar pattern of reduced photosynthesis was observed during the drought stress at flowering stage, with a significant decrease at 6 DAS by 41 % (Fig. 28 a). Transpiration rates were reduced in PFSS and FSS conditions, especially at the flowering stage, with a significant gradual decrease at 9 DAS by 82 % from 46 % at 3 DAS and 68 % at 6 DAS (Fig. 28 b). Stomatal conductance was also similarly decreased in drought stressed plants under PFSS and FSS conditions. At the PFSS condition, gs showed a reduction in drought affected plants but coming to the FSS condition, a drastic decrease was observed, especially at 9 DAS, by 92 % (Fig. 28 d). Water use efficiency increased in drought conditions; a significant increase was observed in FSS conditions as the day progressed, especially at 9 DAS, with a significant increase of 373 % (Fig. 28 c). On the other hand, at PFSS condition, WUE was increased slightly in drought stressed plants by 12% at 9 DAS (Fig. 28 c).

Fig. 28. Photosynthetic physiology of pigeonpea under drought at two developmental stages- preflowering stage (PFSS) and flowering stage (FSS). a) Photosynthetic rate, b) transpiration rate, c) Water use efficiency, and d) stomatal conductance.



# C. Foliar carbohydrates and amino acids analysis under drought

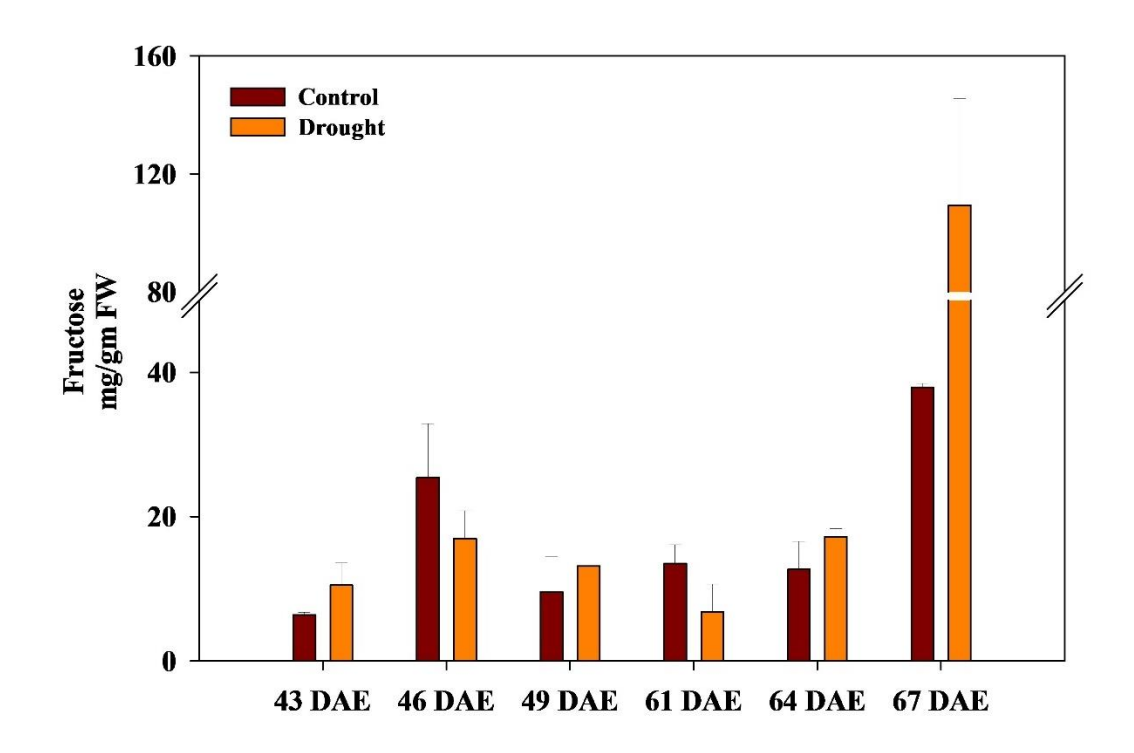
Free sugars like fructose, glucose, and sucrose were analyzed through HLPC. Hexoses were higher in drought stressed plants compared to control at the preflowering stage at 6<sup>th</sup> and 9<sup>th</sup> DAS. Glucose increased at the 6<sup>th</sup> and 9<sup>th</sup> DAS in drought plants at the PFSS stage, with the highest at the 6<sup>th</sup> DAS (81.5 mg/gm). On the other hand, fructose increased only in the 9<sup>th</sup> DAS at drought stress in the PFSS stage. Reduced sucrose levels were observed under drought conditions, especially at the flowering drought stress stage (Fig. 29). In comparison, glucose was reduced significantly at all stages of the FSS condition. Fructose was higher in drought stressed plants than in control, with the highest at 9<sup>th</sup> DAS (109.28 mg/gm) at the FSS stage. On the other hand, sucrose showed a significant decrease in FSS in drought plants as days to stress increased, with the lowest at 9 DAS (18.16 mg/gm). Drought at the flowering stage drastically reduced sugars, primarily glucose and sucrose, compared to preflowering stress.

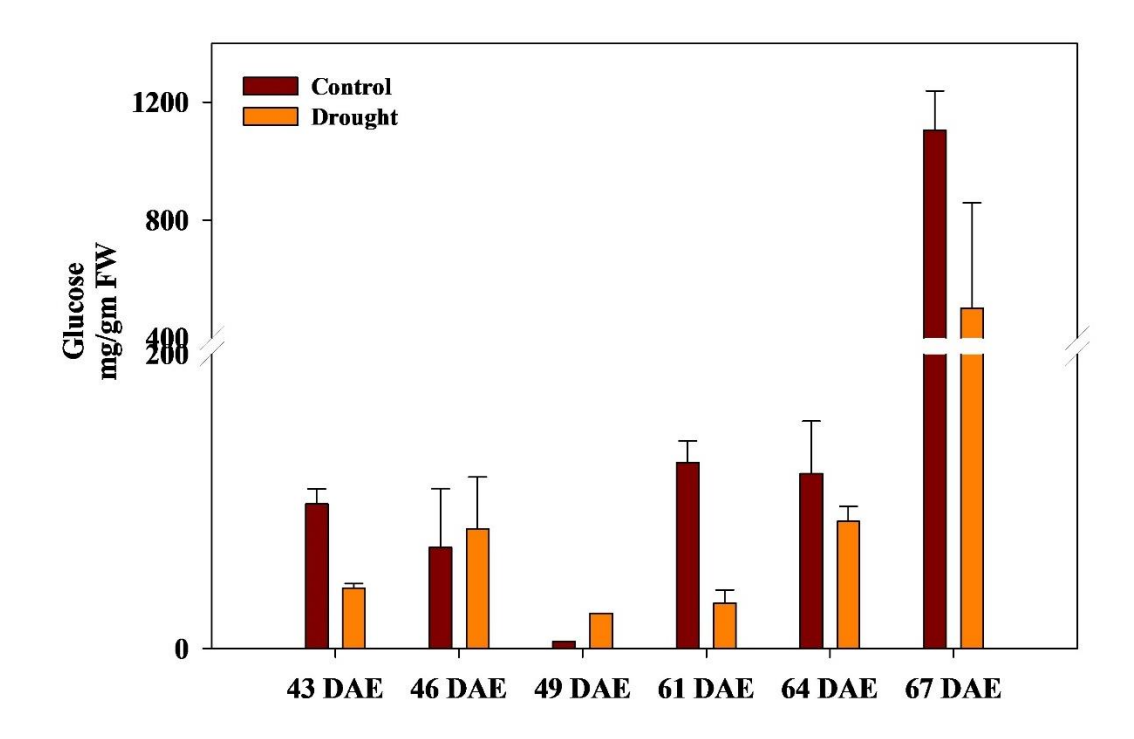
#### D. Changes in foliar amino acids under drought stress

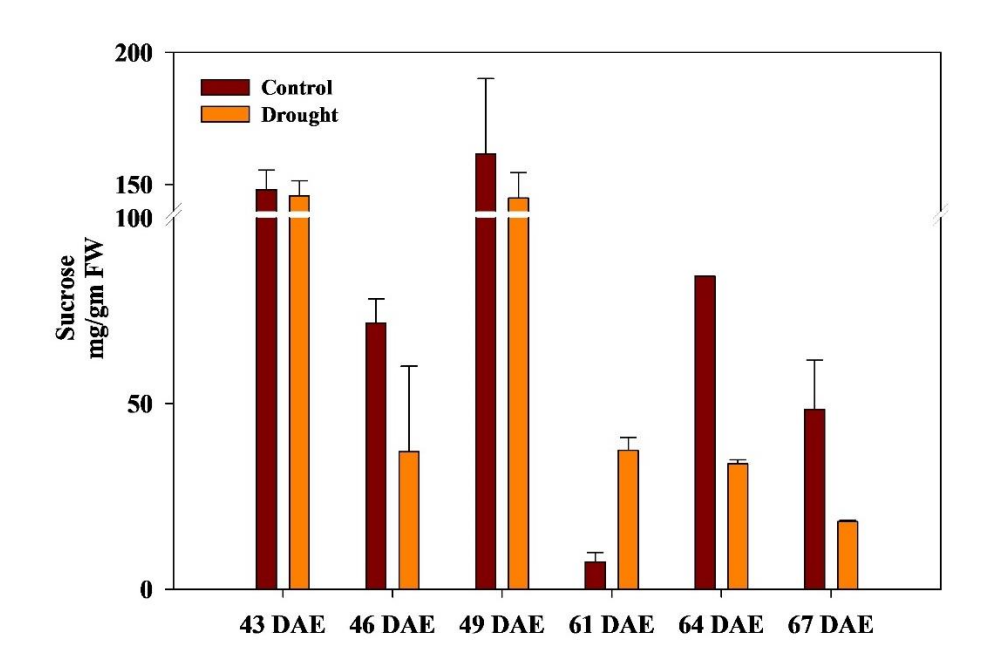
Amino acids were also estimated by HPLC at both PFSS and FSS stages. During the PFSS stage, at 3 DAS, tryptophan, valine, leucine, aspartate, glutamate, serine, and glycine were reduced in drought stressed plants (Fig. 30). At 6 DAS, aspartate and glutamate were decreased while the remaining increased. However, surprisingly, proline was reduced at both 6<sup>th</sup>, and 9<sup>th</sup> DAS in drought stressed plants. On 9<sup>th</sup> DAS, most amino acids, including valine, aspartate, serine, arginine, proline, and glycine, were decreased in drought stressed plants at the preflowering stage. On the other hand, drought, during the flowering stage resulted in a significant increase in proline as days of stress progressed, especially at 9 DAS

(2528.7 μg/gm, 148 %). Amino acids like aspartate, glutamate, serine, alanine, and lysine were decreased significantly in drought subjected plants as days of stress progressed, especially on the 9<sup>th</sup> day of stress (Fig. 31). Increased arginine levels were observed at 9 DAS in the FSS plant (2647 %). Amino acids like histidine, methionine, tryptophan, leucine, glycine, and valine were increased in the FSS plant at 9 DAS (Fig. 31).

Fig. 29. Foliar free sugar contents in pigeonpea under drought stress at two developmental phases- preflowering stage (PFSS) and flowering stage (FSS). Values are given as mean  $\pm$  SD.







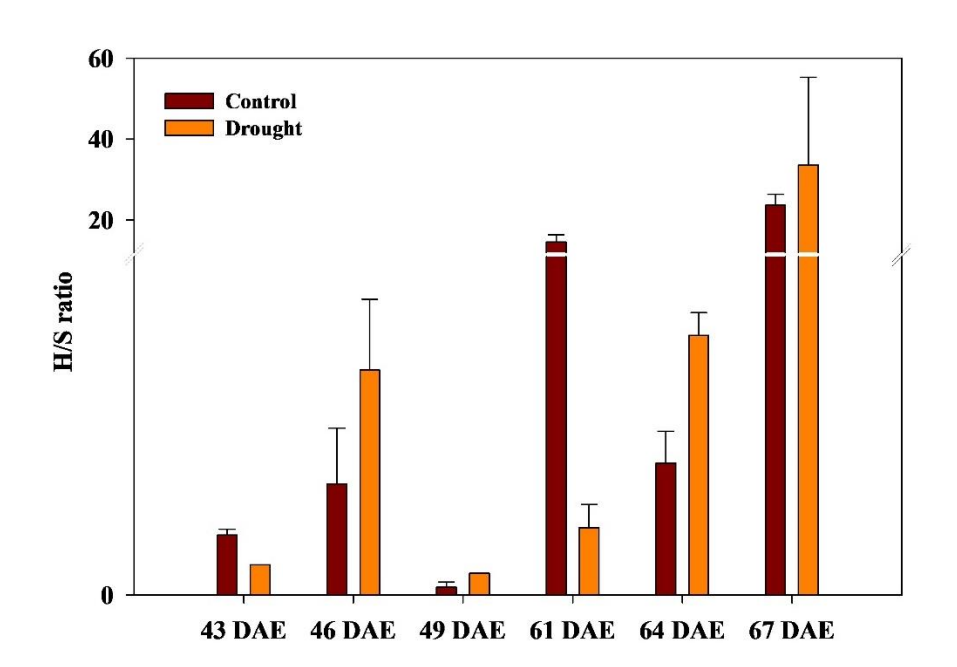
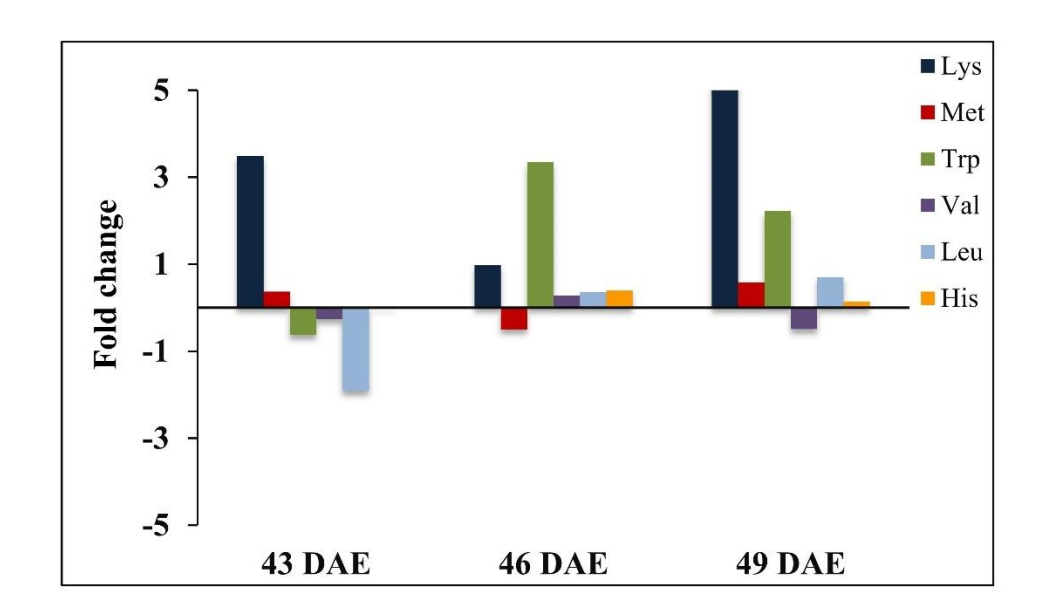




Fig. 30. Fold change of amino acid contents in pigeonpea leaves under drought stress at the preflowering stage (PFSS).



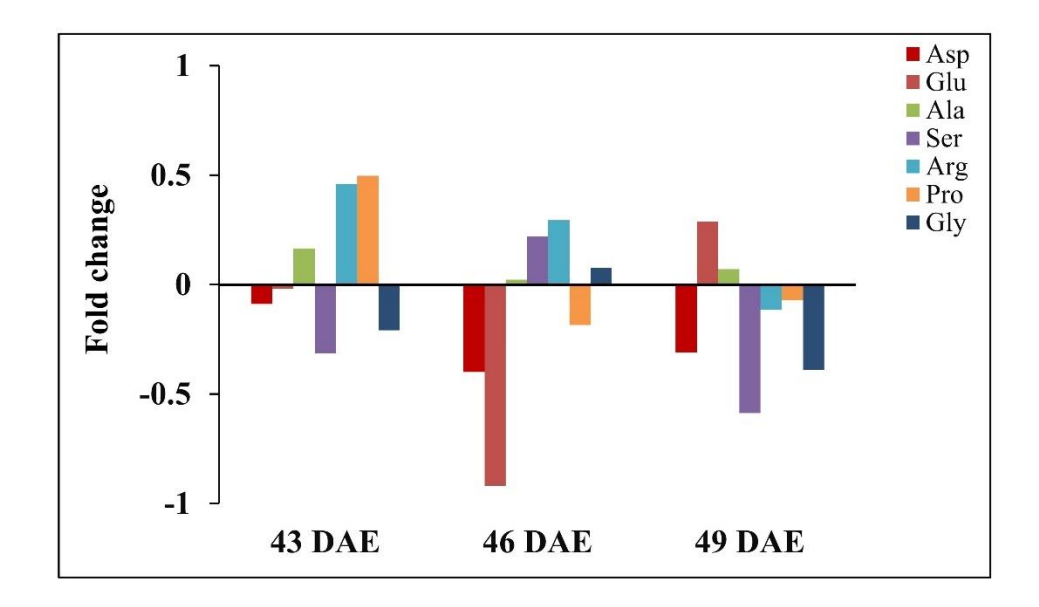
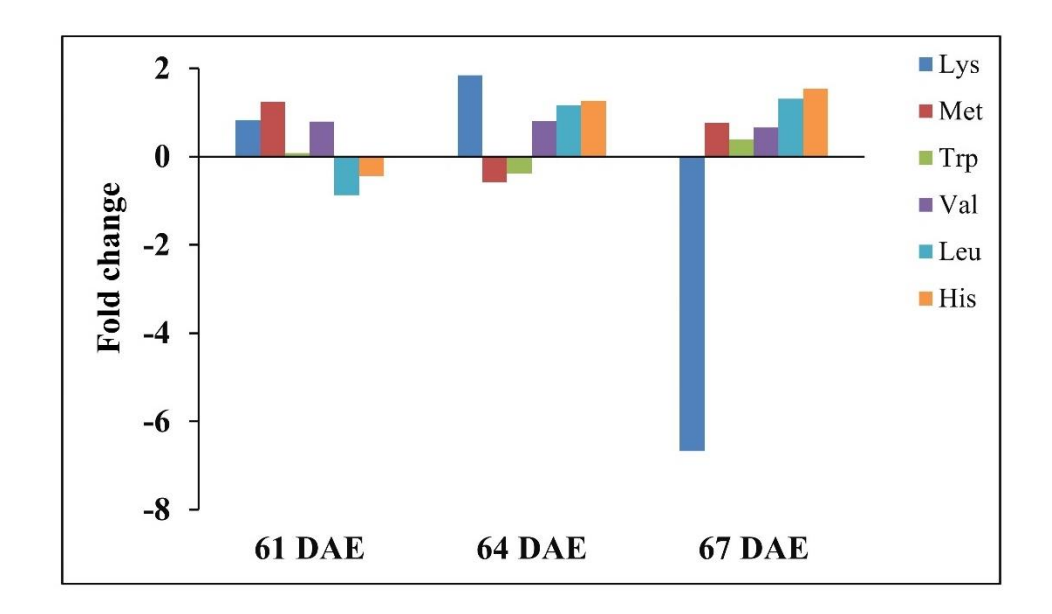
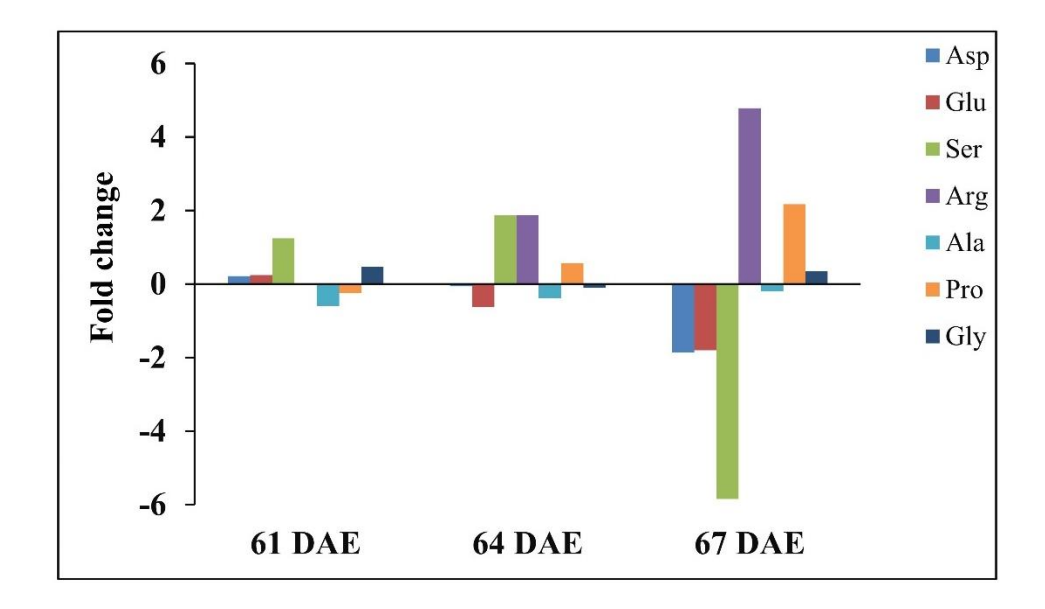




Fig. 31. Fold change of amino acid contents in pigeonpea leaves under drought stress at flowering stage (FSS).

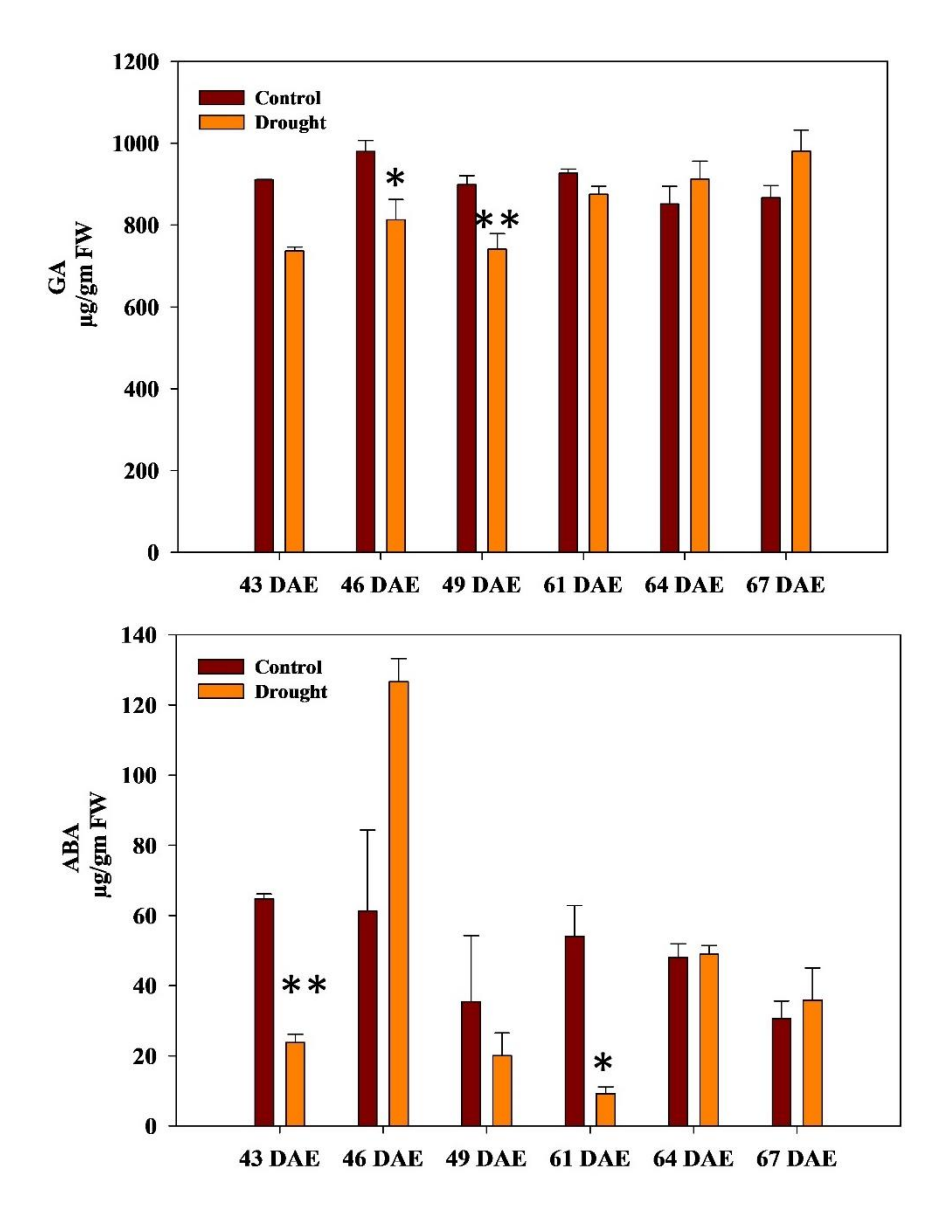


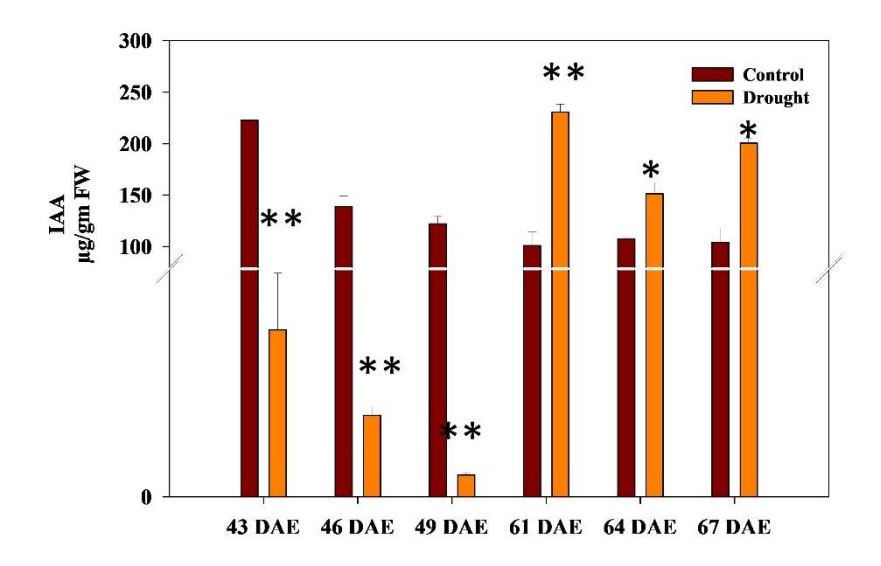


# E. Phytohormones analysis in pigeonpea under drought

Major hormones like gibberellins, abscisic acid, and auxins like IAA and IBA were analyzed under drought conditions. Most of the hormones (GA, ABA, IAA, IBA) were downregulated in PFSS, while all the hormones (GA, ABA, IAA) were significantly increased except for IBA in FSS plants. Auxins like IAA and IBA were reduced in preflowering stressed plants, especially at 9<sup>th</sup> DAS (3.86 μg/gm and 1.78 μg/gm) (Fig. 32). Gibberellins were slightly higher in flowering stage drought stressed plants compared to control plants, but mostly the levels were similar in both control and drought stressed plants. ABA increased in flowering stage drought stressed plants as days of stress advanced, with the highest at 9 DAS (51.8 μg/gm). Auxin, especially IAA levels, were significantly increased in FSS plants compared to control plants at all stages of stress. Pearson correlation was done to understand the relationship among the hormones. At the preflowering stage, only ABA was negatively correlated with IAA and IBA (Fig. 33). At the flowering stage, also IAA and IBA showed a strong negative correlation to ABA (Fig. 34).

Fig. 32. Analysis of major phytohormones (GA3, IAA, ABA, IBA) in pigeonpea leaves under drought stress at the preflowering stage (PFSS) and flowering stage (FSS). Values are given as mean  $\pm$  SD, and significant differences between control and drought stressed plants were calculated wherein \*\*p < 0.001 and \*p < 0.5.





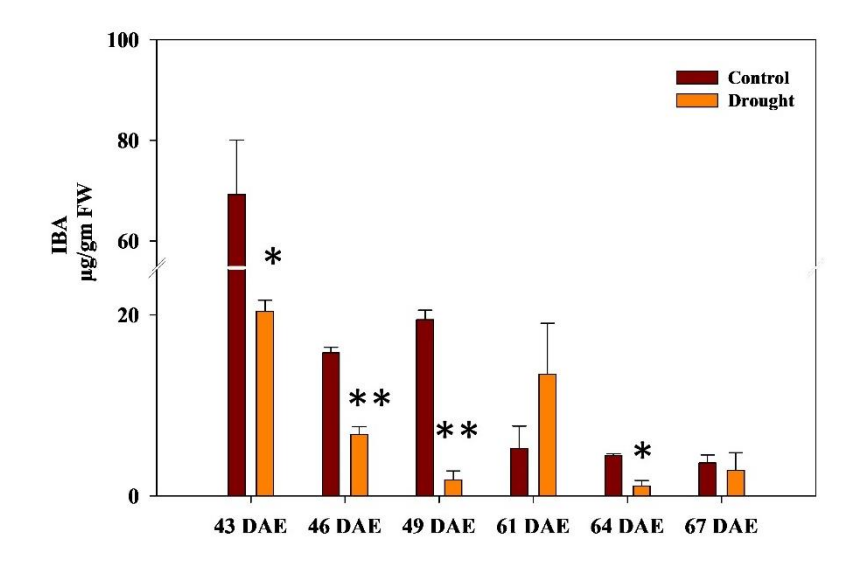




Fig. 33. Correlation heatmap among the phytohormones under PFSS.

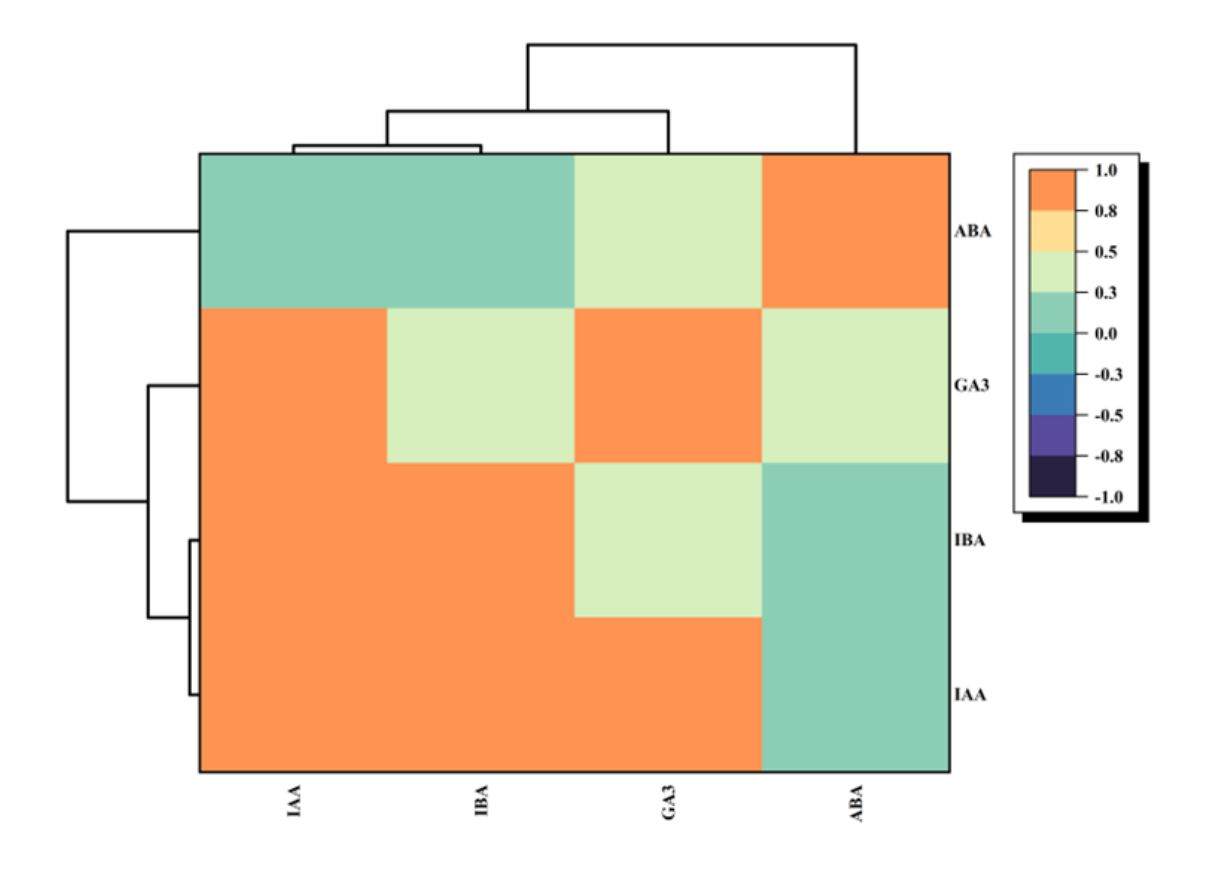
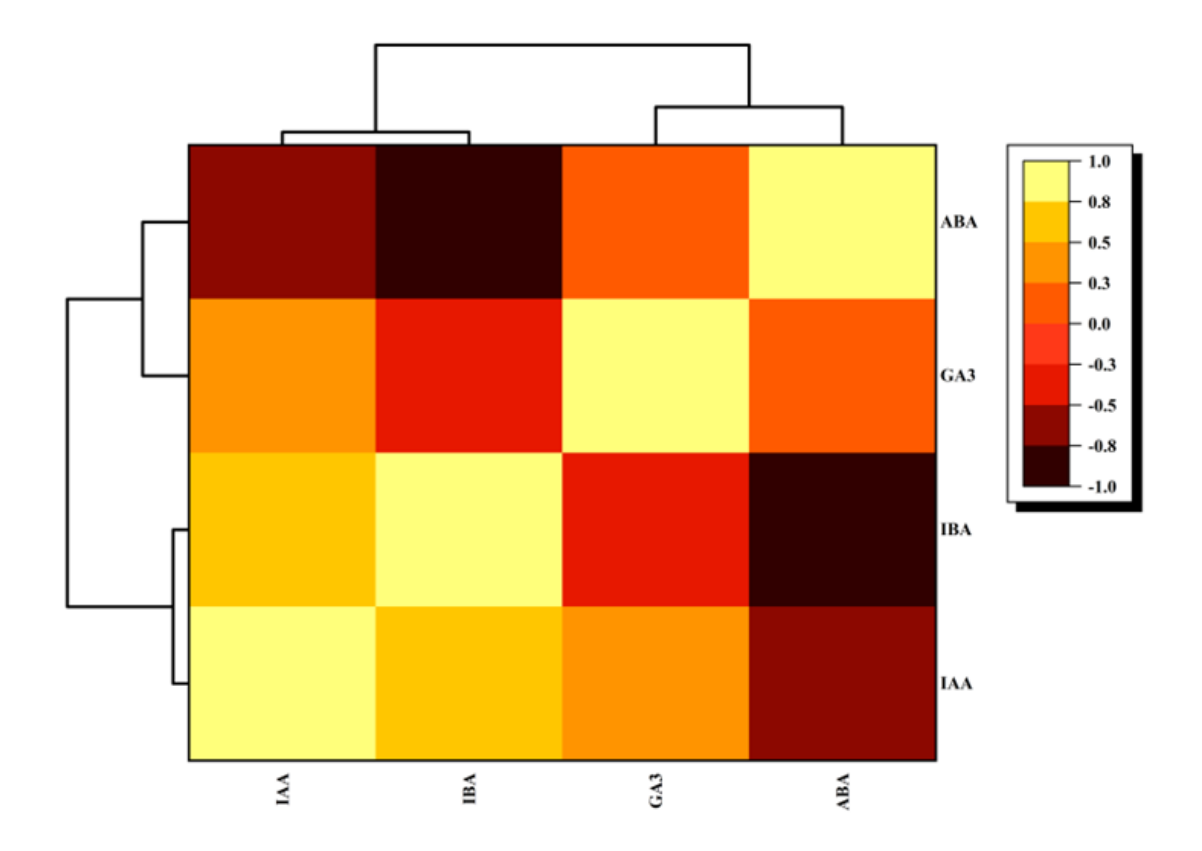


Fig. 34. Correlation heatmap among the phytohormones under FSS.



# F. Correlation between hormones and primary metabolites in pigeonpea leaves under drought

Correlation analysis (Pearson correlation) was performed to understand the association between hormones and primary metabolites and their effect on each other. Correlation coefficient (r) > 0.5 is considered a strong positive correlation, and < -0.5 is a strong negative correlation remaining, following into categories of moderate or no correlation. During the preflowering stage stress, no strong positive correlation was observed among sugars. In contrast, sucrose and fructose showed a strong negative correlation. A strong correlation was observed within amino acids and in amino acids with sugars (Fig. 35). Glucose positively correlated with amino acids glutamate and leucine (+ Gluc: Glu, Leu), whereas it was negatively correlated with serine, histidine, arginine, alanine, and valine (- Gluc: Ser, His, Arg, Ala, and Val). Fructose showed only (+) correlation with amino acids like Asp, Ala, Met, and Pro, while sucrose showed only (-) correlation with lysine in amino acid groups. The correlations within the amino acid group are explained in Table 10 briefly. Amino acids like proline, known for drought tolerance, were positively correlated with Met and negatively correlated with Leu. Hormones showed correlations with both sugars and amino acids like (+) IAA: Gluc, Leu, GA3, IBA, (-) IAA: His, Ala, Trp, Lys; (+) GA3: Asp, Glu, Gly, IAA, (-) GA3: Trp, Lys, and (-) ABA: Suc. On the other hand, during the flowering stage stress, no strong correlations were observed among the sugars. Sugars displayed a strong positive correlation with a few amino acids, e.g., Suc: Gly; Gluc: Ser and Fru: Val, Met, Leu. Sugars showed more negative correlation with amino acids than positive,

including Suc: His, Arg, Pro; Gluc: Asp, Gly, Trp, and Fru: Asp, Glu, Ala, Lys (Fig. 36). Strong correlations, both positive and negative, within amino acids were observed, e.g. (+) Pro: His, Val, Leu; (-) Pro: Glu; (+) Lys: Asp, Ser; (-) Lys: Arg, Trp and remaining elucidated in Table 11. Most hormones except for ABA positively correlated with sugars and amino acids, e.g., IAA: Arg, Val; GA3: Fru, His, Arg, Val, Leu, Pro; IBA: Asp, Glu, Trp. Gibberellin (GA3) was the only hormone negatively correlated with primary metabolites like Suc, Asp, and Glu.



Fig. 35. Correlation heatmap between phytohormones and metabolites under PFSS.

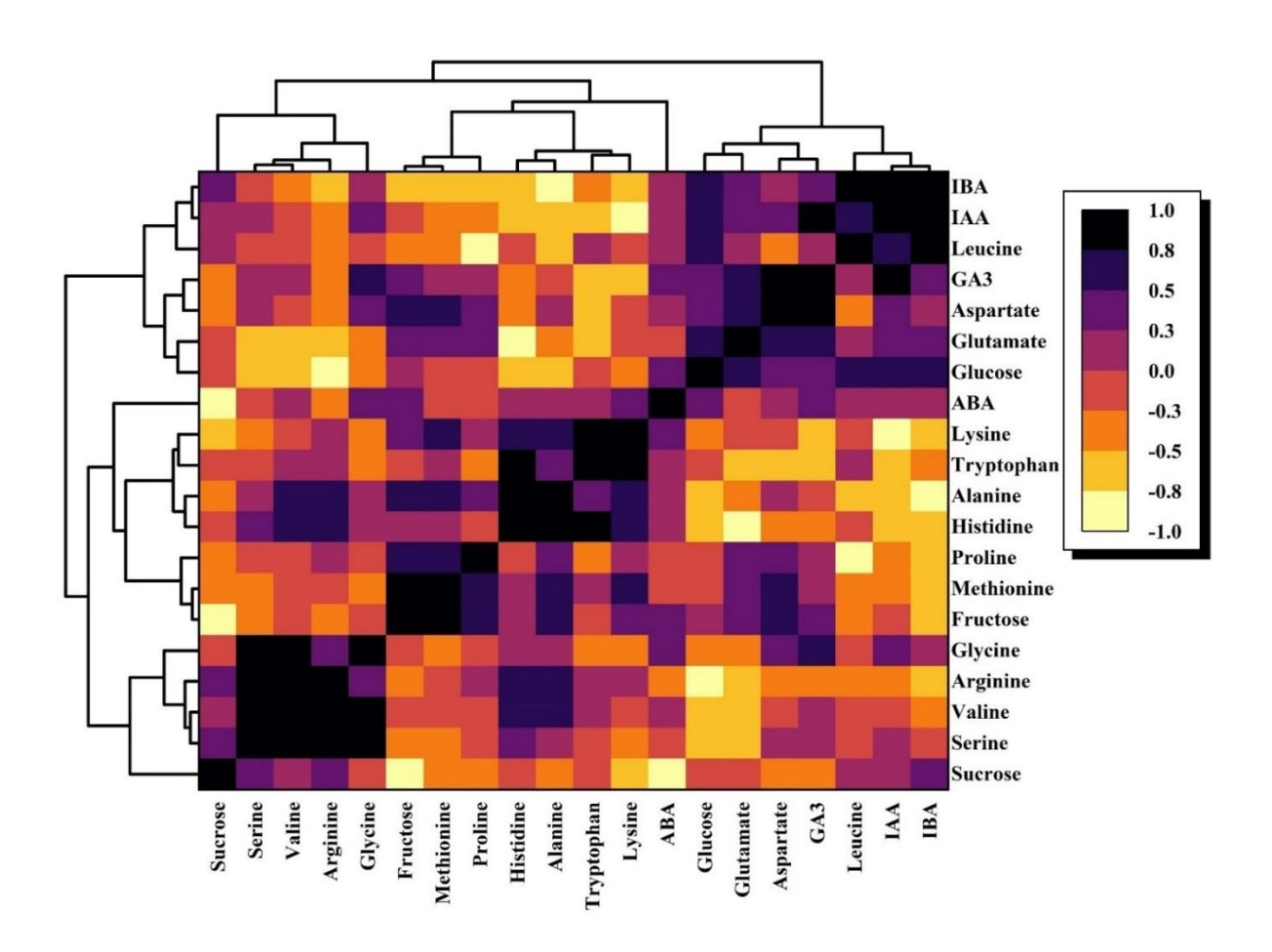
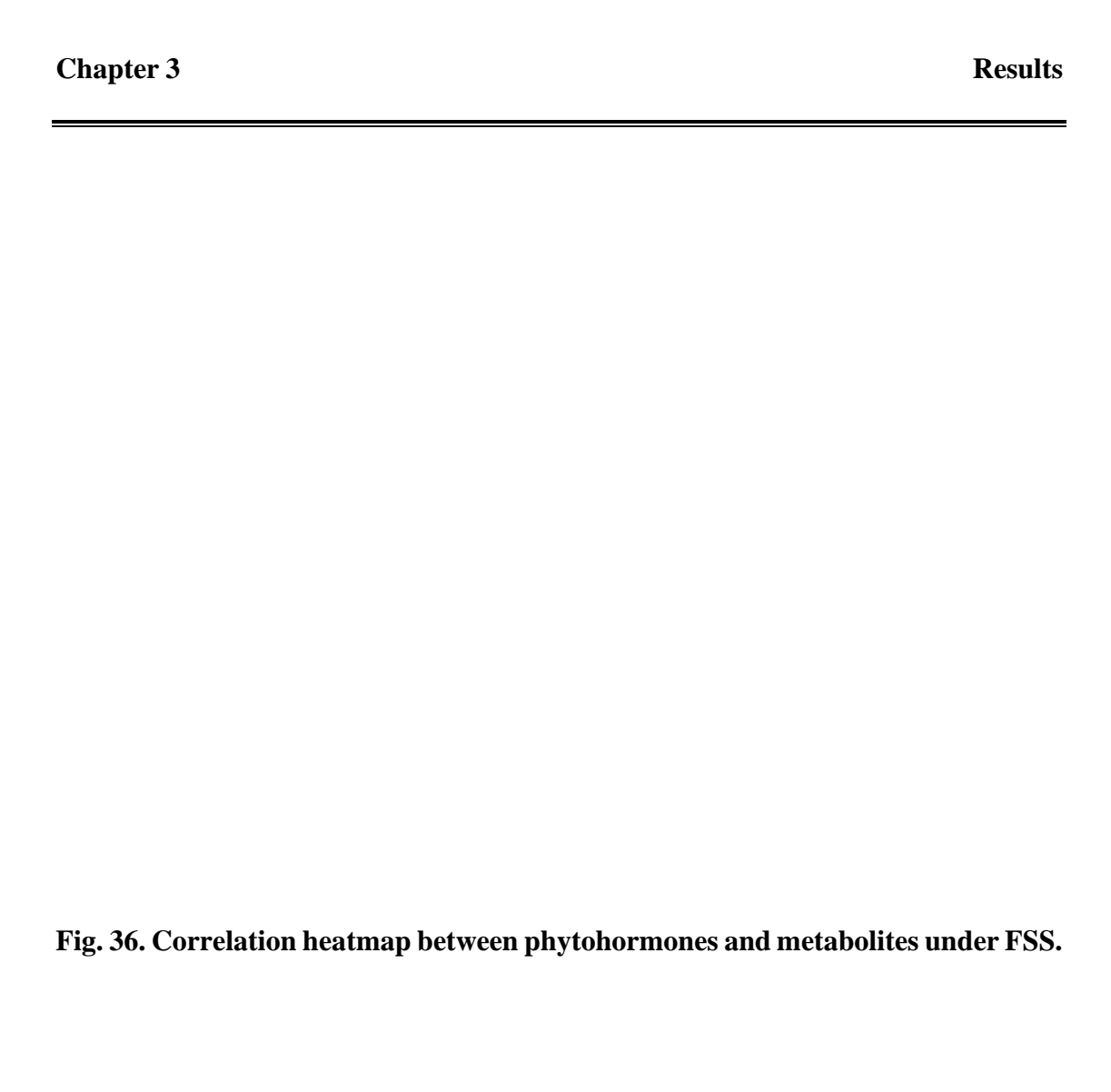


Table. 10 Correlation between metabolites and phytohormones under PFSS. Pearson correlation coefficient (r) > 0.5 is considered a strong positive correlation (red), and < -0.5 is a strong negative correlation (yellow), and follows into categories of moderate or no correlation.

Metabolites	Sucrose	Glucose	Fructose	Aspartate	Glutamate	Serine	Histidine	Arginine	Alanine	Glycine
Sucrose	1	-0.017777	-0.3906799	0.36453328	0.416698402	0.195555	-0.8650408	-0.6810564	-0.213533	0.5096887
Glucose	-0.017777	1	0.45460743	-0.50107996	-0.262385791	0.516543	-0.4637488	-0.2661905	-0.456544	-0.80738
Fructose	-0.39068	0.4546074	1	-0.9875382	-0.870979105	-0.29104	0.23000762	0.4158194	-0.555863	-0.430772
Aspartate	0.3645333	-0.50108	-0.9875382	1	0.902539221	0.228124	-0.1712919	-0.3020237	0.5616602	0.4778578
Glutamate	0.4166984	-0.262386	-0.8709791	0.902539221	1	0.136499	-0.3122827	-0.1962431	0.6123362	0.2709898
Serine	0.1955549	0.5165431	-0.2910395	0.228123814	0.136499365	1	-0.5000617	-0.7098013	-0.383905	-0.266406
Histidine	-0.865041	-0.463749	0.23000762	-0.17129191	-0.312282702	-0.50006	1	0.80137325	0.3312255	-0.029045
Arginine	-0.681056	-0.26619	0.4158194	-0.30202369	-0.196243082	-0.7098	0.80137325	1	0.2718769	-0.083178
Alanine	-0.213533	-0.456544	-0.5558633	0.561660228	0.6123362	-0.38391	0.33122548	0.27187688	1	0.0019513
Glycine	0.5096887	-0.80738	-0.4307719	0.477857842	0.270989829	-0.26641	-0.0290455	-0.0831775	0.0019513	1
Valine	-0.225799	0.2595014	0.75730692	-0.74608548	-0.865638265	0.094341	0.1631257	0.11664573	-0.868861	-0.054178
Methionine	0.3507833	0.1503919	0.66110279	-0.63092889	-0.546465017	-0.30042	-0.2490732	0.06228929	-0.717467	0.2418883
Tryptophan	-0.117646	-0.577299	-0.149985	0.263522054	0.411202413	-0.7852	0.42718339	0.72153896	0.6156809	0.3410039
Lysine	0.1029329	-0.111733	-0.5836998	0.551141532	0.254155043	0.782918	-0.1257058	-0.5388984	-0.149503	0.2200283
Leucine	-0.415046	-0.420922	0.54229873	-0.53127995	-0.76177296	-0.51664	0.63991604	0.43044682	-0.252006	0.2682698
Proline	-0.761325	-0.243297	0.4810655	-0.4963631	-0.739595963	-0.29595	0.80418171	0.44440702	-0.064662	-0.115201
IAA	-0.177609	-0.28098	0.30726036	-0.1704183	-0.195490413	-0.28316	0.39873537	0.60101446	-0.368518	0.3972057
GA3	-0.829794	-0.026976	0.7434161	-0.72048854	-0.783845806	-0.46066	0.80238256	0.69934027	-0.106478	-0.313456
ABA	-0.150123	-0.160797	-0.0425254	-0.08502335	-0.266725132	-0.11702	0.13992965	-0.2733164	0.3131355	-0.126762
IBA	0.1564957	-0.326632	-0.3850879	0.51900495	0.682593103	-0.23002	0.04988378	0.40790827	0.3224106	0.370292

Metabolites	Valine	Methionine	Tryptophan	Lysine	Leucine	Proline	IAA	GA3	ABA	IBA
Sucrose	-0.2258	0.350783261	-0.117645576	0.102933	-0.41505	-0.76133	-0.17761	-0.82979	-0.15012	0.156496
Glucose	0.259501	0.150391922	-0.577299304	-0.11173	-0.42092	-0.2433	-0.28098	-0.02698	-0.1608	-0.32663
Fructose	0.757307	0.661102795	-0.149985001	-0.5837	0.542299	0.481066	0.30726	0.743416	-0.04253	-0.38509
Aspartate	-0.74609	-0.630928894	0.263522054	0.551142	-0.53128	-0.49636	-0.17042	-0.72049	-0.08502	0.519005
Glutamate	-0.86564	-0.546465017	0.411202413	0.254155	-0.76177	-0.7396	-0.19549	-0.78385	-0.26673	0.682593
Serine	0.094341	-0.30042435	-0.785203323	0.782918	-0.51664	-0.29595	-0.28316	-0.46066	-0.11702	-0.23002
Histidine	0.163126	-0.249073195	0.427183391	-0.12571	0.639916	0.804182	0.398735	0.802383	0.13993	0.049884
Arginine	0.116646	0.062289291	0.721538959	-0.5389	0.430447	0.444407	0.601014	0.69934	-0.27332	0.407908
Alanine	-0.86886	-0.717467413	0.615680926	-0.1495	-0.25201	-0.06466	-0.36852	-0.10648	0.313136	0.322411
Glycine	-0.05418	0.241888327	0.341003898	0.220028	0.26827	-0.1152	0.397206	-0.31346	-0.12676	0.370292
Valine	1	0.656068431	-0.446638943	0.015689	0.637613	0.523118	0.518283	0.567739	-0.15653	-0.40399
Methionine	0.656068	1	-0.048876188	-0.46588	0.420234	0.000353	0.451652	0.181693	-0.26904	-0.09312
Tryptophan	-0.44664	-0.048876188	1	-0.50565	0.055374	-0.09297	0.397913	0.089627	-0.28947	0.75084
Lysine	0.015689	-0.465879626	-0.50565099	1	-0.21043	-0.04707	-0.05139	-0.38583	-0.03367	-0.05624
Leucine	0.637613	0.420233559	0.055373773	-0.21043	1	0.86037	0.413358	0.786169	0.316677	-0.37645
Proline	0.523118	0.000352678	-0.092970382	-0.04707	0.86037	1	0.181975	0.894794	0.467926	-0.51599
IAA	0.518283	0.45165181	0.397912863	-0.05139	0.413358	0.181975	1	0.332526	-0.71888	0.536193
GA3	0.567739	0.18169308	0.089627059	-0.38583	0.786169	0.894794	0.332526	1	0.215134	-0.34177
ABA	-0.15653	-0.269042673	-0.28946777	-0.03367	0.316677	0.467926	-0.71888	0.215134	1	-0.76448
IBA	-0.40399	-0.093124498	0.750839736	-0.05624	-0.37645	-0.51599	0.536193	-0.34177	-0.76448	1



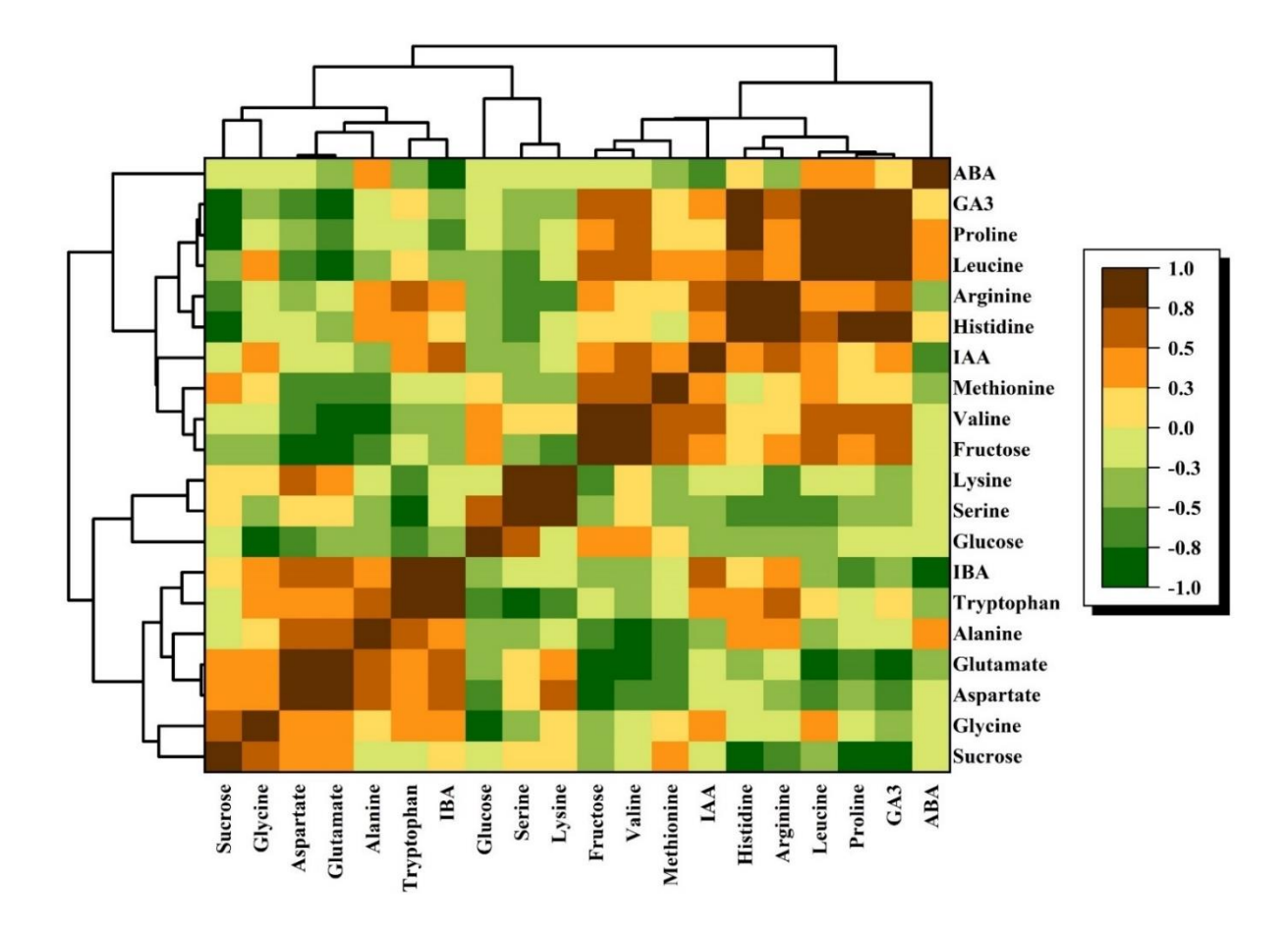


Table. 11 Correlation between metabolites and phytohormones under FSS. Pearson correlation coefficient (r) > 0.5, a strong positive correlation (red), and < -0.5, a strong negative correlation (yellow), and following into categories of moderate or no correlation.

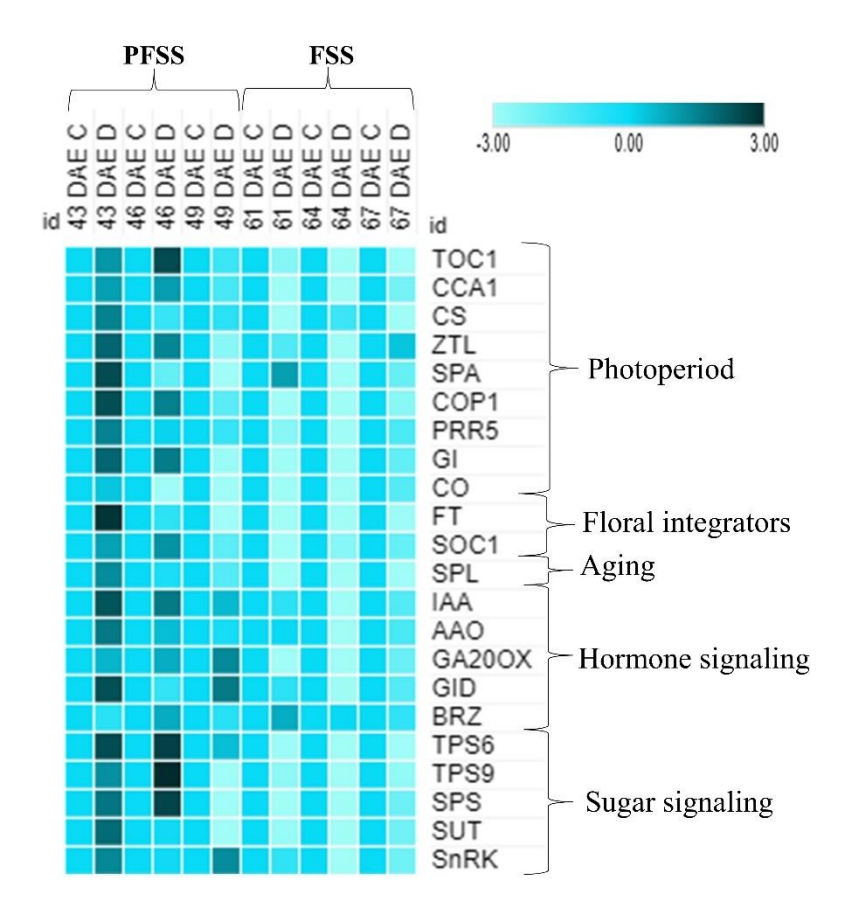
Metabolites	Sucrose	Glucose	Fructose	Aspartate	Glutamate	Serine	Histidine	Arginine	Alanine	Glycine
Sucrose	1	-0.178601	-0.7597012	-0.38747388	-0.140623506	0.356692	-0.2219008	0.39726351	-0.394308	-0.037122
Glucose	-0.178601	1	0.05645514	0.300025231	0.668514224	-0.63655	-0.6986232	-0.9498194	-0.67935	-0.251318
Fructose	-0.759701	0.0564551	1	0.727296415	0.49872861	-0.28941	0.09256814	-0.2619295	0.5809376	-0.108183
Aspartate	-0.387474	0.3000252	0.72729641	1	0.728498059	0.010775	-0.3877859	-0.3540349	0.1040243	0.2629356
Glutamate	-0.140624	0.6685142	0.49872861	0.728498059	1	-0.54413	-0.7643223	-0.7195591	-0.310791	-0.364059
Serine	0.3566919	-0.63655	-0.2894129	0.010774697	-0.544126007	1	0.37318275	0.77992506	0.2487618	0.8355598
Histidine	-0.221901	-0.698623	0.09256814	-0.38778585	-0.764322344	0.373183	1	0.6685363	0.8118102	0.1928708
Arginine	0.3972635	-0.949819	-0.2619295	-0.35403486	-0.719559067	0.779925	0.6685363	1	0.5533634	0.364031
Alanine	-0.394308	-0.67935	0.58093757	0.104024288	-0.310790597	0.248762	0.81181015	0.55336338	1	0.0691757
Glycine	-0.037122	-0.251318	-0.1081829	0.262935648	-0.364058511	0.83556	0.19287084	0.364031	0.0691757	1
Valine	0.1016099	-0.712768	-0.0620076	-0.00378327	-0.634618864	0.917155	0.67813696	0.81092161	0.564779	0.7647283
Methionine	-0.497828	-0.077814	0.89492472	0.524428604	0.440773847	-0.32166	0.22318384	-0.0870843	0.6946379	-0.361792
Tryptophan	-0.161063	-0.243494	-0.1188594	-0.68959076	-0.611641847	-0.17783	0.76039835	0.22988376	0.4267012	-0.305662
Lysine	-0.555512	-0.261743	0.4732651	-0.24617309	-0.237918358	-0.39546	0.68205806	0.08168896	0.7125703	-0.4608
Leucine	0.2267194	0.6635678	-0.4800398	-0.2596502	0.019538339	-0.20653	-0.2014875	-0.4417512	-0.570875	-0.035842
Proline	-0.267671	-0.247038	0.60814948	0.484709481	0.441465383	-0.16331	-0.2210753	0.00638403	0.2915846	-0.227069
IAA	0.2359542	0.6526228	-0.1826965	0.471112709	0.460918736	0.142364	-0.637354	-0.4451356	-0.642023	0.4038264
GA3	-0.30235	0.4759541	0.38395562	0.857133102	0.541615399	0.166524	-0.4583503	-0.4285812	-0.217374	0.5596221
ABA	-0.837723	0.2947134	0.32510451	0.142902916	-0.132300692	-0.16175	0.19758051	-0.3975401	0.0702302	0.3270559
IBA	0.3632232	0.7444738	-0.5398308	0.006875928	0.280563094	-0.10058	-0.684632	-0.5392395	-0.914852	0.1329525

Metabolites	Valine	Methioni	Tryptoph	Lysine	Leucine	Proline	IAA	GA3	ABA	IBA
Sucrose	0.10161	-0.49783	-0.16106	-0.55551	0.226719	-0.26767	0.235954	-0.30235	-0.83772	0.363223
Glucose	-0.71277	-0.07781	-0.24349	-0.26174	0.663568	-0.24704	0.652623	0.475954	0.294713	0.744474
Fructose	-0.06201	0.894925	-0.11886	0.473265	-0.48004	0.608149	-0.1827	0.383956	0.325105	-0.53983
Aspartate	-0.00378	0.524429	-0.68959	-0.24617	-0.25965	0.484709	0.471113	0.857133	0.142903	0.006876
Glutamate	-0.63462	0.440774	-0.61164	-0.23792	0.019538	0.441465	0.460919	0.541615	-0.1323	0.280563
Serine	0.917155	-0.32166	-0.17783	-0.39546	-0.20653	-0.16331	0.142364	0.166524	-0.16175	-0.10058
Histidine	0.678137	0.223184	0.760398	0.682058	-0.20149	-0.22108	-0.63735	-0.45835	0.197581	-0.68463
Arginine	0.810922	-0.08708	0.229884	0.081689	-0.44175	0.006384	-0.44514	-0.42858	-0.39754	-0.53924
Alanine	0.564779	0.694638	0.426701	0.71257	-0.57088	0.291585	-0.64202	-0.21737	0.07023	-0.91485
Glycine	0.764728	-0.36179	-0.30566	-0.4608	-0.03584	-0.22707	0.403826	0.559622	0.327056	0.132953
Valine	1	-0.05588	0.122042	-0.0247	-0.23305	-0.19666	-0.07242	0.073384	0.008859	-0.3546
Methionine	-0.05588	1	0.094671	0.616331	-0.43256	0.535379	-0.33603	0.073999	-0.01345	-0.64845
Tryptophan	0.122042	0.094671	1	0.78463	0.247773	-0.4787	-0.60193	-0.6996	0.20777	-0.35649
Lysine	-0.0247	0.616331	0.78463	1	-0.21737	0.101481	-0.78605	-0.5235	0.280579	-0.72432
Leucine	-0.23305	-0.43256	0.247773	-0.21737	1	-0.87519	0.580067	0.099577	0.149033	0.783468
Proline	-0.19666	0.535379	-0.4787	0.101481	-0.87519	1	-0.35648	0.083171	-0.18431	-0.54554
IAA	-0.07242	-0.33603	-0.60193	-0.78605	0.580067	-0.35648	1	0.773609	0.026104	0.84449
GA3	0.073384	0.073999	-0.6996	-0.5235	0.099577	0.083171	0.773609	1	0.35645	0.403027
ABA	0.008859	-0.01345	0.20777	0.280579	0.149033	-0.18431	0.026104	0.35645	1	0.028591
IBA	-0.3546	-0.64845	-0.35649	-0.72432	0.783468	-0.54554	0.84449	0.403027	0.028591	1

# G. Changes in flowering patterns and gene transcripts under drought stress

Semi-quantitative PCR was performed to understand the regulation of flowering under drought stress. Gene transcripts of significant flowering genes were analyzed at both preflowering stage stress and flowering stage stress. Circadian clock genes, including TOC1 and CCA1, were downregulated as days of stress progressed at the preflowering stage in drought stressed plants, especially at 9 DAS (Fig. 37). Most of the photoperiod genes, including photoreceptors, GI, and CO, downregulated as stress increased, especially at 9 DAS, with CO at a 4-fold decrease in droughtstressed plants at the preflowering stage. All the floral regulators, including FT, SOC1, and SPL were downregulated with the highest at 9 DAS. The genes involved in sugar signaling, including TPS, SPS, and SUT, were downregulated in drought stressed plants at 9 DAS during the preflowering stage except for SnRK (Fig. 37). Genes involved in hormone signaling were also analyzed, wherein genes related to auxin (IAA), and gibberellin (GA20OX, GID) signaling were upregulated while others, including AAO and BRZ, were down-regulated. On the other hand, when drought was subjected at the flowering stage, all genes including photoperiod genes, floral regulators, sugar signaling, and hormone signaling, were downregulated at all stages of stress except for BRZ at 3 and 6 DAS (Fig. 37). FT showed considerable downregulation during drought at the flowering stage, significantly (3-fold) at 9 DAS (Fig. 37). The correlation network during PFSS showed BRZ, GA20OX, and SnRK were negatively correlated with all the significant floral regulatory genes. In contrast, in FSS, only BRZ showed a negative correlation with most of the genes (Fig. 39).

Fig. 37. Transcript levels of flowering regulatory genes, phytohormone, and sugar signaling genes in pigeonpea leaves at PFSS and FSS stress.

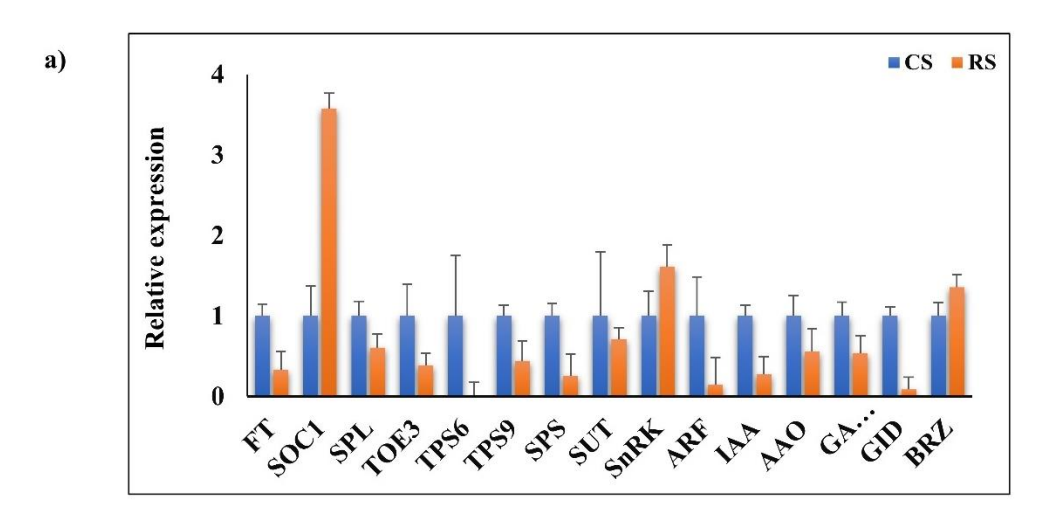


The levels of gene transcripts were also analyzed at the meristem level to understand the effect of drought on floral initiation. Meristem was collected from plants recovered after a drought during the preflowering stage and from drought-subjected plants during the flowering stage. Drought recovered preflowering stage plants showed high Sucrose non-fermenting 1 related kinase (SnRK) and BRZ genes at SAM (Fig. 38 a). All other genes, including FT, SPL, TPS, SUS, hormone signaling,

AAO, and GID, were downregulated in drought recovered meristem compared to control except for SOC1 (Fig. 38 a). Meristem collected from drought at the flowering stage showed upregulated levels of BRZ, AP2, SnRK, LFY, and TPS, and the remaining genes were downregulated (Fig. 38 b). Correlation analysis among the genes was performed to understand the effect of genes and their interactions under stress. SnRK and BRZ showed a negative correlation with all floral regulatory genes, especially the floral integrators in correlation analysis in meristem from PFSS recovered plants (Fig. 40 a). On the other hand, SnRK, BRZ, and AP2 were negatively correlated with major floral integrators in meristem from the FSS plant (Fig. 40 b).



Fig. 38. Transcript levels of flowering regulatory genes, phytohormone, and sugar signaling genes in meristem at a) PFSS and b) FSS stress.



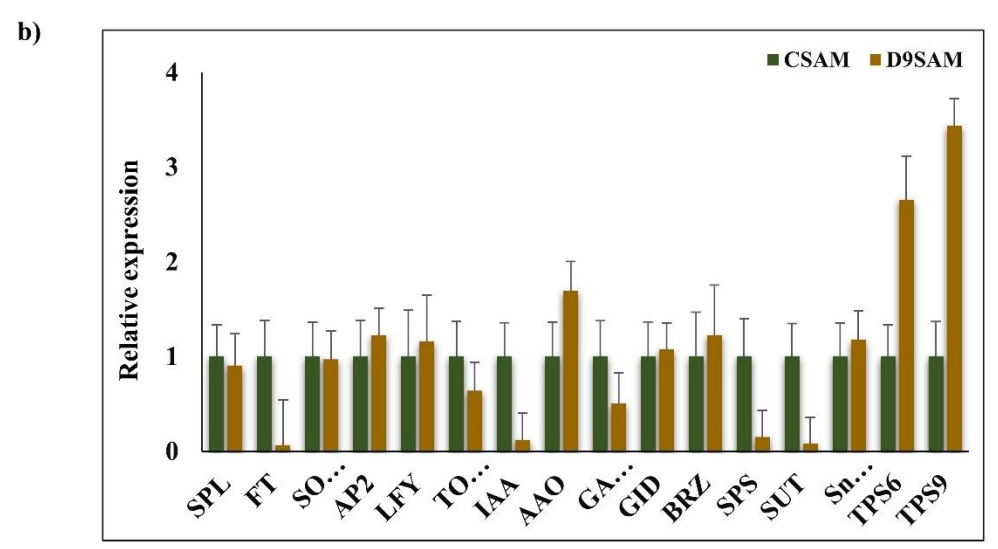
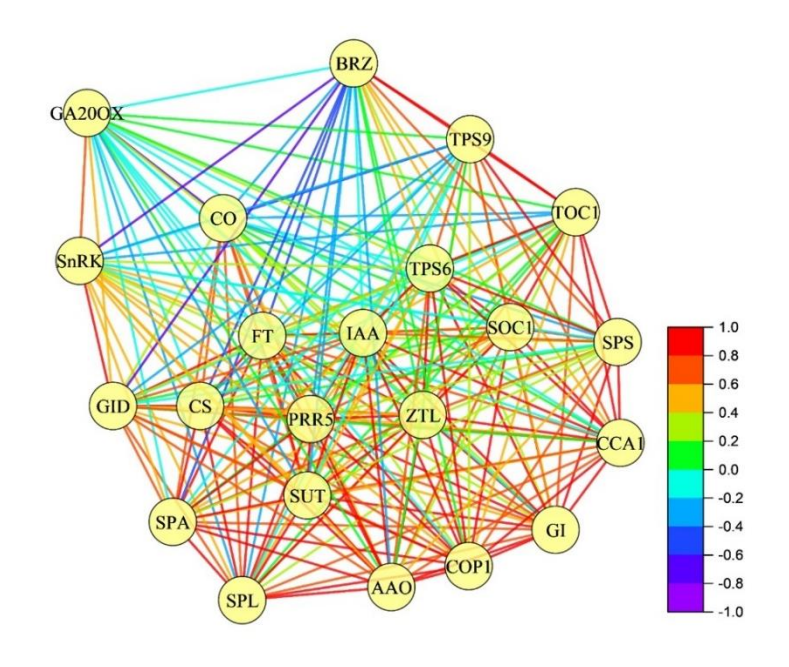
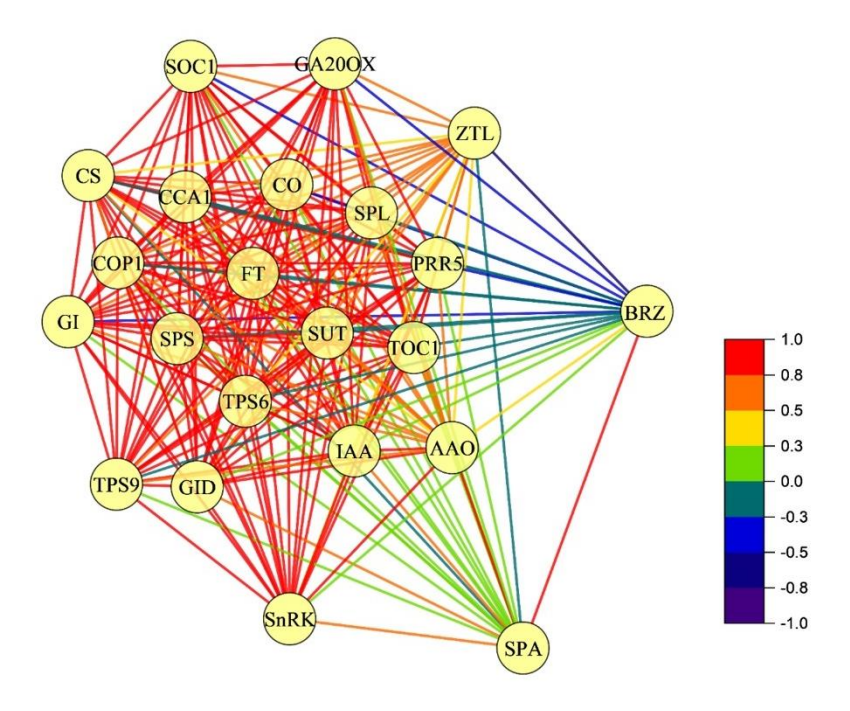




Fig. 39. Correlation network analysis to illustrate relationships among the flowering regulatory genes under a) PFSS and b) FSS stress conditions.

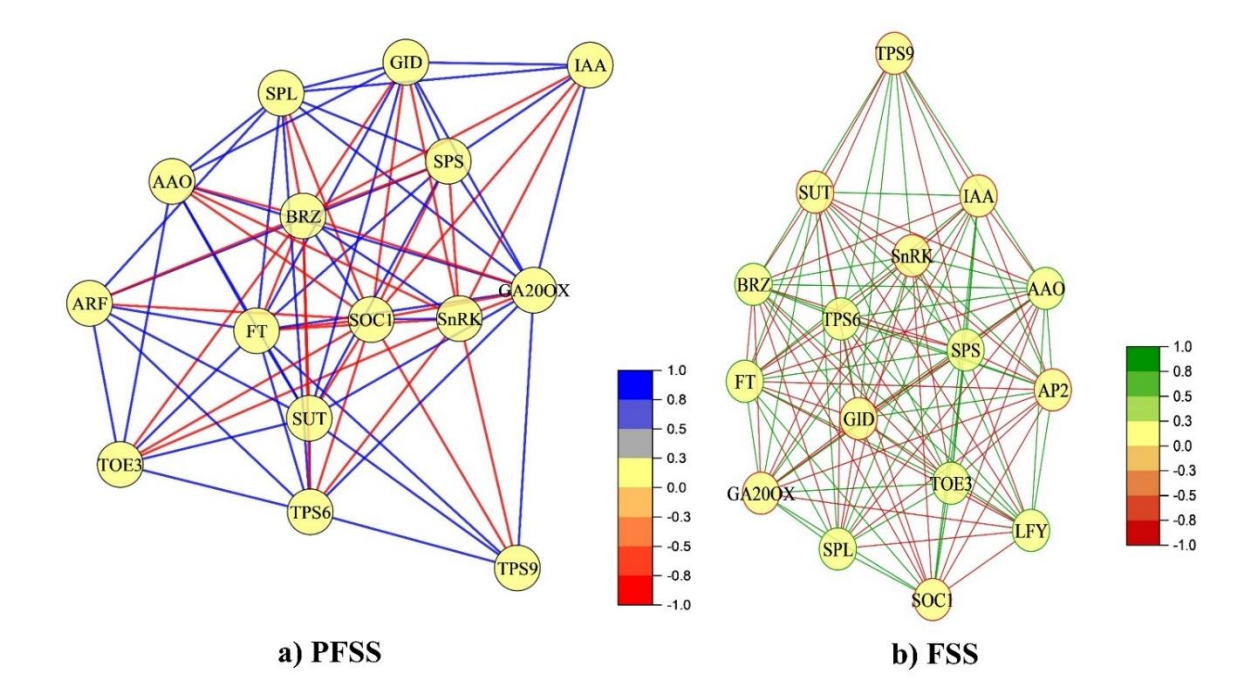


a) PFSS



b) FSS

Fig. 40. Correlation network analysis to illustrate relationships among the flowering regulatory genes in meristem under a) PFSS and b) FSS stress conditions.

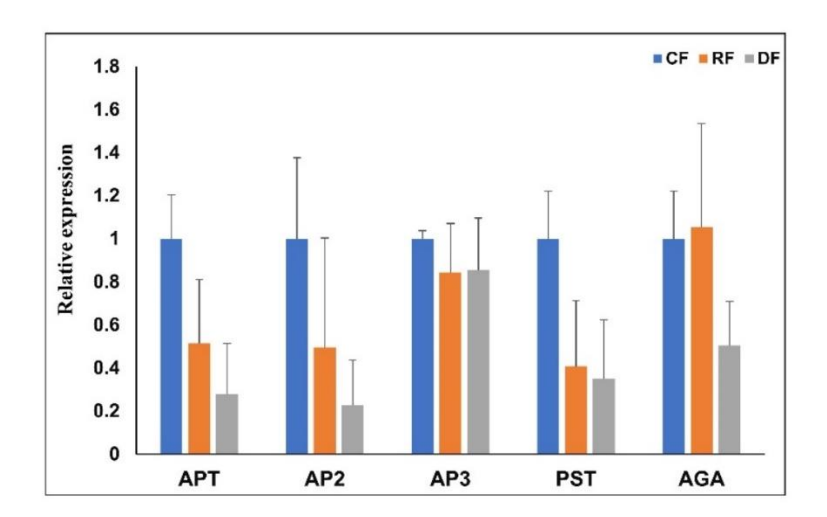


Objective 4 - To investigate the drought-induced changes in reproductive status and seed yields of pigeonpea.

### A. Regulation of ABCE genes under drought

The ABCE gene transcripts were analyzed from inflorescence collected from drought-recovered plants at both developmental stages. All the transcripts were downregulated in drought-recovered samples except for AGA in PFSS-recovered inflorescence. The highest downregulation of ABCE genes was observed in FSS recovered plants (Fig. 41).

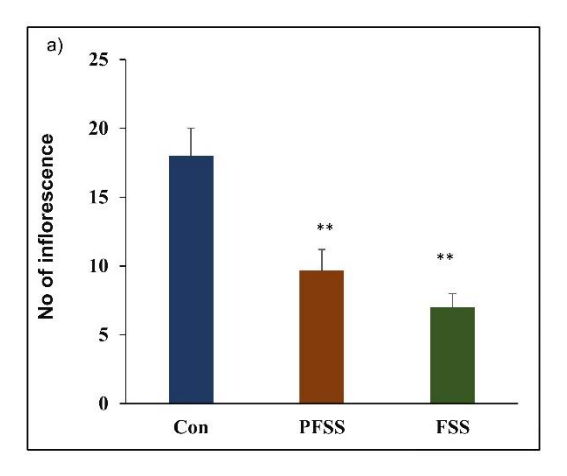
Fig. 41. Transcript analysis of ABCE genes in inflorescence from control plant inflorescence (CF), drought recovered PFSS plants (RF) and inflorescence from drought stressed FSS plants (DF).



### B. Impact of drought on reproductive parameters of pigeonpea

The number of inflorescences decreased to 50% in drought stressed plants under both conditions, with the lowest in the FSS condition (Fig. 42 a). This reduction in the inflorescence is directly translated to its yield patterns, as the number of pods was reduced in both stressed plants even after recovery (Fig. 42 b). Total yield was reduced in drought-recovered plants with a significant reduction when drought was subjected to the flowering stage (34%) (Fig. 43). The same trend of reduced pod weight and seed weight was observed in drought-recovered plants but the highest was at FSS. Weight per 100 seeds increased in drought recovered plants, the highest in FSS recovered plants (1.4%).

Fig. 42. a) Number of inflorescences observed in drought stressed plants, and b) Number of pods observed from drought recovered plants. Statistical analysis shows P value \*\* < 0.01.



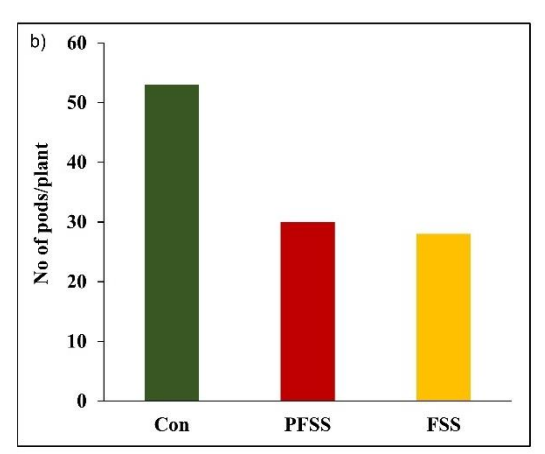
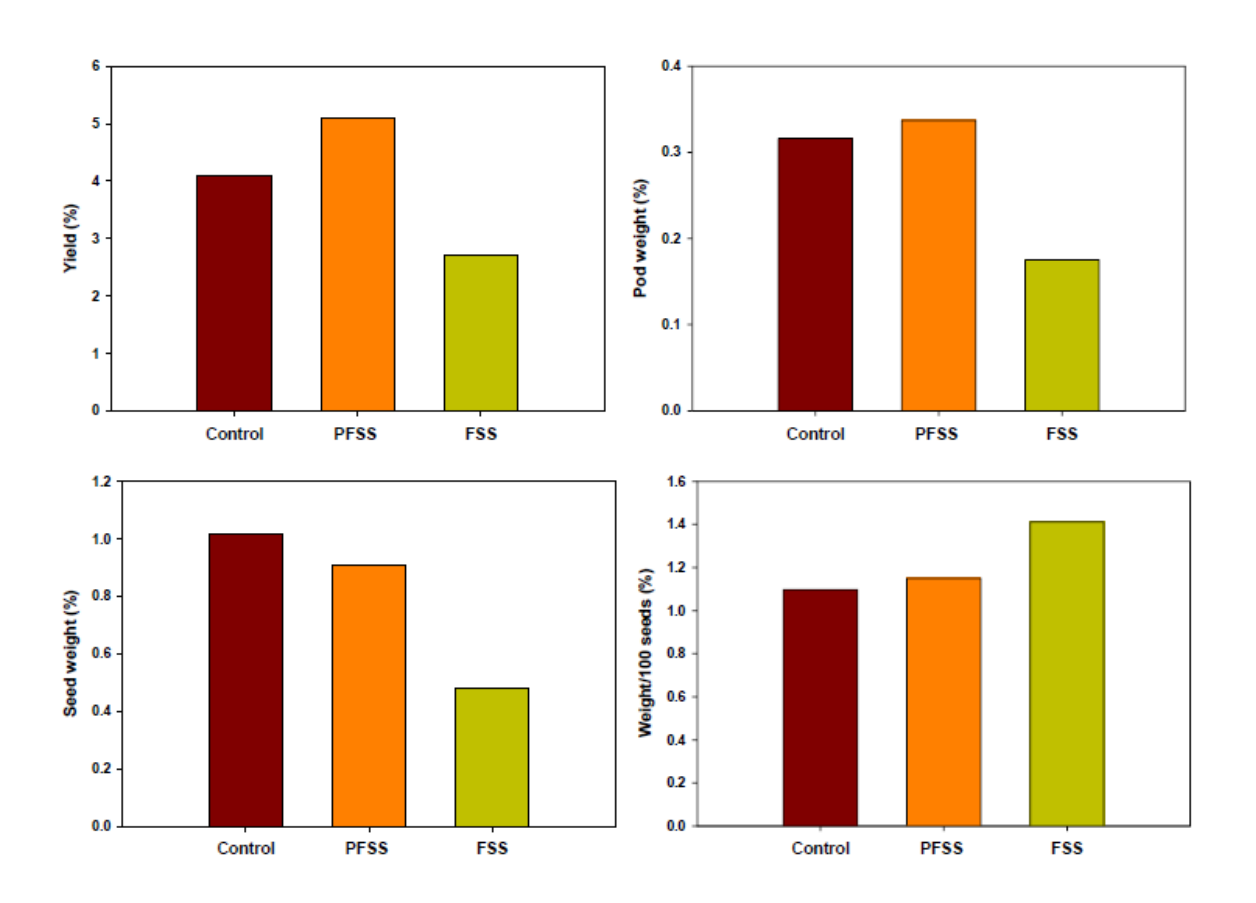


Fig. 43. Analysis of reproductive characteristics from drought recovered pigeonpea plants.

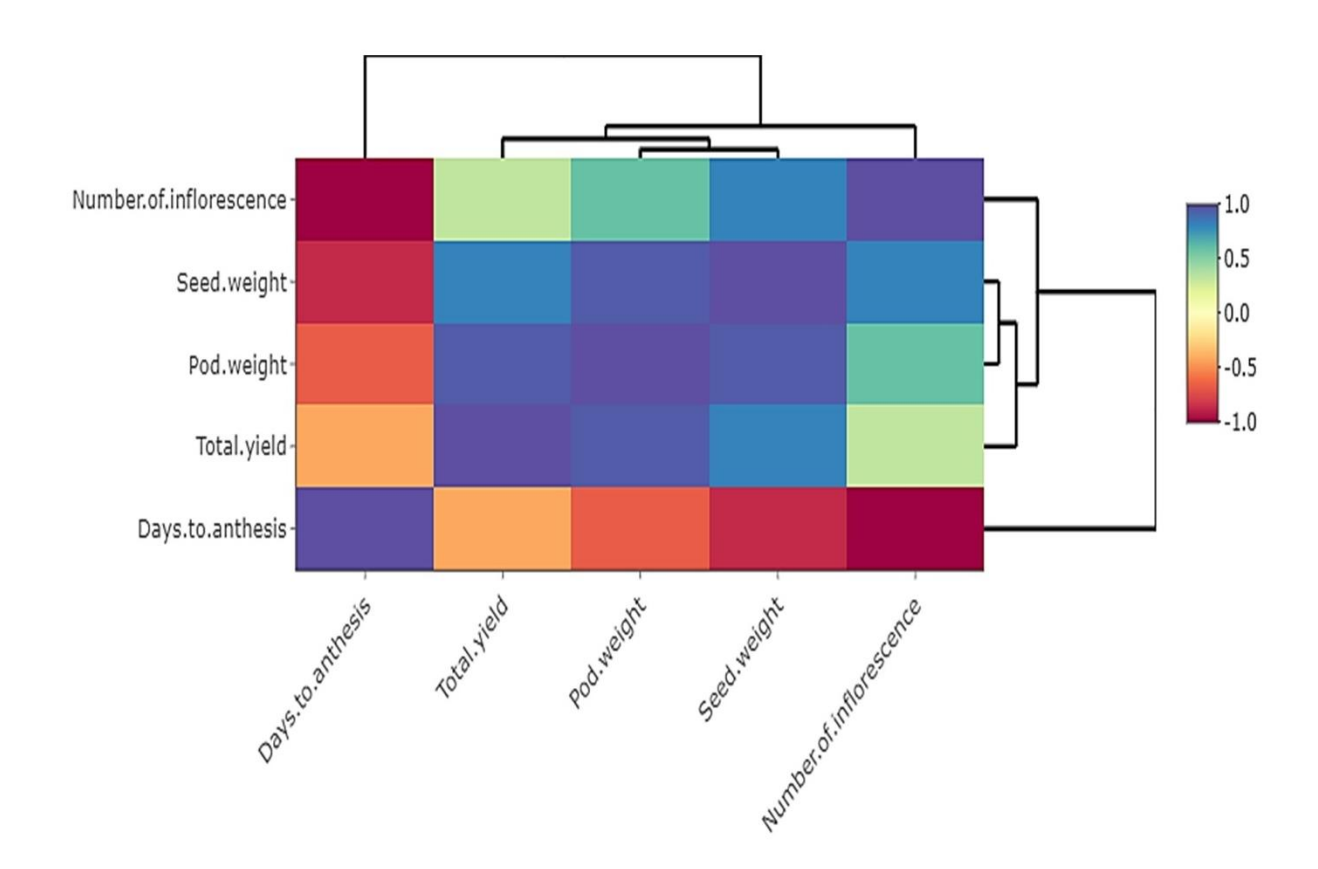


## **C.** Correlation of reproductive parameters

Correlation analysis was performed to understand the effect of drought on the reproductive parameters of pigeonpea. Days to anthesis was negatively correlated with all reproductive parameters confirming that delayed flowering in pigeonpea under drought affects the reproductive characteristics. Days to anthesis showed a strong negative correlation to the number of inflorescences, seed, and pod weight but a moderate negative correlation with total yield. On the other hand, all the remaining reproductive parameters, including the number of inflorescences, total

yield, seed weight, and pod weight, were positively correlated (Fig. 44).

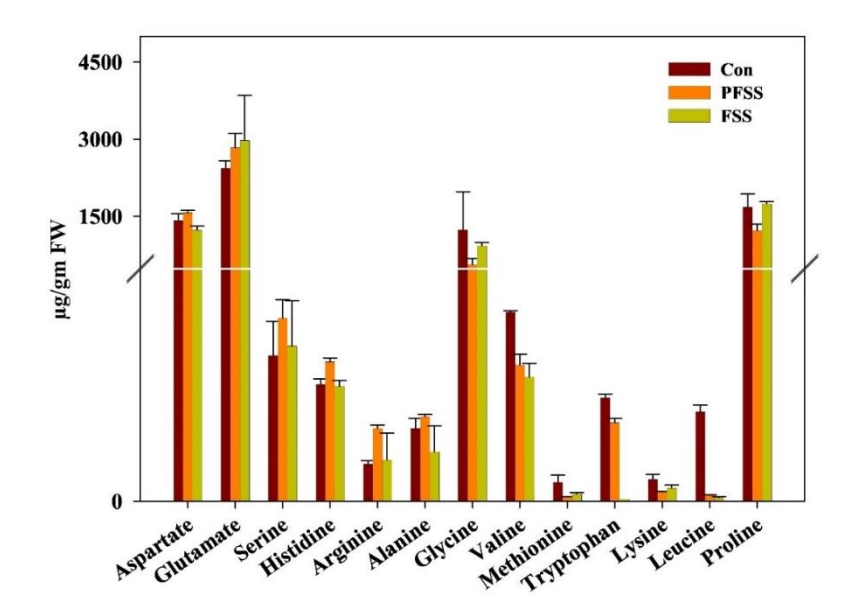
Fig. 44. Correlation heatmap of reproductive characteristics in pigeonpea under drought.



### D. Drought effects on the nutritional quality of pigeonpea seeds

Amino acids were analyzed in seeds obtained from drought-recovered plants. Essential amino acids, including lysine and valine, were decreased in seeds obtained from drought-recovered plants compared to control plants (Fig. 45). Lysine was reduced drastically in seeds from both recovery plants, especially in plants recovered at preflowering stage stress (PFSS Rec) compared to plants recovered at flowering stage stress (FSS Rec); valine decreased significantly in seeds from recovery plants from FSS. Leucine, methionine, tryptophan, and glycine were also reduced drastically in seeds from both drought-recovered plants, especially from the FSS plant. Glutamate and proline were the most increased amino acids observed in seeds of the recovery plant, especially in seeds from the FSS plant. The remaining amino acids, including aspartate, serine, histidine, arginine, and alanine, were higher in seeds collected from drought-recovered plants, especially the PFSS plants.

Fig. 45. Analysis of free amino acids in pigeonpea seeds from drought recovered plants.



# **CHAPTER 4**

# **DISCUSSION**

#### **DISCUSSION**

# Pigeonpea exhibited a positive growth and photosynthetic response under elevated CO<sub>2</sub>

Elevated CO<sub>2</sub> is one of the significant contributors to climate change affecting plant growth and reproduction. Knowledge on crop responses to rising CO<sub>2</sub> is crucial as it holistically influences plant metabolism and will help to design effective breeding programs to develop climate-resilient crops. The species-specific responses vary among C3-C4, legume-non-legume, and crop-tree species. Compared to non-legumes, legumes exchange excess carbon that is fixed due to enhanced photosynthesis for nitrogen with the help of N<sub>2</sub> fixing symbionts, giving them a comparative advantage when grown under elevated CO<sub>2</sub> (Rogers et al., 2009). Pigeonpea showed higher photosynthetic efficiency when grown under elevated CO<sub>2</sub> (Sreeharsha et al., 2015). Pigeonpea showed enhanced photosynthetic efficiency under elevated CO<sub>2</sub> as the plant progresses from one developmental phase to another, maintaining this efficiency throughout the pigeonpea life cycle.

Chlorophyll fluorescence measurements help in the identification of photochemically efficient plants that has better carbon sequestration. Fv/Fm represents the maximum quantum yield of PSII, indicating the photosynthetic efficiency in plants. Pigeonpea grown under elevated CO<sub>2</sub> showed increasing Fv/Fm during all phases of development compared to its control counterpart grown under ambient CO<sub>2</sub>. Fv/Fm ratio increased in elevated CO<sub>2</sub> grown plants from 0.8 in the preflowering phase to 0.82 in the post-flowering phase. This Fv/Fm ratio increase suggests that pigeonpea is photosynthetically more active under elevated CO<sub>2</sub>. On the other hand, decreasing Fo and increasing Fm were observed in elevated CO<sub>2</sub> plants. Reduced Fo shows that

reaction centers are activated more in elevated CO<sub>2</sub> grown plants, as higher Fo values suggest an inefficient function of the oxygen-evolving complex, associated with the inactivation of reaction centers. Increased Fv/Fo was observed at all stages in elevated CO<sub>2</sub> grown plants. Higher Fv/Fo shows an efficient water-splitting complex on the donor side of PSII with increasing ATP production for further dark reactions. ABS/Csm and ETo/Csm were increased, while ABS/RC, TRo/RC, ETo/RC, and DIo/RC were decreased in elevated CO<sub>2</sub> grown plants, further confirming increased photosynthetic efficiency under elevated CO<sub>2</sub>. Parameters like PI (abs) and RC/Csm showed a significant upregulation in elevated CO<sub>2</sub> plants compared to their ambient counterparts confirming the overall photosynthetic efficiency of plants under elevated CO<sub>2</sub>. PI (abs) indicates the overall performance index or efficiency of PSII, and RC/Csm represents the density of active reaction centers per cross-section (Sekhar et al., 2014). Elevated CO<sub>2</sub> grown pigeonpea showed an increase in both parameters, confirming that elevated CO<sub>2</sub> enhances photosynthetic efficiency. Also, a significant upregulation of PI (abs) and RC/Csm was observed as the developmental stage progressed in elevated CO<sub>2</sub> grown plants, with the highest at the post-flowering phase. It confirms that elevated CO<sub>2</sub> does not cause photosynthetic acclimation due to enhanced Rubisco carboxylation suggesting absence of photosynthetic acclimation that other plants, especially nonlegumes, face (Sreeharsha et al., 2015). This enhanced photosynthesis translates to better carbon sequestration, helping in enhanced pigeonpea growth.

Our studies also confirmed that pigeonpea exhibited a positive growth response when grown under elevated CO<sub>2</sub> as shown in growth parameters like the height of the plant, number of nodes, and total biomass, which were also previously reported in our laboratory (Sreeharsa et al., 2015). Under elevated CO<sub>2</sub>, pigeonpea plants showed

increased plant height and number of nodes confirming that elevated CO<sub>2</sub> helps in enhanced growth with the help of excess photosynthates produced at all developmental stages in pigeonpea.

#### Delayed floral transition was observed in pigeonpea under elevated CO<sub>2</sub>

The flowering pattern and its regulation in legumes under elevated CO<sub>2</sub> are not fully characterized. Hence understanding the effect of elevated CO<sub>2</sub> on the onset of flowering in pigeonpea certainly provides valuable information on the flowering cascade in legumes. In pigeonpea, delayed flowering was observed when grown under elevated CO<sub>2</sub> (Fig. 9). A delay of ± 9 days was observed in elevated CO<sub>2</sub> grown plants. Studies on certain plants under elevated CO<sub>2</sub> have shown accelerated and/or delayed flowering (Springer and Ward 2007). However, the varied flowering response in plants under elevated CO<sub>2</sub> has not been fully understood. In this study, the expression pattern of various genes involved in flowering was studied to investigate the effects of elevated CO<sub>2</sub> on floral initiation in pigeonpea. Flowering is controlled by various endogenous factors both at metabolite and gene levels. The transcript levels of the genes were assessed in samples collected from 3 different time points, each representing a phase in the pigeonpea lifecycle- 35 DAE (vegetative phase), 55 DAE (transition phase), and 65 DAE (reproductive phase). Pigeonpea usually flowers after 60 days after emergence. Anthesis was usually observed after 65 DAE in ambient plants and 9 days later in elevated plants; therefore, 65 DAE was regarded as the commencement of the reproductive period in our study. Genes involved in the aging pathway, photoperiod pathway, circadian rhythm, and floral integrators were analyzed through qRT-PCR to check for variation in the regulation of flowering in ambient and elevated CO<sub>2</sub> grown

plants. One of the important contributors to floral initiation is SQUAMOSA PROMOTER BINDING PROTEIN LIKE (SPL) involved in the age-dependent pathway. SPL is a transcriptional factor that promotes flowering by mediating juvenile-to-adult transition in plants by the action of miR172 and MADS-box genes (Wang et al., 2009; Huijser and Schmid. 2011). The miR156 and miR172 are known for plant transition from the vegetative to the reproductive stage. The miR156 delays reproductive transition by repressing SPL, while miR172 promotes the reproductive stage in the age-dependent pathway (Wang et al., 2009, Yamaguchi et al., 2009, Yang et al., 2013, Yu et al., 2013, Quiroz et al., 2021).

As the plant grows, miR156 levels increase till plant maturation, and once the plant enters the adult/reproductive phase, its level decreases, and subsequently, miR172 increases leading to floral initiation (Hujiser and Schmid. 2011, Jung et al., 2011). Our study showed that in all three stages, especially 55 DAE and 65 DAE, SPL expression was decreased in elevated CO<sub>2</sub> grown plants compared to ambient CO<sub>2</sub> grown plants. We also observed that miR156 levels are higher than miR172 at all-time points, especially at 55 DAE as the plant enters the transition period in the elevated CO<sub>2</sub> grown plants. As anthesis could be seen in the ambient plant (65 DAE), the levels of miR156 in the elevated plant were still higher than miR172, causing a delay in flowering. Even though miR172 levels are lower than miR156, an increase in miR172 levels was observed in elevated CO<sub>2</sub> grown plants at 65 DAE compared to the 55 DAE stage. We believe that elevated CO<sub>2</sub> grown plants are preparing for anthesis by the increasing miR172, which is confirmed by the blooming recorded after 9 days.

Among the endogenous cues that affect flowering, trehalose-6-phosphate (T6P) is considered a regulatory carbon signal along with sucrose which is involved in the agedependent pathway (Wu et al., 2009, O'Hara et al., 2013). The T6P levels repress miR152 and activate miR172 expression helping in the transition to flowering through SPLs. UDPG and glucose-6-phosphate are the precursors for trehalose-6-phosphate, wherein TPS is the enzyme involved. In plants, UDPG and glucose-6-phosphate are derived from sucrose; hence, higher sucrose levels are known to repress miR156 (Bolouri et al., 2013, Wahl et al., 2013, Wang et al., 2020). In pigeonpea, low expression of trehalose-6-phosphate synthase gene (TPS6) was observed in elevated CO<sub>2</sub> grown plants compared to ambient plants, but an increment was observed at 65 DAE compared to other time points correlating with miRNA levels. Lower levels of glucose and sucrose during 55 DAE in elevated CO2 grown pigeonpea lead to upregulation of miR156, causing repression of both SPL and miR172, required for the maturation and floral initiation, thus delaying the flowering. It is also known that cell wall invertase (CWIN) has a role in the floral transition. Higher expression of CWIN that cleaves sucrose into glucose and fructose has been shown to accelerate flowering in Arabidopsis (Heyer et al. 2003). From our studies, we have observed lower levels of CWIN throughout the developmental stages in elevated CO<sub>2</sub> grown plants, which correspond to lower levels of the hexoses during the transition phase. We presume this could be another reason for delayed flowering in pigeonpea. Nitrogen (N) is one of the significant macronutrients affecting flowering, wherein an optimal N level promotes flowering while limiting N or high N delays flowering (Lin and Tsay 2017, Weber and Burow 2018). In pigeonpea, N levels remained constant throughout the life cycle when grown under elevated CO<sub>2</sub> (Sreeharsha et al., 2015). We presume that the basis for low

sugars might be due to the redirection of sugars essential for SAM towards the root for increased nodulation leading to higher levels of N (Sreeharsha et al., 2015). We conclude that the sugars (sucrose) are transported toward roots leading to an increase in nitrogen content which results in a prolonged vegetative phase and delay in flowering. This confirms U-shaped flowering where high N delays flowering (Lin and Tsay 2017). Hence, the exchange of sugar to N causes a dip in sugar required for the repression of miR156, leading to the suppression of other genes required for floral transition.

Photoperiod and age-dependent pathways are some other contributors to floral initiation. These pathways, later on, integrate with floral integrators helping in inflorescence meristem development. Genes like GI and CO are part of the photoperiod pathway is affected by the circadian clock genes such as CCA1 and TOC1 which are part of the central oscillator. Along with PRR5, they regulate GI and CO through a feedback loop. Furthermore, ZTL and COP1 photoreceptors regulate CO positively and negatively, respectively (Quiroz et al., 2021). In pigeonpea, as COP1 decreased, there were increased CO levels in elevated plants. Increased ZTL and GI also helped in the upregulation of CO at 65 DAE in elevated plants. Further, the CO gene leads to FT expression, which is subsequently transported to the meristem, where it helps in the expression of inflorescence meristem genes along with SOC1 (Fornara, de Montaigu, and Coupland. 2010). The floral integrator SOC1 acts downstream of FT and encodes a MADS-box transcription factor (Hyun et al., 2016). It is known to integrate multiple flowering signals from different pathways like photoperiod, hormonal, and agedependent (Quiroz et al., 2021). We have analyzed the gene transcripts involved in the photoperiod pathway, which were upregulated in ambient CO<sub>2</sub> grown plants at 35 DAE

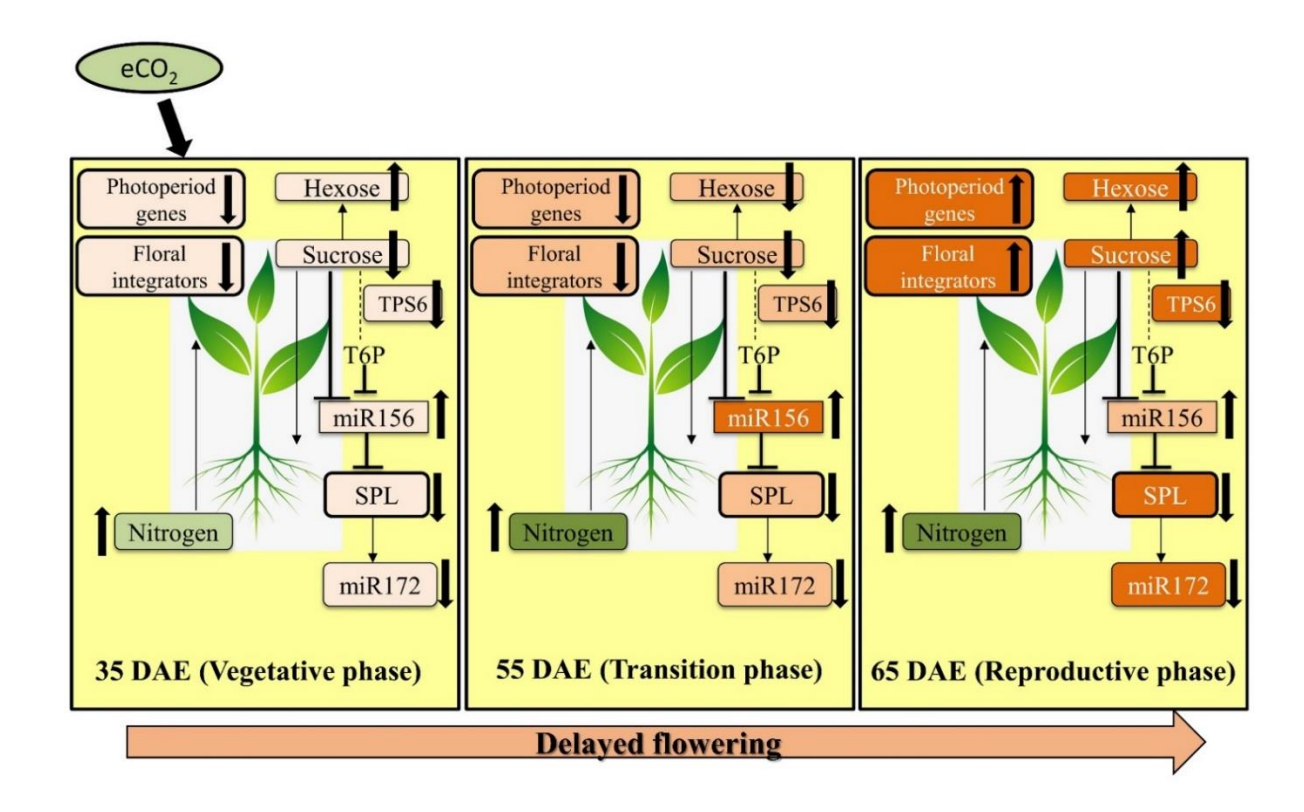
and 55 DAE compared to elevated CO<sub>2</sub> plants. However, at 65 DAE, elevated plants showed higher expression of GI, CO, FT, and SOC1 genes than in ambient CO<sub>2</sub> grown plants. At 55 DAE, the genes for floral initiation were expressed more, thus leading to floral meristem formation. However, the elevated CO<sub>2</sub> grown plants showed lower levels of these floral initiation genes, which can be considered as one of the reasons for the delay in flowering. The higher expression levels of SOC1, TOC1, and FT were observed in the ambient leaf compared to the elevated leaf at 55 DAE, contributing to the delay in flowering. At 65 DAE, most of the floral regulator genes showed increased levels compared to 55 DAE, preparing elevated CO<sub>2</sub> grown plants for flowering.

Correlation network analysis between flowering genes confirmed that miR156 is negatively correlated with all flowering-related genes confirming that it plays a major role in the floral transition. We proposed a model explaining how various factors are involved in delayed flowering in pigeonpea (Fig. 46). As the plant enters from the vegetative phase to the transition phase, the floral regulatory genes are activated in ambient grown pigeonpea. However, these genes were downregulated in elevated CO<sub>2</sub> grown plants. The major reason is the high expression of the vegetative phase promoting miR156, causing decreased levels of SPL and miR172 required for floral transition. The remobilization of sucrose (C) is considered a critical signal for the suppression of TPS, causing enhanced expression of miR156. Even when the plant enters the reproductive phase, the floral activating genes were reduced due to enhanced miR156, causing delayed flowering.

However, this delayed flowering does not affect the inflorescence formation as pigeonpea showed higher inflorescences under elevated CO<sub>2</sub>. To understand the effect

of elevated CO<sub>2</sub> on floral organ differentiation, ABCE genes involved in this differentiation process were analyzed during the inflorescence stage of flowering. During the inflorescence stage, AP3, AP1, PST, AGA, and SEP were highly expressed in elevated CO<sub>2</sub> plants. AP2 and AP1 genes belong to class A genes of the floral model that help to differentiate sepals, while AP3 and PST are class B genes involving the formation of petals. PST is also involved in stamen development, while the AGA class C gene is involved in carpel differentiation. SEP class E gene is known to affect the expression of all other ABC genes (Chen et al., 2018). In elevated CO<sub>2</sub> grown pigeonpea, all genes involved in floral organ formation at the inflorescence stage are upregulated compared to ambient plants, confirming that floral formation is accelerated in elevated CO<sub>2</sub> conditions. This is confirmed by the days required for the bud or inflorescence to form a mature flower which was an average of 4/5 days in elevated CO<sub>2</sub> conditions compared to 7/8 days in ambient conditions. High expression of the floral organ differentiation genes in elevated CO<sub>2</sub> grown plants could be responsible for a higher number of flowers leading to a higher yield in pigeonpea as reported in our recent study (Unnikrishnan et al., 2021).

Fig. 46. Proposed model on the molecular regulation of delayed flowering under elevated CO<sub>2</sub>. The brown color shows the presence of metabolites and gene transcripts in leaves and green in roots, and the ascending intensity of the color shows an increase in concentration at the time point in elevated CO<sub>2</sub> grown plants. The arrow represents upregulation or downregulation compared to ambient CO<sub>2</sub> grown plants. The remobilization of sucrose (C) is considered a signal for the suppression of TPS, causing enhanced expression of miR156, which results in the suppression of various other genes required for floral initiation.



The sequential effect of elevated CO<sub>2</sub> shows a positive response on the reproductive physiology of pigeonpea

In general, many C3 plants showed enhanced photosynthesis under elevated CO<sub>2</sub> due

to increased RUBISCO carboxylation leading to enhanced carbon fixation but experience photosynthetic acclimation after a certain period due to N limitation and source-sink imbalance (Sreeharsha et al., 2015). Pigeonpea, a legume crop, was shown to overcome the problem of photosynthetic acclimation by maintaining a balance between C: N ratio due to its ability to fix nitrogen, thus improving growth and yield (Sreeharsha et al. 2015). Our results follow the above growth patterns and infer that the plant utilized the enhanced C levels due to increased photosynthesis to increase its growth, pod production, and seed yield. Similar increases in the seed yield were reported in wheat and soybean when grown under elevated CO<sub>2</sub> (Bunce 2016; Soba et al., 2019). Our study showed only a slight decrease in N, which may be due to N dilution with growth because of C accumulation (Bourgault et al., 2016; Bourgault et al., 2017). Usually, the levels of metabolites including sugars fluctuate with the progression of seed development. During the initial stages of seed development, a higher hexose/sucrose ratio is known to promote cell and nuclear division in the embryo and endosperm. As the seed reaches maturity, hexose: sucrose ratios gradually decrease to maintain the sink strength. These prestored sugars, especially sucrose and sugar polymers, are known in seed desiccation tolerance mechanisms, in turn maintaining seed vigor (Wang et al., 2017). Elevated CO<sub>2</sub> grown pigeonpea seeds have shown higher sucrose content than ambient seed due to increased photosynthesis and enhanced C assimilation, thus reducing the seed desiccation cycle and subsequent increase in seed

vigor (Wang et al., 2017). These legume-specific sugar monomers collectively contributed to higher total carbohydrates in elevated CO<sub>2</sub> grown pigeonpea seed. These slowly digesting legume carbohydrates make elevated CO<sub>2</sub> grown pigeonpea seed with a low glycemic index food suitable for diabetes (Maphosa and Jideani 2017). Also, resistant starch and other oligosaccharides make the pigeonpea seed a good dietary fiber source. They also can act as prebiotics for the beneficial gut bacteria, which form shortchain fatty acids like butyrate upon fermentation and lead to a healthier gut microbiome. It can be inferred from the GC-MS analysis that elevated CO<sub>2</sub> grown seeds have more dietary fiber than in the ambient CO<sub>2</sub> grown seeds. However, excess intake of these sugars, especially raffinose, may cause bloating, and this can be avoided by various food processing techniques like boiling, soaking, cooking, and germination (Maphosa and Jideani 2017). Four essential amino acids were upregulated, including lysine, valine, histidine, and threonine; the rest were non-essential amino acids. Amino acids like leucine, glutamine, aspartic acid, and norvaline were down-regulated in elevated CO<sub>2</sub> grown pigeonpea seed. The amino acids lysine, methionine, threonine (Asp family), phenylalanine, and tryptophan of the aromatic group, valine, leucine, isoleucine (BCAA family), and histidine are considered essential amino acids for humans (Galili et al., 2016; Amir et al., 2018). Lack of these amino acids can cause protein malnutrition, like lower disease resistance and decreased blood proteins, resulting in mental and physical retardness in children (Galili et al., 2013). Lysine is an essential amino acid not present in cereals; hence, legumes rich in lysine are combined with cereals for complete nutrition. In the present study, we have recorded that elevated CO<sub>2</sub> grown seeds contained a higher percentage of these essential amino acids (lysine, threonine, valine, and histidine) than the ambient seeds, thus increasing the nutritional

status of elevated CO<sub>2</sub> grown seeds (Dam et al., 2009). Lysine and threonine, derived from aspartic acid, were found to be higher in elevated seed while aspartic acid was reduced, indicating enhanced conversion of aspartic acid to lysine and threonine and subsequently to glycine. Asp kinase (AK), a regulatory enzyme in Asp conversion, is allosterically inhibited by both lysine and threonine (Galili et al., 2016). Nevertheless, from our study, we can assume that the overproduced lysine and threonine might be accumulating inside the vacuole and hence might not inhibit plastidic AK activity, which was also shown in lysine enhanced Arabidopsis mutant (Angelovici et al., 2011). High lysine negatively regulates TCA metabolites since pyruvate, a precursor of the TCA cycle, enters the lysine biosynthesis pathway (Angelovici et al., 2011). In the current study, fumarate and succinate were found to be less in elevated CO<sub>2</sub> grown seed, and this might be due to high lysine content. Among the amino acids derived from the BCAA family, only valine was higher in the elevated CO<sub>2</sub> grown seed, while leucine was higher in the ambient seed. The possible reason could be an increased amount of 3-methyl-2-oxobutanoate, which might be used for valine biosynthesis and hence produce less leucine because 3-methyl-2-oxobutanoate branches off for the biosynthesis of leucine in the main pathway (Galili et al., 2016).

Higher levels of proline were observed in elevated seeds, which mediates storage protein biosynthesis and function as an osmoprotectant to avoid desiccation of seeds as well as in the development of the embryo (Mattioli et al., 2009). Higher free amino acids with relatively low protein content in elevated CO<sub>2</sub> grown pigeonpea seeds suggest that the elevated CO<sub>2</sub> grown seeds were better prepared for desiccation and subsequent germination as these biological processes require decreased C/N ratio and accumulation of free amino acids (Fait et al., 2006). Our data also represented two fatty

acids, including hexadecanoic acid (palmitic acid) and octadecanoic acid (stearic acid), which are helpful for energy generation during germination, were upregulated in elevated CO<sub>2</sub> grown pigeonpea seed. The levels of 3 cyclitols, including inositol, myoinositol, and pinitol, decreased in elevated CO<sub>2</sub> grown pigeonpea seed. During the seed development process, seeds mostly enter into the desiccation stage, wherein loss of water results in the dry seed entering a stationary state and remaining dormant till germination. The seeds used for proteomic analysis were fully mature seeds that had entered the desiccation stage. The seeds in plants, including pigeonpea, growing under semi-arid climates, undergo the desiccation phenomenon to escape the unfavorable environment. Seed desiccation is also an important stage where several changes occur transcriptionally and metabolically (Angelovici et al., 2010), and similar patterns were observed in our studies. Transcripts associated with DNA repair and transport were upregulated in elevated CO<sub>2</sub> grown pigeon pea seed compared to ambient CO<sub>2</sub> grown pigeonpea seed. The transcripts related to signaling, transport, transcription, lipid, and development were found to be down-regulated in elevated CO<sub>2</sub> grown pigeonpea seed. Among proteins identified, a higher number of transposons were observed in elevated CO<sub>2</sub> grown pigeonpea seeds (Fig. 24). Transposons are also known as jumping genes for their ability to move from one position to another in the genome. They help to create genetic diversity and are used in phylogenetic analysis. They play a huge role in genome organization and regulation of gene expressions. Due to their ability to move, TEs are also used in crop improvements of many plants (Singh et al., 2019). Pigeonpea genome sequencing has predicted 12,511 transposable related genes out of 510,809,477 bp of sequence (Singh et al., 2012). It is well known by genome sequencing that the pigeonpea genome comprises a large number of repeat elements categorized as class I-

retrotransposons (RTR) and class II- DNA transposons. Among REs observed, the majority were RTRs with 23.59%, within which LTR retrotransposons- Copia and Gypsy were predominant with 6.10% and 16.02%. Our proteome data showed that copia and gypsy TEs were upregulated in elevated CO<sub>2</sub> conditions. Among the proteins which were exclusively expressed in elevated CO<sub>2</sub> conditions 45.37% constituted copia and 1.84% gypsy proteins. Previous studies have shown that TEs in legumes (pigeonpea, soybean, common bean) were near to nucleotide binding leucine-rich repeats genes and help to develop disease resistant varieties to enhance yield and quality (Singh et al., 2019). From our present study, we believe that a higher number of TEs observed in elevated CO<sub>2</sub> grown pigeonpea seeds play a major role in enhanced yield as well as in creating tolerance in response to stress due to their role in epigenetic changes. Proteins involved in secondary metabolism were also upregulated in elevated CO<sub>2</sub> grown pigeonpea seed. One of the upregulated proteins is 4-hydroxy-3-methylbut-2-en-1-yl diphosphate synthase which is part of terpenoid biosynthesis (Table 8). They catalyze the conversion of 2-C-methyl-D-erythritol 2,4-cyclodiphosphate to 4-hydroxy-3-methylbut-2-en-1-yl diphosphate during the MEP pathway of isoprene biosynthesis. These secondary metabolites act as defense mechanism against biotic stress and help to attract seed dispersal organisms (Wink 2013). The conjugated forms of these metabolites are easily soluble in water; hence upon seed imbibition, they are released into the soil as signals to deter pathogens and help attract symbionts, especially in the case of legumes, in turn helping the emerging seedling (Ndakidemi and Dakora 2003). The impact of elevated CO<sub>2</sub> on the levels of secondary metabolites varies from plant to plant. For example, the levels of monoterpenes in Scots pine needles were decreased under elevated CO<sub>2</sub> (Raisanen et al., 2008). However, in our case, the protein (4-

hydroxy-3-methylbut-2-en-1-yl diphosphate synthase) involved in terpenoid biosynthesis was upregulated in elevated CO<sub>2</sub> grown pigeonpea seed. The upregulated protein is a part of the MEP pathway in which pyruvate and G3P are its precursors. Hence, we can assume that in elevated CO<sub>2</sub> grown pigeonpea seed, the pyruvate enters into terpenoid and other amino acid biosynthetic pathways, leading to reduction in pyruvate content entering the TCA cycle, whereas metabolites were found to be decreased in the TCA cycle which is in accordance with our metabolite analysis. Since desiccant seeds undergo stress at remarkable levels, protecting genetic material in the seeds is highly crucial. In most recalcitrant seeds, the proteins involved in DNA repair were observed which help to restore the damage to DNA (Waterworth et al., 2019). In our case, elevated CO<sub>2</sub> grown pigeonpea seed had increased levels of the proteins involved in DNA repair (eg- Helicase SEN 1, Replication factor C subunit 3), thus increasing its longevity and vigor. Our data also infer that elevated CO<sub>2</sub> grown pigeonpea seed is better prepared for germination than ambient CO<sub>2</sub> grown pigeonpea seed. Recently, Krishnan et al. 2017 identified various stress-related proteins like embryonic DC-8, EMB1, heat shock proteins, and elongation factor 2, which were also observed in the present study. Elevated CO<sub>2</sub> grown pigeonpea seed showed the presence of Bowman-Birk type proteinase inhibitor 2 (BBI) and Kunitz-type trypsin inhibitorlike 2 protein which are protease inhibitors, which help to act against pathogens, insects, and also as part of the immune response. These inhibitors are known to play the role of anticarcinogen. Proteins synthesizing secondary metabolites like lignin, terpenoid, and flavonoids were exclusively expressed in elevated CO<sub>2</sub> grown seeds (Table 9). GTP cyclohydrolase involved in folate biosynthesis was also exclusively expressed in elevated CO<sub>2</sub> grown seeds. Folate is known for methylation reactions necessary for

gene regulation and synthesis of lipids, proteins, and lignin (Gorelova et al., 2017). Folate (B9 vitamin) is also important for health and is synthesized only in plants (Gorelova et al., 2017). Expression of folate biosynthesis protein in elevated CO<sub>2</sub> grown seeds confirms that the nutritional quality of pigeonpea seeds increased under elevated CO<sub>2</sub>. Protein isoforms belonging to the subfamily of serine/threonine protein phosphatases were observed exclusively in elevated CO<sub>2</sub> grown pigeonpea seed which are known to play a positive role in stress signaling and protect the macromolecules of seed from stress during the desiccation period (Wang et al., 2015). In elevated CO<sub>2</sub> grown pigeonpea seeds, a large number of stress related proteins were identified (Table 9). The proteome analysis of seeds grown in elevated CO<sub>2</sub> demonstrates that seeds are better equipped to maintain seed vigor by accumulating macromolecules, including lipids and stress-related proteins during the desiccation period. Pigeonpea is one of the underutilized legumes in terms of its nutritional status compared to other legumes. In the current study, the nutritional quality of pigeonpea seeds grown under elevated CO<sub>2</sub> has been established, which showed higher amounts of essential amino acids making the crop nutritionally superior to its ambient counterparts. The proteome analysis of seeds also showed that elevated CO<sub>2</sub> grown pigeonpea seed was better programmed for the desiccation stage.

The developmental stage of pigeonpea plays a role in the negative response to short-term drought

It is a well-known fact that elevated CO<sub>2</sub> influences drought at present. Hence, understanding plants' behavior under drought is essential for crop improvement studies. Plants respond to drought based on the severity and the environment they are grown in. Short-term drought response or dehydration avoidance entails stomatal closure, decreased C assimilation, multi-stress sensing, gene responses, inhibition of growth, and signal transport in plants (Farooq et al., 2009). Pigeonpea being a semi-arid crop, is known for drought tolerance. Here in our study, we have subjected drought at two different developmental stages of pigeonpea to understand the effect of drought on pigeonpea and the severity depending on the stage to which it is exposed. Drought was subjected at the preflowering stage of pigeonpea, i.e., 40-50 days after emergence (DAE), and flowering stage, i.e., 55-70 DAE starting from 59 DAE. Drought at the preflowering stage showed decreased photosynthetic rate. The photosynthetic rate decreased mainly at 9 DAS with 29 %. Transpiration rate and stomatal conductance were also reduced, but no significant difference was observed under PFSS. Drought at the flowering stage also showed decreased photosynthetic rates compared to control plants.

However, stomatal conductance and transpiration rate decreased significantly at flowering stage drought (FSS) compared to preflowering stage drought (PFSS). Both stomatal conductance and transpiration rates decreased as the stress progressed during drought at the flowering stage, with a significant reduction at 9 DAS. Water use efficiency (WUE) was increased without significant changes in PFSS pigeonpea

compared to control, but a steep increase was observed in pigeonpea when drought was subjected to the flowering stage. This increase in WUE at FSS is due to the reduction of transpiration rate and low stomatal conductance. The above results on photosynthesis and transpiration clearly demonstrate the resilient response of pigeonpea to low levels of water availability. The data also confirm that drought at the flowering stage is perceived as severe stress as observed by the reduced stomatal conductance and transpiration. High water use efficiency is correlated with stomatal closure to reduce transpiration under a limited water supply. Reduction in photosynthesis under drought is due to various mechanisms, wherein one of them is limited CO<sub>2</sub> intake due to stomatal closure leading to limited carboxylation (Faroog et al., 2009). In the present study, decreased photosynthesis under drought can be attributed to increased stomatal closure causing limitation in carboxylation. Drought tolerant species have been shown to maintain WUE by reducing water loss under severe drought as part of their tolerance mechanism (Farooq et al., 2009). Leaf relative water content was reduced in droughtstressed plants at both the preflowering and flowering stages. At 9 DAS, LRWC was reduced to the highest by 71 % at both PFSS and FSS conditions, confirming that the effect of drought stress increased progressively. LMC is also reduced in drought stressed plants at both developmental stages, suggesting that drought reduced plant water status in pigeonpea under both developmental stages- preflowering and flowering.

In response to drought, plants initiate various physiological mechanisms, including variations in the contents of sugars, amino acids, and plant growth regulators. Drought, at the preflowering stage, showed a decrease in sugar levels, especially sucrose, while hexoses were increased in drought-stressed plants. In comparison, drought at the

flowering stage showed a reduction of both glucose and sucrose while fructose was increased. Among glucose and sucrose, sucrose was reduced drastically at 9 DAS at the FSS condition. These reduced sugars, especially sucrose, are due to reduced photosynthetic rates as shown in Fig. 29. This decreased carbon assimilation aids in protection from stress as the energy required for growth is redirected to maintain homeostasis during stress.

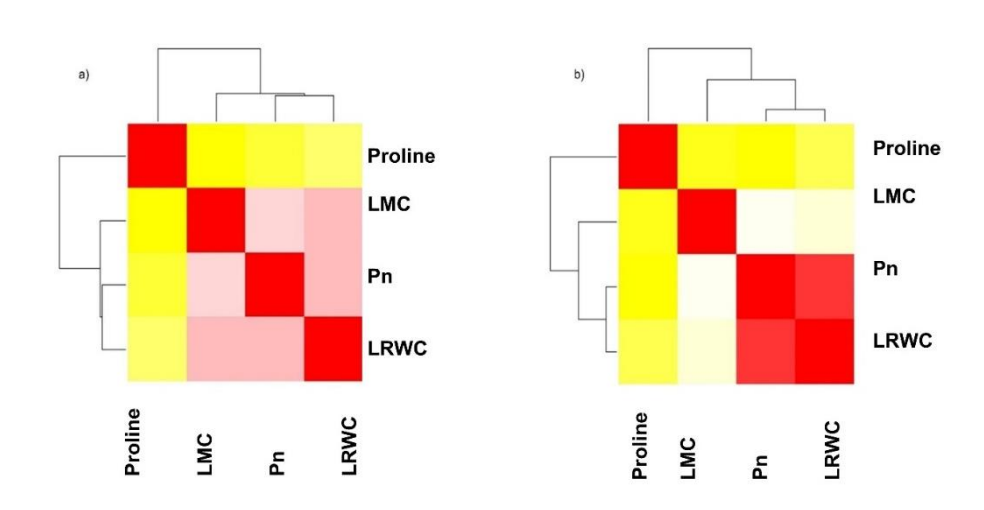
Most drought studies have shown that sugars, mainly sucrose, are upregulated under drought conditions as part of the protection system by acting as an osmoprotectant (Faroog et al., 2009). However, in this study, drought at both developmental stages in pigeonpea has shown reduced sucrose levels. This might be due to decreased photosynthesis, leading to low C assimilation. Plants under drought undergo either of the following- drought escape, drought avoidance, and drought tolerance. Plants undergoing drought avoidance response have been shown to have decreased C assimilation. We can infer that the drought at both developmental stages in pigeonpea has elicited a drought avoidance response. Sugars, especially the soluble sugars (sucrose, glucose, and fructose) are increased in leaves of drought susceptible rice varieties and reduced in resistant or tolerant varieties (Xu et al., 2015). On the other hand, drought in soybean tolerant variety has shown no change in sucrose levels among the drought treated and control plants, especially at vegetative stages of growth which confirms that sugars might not play a significant role in a plant's osmoprotection under stress during early life stages (Silvente et al., 2012). In our study, drought at the preflowering stage showed a decrease in sucrose confirming that sucrose might not play an important role in osmoprotection under stress during the early stages of the plant life cycle. On the contrary, sucrose was reduced significantly at the flowering stage showing

the severity of stress based on the developmental stage to which it is exposed. Studies on Lanzhou lily during different growth stages showed reduced sugar (sucrose) levels under drought (Li et al., 2020). Our data show that total amino acid content was decreased in leaves of drought stressed plants, but few of the amino acids were upregulated. Amino acids, including lysine and leucine, were increased at 9 DAS, while proline was decreased at PFSS. The cause for the decrease in proline can only be attributed to the fact that the drought subjected at the preflowering stage must not have been perceived as severe stress. On the other hand, a drastic increase in proline was observed in FSS, especially at 9 DAS, confirming that drought at flowering is more severe. Drought on soybean in the vegetative phase also did not enhance proline levels, while at the reproductive phase, proline increased, concluding that proline only increased once perceived the drought as severe stress (Silvente et al., 2012). Other amino acids like arginine, glycine, methionine, tryptophan, valine, leucine, and histidine were also increased in drought stressed plants at 9 DAS in FSS conditions. Proline is one of the osmoprotectants that scavenge ROS under drought stress. At the FSS, proline was upregulated as the day of stress progressed, confirming that drought had severe effects when subjected at the flowering stage. Also, the free amino acids level was higher in drought stressed plants than in control plants at the flowering stage at all stress levels. Free amino acid levels were observed to be upregulated in plants affected by stress mainly as most amino acids act as osmoprotectants, precursors for secondary metabolites, alternate substrates for mitochondrial respiration, immune signaling, and much more (Silva et al., 2018, Hildebrandt et al., 2018). It is observed in our case that at both drought stages, i.e., PFSS and FSS, sugars (especially sucrose) were low due to reduced photosynthesis and in such cases, plants use the free amino

acids as alternate substrates for mitochondrial respiration (Silva et al., 2018, Hildebrandt et al., 2018).

The correlation heatmap during the FSS condition shows that proline is negatively correlated to glutamate, which can be observed from the amino acid quantification wherein proline and glutamate levels were inversely proportional. During stress (mainly abiotic stress) like salt or drought, glutamate is converted to form proline. Drought at the flowering stage showed high proline and low glutamate, confirming that the glutamate was being redirected to the formation of proline for mitigating the stress (Szabados and Savoure 2009). Proline acts as a molecular chaperone to protect protein integrity, and ROS scavenging system during stress (Szabados and Savoure 2009). Correlation analysis among LRWC, LMC, photosynthetic rate, and proline at both drought conditions have shown that proline was negatively correlated with all the above parameters (Fig. 47). This confirms the negative impact of drought on plant water status resulting in the production of osmoprotectants including proline.

Fig. 47. Correlation analysis among LMC, Pn, LRWC, and Proline under drought stress a) PFSS and b) FSS conditions. (Red-positive, Yellow-negative).



Plant growth regulators also play an essential role in stress signaling and tolerance mechanisms. Most of the hormones were downregulated under PFSS conditions due to the minimal severity of stress at the preflowering stage. However, drought at the flowering stage showed upregulation of most phytohormones- gibberellin, auxin, and abscisic acid. An increase in ABA is well known for mitigating drought stress as it helps in stomatal closure and minimizing water loss. The levels of ABA vary, causing different responses based on stress severity. ABA is known to regulate the transcription of drought responsive genes, the production of osmolytes, and maintain membrane structure and integrity (Mubarik et al., 2021, Raja et al., 2020, Verslues et al., 2006).

In comparison to preflowering stage, drought at the flowering stage showed a steep increase in ABA levels as stress progressed, confirming that drought was much more severe at the flowering phase of the plant. Increased levels of ABA also correlated with reduced stomatal conductance and transpiration rate and increased WUE confirming the role of ABA in maintaining the water status. Exogenous application of ABA on soybean under drought has shown improved WUE (He et al., 2019). ABA helps in drought tolerance or avoidance by mitigating ROS and stomatal closure. The protein kinase SnRKs activates ABA signaling, and these SnRKs are activated under starvation or low levels of sugars. Under both drought conditions, sucrose was reduced but significantly only at FSS leading to higher ABA levels at FSS. Higher levels of auxin are also known for drought tolerance which also showed an increase in other hormones including ABA, GA, and JA, ultimately helping to mitigate the stress (Zhang et al., 2020). At FSS conditions, drought stressed plants showed increased levels of auxin (IAA) at all stages of stress. We can thus infer that the increased severity of the drought stress at the flowering stage leads to the upregulation of certain growth hormones to

mitigate stress. Auxin activates antioxidant systems in plants, helping minimize the effect of drought (Sharma et al., 2015). Most of the hormones increased at FSS conditions as days of stress progressed, significantly higher at 9 DAS. Correlation analysis between hormones and metabolites showed that the relationship varied depending on the phase when drought was subjected. Auxin is produced from one of the amino acid tryptophan through several enzymatic pathways.

On the other hand, sucrose was negatively correlated with ABA suggesting that sucrose downregulates ABA synthesis. Auxin showed a negative correlation to histidine, alanine, tryptophan, and lysine in drought stressed plants at the preflowering stage. Coming to other hormones, GA3 showed a negative correlation with tryptophan and lysine. Gibberellin was positively correlated with multiple amino acids, including proline, in FSS. Gibberellins thus help to mitigate stress by accumulating osmoprotectants like proline. Under FSS conditions, GA3 was negatively correlated to sucrose. Downregulation of sucrose creates an energy-deficient condition in plants, activating SnRKs which sense the energy availability and inhibit plant growth and development during stress to maintain homeostasis. It is a part of the dehydration avoidance strategy commonly seen in plants undergoing drought, and hence we could observe delayed flowering as a part of this strategy to overcome the stress effects.

# Delayed flowering in pigeonpea as part of drought avoidance mechanism

Delayed flowering was observed in pigeonpea under both drought conditions. This delayed flowering might be due to the dehydration strategy by the plants in response to drought. The low sugars activate these strategies as a part of stress mitigation, causing these developmental changes. Even if delayed flowering was observed under drought

conditions, the severity of the stress perceived by the pigeonpea varied. Drought, when exposed at the flowering stage, was much more severe. Also, delayed flowering under drought is associated with a dehydration avoidance strategy (Kooyers 2015). The late flowering is usually associated with high WUE, a part of the dehydration avoidance strategy. High WUE correlates to decreased photosynthetic rates leading to the limitation in the amount of carbon fixed, causing delayed flowering, which was observed in the stressed conditions during different growth stages.

To understand the molecular mechanisms behind the delayed flowering under drought, expression patterns of various flowering gene transcripts were studied under drought conditions – PFSS and FSS. At PFSS conditions, most circadian clock and photoreceptor genes were upregulated at the initial stages of drought, i.e., 3 DAS and 6 DAS (Fig. 36). As drought progressed, most of these transcripts were downregulated at 9 DAS, including TOC1 and CCA1. The photoperiod genes like GI and CO were initially upregulated in drought stressed plants but downregulated by 3-fold and 4-fold at 9 DAS. Transcript levels of genes, including FT, SOC1, and SPL, followed similar trend. Photoperiod pathway, floral regulatory, and aging pathway genes (GI, CO, FT, SOC1, SPL) were well known involved in the floral transition (Quiroz et al., 2021).

On the other hand, genes involved in gibberellin signaling were upregulated at 9 DAS. IAA/ AUX transcript levels involved in auxin signaling were upregulated at all stress stages which correlates with reduced levels of auxin observed at PFSS plants at all stages of stress. AUX/IAA are repressor proteins and auxin triggers the degradation of these proteins. Genes related to sugar signaling were downregulated at 9 DAS, except for SnRK. The downregulated sugar signaling genes (SPS, SUT) correlate with low

sugars observed under drought stress. It is believed that the effect of drought on the preflowering stage was observed more towards the end of stress as most flowering regulatory genes were downregulated during that time. The downregulation of these floral regulatory genes and all other associated physiological mechanisms contributed to delayed flowering in pigeonpea. As initially discussed, low sucrose inhibits developmental processes in plants to save energy with the help of SnRK. High sucrose leads to high trehalose 6 phosphate levels, one of the plants' signals for floral transition. High sucrose or T6P levels inhibit the levels of SnRK in plants and on the other hand lower sucrose levels activate SnRK. As already stated, low sucrose levels as days of stress progressed at PFSS conditions, resulted upregulation of SnRK at 9 DAS and delayed flowering. After 9 days of stress, plants recovered on the 10th day and the PFSS recovered plants flowered 6 days later compared to control plants.

Shoot apical meristem was collected from PFSS recovered plants to check the expression patterns of floral regulatory genes as influenced by drought. Most of the floral regulatory genes required to shift to inflorescence meristem to the floral initiation were downregulated in PFSS recovered plants. SnRK and BRZ transcript levels were upregulated in PFSS recovered SAM, causing a delay in floral initiation. Both SnRK and BRZ are known to be floral repressors (Conti 2017, Mubarik et al., 2021). BRZ is involved in brassinosteroid signaling and the brassinosteroids are known to repress flowering in some plants. Most hormones like auxin, gibberellin, and abscisic acid are known for their duality depending on the environment to initiate or repress flowering (Conti 2017). In this study, drought at the preflowering stage showed reduced levels of phytohormones and delayed flowering. We can hypothesize that drought at the preflowering stage caused the effects towards the end of the stress, wherein

various floral repressors like SnRK and BRZ were upregulated. Correlation network analysis between the gene transcripts also showed that SnRK and BRZ were negatively correlated with most floral regulatory genes confirming their prominent role in the delayed flowering. These after-effects were still carried on the SAM of the PFSS recovered plants wherein floral repressors, including SnRK and BRZ, were upregulated, further delaying the floral initiation.

Drought at the flowering stage showed downregulation of all genes involved in floral regulation at all stages of stress. It might be due to the increased severity of the stress perceived by the pigeonpea. The flowering stage is a crucial developmental stage in the plant life cycle and hence any stress subjected at that phase has a detrimental effect on the plant life cycle. We could observe that under FSS conditions, sucrose levels were drastically reduced while osmoprotectants like proline and certain growth hormones were increased along with the downregulation of floral regulatory genes leading to delayed flowering. Even though the hormones (GA, IAA and ABA) were increased, delayed floral transition was observed. The plausible reason for this contradictory phenomenon can only be attributed to the fact that the perception of stress by pigeonpea is varied and the function of these plant growth regulators was modulated accordingly. It is well known the duality of phytohormone functions during flowering (Conti 2017). Most of the genes involved in sugar signaling were reduced in drought stressed plants. Correlation network analysis showed BRZ was negatively correlated with all floral regulatory genes. The expression patterns of floral initiation genes were also analyzed in shoot apical meristem collected from FSS drought stressed plants to check for variations. The upregulated levels of floral repressors, including AP2, SnRK, BRZ, and

AAO resulted an interruption in floral initiation. Correlation network analysis of gene transcripts in SAM also showed that SnRK, AP2, and BRZ were negatively correlated to all floral regulatory genes. Drought at the preflowering stage elicited physiological responses including reduced photosynthesis, increased WUE, and reduced sucrose compared to control plants causing a collective response of delayed flowering along with downregulation of most of the floral regulatory genes (Fig. 48). The delayed flowering also affected reproductive physiology and reducing yield. In comparison, drought at the flowering stage elicited much more severe responses like reduced photosynthesis, highly increased WUE, significant reduction of sucrose, an increase of osmoprotectant like proline, increased levels of phytohormones in combination leading to downregulation of floral regulatory genes triggering delayed flowering and severe yield reduction (Fig. 49). We can conclude that drought elicited various physiological and molecular responses in pigeonpea even though the extent of these responses varied based on the developmental stage ultimately leading to delayed flowering.

Fig. 48. Proposed model on delayed flowering and sequential effects on the reproductive physiology of pigeonpea under drought at the preflowering stage. The arrows show upregulation and downregulation in drought stressed plants compared to the control.

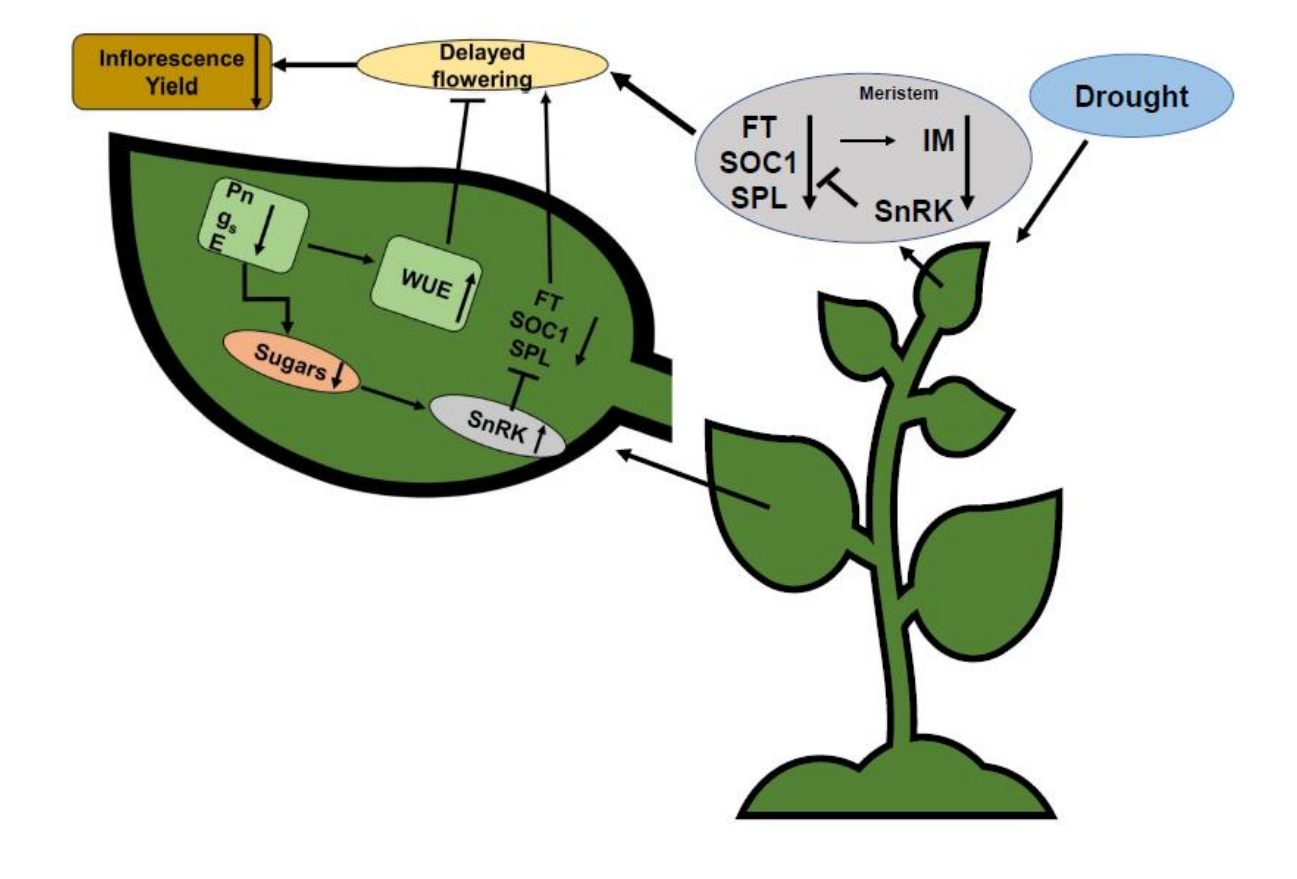
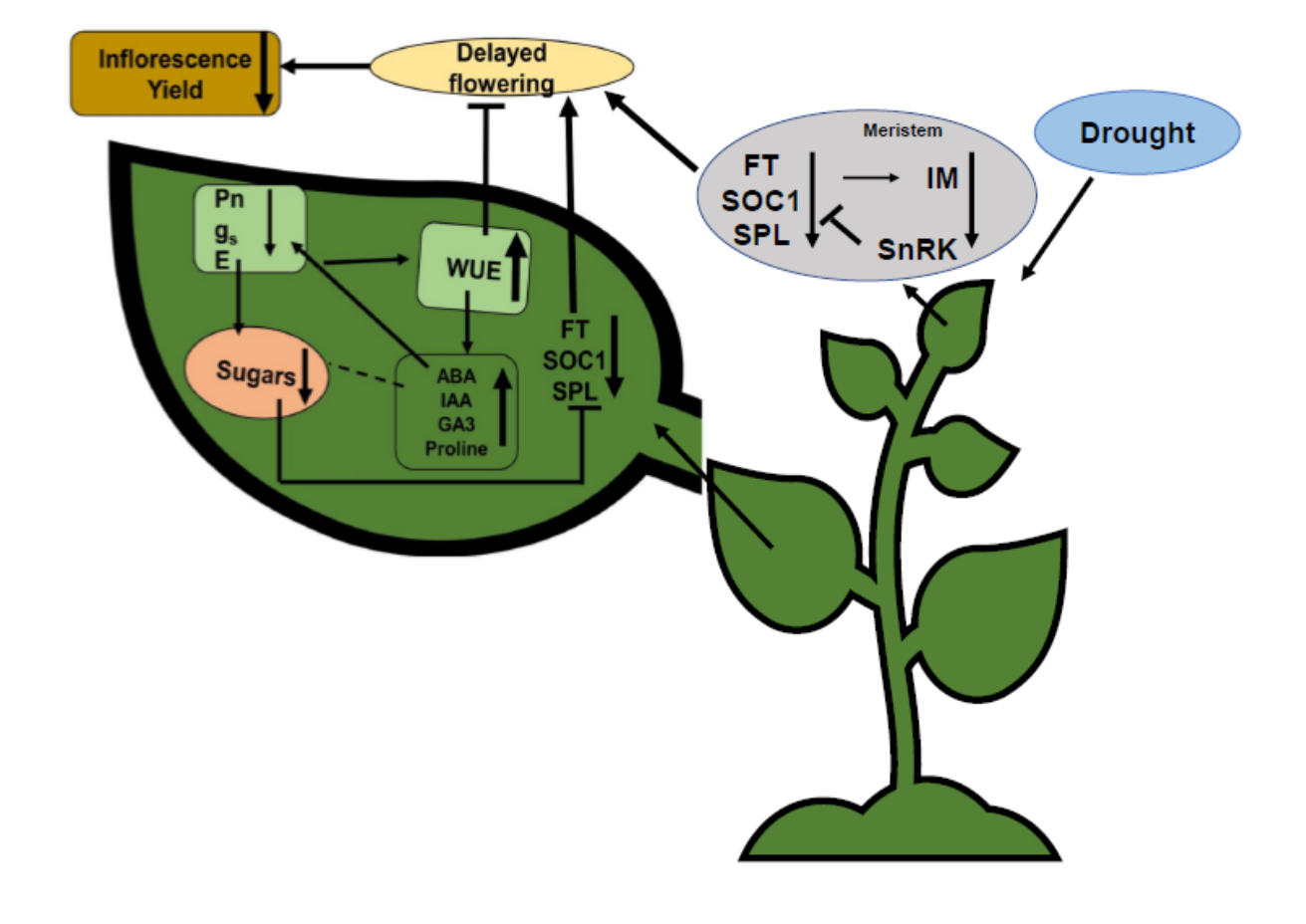


Fig. 49. Proposed model on delayed flowering and sequential effects on the reproductive physiology of pigeonpea under drought at flowering stage. The arrows show upregulation and downregulation in drought stressed plants compared to the control. The width of the arrows shows an increase in the intensity of either upregulation or downregulation compared to the control plants and PFSS drought stressed plants.



#### Negative response on the reproductive physiology of pigeonpea under drought

The delayed flowering as a result of drought severely affected the inflorescence numbers. Drought at both PFSS and FSS resulted in a decrease in inflorescence, with almost a 50% reduction at PFSS and even more at FSS. Conferring that drought had a detrimental effect when subjected at the flowering stage. As recorded, the aftereffects were then translated into reproductive parameters like decreased number of pods per plant in drought recovered plants. The expression patterns of ABCE genes involved in inflorescence formation were analyzed in drought recovered plants and were found to be downregulated mainly in FSS plants compared to control pigeonpea plants causing a decreased number of flowers and consequently reduced number of pods. Other reproductive parameters like total yield, pod weight, and seed weight were also reduced in drought recovered plants, mainly the FSS recovered plants. Farooq et al 2014 showed that drought on wheat during the post-anthesis period reduced yields by 30 %, while drought subjected throughout the flowering and grain filling period showed yield reduction by more than 58 %. Weight per 100 seeds was more in FSS recovered plants, possibly due to the increased seed size under drought. One of the pathways for delayed flowering is due to low levels of GI and higher levels of AP2. Here in drought stressed plants, GI levels were lower, especially at FSS, and AP2 levels were also increased. So, we can hypothesize that seed size was increased in drought recovered plants as an aftereffect of low GI and high AP2 levels (Lv et al., 2019).

The seeds were analyzed for the amino acid contents to understand the effects of drought during different developmental stages of pigeonpea, consequentially affecting seed nutrition. The seeds collected from PFSS recovered plants had reduced proline and

increased glutamate content suggesting that glutamate was not actively converted into proline in PFSS recovered plants. More contents of alanine and glutamate in PFSS recovered seeds might be a potential source of nitrogen storage in the seeds. On the other hand, FSS recovered seeds showed increased levels of both proline and glutamate, confirming that drought at the flowering stage was much more severe and the osmoprotectant proline proved its effectiveness to protect the seeds. The majority of amino acids were also reduced in FSS recovered seeds compared to PFSS recovered seeds confirming that the developmental stage of the plant subjected to drought stress is crucial in determining the reproductive yields and quality.

# CHAPTER 5 SUMMARY AND CONCLUSIONS

#### **SUMMARY AND CONCLUSIONS**

The present study attempts to understand the molecular mechanisms behind floral initiation in pigeonpea and how these developmental processes are affected in response to environmental stresses including elevated CO<sub>2</sub> and drought. Pigeonpea flowering was delayed both under elevated CO<sub>2</sub> and drought. However, the pigeonpea crop perceived them differently. Elevated CO<sub>2</sub> positively affected the pigeonpea life cycle at all developmental phases. However, delayed flowering in pigeonpea under elevated CO<sub>2</sub> did not affect the reproductive characteristics like inflorescence number and yield and they were increased under elevated CO<sub>2</sub>. Coming to the effects of drought on pigeonpea growth, a negative response was observed when drought was subjected to two developmental phases with the severity varied. Drought at the flowering stage had much more severity which could be seen from the enhanced levels of proline and phytohormones. Flowering was delayed at both stages of drought stress. Nevertheless, this delayed flowering was to escape the stress by maintaining homeostasis but it negatively affected the reproductive yields in pigeonpea. The effects of elevated CO<sub>2</sub> and drought have been more crucial during the reproductive stages than the vegetative growth developmental stages. In conclusion, the life cycle of pigeonpea was more beneficial from the elevated CO<sub>2</sub> stress than the drought stress.

Summary of the significant findings.

- ➤ Pigeonpea showed a positive growth response when grown under elevated CO<sub>2</sub>.

  Delayed flowering was observed in pigeonpea under elevated CO<sub>2</sub> although it did not reduce the inflorescence number.
- ➤ Pigeonpea grown under elevated CO₂ showed increased photosynthetic efficiency, ultimately increasing C levels which can be used for efficient N acquisition. This remobilization of C to other sinks, including roots instead of

the meristem, along with increased floral repressors miR156 and suppression of all floral activators resulting delay in floral initiation. The delayed floral initiation did not affect the inflorescence number due to enhanced expression of ABCE genes in the inflorescence, which was further associated with a more significant number of flowers.

- ➤ Elevated CO<sub>2</sub> had a highly positive influence on growth and seed yields in pigeonpea. Total carbohydrates were increased in elevated CO<sub>2</sub> grown seeds while starch content was unchanged.
- ➤ Total protein content was slightly reduced, while nitrogen levels were constant in elevated CO<sub>2</sub> grown seeds.
- Essential amino acid contents were increased in elevated CO<sub>2</sub> grown seeds when analyzed through GC MS. It is fascinating to note that the reproductive status of pigeonpea fares better than other crops, especially the non-legumes grown under elevated CO<sub>2</sub>, with increased yields and better nitrogen levels. The increased essential amino acid content in elevated CO<sub>2</sub> grown pigeonpea seeds showed a nutritional superiority compared to those in ambient seeds.
- The proteome analysis of seeds grown in elevated CO<sub>2</sub> demonstrates that seeds are better equipped to maintain seed vigor by accumulating macromolecules, including lipids and stress-related proteins, during the desiccation period.
- ➤ Drought, on the other hand, caused a negative response on pigeonpea. The effects of drought also varied depending on the developmental phase of pigeonpea.

- During the preflowering phase drought showed a moderate stress effect, while at the flowering stage the effects of drought were more severe and detrimental as evidenced by lower relative water content, decreased photosynthesis, and increased water use efficiency which confirms that drought severely affects pigeonpea during the flowering phase.
- The number of inflorescences was decreased in drought stressed plants, with the lowest in the FSS. This reduction in the inflorescence is directly translated to its yield pattern, as the number of pods was reduced in stressed plants.
- A decrease in sugar levels, majorly sucrose, was observed at PFSS. Growth hormone contents were lower in drought-stressed plants compared to control, showing that drought at the preflowering stage was sensed as moderate stress as no phytohormones. On the other hand, drought at the flowering stage caused a drastic drop in sucrose compared to the case of drought at the preflowering stage.
- An increase in proline, ABA, auxin, and gibberellin occurred in the FSS plant.

  Increased amounts of ABA help mitigate stress by leading to stomatal closure, which can be observed in our FSS plant.
- ➤ Delayed flowering under drought stress can be attributed to upregulated levels of floral repressors (SnRK, BRZ, AP2) and the accumulation of crucial metabolites including ABA, GA, IAA and proline.
- The drought stress induced delayed flowering led to a reduction in all yield parameters including total yield, pod weight, and seed weight in all drought subjected plants, especially at the flowering stage.

- The effects of drought stress in pigeonpea depend on the plant's developmental stage and the level of perception of the stress by the plant during growth.
- ➤ In conclusion, the growth and development of pigeonpea was more benefited by elevated CO<sub>2</sub> stress than the stress associated with limited water availability.

# CHAPTER 6 LITERATURE CITED

#### LITERATURE CITED

- Ainsworth E A, and Long S P (2005) What have we learned from 15 years of free-air CO<sub>2</sub> enrichment (FACE)? A meta-analytic review of the responses of photosynthesis, canopy properties and plant production to rising CO<sub>2</sub>. New phytologist 165: 351-372.
- Ainsworth E A, and Long S P (2021) 30 years of free-air carbon dioxide enrichment (FACE): what have we learned about future crop productivity and its potential for adaptation? Global Change Biology 27: 27-49.
- Ainsworth E A, and Rogers A (2007) The response of photosynthesis and stomatal conductance to rising [CO<sub>2</sub>]: mechanisms and environmental interactions. Plant, cell and environment 30: 258-270.
- Ainsworth E A, Davey P A, Bernacchi C J, Dermody O C, Heaton E A, Moore D J, et al. (2002). A meta-analysis of elevated [CO<sub>2</sub>] effects on soybean (Glycine max) physiology, growth and yield. Global change biology 8: 695-709.
- Amir R, Galili G, and Cohen H (2018) The metabolic roles of free amino acids during seed development. Plant Science 275:11-18.
- Angelovici R, Fait A, Fernie AR and Galili G (2011) A seed high-lysine trait is negatively associated with the TCA cycle and slows down Arabidopsis seed germination. New Phytologist 189: 148-159.
- Angelovici R, Galili G, Fernie AR, and Fait A (2010) Seed desiccation: a bridge between maturation and germination. Trends in Plant Science 15:211-218.
- Batista-Silva W, Heinemann B, Rugen N, Nunes-Nesi A, Araújo W L, Braun H P, and Hildebrandt T M (2019) The role of amino acid metabolism during abiotic stress release. Plant, cell & environment 42: 1630-1644.

Bäurle I, and Dean C (2006) The timing of developmental transitions in plants. Cell 125: 655-664.

- Becklin K M, Walker S M, Way D A, and Ward J K (2017) CO<sub>2</sub> studies remain key to understanding a future world. New Phytologist 214: 34-40.
- Bhargava S, and Mitra S (2021) Elevated atmospheric CO<sub>2</sub> and the future of crop plants. Plant Breeding 140: 1-11.
- Bolouri Moghaddam MR and Vanden Ende W (2013) Sugars, the clock and transition to flowering. Frontiers in Plant Science 4:22.
- Bourgault M, Brand J, Tausz M, and Fitzgerald GJ (2016) Yield, growth and grain nitrogen response to elevated CO<sub>2</sub> of five field pea (*Pisum sativum* L.) cultivars in a low rainfall environment. Field Crops Research 196:1–9.
- Bourgault M, Brand J, Tausz-Posch S, Armstrong RD, O'Leary GL, et al. (2017) Yield, growth and grain nitrogen response to elevated CO<sub>2</sub> in six lentil (*Lens culinaris*) cultivars grown under Free Air CO<sub>2</sub> Enrichment (FACE) in a semiarid environment. European Journal of Agronomy 87:50–58.
- Bunce JA (2016) Responses of soybeans and wheat to elevated CO<sub>2</sub> in free-air and open top chamber systems. Field Crops Research 186:78–85.
- Burkey OK, Booker FL, Pursley WA and Heagle AS (2007) Elevated Carbon Dioxide and Ozone Effects on Peanut: II. Seed Yield and Quality. Crop Science 47:1488-1497.
- Cen Y P, and Sage R F (2005) The regulation of Rubisco activity in response to variation in temperature and atmospheric CO<sub>2</sub> partial pressure in sweet potato. Plant physiology 139: 979-990.

Chen D, Yan W, Fu LY and Kaufmann K (2018) Architecture of gene regulatory networks controlling flower development in Arabidopsis thaliana. Nature Communications 9:4534.

- Chen X (2005) MicroRNA biogenesis and function in plants. FEBS Letters 579: 5923–5931.
- Cho A R, Chung S W, and Kim Y J (2020) Flowering responses under elevated CO<sub>2</sub> and graded nutrient supply in Phalaenopsis Queen Beer 'Mantefon'. Scientia Horticulturae 273: 109602.
- Cho LH, Yoon J and An G (2017) The control of flowering time by environmental factors. The Plant Journal 90:708–719.
- Conti Lucio (2017) Hormonal control of the floral transition: Can one catch them all?

  Developmental Biology 430: 288-301.
- Dam S, Laursen BS, Ornfelt JH, Jochimsen B, Staerfelt HH, Friis C, Nielsen K et al (2009) The Proteome of Seed Development in the Model Legume *Lotus japonicas*. Plant Physiology 149:1325-1340.
- Fait A, Angelovici R, Less H, Ohad I, Wochnak EW, et al. (2006) Arabidopsis seed development and germination is associated with temporally distinct metabolic switches. Plant Physiology 142: 839-854.
- Fang Y, and Xiong L (2015) General mechanisms of drought response and their application in drought resistance improvement in plants. Cellular and molecular life sciences 72: 673-689.
- Farooq M, Hussain M, and Siddique K H (2014) Drought stress in wheat during flowering and grain-filling periods. Critical reviews in plant sciences 33: 331-349.

Farooq M, Wahid A, Kobayashi N S M A, Fujita D B S M A, and Basra S M A (2009)

Plant drought stress: effects, mechanisms and management. In Sustainable agriculture (pp. 153-188). Springer, Dordrecht.

- Fornara F, de Montaigu A and Coupland G (2010) SnapShot: Control of Flowering in Arabidopsis. Cell 141: 550.
- Galili G and Amir R (2013) Fortifying plants with the essential amino acids lysine and methionine to improve nutritional quality. Plant Biotechnology Journal 11:211–222.
- Galili G, Amir R and Fernie AR (2016) The Regulation of Essential Amino Acid Synthesis and Accumulation in Plants. Annual Review of Plant Biology 67:153–178.
- Giannoccaro E, Wang YJ and Chen P (2006) Effects of solvent, temperature, time, solvent to sample ratio, sample size, and defatting on the extraction of soluble sugars in soybean. Journal of Food Science 71: 59-64.
- Gorelova V, Ambach L, Rébeillé F, Stove C, and Van Der Straeten D (2017) Folates in plants: research advances and progress in crop biofortification. Frontiers in chemistry 5: 21.
- Hampton JG, Boelt B, Rolston MP and Chastain TG (2012) Effects of elevated CO<sub>2</sub> and temperature on seed quality. Journal of Agricultural Science 151:154–162.
- He J, Jin Y, Palta J A, Liu H Y, Chen Z, and Li F M (2019) Exogenous ABA induces osmotic adjustment, improves leaf water relations and water use efficiency, but not yield in soybean under water stress. Agronomy 9: 395.
- Hedge JE and Hofreiter BT (1962) in Methods in Carbohydrate Chemistry, Vol.17, ed. Academic Press, New York, p.420.

Heyer AG, Raap M, Schroeer B, Marty B and Willmitzer L (2003) Cell wall invertase expression at the apical meristem alters floral, architectural, and reproductive traits in Arabidopsis thaliana. The Plant Journal 39: 161-169.

- Hikosaka K, Kinugasa T, Oikawa S, Onoda Y and Hirose T (2011) Effects of elevated CO<sub>2</sub> concentration on seed production in C<sub>3</sub> annual plants. Journal of Experimental Botany 62:1523-1530.
- Hildebrandt T M (2018) Synthesis versus degradation: directions of amino acid metabolism during Arabidopsis abiotic stress response. Plant molecular biology 98: 121-135.
- Hogy P and Fangmeier A (2008) Effects of elevated atmospheric CO<sub>2</sub> on grain quality of wheat. Journal of Cereal Science 48:580-591.
- Hogy P, Zorb C, Langenkamper G, Betsche T and Fangmeier A (2009) Atmospheric CO<sub>2</sub> enrichment changes the wheat grain proteome. Journal of Cereal Science 50:248-254.
- Hu W, Tian S B, Di Q, Duan S H, and Dai K (2018) Effects of exogenous calcium on mesophyll cell ultrastructure, gas exchange, and photosystem II in tobacco (Nicotiana tabacum Linn.) under drought stress. Photosynthetica 56: 1204-1211.
- Huang T, and Jander G (2017) Abscisic acid-regulated protein degradation causes osmotic stress-induced accumulation of branched-chain amino acids in Arabidopsis thaliana. Planta 246: 737-747.
- Huijser P and Schmid M (2011) The control of developmental phase transitions in plants. Development 138:4117-4129.

Hussain S, Ulhassan Z, Brestic M, Zivcak M, Zhou W, Allakhverdiev S I, and Liu W et al (2021) Photosynthesis research under climate change. Photosynthesis Research 150: 5-19.

- Hyun Y, Richter R, Vincent C, Martinez-Gallegos R, Porri A and Coupland G (2016)

  Multi-Layered Regulation of SPL15 and Cooperation with SOC1 Integrate

  Endogenous Flowering Pathways at the Arabidopsis Shoot Meristem.

  Developmental Cell 37:254–266.
- Irigoyen, J., Goicoechea, N., Antolín, M., Pascual, I., Sánchez-Díaz, M., Aguirreolea, J., & Morales, F. (2014). Growth, photosynthetic acclimation and yield quality in legumes under climate change simulations: An updated survey. Plant Science 226: 22-29.
- Irish V (2017) The ABC model of floral development. Current Biology 27: R853–R909.
- Jack T (2004) Molecular and Genetic Mechanisms of Floral Control. The Plant Cell 16: S1–S17.
- Jena U R, Swain D K, Hazra K K, and Maiti M K (2018) Effect of elevated [CO<sub>2</sub>] on yield, intra-plant nutrient dynamics, and grain quality of rice cultivars in eastern India. Journal of the Science of Food and Agriculture 98: 5841-5852.
- Jogawat A, Yadav B, Chhaya, Lakra N, Singh AK, and Narayan OP (2021) Crosstalk between phytohormones and secondary metabolites in the drought stress tolerance of crop plants: A review. Physiologia Plantarum. 172:1106–1132.

Jung JH, Seo PJ, Kang SK, and Park CM (2011) MiR172 Signals are Incorporated intothe MiR156 Signaling Pathway at the SPL3/4/5 Genes in ArabidopsisDevelopmental Transitions. Plant Molecular Biology 76:35–45.

- Kaur G, and Asthir B (2017) Molecular responses to drought stress in plants. Biologia Plantarum 61: 201-209.
- Kazan K, and Lyons R (2016) The link between flowering time and stress tolerance. Journal of experimental botany 67: 47-60.
- Kenney A M, McKay J K, Richards J H, and Juenger T E (2014) Direct and indirect selection on flowering time, water-use efficiency (WUE, δ13C), and WUE plasticity to drought in Arabidopsis thaliana. Ecology and evolution 4: 4505-4521.
- Kooyers N J (2015) The evolution of drought escape and avoidance in natural herbaceous populations. Plant science 234:155-162.
- Kopka J and Schauer N et al (2005) GMD@ CSB.DB: the Golm metabolome database. Bioinformatics 21:1635-1638.
- Krishnan HB, Natarajan SS, Oehrle NW, Garrett NW and Darwish O (2017) Proteomic Analysis of Pigeonpea (Cajanus cajan) Seeds Reveals the Accumulation of Numerous Stress-Related Proteins. Journal of Agriculture Food Chemistry 65:4572-4581.
- Kumar S, Chaitanya B S, Ghatty S, and Reddy A R (2014) Growth, reproductive phenology and yield responses of a potential biofuel plant, Jatropha curcas grown under projected 2050 levels of elevated CO<sub>2</sub>. Physiologia Plantarum 152: 501-519.

Kuromori T, Fujita M, Takahashi F, Yamaguchi-Shinozaki K, and Shinozaki K (2022)

Inter-tissue and inter-organ signaling in drought stress response and phenotyping of drought tolerance. The Plant Journal 109: 342-358.

- Laxa M, Liebthal M, Telman W, Chibani K, and Dietz K J (2019) The role of the plant antioxidant system in drought tolerance. Antioxidants 8: 94.
- Li W, Pang S, Lu Z, and Jin B (2020) Function and mechanism of WRKY transcription factors in abiotic stress responses of plants. Plants 9: 1515.
- Li Y, Yu Z, Jin J, Zhang Q, Wang G, Liu C, Wu J, Wang C, and Liu X (2018). Impact of Elevated CO<sub>2</sub> on Seed Quality of Soybean at the Fresh Edible and Mature Stages. Frontiers in Plant Science 9:1413.
- Lin YL and Tsay YF (2017) Influence of differing nitrate and nitrogen availability on flowering control in Arabidopsis. Journal of Experimental Botany 68: 2603-2609.
- Liu X, Zhang H, Wang J, Wu X, Ma S, Xu Z et al. (2019) Increased CO<sub>2</sub> concentrations increasing water use efficiency and improvement PSII function of mulberry seedling leaves under drought stress. Journal of Plant Interactions 14:213-223.
- Livak KJ and Schmittgen TD (2001) Analysis of Relative Gene Expression Data Using Real-Time Quantitative PCR and the  $2^{-\Delta\Delta CT}$  Method. Methods 25:402–408.
- Loladze I (2014) Hidden shift of the ionome of plants exposed to elevated CO<sub>2</sub> depletes minerals at the base of human nutrition. elife 3: e02245.
- López-Cubillos S, and Hughes L (2016) Effects of elevated carbon dioxide (CO<sub>2</sub>) on flowering traits of three horticultural plant species. Australian Journal of Crop Science 10: 1523-1528.

Lv M J, Wan W, Yu F, and Meng L S (2019) New insights into the molecular mechanism underlying seed size control under drought stress. Journal of agricultural and food chemistry 67: 9697-9704.

- Malhi GS, Kaur M, Kaushik P (2021) Impact of Climate Change on Agriculture and its Mitigation Strategies: A Review. Sustainability 13: 1318.
- Maphosa Y and Jideani VA (2017) The Role of Legumes in Human Nutrition, Functional Food Improve Health through Adequate Food, Maria Chavarri Hueda, IntechOpen.
- Mattioli R, Costantino P and Trovato M (2009) Proline accumulation in plants. Plant Signaling and Behavior 4:1016-1018.
- McGill and C Figueiredo (1993) Total Nitrogen, Soil Sampling and Methods of Analysis. Lewis Publ, Boca Raton, FL pp. 201–211.
- Miller JL (1972) Use of dinitrosalicylic acid reagent for determination of reducing sugar. Analytical Chemistry 31:426–428.
- Mubarik M S, Khan S H, Sajjad M, Raza A, Hafeez M B, Yasmeen T, et al. (2021). A manipulative interplay between positive and negative regulators of phytohormones:
  A way forward for improving drought tolerance in plants. Physiologia Plantarum 172: 1269-1290.
- Mukarram M, Choudhary S, Kurjak D, Petek A, and Khan M M A (2021) Drought: Sensing, signalling, effects and tolerance in higher plants. Physiologia Plantarum 172: 1291-1300.

Myers S, Zanobetti A, Kloog I et al. (2014) Increasing CO<sub>2</sub> threatens human nutrition. Nature 510: 139–142.

- Nadeem M, Li J, Yahya M, Sher A, Ma C, Wang X, and Qiu L (2019) Research progress and perspective on drought stress in legumes: A review. International journal of molecular sciences 20: 2541.
- Ndakidemi PA, Dakora FD (2003) Legume seed flavonoids and nitrogenous metabolites as signals and protectants in early seedling development. Functional Plant Biology 30:729-745.
- O'Hara LE, Paul M and Wingler A (2013) How Do Sugars Regulate Plant Growth and Development? New Insight into the Role of Trehalose-6-Phosphate. Molecular Plant 6: 261-274.
- Pan C, Ahammed G J, Li X, and Shi K (2018) Elevated CO<sub>2</sub> improves photosynthesis under high temperature by attenuating the functional limitations to energy fluxes, electron transport and redox homeostasis in tomato leaves. Frontiers in plant science 9:1739.
- Pan X, Welti R and Wang X (2010) Quantitative analysis of major plant hormones in crude plant extracts by high-performance liquid chromatography—mass spectrometry. Nature Protocols 5: 986-992.
- Parvin S, Uddin S, Tausz-Posch S, Fitzgerald G, Armstrong R, and Tausz M (2019) Elevated CO<sub>2</sub> improves yield and N<sub>2</sub> fixation but not grain N concentration of faba bean (Vicia faba L.) subjected to terminal drought. Environmental and Experimental Botany 165:161-173.

Pereyda-González J M, De-la-Peña C, Tezara W, Zamora-Bustillos R, Andueza-Noh R H, Noh-Kú J G, and Garruña R (2022) High Temperature and Elevated CO<sub>2</sub> Modify Phenology and Growth in Pepper Plants. Agronomy 12: 1836.

- Pignon C P, and Long S P (2020) Retrospective analysis of biochemical limitations to photosynthesis in 49 species: C4 crops appear still adapted to pre-industrial atmospheric [CO<sub>2</sub>]. Plant, Cell & Environment 43: 2606-2622.
- Piikki K, De Temmerman L, Ojanpera K, Danielsson H and Pleijel H (2008) The grain quality of spring wheat (*Triticum aestivum* L.) in relation to elevated ozone uptake and carbon dioxide exposure. European Journal of Agronomy 28:245-254.
- Pilbeam D J (2015) Breeding crops for improved mineral nutrition under climate change conditions. Journal of experimental botany 66: 3511-3521.
- Pinheiro C, and Chaves M M (2011) Photosynthesis and drought: can we make metabolic connections from available data? Journal of experimental botany 62: 869-882.
- Putterill J, Laurie R, and Macknight R (2004) It's time to flower: the genetic control of flowering time. Bioessays 26: 363-373.
- Putterill J, Robson F, Lee K, Simon R and Coupland G (1995) The CONSTANS Gene of Arabidopsis Promotes Flowering and Encodes a Protein Showing Similarities to Zinc Finger Transcription Factors. Cell 80: 847–857.
- Quiroz S, Yustis JC, Chávez-Hernández EC, Martínez T, et al (2021) Beyond the Genetic Pathways, Flowering Regulation Complexity in Arabidopsis thaliana. International Journal of Molecular Sciences 22: 5716.

Raisanen T, Ryyppo A, Julkunen-Tiitto R and Kellomaki S (2008) Effects of elevated CO<sub>2</sub> and temperature on secondary compounds in the needles of Scots pine (*Pinus sylvestris* L.). Trees 22:121-135.

- Raja V, Qadir SU, Alyemeni MN and Ahmad P (2020) Impact of drought and heat stress individually and in combination on physio-biochemical parameters, antioxidant responses, and gene expression in Solanum lycopersicum. 3 Biotechnology 10: 1–8.
- Reddy A R, Chaitanya K V, and Vivekanandan M (2004). Drought-induced responses of photosynthesis and antioxidant metabolism in higher plants. Journal of plant physiology 161: 1189-1202.
- Riboni M, Galbiati M, Tonelli C, and Conti L (2013) GIGANTEA enables drought escape response via abscisic acid-dependent activation of the florigens and SUPPRESSOR OF OVEREXPRESSION OF CONSTANS1. Plant physiology 162: 1706-1719.
- Rogers A, Ainsworth EA and Leakey ADB (2009) Will Elevated Carbon Dioxide Concentration Amplify the Benefits of Nitrogen Fixation in Legumes? Plant Physiology 151: 1009–1016.
- Saha S, Sehgal V K, Nagarajan S, and Pal M (2012) Impact of elevated atmospheric CO<sub>2</sub> on radiation utilization and related plant biophysical properties in pigeon pea (Cajanus cajan L.). Agricultural and Forest Meteorology 158: 63-70.
- Sasaki H, Hara T, Ito S, Miura S, Hoque M M, Lieffering M, Kim H, Okada M and Kobayashi K (2005) Seasonal changes in canopy photosynthesis and respiration, and

partitioning of photosynthate, in rice (Oryza sativa L.) grown under free-air CO<sub>2</sub> enrichment. Plant and cell physiology 46: 1704-1712.

- Schwab R, Palatnik J F, Riester M, Schommer C, Schmid M, and Weigel D (2005)

  Specific effects of microRNAs on the plant transcriptome. Developmental cell 8:
  517-527.
- Sekhar K M, Rachapudi V S, Mudalkar S, and Reddy A R (2014) Persistent stimulation of photosynthesis in short rotation coppice mulberry under elevated CO<sub>2</sub> atmosphere. Journal of Photochemistry and Photobiology B: Biology 137: 21-30.
- Sharma E, Sharma R, Borah P, Jain M, and Khurana J P (2015) Emerging roles of auxin in abiotic stress responses. Elucidation of abiotic stress signaling in plants 299-328.
- Silvente S, Sobolev A P, and Lara M (2012) Metabolite adjustments in drought tolerant and sensitive soybean genotypes in response to water stress. PLoS One 7: e38554.
- Singh G, Ratnaparkhe M and Kumar A (2019) Comparative Analysis of Transposable Elements from *Glycine max, Cajanus cajan and Phaseolus vulgaris*. Journal of Experimental Biology and Agricultural Sciences 7: 167-177.
- Singh N K, Gupta D K, Jayaswal P K, Mahato A K, Dutta S, Singh S, and Sharma T R et al (2012) The first draft of the pigeonpea genome sequence. Journal of plant biochemistry and biotechnology 21: 98-112.
- Singha KT, Sreeharsha RK, Mariboina S and Reddy AR (2019) Dynamics of metabolites and key regulatory proteins in the developing seeds of *Pongamia pinnata*, a potential biofuel tree species. Industrial Crops and Products 140: p.111621.

Smith M R, Veneklaas E, Polania J, Rao I M, Beebe S E, and Merchant A (2019) Field drought conditions impact yield but not nutritional quality of the seed in common bean (Phaseolus vulgaris L.). PLoS One 14: e0217099.

- Soares J C, Santos C S, Carvalho S M, Pintado M M, and Vasconcelos M W (2019)

  Preserving the nutritional quality of crop plants under a changing climate:
  importance and strategies. Plant and Soil 443: 1-26.
- Soba D, Mariem SB, Mendizabal TF, Mendez-Espinoza AM, Gulard F, Gonzalez-Murua C, et al. (2019) Metabolic Effects of Elevated CO<sub>2</sub> on Wheat Grain Development and Composition. Journal of Agricultural Food Chemistry 67:8441-8451.
- Springer JC, Orozco RA, Kelly JK and Ward JK (2008) Elevated CO<sub>2</sub> influences the expression of floral-initiation genes in Arabidopsis thaliana. New Phytologist 178: 63-67.
- Sreeharsha RV, Mudalkar S, Sengupta D, Unnikrishnan D and Reddy A.R (2019) Mitigation of drought-induced oxidative damage by enhanced carbon assimilation and an efficient antioxidative metabolism under high CO<sub>2</sub> environment in pigeonpea (Cajanus cajan L.). Photosynthesis Research 139: 425–439.
- Sreeharsha RV, Sekhar KM, and Reddy AR (2015) Delayed flowering is associated with lack of photosynthetic acclimation in Pigeon pea (*Cajanus cajan* L.) grown under elevated CO<sub>2</sub>. Plant Science 231:82-93.
- Sun X, Lin L, and Sui N (2019) Regulation mechanism of microRNA in plant response to abiotic stress and breeding. Molecular Biology Reports 46: 1447-1457.

Szabados L, and Savouré A (2010). Proline: a multifunctional amino acid. Trends in plant science 15: 89-97.

- Tomimatsu H, and Tang Y (2016) Effects of high CO<sub>2</sub> levels on dynamic photosynthesis: carbon gain, mechanisms, and environmental interactions. Journal of Plant Research 129: 365-377.
- Unnikrishnan D, Sreeharsha R and Reddy A (2021) Growth, seed yield and nutritional characteristics of pigeonpea grown under elevated CO<sub>2</sub> atmosphere. Acta Physiologiae Plantarum 43: 1-15.
- Venkatappa M, Sasaki N, Han P, and Abe I (2021) Impacts of droughts and floods on croplands and crop production in Southeast Asia—An application of Google Earth Engine. Science of the Total Environment 795: 148829.
- Verslues P E, Agarwal M, Katiyar-Agarwal S, Zhu J, and Zhu J K (2006) Methods and concepts in quantifying resistance to drought, salt and freezing, abiotic stresses that affect plant water status. The Plant Journal 45: 523-539.
- Wahab A, Abdi G, Saleem M H, Ali B, Ullah S, Shah W, and Marc R A et al (2022).

  Plants' physio-biochemical and phyto-hormonal responses to alleviate the adverse effects of drought stress: A comprehensive review. Plants 11: 1620.
- Wahl V, Ponnu J, Schlereth A, et al. (2013) Regulation of Flowering by Trehalose-6-Phosphate Signaling in Arabidopsis Thaliana. Science 339:704–707.
- Wang A, Lam S K, Hao X, Li F Y, Zong Y, Wang H, and Li P (2018). Elevated CO<sub>2</sub> reduces the adverse effects of drought stress on a high-yielding soybean (Glycine max (L.) Merr.) cultivar by increasing water use efficiency. Plant physiology and biochemistry 132: 660-665.

Wang et al. (2020) Sugar Signaling and Post-transcriptional Regulation in Plants: An Overlooked or an Emerging Topic? Frontiers in Plant Science 11:578096.

- Wang JW, Czech B and Weigel D (2009) miR156-Regulated SPL Transcription Factors

  Define an Endogenous Flowering Pathway in Arabidopsis thaliana. Cell 138: 738–749.
- Wang L, Patrick JW and Ruan YL (2017) Live Long and Prosper: Roles of Sugar and Sugar Polymers in Seed Vigor. Molecular Plant 11:1-3.
- Wang WQ, Liu SH, Song SQ and Moller IM (2015) Proteomics of seed development, desiccation tolerance, germination and vigor. Plant Physiology Biochemistry 86:1-15.
- Waterworth WM, Bray CM, and West CE (2019) Seeds and the art of genome maintenance. Frontiers in Plant Science 10:706.
- Weber K and Burow M (2018) Nitrogen essential macronutrient and signal controlling flowering time. Physiologia Plantarum 162: 251–260.
- Wink M (2013) Evolution of secondary metabolites in legumes (Fabaceae). South African Journal of Botany 164-175.
- Wu G, Park MY, Conway SR, Wang JW, Weigel D and Poethig RS (2009) The Sequential Action of MiR156 and MiR172 Regulates Developmental Timing in Arabidopsis. Cell 138:750–759.
- Xu W, Cui K, Xu A, Nie L, Huang J, and Peng S (2015) Drought stress condition increases root to shoot ratio via alteration of carbohydrate partitioning and enzymatic activity in rice seedlings. Acta physiologiae plantarum 37: 1-11.

Xu Z, Jiang Y, and Zhou G (2015) Response and adaptation of photosynthesis, respiration, and antioxidant systems to elevated CO<sub>2</sub> with environmental stress in plants. Frontiers in plant science 6: 701.

- Yadav A K, Carroll A J, Estavillo G M, Rebetzke G J, and Pogson, B J (2019) Wheat drought tolerance in the field is predicted by amino acid responses to glasshouse-imposed drought. Journal of Experimental Botany 70: 4931-4948.
- Yamaguchi A Wu MF, Yang L, Wu G, Poethig RS, and Wagner D (2009) The MicroRNA-Regulated SBP-Box Transcription Factor SPL3 Is a Direct Upstream Activator of LEAFY, FRUITFULL, and APETALA1. Developmental Cell 17: 268–278.
- Yang L, Xu M, Koo Y, He J, and Poethig RS (2013) Sugar promotes vegetative phase change in Arabidopsis thaliana by repressing the expression of MIR156A and MIR156C. eLife 2: e00260.
- Yu et al. (2013) Sugar is an endogenous cue for juvenile-to-adult phase transition in plants. eLife 2: e00269.
- Zhang J, Jia W, Yang J, and Ismail A M (2006) Role of ABA in integrating plant responses to drought and salt stresses. Field Crops Research 97: 111-119.
- Zhang Y, Li Y, Hassan M J, Li Z, and Peng Y (2020). Indole-3-acetic acid improves drought tolerance of white clover via activating auxin, abscisic acid and jasmonic acid related genes and inhibiting senescence genes. BMC plant biology 20: 1-12.
- Zhao X, Zhou N, Lai S, Frei M, Wang Y, and Yang L (2019) Elevated CO<sub>2</sub> improves lodging resistance of rice by changing physicochemical properties of the basal internodes. Science of The Total Environment 647: 223-231.

Zhu S, Chen, SW and Li Y (2020) Simultaneous analysis of thirteen phytohormones in fruits and vegetables by SPE-HPLC-DAD. Food Science and Biotechnology 29: 1587–1595.

### **PUBLICATIONS**

#### **Publications**

- ➤ Unnikrishnan Divya, Sreeharsha Rachapudi, and Attipalli R Reddy (2021).

  Growth, seed yield and nutritional characteristics of pigeonpea grown under elevated CO₂ atmosphere. Acta Physiologiae Plantarum. 43:1-15.
- ➤ Sreeharsha Rachapudi, Mudalkar Shalini, **Unnikrishnan Divya**, Venkata Mohan S and Attipalli R Reddy (2021). Improving Nitrogen Use Efficiency of Legumes Under Changing Climate Through Omics Technologies.
- ➤ Sreeharsha Rachapudi, Mudalkar Shalini, Sengupta Debashree, **Unnikrishnan Divya**, and Attipalli R Reddy (2019). Mitigation of drought-induced oxidative damage by enhanced carbon assimilation and an efficient antioxidative metabolism under high CO₂ environment in pigeonpea (Cajanus cajan L.). Photosynthesis Research 139: 425–439.
- ➤ Sengupta Debashree, Marriboina Suresh, **Unnikrishnan Divya**, and Attipalli R Reddy (2019). Photosynthetic performance and sugar variations during key reproductive stages of soybean under potassium iodide-simulated terminal drought. Photosynthetica 57: 458-469.

#### **ORIGINAL ARTICLE**



## Growth, seed yield and nutritional characteristics of pigeonpea grown under elevated CO<sub>2</sub> atmosphere

Divya K. Unnikrishnan<sup>1</sup> · Rachapudi V. Sreeharsha<sup>2</sup> · Attipalli R. Reddy<sup>1</sup>

Received: 27 March 2020 / Revised: 28 September 2020 / Accepted: 19 April 2021 / Published online: 29 April 2021 © Franciszek Górski Institute of Plant Physiology, Polish Academy of Sciences, Kraków 2021

#### Abstract

In the present study, we have analyzed the seed yield and seed quality of pigeonpea grown under elevated  $CO_2$ . Pigeonpea was grown for its complete life cycle in open top chambers under elevated  $CO_2$  (600 µmol/mol) and atmospheric ambient  $CO_2$  (400 µmol/mol). The growth, biomass and seed yield were increased under elevated  $CO_2$  when compared to plants grown at ambient  $CO_2$  concentrations. The mature seeds were collected after 120 days for various biochemical analyses to determine their nutritional quality. The biochemical analyses indicated that elevated  $CO_2$  grown pigeonpea seeds did not show any significant decrease in nitrogen and protein contents but showed an increase in total carbohydrates. The metabolomics of seeds revealed changes in sugars, amino acids, organic acids and fatty acid levels under elevated  $CO_2$  growth. The seeds collected from elevated  $CO_2$  grown pigeonpea showed higher levels of essential amino acids inferring their better nutritional quality. The total proteome of pigeonpea seed was studied through label-free quantification and recorded an increase in several seed specific proteins including certain stress related proteins in elevated  $CO_2$  grown pigeonpea seeds. The proteome and metabolome data demonstrate better seed vigor in elevated  $CO_2$  grown pigeonpea.

**Keywords** Elevated CO<sub>2</sub> · Metabolome · Nutritional quality · Pigeonpea · Proteome · Seed protein

#### Introduction

Climate change due to rising atmospheric  $CO_2$  levels  $[CO_2]$  is posing a threat to the natural ecosystems and biotic communities including crop plants. The  $[CO_2]$  levels have increased from 270 ppm during the preindustrial era to the current 400 ppm and are expected to rise to 550 ppm by the year 2050 (IPCC 2017). The biological functions of a plant including photosynthesis, transpiration, biomass production and seed yields are tuned according to increasing  $[CO_2]$  levels thus influencing the future agronomy. In general, plants gain a pseudo-advantage from elevated  $CO_2$ , where they

Communicated by S. Esposito.

- Attipalli R. Reddy attipalli.reddy@gmail.com
- Photosynthesis and Climate Change Laboratory, Department of Plant Sciences, University of Hyderabad, Hyderabad, India 500046
- Department of Energy and Environmental Engineering, CSIR-Indian Institute of Chemical Technology (CSIR-IICT), Hyderabad 500 007, India

show enhanced photosynthesis and C sequestration during the initial growth stages. However, upon prolonged growth under N-limiting conditions, the increased C reserves and saturated sink tissues mediate feedback inhibition on Ribulose-1,5-bisphosphate carboxylase/oxygenase (Rubisco) resulting in photosynthetic acclimation (Ainsworth and Rogers 2007). The effects of elevated CO<sub>2</sub> differ from vegetative to reproductive tissues wherein, a meta-analysis of crop plants showed an increase of 31% in vegetative biomass while fruit and seed production showed only 12 and 25% increase respectively under elevated CO<sub>2</sub> (Hikosaka et al. 2011). Though there was a quantitative enhancement in seed biomass, major non-legume food crops with few exceptions showed an average of 14% decrease in seed N content under elevated CO<sub>2</sub> thus making the seed deficient of crucial proteins and amino acids, leading to diminished seed nutritional quality (Burkey et al. 2007; Hogy and Fangmeier 2008; Piikki et al. 2008; Hikosaka et al. 2011; Hampton et al. 2012). Furthermore, majority of non-legumes show photosynthetic acclimation when grown under elevated CO<sub>2</sub> due to insufficiency in leaf N content, in the absence of external supply of fertilizer (Sekhar et al. 2015; Kumar et al. 2017).



## Improving Nitrogen Use Efficiency of Legumes Under Changing Climate Through Omics Technologies

7

Rachapudi Venkata Sreeharsha, Shalini Mudalkar, Divya K. Unnikrishnan, S. Venkata Mohan, and Attipalli R. Reddy

#### Abstract

The assimilation rate of carbon per unit of nitrogen in the foliage is termed as nitrogen use efficiency (NUE) and this clearly depends on various factors including soil nitrogen availability, environmental conditions and climatic factors. In legumes, symbiotic nitrogen fixation occurs in root nodules which contain millions of nitrogen-fixing bacteroids. Root nodules possess leghaemoglobin as main constituent and the activity mainly depends on antioxidant levels and reactive oxygen species (ROS). Symbiotic N fixation influences a wide array of plant metabolic pathways including photosynthesis, protein metabolism in turn modulating the plant nitrogen use efficiency in response to different environmental conditions, viz. elevated CO<sub>2</sub>, drought stress, elevated temperature, etc. Under elevated CO<sub>2</sub> conditions, several C3 plants experience photosynthetic acclimation due to the imbalance in C/N supply. Several legumes including pigeonpea, soybean were reported to enhance their nitrogen fixation capacity in response to increased carbon supply and overcame photosynthetic acclimation. Also, there was an increase in photosynthetic nitrogen use efficiency channelizing most of the fixed N to biosynthesis of photosynthetic enzymes. Abiotic stresses modulate the antioxidant system of root by increasing the ROS levels thus influencing the N fixation process and subsequently hampers plant metabolism and growth. Crops, shrubs and annuals are the most commonly explored species for their nitrogen-

Department of Energy and Environmental Engineering, CSIR-Indian Institute of Chemical Technology (CSIR-IICT), Hyderabad, India

Forest College and Research Institute, Hyderabad, Telangana, India

D. K. Unnikrishnan · A. R. Reddy

Department of Plant Sciences, University of Hyderabad, Hyderabad, India

R. V. Sreeharsha ( $\boxtimes$ ) · S. Venkata Mohan

S. Mudalkar

<sup>©</sup> The Author(s), under exclusive license to Springer Nature Singapore Pte Ltd. 2021

## Photosynthetic performance and sugar variations during key reproductive stages of soybean under potassium iodide-simulated terminal drought

D. SENGUPTA\*, S. MARRIBOINA\*, D. K. UNNIKRISHNAN\*, and A.R. REDDY\*,\*\*\*,+

Department of Plant Sciences, School of Life Sciences, University of Hyderabad, 500046 Hyderabad, India\* Yogi Vemana University, 516003 Kadapa, Andhra Pradesh, India\*\*

#### **Abstract**

Importance of utilizing chemical desiccants to simulate terminal drought effects is gradually increasing. In the present study, a potassium iodide (KI)-simulated terminal drought stress was imposed during the full bloom (R2), pod elongation (R4), and seed initiation (R5) stages of soybean; the KI-induced desiccation effects were assessed at 1, 3, and 5 d after spraying (DASP). Plants responded to KI-simulated terminal drought stress within 1 DASP of KI-treatment, in terms of photosynthetic and transpiration rates. Seed initiation stage was found to be comparatively tolerant to KI-induced desiccation, with respect to chlorophyll degradation and PSII efficiency, which correlated well with the high hexose accumulation during this period. The present study provides a basic understanding regarding the stage-specific responses of soybean towards KI-simulated terminal drought, with respect to photosynthetic performance and sugar status and a correlation between the two traits, which could be useful for developing terminal drought-tolerant varieties.

Additional key words: chemical desiccation; Glycine max; hexose to sucrose ratio; linear regression; photosynthetic carbon exchange rate.

#### Introduction

Being the major source of edible oil, animal feed and other industrial products, soybean [Glycine max (L.) Merril] has become one of the most important grain legumes worldwide (Pagano and Miransari 2016). In India, soybean cultivation area increased from 0.03 Mha in 1970 to 11.67 Mha in 2016, with a corresponding increase in yield from 426 to 737 kg ha-1 (Agricultural Statistics at a Glance 2016). One of the major limitations to soybean productivity is the rain-fed cultivation system, with highly erratic monsoon patterns. Drastic spatio-temporal variations in rainfall often cause terminal drought stress, i.e., water deprivation during the key reproductive stages, which substantially hampers the final grain yield (Daryanto et al. 2015). Physiologically, terminal drought effects include decreased photosynthetic carbon exchange rates (CER), early leaf senescence and maturity, and a reduced seed yield (Manavalan et al. 2009). Hence, the ability to remobilize stem carbohydrates towards developing pods/seeds is the key trait, which determines terminal drought tolerance in soybean. Screening and selection of cultivars with effective stem reserve mobilization marks the first step for subsequent breeding strategies for terminal drought tolerance. However, due to variation in soil moisture, field screening for terminal drought is quite difficult due to lack of uniformity and reproducibility of plant responses to the stress factor (Tuberosa 2012, Bhatia et al. 2014). Thus, to mimic terminal drought stress effects, chemical desiccants, such as potassium iodide (KI) were used (Regan et al. 1993, Royo and Blaco 1998, Bhatia et al. 2014). KI was reported to act as a contact desiccant and rapidly inhibits photosynthesis without showing any direct toxic effect to grain filling from the translocated carbohydrates (Nicolas and Turner 1993). The possible mechanism behind KI-induced desiccation is the interference with plant water relations. Hygroscopicity of the salt solution was also included as one of the major factors causing 'hydraulic activation of stomata' (HAS), which affects the stomatal conductance, transpiration rates, and ultimately photosynthesis (Burkhardt 2010). Also, desiccation leads to osmotic stress and triggers osmotic stress-inducible gene expression (Shapiguzov et al. 2005). Detailed physiochemical responses of soybean to KIinduced desiccation, with respect to specific reproductive growth stage, are not yet reported. Moreover, for wide

Received 28 May 2018, accepted 14 November 2018.

\*Corresponding author; phone:+91 4023134508, fax: +91 4023010120, e-mail: attipalli.reddy@gmail.com

Abbreviations: CER – carbon exchange rate; Chl – chlorophyll; DASP – days after spraying; DMSO – dimethyl sulfoxide; H/S – hexose to sucrose ratio; Kn – nonphotochemical deexcitation rate constant; Kp –photochemical deexcitation rate constant; PDA – photodiode array;  $\Delta V_{OI}$  – kinetic difference of variable fluorescence between phase O and J with respect to 1 day control;  $\Delta V_{OK}$  – kinetic difference of variable fluorescence between phase O and K with respect to 1 day control;  $\delta_{(Ro)}$  – reduction efficiency/electron transport;  $\Phi_{(Po)}$  – trapping/absorbance;  $\psi_{(Eo)}$  – electron transport/trapping.

Acknowledgements: The present work is supported by the Young Scientist Start-Up grant to Dr. Debashree Sengupta (YSS/2015/000635) from Science and Engineering Research Board (SERB), a statutory body of Department of Science and Technology (DST), Govt. of India. Sureshbabu Marriboina acknowledges the fellowship from University Grant Commission (UGC), Govt. of India.

#### **ORIGINAL ARTICLE**



## Mitigation of drought-induced oxidative damage by enhanced carbon assimilation and an efficient antioxidative metabolism under high ${\rm CO_2}$ environment in pigeonpea (*Cajanus cajan* L.)

Rachapudi Venkata Sreeharsha<sup>1</sup> · Shalini Mudalkar<sup>1</sup> · Debashree Sengupta<sup>1</sup> · Divya K. Unnikrishnan<sup>1</sup> · Attipalli Ramachandra Reddy<sup>1,2</sup>

Received: 20 June 2018 / Accepted: 14 September 2018 / Published online: 22 September 2018 © Springer Nature B.V. 2018

#### **Abstract**

In the current study, pigeonpea ( $Cajanus\ cajan\ L.$ ), a promising legume food crop was assessed for its photosynthetic physiology, antioxidative system as well as C and N metabolism under elevated  $CO_2$  and combined drought stress (DS). Pigeonpea was grown in open top chambers under elevated  $CO_2$  ( $600\ \mu mol\ mol\ ^{-1}$ ) and ambient  $CO_2$  ( $390\pm20\ \mu mol\ mol\ ^{-1}$ ) concentrations, later subjected to DS by complete water withholding. The DS plants were re-watered and recovered (R) to gain normal physiological growth and assessed the recoverable capacity in both elevated and ambient  $CO_2$  concentrations. The elevated  $CO_2$  grown pigeonpea showed greater gas exchange physiology, nodule mass and total dry biomass over ambient  $CO_2$  grown plants under well-watered (WW) and DS conditions albeit a decrease in leaf relative water content (LRWC). Glucose, fructose and sucrose levels were measured to understand the role of hexose to sucrose ratios (H:S) in mediating the drought responses. Free amino acid levels as indicative of N assimilation provided insights into C and N balance under DS and  $CO_2$  interactions. The enzymatic and non-enzymatic antioxidants showed significant upregulation in elevated  $CO_2$  grown plants under DS thereby protecting the plant from oxidative damage caused by the reactive oxygen species. Our results clearly demonstrated the protective role of elevated  $CO_2$  under DS at lower LRWC and gained comparative advantage of mitigating the DS-induced damage over ambient  $CO_2$  grown pigeonpea.

**Keywords** Cajanus cajan · Elevated CO<sub>2</sub> · Drought stress · Antioxidative system · Amino acids

#### Introduction

An unprecedented rise in atmospheric CO<sub>2</sub> concentrations is a serious concern to global food security as it influences the physiology, growth and yield of food crops. Plant responses to climate change are further perplexed by the concurrent exposure to multiple and frequent abiotic stresses such as

**Electronic supplementary material** The online version of this article (https://doi.org/10.1007/s11120-018-0586-9) contains supplementary material, which is available to authorized users.

- Attipalli Ramachandra Reddy attipalli.reddy@gmail.com
- Photosynthesis and Climate Change Laboratory, Department of Plant Sciences, University of Hyderabad, Hyderabad 500046, India
- Yogi Vemana University, Kadapa, Andhra Pradesh 516003, India

drought. The additive effects of the abiotic stress and elevated CO<sub>2</sub> can be better understood by treating the plants with these factors together rather than individual elements. In C<sub>3</sub> plants, elevated CO<sub>2</sub> enhances the RUBISCO carboxylation efficiency by increasing the intercellular CO<sub>2</sub> thereby stimulating the light-saturated net photosynthetic rate  $(A_{sat})$ (Ainsworth and Rogers 2007). However, during long-term growth under elevated CO<sub>2</sub>, the carbon-nitrogen (C-N) interactions result in a gradual decrease in leaf N (especially on a mass basis) owing to enhanced C uptake. This leads to acclimation of photosynthesis by decreasing the carboxylation capacity (Vc<sub>max</sub>) driven by reduced RUBISCO amount and activity (Ainsworth and Rogers 2007; Ellsworth et al. 2004; Nowak et al. 2004; Sekhar et al. 2017). In addition to N limitation, the factors like feedback inhibition due to excessive carbohydrate accumulation, stomatal resistance and chlorophyll dilution also play crucial role in photosynthetic acclimation under elevated CO<sub>2</sub> (Ainsworth and Long 2005; Rogers et al. 2004).



# Regulation of Floral Ontogeny in Pigeonpea (Cajanus cajan L.) Under Elevated CO2 and Drought Stress.

by Divya K Unnikrishnan

**Submission date:** 15-Dec-2022 05:10PM (UTC+0530)

**Submission ID:** 1981934059

File name: Divya K U Thesis.pdf (352.27K)

Word count: 21771

Character count: 118655

Regulation of Floral Ontogeny in Pigeonpea (Cajanus cajan L.) Inder Elevated CO2 and Drought Stress.

RIGINALITY REPORT

SIMILARITY INDEX

12% INTERNET SOURCES

STUDENT PAPERS

RIMARY SOURCES

link.springer.com

Internet Source

Rachapudi Venkata Sreeharsha, Kalva Madhana Sekhar, Attipalli Ramachandra Reddy. "Delayed flowering is associated with lack of photosynthetic acclimation in Pigeon pea (Cajanus cajan L.) grown under elevated CO2", Plant Science, 2015 Publication

Mohammad Mukarram, Sadaf Choudhary, Daniel Kurjak, Anja Petek, M. Masroor A. Khan. "Drought: Sensing, Signalling, Effects and Tolerance in Higher Plants", Physiologia Plantarum, 2021

Publication

Divya K. Unnikrishnan, Rachapudi V. Sreeharsha, Attipalli R. Reddy. "Growth, seed yield and nutritional characteristics of Prof. pigeonpea grown under elevated CO2

## atmosphere", Acta Physiologiae Plantarum, 2021

Publication

Internet Source

5	"Photosynthesis: Mechanisms and Effects", Springer Science and Business Media LLC, 1998 Publication	<1%
6	Submitted to University of Hyderabad, Hyderabad Student Paper	<1%
7	"Agricultural Proteomics Volume 2", Springer Science and Business Media LLC, 2016 Publication	<1%
8	Guo, Huijuan, Sun Yucheng, Yuefei Li, Bin Tong, Marvin Harris, Keyan Zhu-Salzman, and Feng Ge. "Pea aphid promotes amino acid metabolism both in Medicago truncatula and bacteriocytes to favor aphid population growth under elevated CO2", Global Change Biology, 2013. Publication	<1%
9	coek.info Internet Source	<1%
10	Molecular Biology, 2014.  Publication	<1%
11	bbrc.in	

12	www.mdpi.com Internet Source	<1%
13	Girish K. Rasineni, Anirban Guha, Attipalli R. Reddy. "Responses of Gmelina arborea, a tropical deciduous tree species, to elevated atmospheric CO2: Growth, biomass productivity and carbon sequestration efficacy", Plant Science, 2011	<1%
14	ir.lib.uwo.ca Internet Source	<1%
15	www.frontiersin.org Internet Source	<1%
16	fenix.isa.ulisboa.pt Internet Source	<1%
17	Environmental Adaptations and Stress Tolerance of Plants in the Era of Climate Change, 2012. Publication	<1%
18	Rachapudi Venkata Sreeharsha, Shalini Mudalkar, Debashree Sengupta, Divya K. Unnikrishnan, Attipalli Ramachandra Reddy. "Mitigation of drought-induced oxidative damage by enhanced carbon assimilation and an efficient antioxidative metabolism under an efficient antioxidative metabolism under the high CO2 environment in pigeonpea (Carantal Solito Plant Plant Solito Plant	<1% Sciences Sciences Nyderabad O46, India.  OPAL Sences Serabad O46.

Publication

D. EAMUS. "The interaction of rising CO2 and <1% 19 temperatures with water use efficiency", Plant Cell and Environment, 10/1991 Publication Submitted to Heriot-Watt University <1% 20 Student Paper Yusuf Y Muhammad, Sean Mayes, Festo 21 Massawe. " Effects of short-term water deficit stress on physiological characteristics of Bambara groundnut ((L.) Verdc.) ", South African Journal of Plant and Soil, 2015 Publication dokumen.pub <1% 22 Internet Source Clint J. Springer. "Flowering time and elevated 23 atmospheric CO2", New Phytologist, 8/23/2007 Publication Ellen Broucke, Thi Tuong Vi Dang, Yi Li, Sander <1% 24 Hulsmans et al. "SnRK1 inhibits anthocyanin biosynthesis through both transcriptional regulation and direct phosphorylation and dissociation of the MYB/bHLH/TTG1 MBW complex", Cold Spring Harbor Laboratory, 2022

25

Fui-Ching Tan. "Genetics of flower initiation and development in annual and perennial plants", Physiologia Plantarum, 9/2006

<1%

26

Madhana Sekhar, Kalva, Venkata Sreeharsha Rachapudi, Shalini Mudalkar, and Attipalli Ramachandra Reddy. "Persistent stimulation of photosynthesis in short rotation coppice mulberry under elevated CO2 atmosphere", Journal of Photochemistry and Photobiology B Biology, 2014. <1%

Publication

Exclude quotes

On

Exclude matches

< 14 words

Exclude bibliography